

**EFFECTS OF THYROID HORMONE ON  
CARDIOMYOCYTES AND ON GLIOMA  
DIFFERENTIATION AND PROLIFERATION**

Alexandros Liappas BSc, MSc

A thesis submitted in partial fulfillment for the requirements for  
the degree of Doctor of Philosophy at the University of Central  
Lancashire in collaboration with the University of Athens  
Medical School, Greece.

School of Pharmacy and Biomedical Sciences

**August 2012**

## **Abstract**

The action of thyroid hormone (TH) on cell growth, differentiation and survival during development may be of therapeutic relevance. The present study investigated the potential effects of long-term TH treatment on cardiomyocytes and on glioma tumour cell lines. This study employed neonatal cardiomyocytes, 1321N1 cell line, an astrocytoma grade II, and U87MG, a glioblastoma grade IV. Cells were exposed for 2 and 4 days in culture medium deprived of T3 (non-treated cells) and in a medium containing either 1 nM T3 (at near physiological range) or 500 nM T3 (supraphysiological). From the initial study on cardiomyocytes, the results show that phenylephryne (PE) can induce cell growth and this effect was mediated by T3. For the glioma cell lines the results show that T3 at 1 nM can promote cell re-differentiation in both cell lines. However, T3 had a preferential effect on suppressing cell proliferation only in the high grade glioma cell line. Thus, in 1321N1 cell line, T3 increased cell proliferation (2 days) which declined thereafter (4 days) without having any effect on cell survival. In U87MG cell line, T3 resulted in marked suppression of cell proliferation without increasing cell injury. At the molecular level, a 2.9 fold increase in the expression of TR $\alpha$ 1 receptor was observed in U87MG cells as compared to 1321N1,  $p < 0.05$ . TR $\beta$ 1 receptor was undetectable in both cell lines. These changes corresponded to a distinct pattern of growth signalling activation induced by T3 treatment. The results also show that T3 had no significant effect on ERK activation in both cell lines, but significantly ( $p < 0.05$ ) increased phospho-Akt levels in 1321N1 cell line. At higher dose, T3 also induced cell differentiation in both cell lines and suppressed proliferation while increased cell injury in U87MG cells. It can be concluded from these results that T3 can re-differentiate glioma tumour cells. However, the effect of T3 on cell proliferation appears to be dependent on the type of

tumour cell line with aggressive tumours to be more sensitive to thyroid hormone treatment. TR $\alpha$ 1 receptor may, at least in part, be implicated in this response.

## **Acknowledgments**

I sincerely thank Professor Costas Pantos and Dr Iordanis Mourouzis for their valuable support and guidance over the three years of the study concerning the planning the materialization and the supervising of my thesis. I regard myself as being very privileged to have had the chance to conduct my PhD in the Laboratory of Pharmacology Sciences of the University of Athens Medical School in collaboration with the School of Pharmacy and Biomedical Sciences of the University of Central Lancashire. Especially, I would like to thank Professor Robert W. Lea and Professor Jai Paul Singh for their continuous and valuable advice, as well as his exceptional help in the preparation of the thesis.

Finally many thanks to my family and Petros Malitas for their assistance, guidance and love.



## **Student Declaration**

### **Concurrent registration for two or more academic awards**

I declare that while registered as a candidate for the research degree, I have not been a registered candidate or enrolled student for another award of the University or other academic or professional institution

### **Material submitted for another award**

I declare that no material contained in the thesis has been used in any other submission for an academic award and is solely my own work

### **Collaboration**

Where a candidate's research programme is part of a collaborative project, the thesis must indicate in addition clearly the candidate's individual contribution and the extent of the collaboration. Please state below:

**This thesis was done in collaboration with the Department of Pharmacology, University of Athens Medical School, Athens, Greece**

**Signature of Candidate**

**Alexandros Liappas**

**Type of Award**

**PhD Doctoral**

**School of Pharmacy and Biomedical Sciences, University of Central Lancashire, Preston UK**

**This thesis is dedicated to my parents, Ioannis and Konstantina Liappas, my family and friends, my godfather Ioannis Soukos, and my beloved Grand dad.**

## **TABLE OF CONTENTS**

Abstract	2
Acknowledgements	4
Declaration	5
Dedication	6
Table of contents	7
Abbreviations	13
<b><u>Chapter 1. Introduction</u></b>	16
1.1. General introduction	17
1.2. Gliomas	18
1.3. Identification and grading of brain tumours	22
1.3.1. Astrocytic tumours	24
1.3.2. Pilocytic astrocytomas	25
1.3.3. Diffuse astrocytomas	26
1.3.4. Low grade diffuse astrocytomas	27
1.3.5. Fibrillary astrocytomas	28
1.3.6. Gemistocytic astrocytomas	28
1.3.7. Protoplasmic astrocytomas	28
1.3.8. Anaplastic astrocytomas	29
1.3.9. Glioblastomas	30
1.4. Molecular aspects of glioma tumourigenesis	32
1.4.1. Growth kinase signaling in cell proliferation and survival	32
1.4.1.1. MAPK and cancer	32
1.4.1.2. ERK	33
1.4.1.3. Akt	34
1.4.2. Growth kinase signaling in gliomas	37
1.4.2.1. ERK and gliomas	37

1.4.2.2. Akt and gliomas	37
1.5. Current treatment for brain malignant tumours	38
1.5.1. Surgery	38
1.5.2. Radiotherapy	39
1.5.3. Chemotherapy	40
1.5.3.1. Current standard therapy for GBM	41
1.5.3.2. Targeted therapies	42
1.5.3.3. EGFR inhibitors	42
1.5.3.4. Mammalian target of Rapamycin inhibitors	43
1.6. Therapeutic approaches related to redifferentiation of cancer cells	45
1.6.1 Cancer as maladaptive response to stress: a shift to a paradigm	45
1.6.2. Thyroid hormone as novel cancer treatment	47
1.7. Thyroid hormone: metabolism and transport	49
1.7.1. Thyroid hormone: cellular action	52
1.7.1.1. Genomic action-thyroid hormone receptors	52
1.7.1.2. Non genomic action of thyroid hormone	53
1.7.2. Novel thyroid hormone signaling	55
1.7.3. Thyroid hormone and tissue differentiation	57
1.7.4. Thyroid hormone and brain development	62
1.7.5. Changes of thyroid hormone signaling in disease	65
1.7.6. Changes in thyroid hormone signaling in heart diseases	65
1.7.7. Changes in thyroid hormone signaling in cancer	66
1.7.8. Thyroid hormone as potential treatment for cancer	68
1.7.8.1. Changes in thyroid hormone signaling in brain cancer	70
1.7.9. Thyroid hormone treatment	70
1.8. Working hypothesis	71
1.9. Aims of the study	72

<b><u>Chapter 2. Materials and Methods</u></b>	73
Materials	74
2.1. Studies on cardiac cell based models	77
2.1.1. Cell culture	77
2.1.2. Measurement of neonatal cardiomyocytes Axes and cell size	77
2.1.3. Determination of cardiomyocyte growth (cellular protein content)	78
2.1.4. Myosin Heavy Chain (MHC)	78
2.1.5. Immunocytochemistry	79
2.1.6. Experimental protocol	80
2.2 Studies on glioma cell lines	81
2.2.1. Cell culture	81
2.2.2. Subculture	82
2.2.3. Cell freezing	82
2.2.4. Culturing cells from frozen	83
2.2.5. Cell assays	83
2.2.5.1. Cell counting	83
2.2.5.2. Cell morphology	84
2.2.5.3. Cell proliferation	85
2.2.5.4. Cell apoptosis	86
2.2.5.5. Cell injury	86
2.2.5.6. Molecular analysis	86
2.2.5.7. Measurement of thyroid receptors	87
2.2.5.8. Construction of growth curves	88
2.3. Experimental protocols	90
2.4. Experimental studies	90
2.5. Statistical analysis	93
<b><u>Chapter 3. Results</u></b>	94
3.1. Studies in cardiac cell based models	95
3.1.1. Cell geometry, shape and $\alpha$ -myosin in untreated neonatal cells	95
3.1.2. Cell geometry, shape and growth in phenylephrine treated cardiomyocytes	95
3.1.3. Myosin heavy chain isoform expression in phenylephrine treated neonatal cardiomyocytes	97
3.1.4. Re-expression of TR $\alpha$ 1 in phenylephrine treated neonatal cardiomyocytes	99
3.1.5. Cell geometry and shape in T3 treated undifferentiated cardiomyocytes	100

3.1.6. Cell area, protein synthesis in T3 treated undifferentiated cardiomyocytes	102
3.1.7. Myosin heavy chain isoform expression in T3 treated undifferentiated cardiomyocytes	104
3.1.8. Cell geometry and shape in T3 treated dedifferentiated cardiomyocytes	106
3.1.9. Cell area, protein synthesis in T3 treated dedifferentiated cardiomyocytes	108
3.1.10. Myosin isoform expression in T3 treated dedifferentiated cardiomyocytes	108
3.2. Studies in glioma cell lines	111
3.2.1. Growth curves of 1321N1 and U87MG glioma cell lines	111
3.2.2. Morphological characteristics of glioma cell lines	113
3.2.2.1. Cell morphology 2days	113
3.2.2.2. Cell morphology 4 days	117
3.2.3. Cell count of glioma cell lines	119
3.2.3.1. Total cell number count 2 days	119
3.2.3.2. Total cell number count 4 days	121
3.2.4. Cell proliferation of glioma cell line	123
3.2.4.1. Cell proliferation 2 days	123
3.2.4.2. Cell proliferation 4 days	127
3.2.5. Levels of injury on glioma cell lines	131
3.2.5.1. Cell necrosis 2 days	131
3.2.5.2. Cell necrosis 4 days	133
3.2.6. Levels of apoptosis on glioma cell lines	135
3.2.6.1. Cell apoptosis 2 days	135
3.2.6.2. Cell apoptosis 4 days	140
3.2.7. Molecular detection of kinase signaling in glioma cell lines	144
3.2.7.1. Kinase signaling activation 2 days	144
3.2.7.2. Kinase signaling activation 4 days	148

3.3.1. Morphological characteristics of glioma cell lines	152
3.3.1.1. Cell morphology 2 days	152
3.3.1.2. Cell morphology 4 days	156
3.3.2. Cell count of glioma cell lines	158
3.3.2.1. Total cell number count 2 days	158
3.3.2.2. Total cell number count 2 days	160
3.3.3. Cell proliferation of glioma cell lines	162
3.3.3.1. Cell proliferation 2 days	162
3.3.3.2. Cell proliferation 4 days	166
3.3.4. Levels of injury on glioma cell lines	170
3.3.4.1. Cell necrosis 2 days	170
3.3.4.2. Cell necrosis 4 days	172
3.3.5. Levels of apoptosis on glioma cell lines	174
3.3.5.1. Cell apoptosis 2 days	174
3.3.5.2. Cell apoptosis 4 days	179
3.3.6. Molecular detection of kinase signaling in glioma cell lines	183
3.3.6.1. Kinase signaling activation 2 days	183
3.3.6.2. Kinase signaling activation 4 days	187
3.3.7. Molecular detection of TR $\alpha$ 1 receptors in glioma cell lines	191
3.3.7.1 Thyroid hormone receptors expression	191
<b><u>Chapter 4. Discussion</u></b>	193
4.1 Discussion	194
4.2 T3 has the ability to differentiate neonatal cardiomyocytes	195
4.3 PE induces dedifferentiation in neonatal cardiomyocytes	196
4.4 T3 differentiates dedifferentiated cells	196
4.5 Glioma cell line models	197
4.6 Thyroid hormone and brain tumours	198
4.7. T3 effect on glioma cell differentiation	199

4.8. T3 effect on cell growth and survival	200
4.9. Molecular aspects of T3 action on glioma tumours	201
4.9.1. The potential role of TR receptors	201
4.9.2. TR $\alpha$ 1: a common player in pathological cardiac growth and cancer	205
4.9.3. The potential role of growth signaling	205
4.10. Conclusions	211
4.11. Clinical and therapeutic relevance- future directions	211
4.12. Scope for future studies	212
<b><u>Publication</u></b>	213
<b><u>References</u></b>	215

## ABBREVIATIONS

Akt: protein-serine/threonine kinase

ATP: adenosine triphosphate

Bax: proapoptotic protein

Bcl2: B cell leukemia protooncogene

B-Raf: Serine/Threonine Kinase

CDK4: cyclin dependent kinase 4

CNS: Central nervous system

COX: cyclooxygenase

DT: Diffusion tensor

EGFR: epithelial growth factor receptor

ELISA: enzyme linked immunosorbent assay

ERK: extracellular signal regulated kinase

fMRI: functional magnetic resonance imaging

GBM: glioblastoma multiforme

GFAP: glial fibrillary acidic protein

HCL: hydrogen chloride

HGF: hepatocyte growth factor

LDH: lactate dehydrogenase

LOH: loss of heterozygosity

MAB: monoclonal antibodies

MAPK: mitogen activated protein kinase

MCT: monocarboxylate transporter

MEK 1/2: cell migration kinase

MGMT: Methyl Guanine Methyl Transferase

MLCK: myosine light-chain kinase

MMP: matrix metalloproteinase

MST: mean survival time

mTORC1: mammalian target of rapamycin

Na<sup>+</sup>: sodium

OATP: organic anion transporting polypeptide

PDGFR: platelet-derived growth factor receptor 1

PE: phenylephrine

PI-103: dual inhibitor of Class IA phosphatidylinositol 3-kinase

PKC: protein kinase C

PTEN/MMAC1: phosphatase that dephosphorylates

Ras-1: protein pathway

RB: retinoblastoma

RTOG: Radiation Therapy Oncology Group

SEM: standard error of mean

STAT: signal transducers and activators

TH: Thyroid hormone

TKI: tyrosine kinase inhibitors

TREs: thyroid hormone response elements

TRs: thyroid hormone receptors

TR $\alpha$ 1: thyroid hormone receptor alpha 1

TR $\beta$ 1: thyroid hormone receptor beta 1

VEGFR: vascular endothelial growth factor receptor

# Chapter One

## Introduction

## **1.1. General introduction**

Brain tumours are masses of growth of abnormal cells in the brain and typically are categorized as either primary or secondary. Primary brain tumours originate in the brain and can be non-cancerous (benign) or cancerous (malignant). Secondary brain tumours result from cancer that began elsewhere and has spread to the brain. Primary brain tumours are less common than secondary brain tumours (Aminoff, 2004). Benign brain tumours are usually slower growing, easier to remove (depending the location), and less likely to recur than are malignant brain tumours. Benign brain tumours do not invade the surrounding normal brain or other nearby structures, but they can still place pressure on sensitive areas of the brain. Malignant brain tumours can grow more rapidly, invading or destroying nearby brain tissue. However, unlike cancers elsewhere in the body, primary malignant brain tumours rarely spread from the brain (Aminoff, 2004).

Signs and symptoms of the brain tumour depend on its size, location and rate of growth (Aminoff, 2004).

A brain tumour- either primary or secondary- may cause a variety of signs and symptoms because it may directly press on or invade brain tissue. This can damage or destroy areas responsible for sight, movement, balance, speech, hearing, memory or behaviour. Pressure from a brain tumour can also cause surrounding brain tissue to swell (oedema), further increasing pressure and symptoms (Aminoff, 2004).

Since it is not known exactly what causes primary brain tumours, it is difficult to pinpoint risk factors. In rare cases, brain tumours strike several members of a family, suggesting heredity may be a risk factor. This accounts for only a fraction of cases. Some types of brain tumours appear to occur more frequently in people who are

exposed in radiation or certain chemicals, such as those who work in oil refining, rubber manufacturing, and chemical and nuclear industries (American Cancer Society, 2007). However, a definite link between exposure to chemicals and brain tumours has not been proved. Similarly, electromagnetic fields and the use of cell phones have been studied as causes of primary brain tumours, but no definitive evidence indicates that either are the cause of brain tumours (American Cancer Society 2007; Munchi 2011; Cardis *et al.*, 2011).

This study is concerned mainly with gliomas, a type of brain tumour which derives from astroglial cells and which have attracted much recent attention. In particular, this thesis focuses on the potential role of thyroid hormone (TH) signalling in gliomas.

## **1.2. Gliomas**

Gliomas are the most common tumour of the central nervous system (CNS) with a lethality rate approaching 80% in the first year of diagnosis and comprise about 5% of all newly diagnosed cancers each year (Avgeropoulos *et al.*, 1999; Lemke, 2004). Generally, the incidence of malignant gliomas equals that of leukaemia and comprises about 50% of all intracranial tumours in the adult. The American Cancer Society estimated that the number of new cases of primary CNS malignant disorders was 16,500, per year with an estimated 13,000 deaths in the USA alone in 2000 (Greenlee *et al.*, 2000). In the USA, about 7,000 cases of malignant brain tumours were newly diagnosed in 1987 (Kimmel *et al.*, 1987) whilst in American's Cancer Society survey in 2007 it was found that almost 20,500 new cases of malignant brain tumours were diagnosed. In the UK the average annual incidence of cerebral glioma in the age range 15-64 years was 5.9 per 100,000 per year (Grant *et al.*, 1996) and a later study showed

that glioblastomas have an incidence with 3.55 new cases per 100,000 population per year (Ohgaki and Kleihues, 2007).

These neoplasms cause a disproportionate burden of cancer-related disability and death. The five year survival rates for brain tumours are the third lowest among all types of cancer (pancreas and lung are first and second, respectively) (Avgeropoulos *et al.*, 1999).

In the USA, the median survival of patients with gliomas treated conservatively is 14 weeks; by surgical resection alone 20 weeks; by surgery and radiation 36 weeks; and by the addition of chemotherapy 40-50 weeks (Salcman, 1980; Fine *et al.*, 1993; Salcman *et al.*, 1994; Huncharek *et al.*, 1998; Avgeropoulos *et al.*, 1999; Stupp *et al.*, 2005; Tabatabai *et al.*, 2012; Weller *et al.*, 2012).

Genetic mutations, specifically gene p53 chromosome 17, have been identified in 50% of cancers and 75% of glioblastoma multiform (Madjian *et al.*, 1999; Ali *et al.*, 2000; Gutin *et al.*, 2000; Strickler *et al.*, 2000; Caruthers, 2001; Paterson, 2001; Hickey, 2004; Ohgaki and Kleihues, 2007). Additional agents suspected as being carcinogenic include non-ionizing radiation (from cell phones and microwaves), pesticides, toxic water and high voltage power lines (American Cancer Society, 2007). Current research investigating these agents remains inconclusive.

Finally, the presenting symptoms of brain cancer are related to the decompensation of the brain resulting from an expanding mass. According to the 'Monroe Kelly Theory'; equilibrium must be maintained between three components within the skull: brain tissue (80%), cerebral spinal fluid (10%) and interstitial and vascular supply (10%). If there is enlargement of one of these components or an expanding mass within the skull, there will be compression to one or both of the other components (Hickey,

2004). As the brain tumour grows, oedema will occur, which further compromises the closed system (Strickler *et al.*, 2000; Caruthers, 2001; Hickey, 2004). Symptoms occur when the brain is no longer able to compensate for the increase in mass effect, and include headaches, seizures, or neurologic deficits (Chamberlain *et al.*, 1998; Armstrong *et al.*, 2000; Chang *et al.*, 2000; Short *et al.*, 2000; Strickler *et al.*, 2000; Caruthers, 2001; DeAngelis, 2001; Peterson, 2001; Lovely, 2002; Hickey, 2004).

High-grade tumours, such as anaplastic astrocytoma and glioblastoma multiforme (WHO grade III and IV, respectively), account for roughly half of astrocytic tumours (Cavenee *et al.*, 2000) and are referred to as high-grade gliomas (Table 1.1).

Depending on the cell origin, there are three main types of glial tumours: astrocytoma, oligodendroglioma andependymoma. The term 'glioma' generally refers to an astrocytoma. Furthermore, astrocytomas account for the majority of malignant gliomas in adults and are graded into four groups according to the WHO classification. Grade I tumours are more common in children than in adults and comprise a distinct entity called pilocytic astrocytomas, characterized histologically by the presence of Rosenthal fibres. Hypercellularity and cellular pleomorphism are the basic characteristics of grade II astrocytomas, whilst grade III astrocytomas show strong mitotic activity along with hypercellularity and pleomorphism (Ohgaki and Kleihues, 2007).

When the tumour shows vascular endothelial proliferation and/or the presence of necrosis, it is graded as grade IV (Glioblastoma). Grade III and IV astrocytomas are generally referred to as malignant astrocytomas. Oligodendrogliomas and ependymomas are much less common and have three grades I, II, and III. Molecular

biology studies suggest two types of glioblastoma, primary (de novo) and secondary (evolving from a pre-existing low-grade glioma).

Primary tumours exhibit frequent occurrences of loss of heterozygosity 10q (70% of cases) EGRF (Epithelial growth factor receptor) amplification (36%), p16<sup>INK4a</sup> deletion (31%) and PTEN mutations (25%), whereas secondary tumours show more frequent p53 mutation (Benjamin *et al.*, 2003; Ohgaki and Kleihues, 2007).

Surgery, radiotherapy or chemotherapy are the main treatment options and may be used alone or in combination, depending on the type of tumour. Surgery is the first treatment option for most primary brain tumours. As much of the tumour as possible is removed by making an opening in the skull called a craniotomy. A course of radiotherapy and/or chemotherapy often follows (Mao *et al.*, 1991).

Radiotherapy works by targeting radiation to damage the cancer cells and prevent them growing. It may be used before surgery to reduce the size of the tumour, after surgery to kill any tumour cells that were not removed, or as an alternative to surgery (Frelick *et al.*, 1992)

Chemotherapy uses drugs that attack cancer cells or prevent them multiplying. It is used alone or in combination with radiotherapy to treat primary brain tumours that cannot be removed surgically, or to treat secondary brain tumours. It is usually given as tablets or by injection (Davis *et al.*, 1991).

Steroids, such as dexamethasone, are often given to reduce the swelling caused by brain tumours. They will not remove the tumour, but should improve the symptoms and may be given before or after surgery or radiotherapy (Riggs *et al.*, 1995).

### **1.3. Identification and grading of brain tumours**

Gliomas (cancer cells) are identified depending on the specific cell type they largely bear a resemblance to or originate from (Table 1.1). There are three main types of glioma; astrocytomas originating from astrocytes, oligodendroglioma (oligodendrocytes) and ependymomas (ependymal cells), (World Health Organization WHO 1990). Gliomas are further categorised into a grading system by histological examination. Many different methods are employed to grade tumours but the one most commonly used is that of the World Health Organisation (WHO). The WHO grading system grades gliomas into 4 categories, grades I-IV, I being the least aggressive and IV being the most aggressive, prognosis is strongly related to histological grade (Table 1.1).

**Table 1.1.** Summary of grading system for astrocytomas. Table obtained from WHO (World Health Organisation 2007).

<b>Grading of astrocytomas</b>		
<b>WHO Grade</b>	<b>Designation</b>	<b>Histological Criteria</b>
I	Pilocytic Astrocytoma	Rosenthal fibres, eosinophilic granular bodies and microcystes
II	Diffuse Astrocytoma	Nuclear atypia, hypercellularity and pleomorphism.
III	Anaplastic astrocytoma	Nuclear atypia and strong mitotic activity
IV	Glioblastoma multiform	Atypia, mitoses, vascular endothelial proliferation, necrosis

Grade I glioma or pilocytic astrocytomas are considered to commonly be a childhood tumour as they occur predominantly in children, involving the midline, posterior and basal fossae. They are characterised histological by the presence of Rosenthal fibres, eosinophilic granular bodies and microcystes (Nishio *et al*, 1995). Grade II gliomas are termed diffuse astrocytoma and often show evidence of hypercellularity and cellular pleomorphism (Surawicz *et al*, 1999). Grade III glioma or anaplastic astrocytoma occur mainly in adults with a median age at diagnosis of 51 years of age and account for roughly 7% of primary brain tumours. They exhibit strong mitotic activity along with hypercellularity and pleomorphism (Bondy *et al*, 1991). Grade IV glioma or glioblastoma multiform (GBM), is the most common form of glioma

accounting for roughly 45%-52% of all reported brain tumours. These are the most aggressive tumours and often recur which contributes to the poor survival time associated with these tumours. GBM are distinguished from grade III glioma by the presence of necrotic tissue alongside proliferating anaplastic cells, grade III glioma has no necrotic tissue. Within both the different areas of the same tumour and between different GBM's there is often discernible heterogeneity in histological and cytological appearance (Preston-Martin *et al*, 1995; Christians *et al.*, 2012; Karina *et al.*, 2012; Gupta *et al.*, 2012).

Over the past few decades there has been increased interest in glioma research with new and more effective ways of treating glioma; nonetheless improvement in prognosis has been limited (Li *et al.*, 2012; Minniti *et al.*, 2009). Because of their profound devastating effect much research is currently being carried out to investigate gliomas and it seems that the chemosensitivity of gliomas, i.e. the analysis of glioma response to a specific drug, is a focal point of developing treatment, and more recently an idea of prevention (Gurney *et al*, 1996).

### 1.3.1. Astrocytic tumours

Astrocytomas are defined as tumours composed predominantly of neoplastic astrocytes. If not stated otherwise, this term applies to diffusely infiltrating neoplasms which, according to their biological behavior, are subdivided into low grade astrocytoma (WHO Grade II), anaplastic astrocytoma (WHO Grade III) and glioblastoma (WHO Grade IV) (Dillman *et al*, 2004). A distinct entity is the pilocytic astrocytoma, which has a different location, age distribution, biological behavior and genetic basis (Chan *et al*, 2005).

The term astrocytoma was already used in the late nineteenth century by Virchow (Barker *et al*, 1998) but was firmly introduced into histopathological classification in 1926 by Bailey (Cushing Brem *et al*, 1995). A detailed account of the historical evolution of the astrocytoma terminology has been given by Zulch (Amiratti *et al*, 1987) and Russell and Rubinstein (Choucair *et al*, 1986). More recent reviews on the pathology of astrocytic neoplasms include those by VandenBerg Cohen *et al*, (1995), Davis *et al*, (1998), Schiffer Kleihues *et al*, 2000, Parisi and Scheithauer, (Mahajan *et al*, 2005), and Burger and Scheithauer, (O'Reilly *et al*, 2006).

### 1.3.2. Pilocytic astrocytomas

The pilocytic astrocytoma is a slow growing astrocytic tumour predominantly of childhood, with preferential location in midline structures of the CNS. The term piloid/ pilocytic astrocytoma was introduced by Penfield in 1931 (Salzman *et al*, 1994). Pilocytic astrocytoma is now the generally acknowledged term and recommended in the WHO Histopathological Typing of Tumours of the CNS (Stupp *et al*, 2002; Black *et al*, 1991). Pilocytic astrocytoma amounts to approximately 6% of intracranial tumours. More than 75% of pilocytic astrocytomas manifest in children below the age of 20 years, and peak incidence is between 8 and 13 years (Aronen *et al*, 2002)

Pilocytic astrocytomas are preferentially located axially, i.e. close to the ventricles and to midline structures of the CNS, i.e. visual system, hypothalamus, cerebellum, brain stem and spinal cord. The cerebellum is most frequently affected, preferentially the cerebellar hemispheres (>80%), less frequently the vermis (20%) (Colombo *et al*, 2005).

Since pilocytic astrocytomas are slowly growing neoplasms, the clinical history often precedes clinical diagnosis and surgical intervention by several months, often years. In the cerebellum, the pilocytic astrocytoma is macroscopically well delineated and appears to expand rather than infiltrate into adjacent brain structures. Pilocytic astrocytomas may display a remarkable degree of nuclear polymorphism; even multinuclear giant cells may occur. Vascular proliferation may be extensive and often includes formation of typical glomeruli (Yoshida *et al*, 2000; Scharfen *et al*, 1992).

Cytogenetic analysis of pilocytic astrocytomas was revealed either or a normal karyotype of a variety of aberrations but no distinct pattern suggesting the loss of a particular tumour suppressor gene (Osoba *et al*, 2000; Mahajan *et al*, 2005) with the exception of a frequent (33%) occurrence of trisomy 7 and 8 (O'Reilly *et al*, 2006). In contrast to diffusely infiltrating astrocytomas, pilocytic astrocytomas have no intrinsic tendency for progression to malignant astrocytoma.

### 1.3.3. Diffuse astrocytomas

Astrocytic neoplasms are characterized by a high degree of cellular differentiation, slow growth and diffuse infiltration of neighbouring brain structures. These lesions typically affect young adults and have an intrinsic tendency for malignant progression to anaplastic astrocytoma and ultimately, glioblastoma. The term 'diffuse astrocytoma' refers to low grade astrocytomas of adults (Kleihues *et al.*, 1993).

Diffuse astrocytomas represent 10-15% of all astrocytic tumours, with an incidence of approximately 1.4 new case per 1 million population per year (Davis *et al.*, 1998) the

peak incidence occurs in young adults between 30 and 40 years of age (25% of all cases). Diffuse astrocytomas may be located in any region of the CNS.

Seizures are a common presenting manifestation of tumour. It is clear that the symptoms and the signs of the patient depend upon the location of the tumour.

Diffuse astrocytomas are composed of well-differentiated fibrillary or gemistocytic neoplastic astrocytes. Cellularity is moderately increased and occasional nuclear atypia is a typical feature. Mitotic activity is generally absent and the presence of necrosis or microvascular proliferation is incompatible with the diagnosis of diffuse astrocytoma (Kleihues and Cavenee, 1999)

#### 1.3.4. Low grade diffuse astrocytomas

Low grade diffuse astrocytomas progressing to glioblastomas present mutation frequencies on TP53 of greater than 60% (Reifenberg *et al.*, 1996; Watanabe *et al.*, 1997). Frequency of TP53 mutation does not increase during malignant progression of low grade astrocytomas indicating that this genetic change is an early event (von Deimling *et al.*, 1992; Sidransky *et al.*, 1992; Watanabe *et al.*, 1996; Watanabe *et al.*, 1997; Ruda *et al.*, 2012; Hasegawa *et al.*, 2011). If the mutations were the initial event (Kinzler *et al.*, 1998) it would be expected that patients with inherited TP53 germline mutations would also develop brain tumours preferentially of astrocytic lineage and this is indeed the case (Kleihues *et al.*, 1997). Other genetic changes observed in diffuse astrocytomas concern platelet derived growth factor receptor  $\alpha$  (PDGFR $\alpha$ ). Mean survival after surgical intervention shows a range of 6-8 years (Roelcke *et al.*, 1999). The total length of disease is mainly influenced by the dynamics of malignant

progression to glioblastoma, which tends to occur after a mean time of 4-5 years (Vestrosick *et al.*, 1991; McCormack *et al.*, 1992; Watanabe *et al.*, 1997; Roelcke *et al.*, 1999).

#### 1.3.5. Fibrillary astrocytomas

This is by far the most frequent histological variant of astrocytoma. The occasional or regional occurrence of gemistocytic neoplastic cells is compatible with the diagnosis of fibrillary astrocytomas (Maxwell, 1991).

#### 1.3.6. Gemistocytic astrocytomas

This variant of astrocytoma is predominantly composed of gemistocytic neoplastic astrocytes. The gemistocytic neoplastic astrocytes consistently express GFAP (like most of the gliomas do) in their perikarya and cell process. Electron microscopy confirms the presence of abundant, compact glial filaments in the cytoplasm and in the cell process. Enlarged mitochondria have also been noted (Choucair *et al.*, 1986; Combs *et al.*, 2005).

#### 1.3.7. Protoplasmic astrocytomas

This rare variant is characterized by neoplastic astrocytes showing a small cell body with few, thin processes with a low content of glial filaments. Nuclei are uniformly round to oval. Cellularity is low and mitotic activity absent (Jaeckle *et al.*, 2003).

### 1.3.8. Anaplastic astrocytomas

The anaplastic astrocytoma is a diffusely infiltrating tumour with focal or dispersed anaplasia and a marked proliferative potential. These tumours arise from low-grade astrocytomas but are also diagnosed at biopsy without a less malignant precursor lesion and have an intrinsic tendency for malignant progression to glioblastoma. The anaplastic astrocytoma corresponds to WHO grade III. The main incidence of these tumours occurs between 40 and 49 years of age in males and 30-39 years for females (Kleihues and Cavenee 1999). Moreover, they are more frequent in males than females with a male to female ratio of 1.8:1. Localization corresponds to that of other diffusely infiltrating astrocytomas, with a preference for the cerebral hemispheres. Symptoms are similar to those referred to previously for patients with diffuse astrocytomas WHO grade II (Kleihues and Cavenee 1999).

The principal histopathological features of anaplastic astrocytoma are those of diffuse infiltrating astrocytomas with increased cellularity, distinct nuclear atypia and marked mitotic activity (Watanabe *et al.*, 1997).

Anaplastic astrocytomas show a high frequency of TP53 mutation similar to that of diffuse astrocytomas found in over 90% of the cases (Watanabe *et al.*, 1997). Additional genetic changes reflect the high degree of malignancy such as RB alterations (25%), p19<sup>ARF</sup> deletion (15%) and CDK4 amplification (10%) (Kleihues and Cavenee 1999). Also PTEN/MMAC1 mutations and LOH on chromosome 10q have been reported in 15% and 30% respectively (Kleihues and Cavenee 1999). Finally, approximately 40% of anaplastic astrocytomas have shown a LOH on chromosome 19q (von Deimling *et al.*, 1994) and in 30% a LOH on chromosome 22q (Ischimura *et al.*, 1998).

The key prognostic factor is progression of anaplastic astrocytoma to glioblastoma. The time interval varies with a mean of 2 years (Watanabe *et al.*, 1997) and a total length of disease of 3 years (Donahue *et al.*, 1997).

### 1.3.9. Glioblastomas

Glioblastoma multiform (GBM) is the most aggressive form of primary brain tumours known collectively as gliomas. These tumours arise from the supporting, glial cells of the brain during childhood and in adults. These growths do not spread throughout the body like other forms of cancer, but cause symptoms by invading the brain (Scott *et al.*, 1998). Gliomas are graded by their microscopic appearance. As a rule, their behaviour can be predicted from this histology: grade I (pilocytic astrocytomas) and grade II (benign astrocytomas) tumours grow slowly over many years while grade IV (GBM) grows rapidly, invading and altering brain function. Untreated, GBM's are rapidly lethal (Sipos *et al.*, 1997).

The area of the brain first involved by the tumour influences the first symptoms of GBM. Progressive weakness, speech or visual loss occurs when "eloquent" brain regions are involved. More "silent" areas of the brain allow the tumours to become large before symptoms arise. In this case increased pressure in the head produces headache and rarely, visual loss from swelling of the optic nerves (Tuettenberg *et al.*, 2005). The tumours also irritate the brain, causing epileptic seizures. Rarely, spontaneous haemorrhage into the tumour yields a stroke syndrome, with the sudden development of a neurological deficit.

GBM usually arise *de novo* or may develop from lower grade gliomas after many years. Distinct genetic alterations in primary and secondary GBM's have been identified. As a rule, they do not run in families (Wald *et al*, 1997). Once symptoms occur, the diagnosis of GBM is usually straightforward. The tumour can be imaged by contrast-enhanced MRI scan. Progressive growth of the lesion on serial MR scans differentiates tumour from stroke. A PET scan showing increased uptake of glucose can also help separate a diagnosis of tumour from stroke. An open or needle biopsy provides tissue for microscopic diagnosis. Glioblastoma is the most frequent brain tumour and accounts for approximately 12-15% of all intracranial neoplasms (Lurching *et al*, 1975), and 50-60% of all astrocytic tumours. The incidence in the general population is in the range of two to three new cases per 100000 per year for most European and North American countries. Glioblastomas may manifest at any age, but preferentially affect adults, with a peak incidence between 45 and 70 years (Brandes *et al*, 2002).

The preferred location of glioblastomas is the cerebral hemispheres, in particular the frontotemporal and parietal regions. Tumour infiltration often extends into the basal ganglia. Glioblastomas of the brain stem (malignant brain stem glioma) are less frequent and often affect children (Dillman *et al*, 2004), while cerebellum and spinal cord are rare sites for this neoplasm. It has long been observed that some glioblastomas develop over months or years from low grade or anaplastic astrocytomas and these have traditionally been termed secondary glioblastomas. The less malignant precursor lesions usually manifest at middle age (30-45 years). In contrast, primary glioblastomas develop with a short clinical history of usually less than 6 months *de novo*, i.e. without clinical or histopathological evidence of a pre-existing, less malignant precursor lesion (Groves *et al*, 2002).

## **1.4. Molecular aspects of glioma tumorigenesis**

### **1.4.1. Growth kinase signalling in cell proliferation and survival**

#### **1.4.1.1. MAPK and cancer**

Mitogen-activated protein kinases (MAPKs) are serine-threonine kinases that mediate intracellular signalling associated with a variety of cellular activities including cell proliferation, differentiation, survival, death and transformation (McCubret *et al.*, 2006, Torii *et al.*, 2006; Dhillon *et al.*, 2007). MAPK pathways are usually activated through complex signalling that contains multiple kinases guided by scaffold protein or as a result of binary interactions between kinase components. Kinase suppressor of Ras-1 (KSR) and MEK partner 1 (MP1) function as scaffold proteins for the ERK signaling pathway (Morrison *et al.*, 2003; Whitmarsh *et al.*, 2006).

In the ERK signalling pathway, ERK1 or ERK2 is activated by MEK1/2, which in turn is activated by a Raf isoform such as A-Raf, B-Raf or Raf-1. Members of the Ras family of protein play a key role in transmission of extracellular signals into the cell (Malumbres *et al.*, 2003).

Associated with cellular activities the MAPK signalling pathways have been implicated in the pathogenesis of many human diseases such as cancer, Alzheimer's, Parkinsons and amyotrophic lateral sclerosis (Dhillon *et al.*, 2007).

Ras and B-Raf that play a key role in the ERK signalling pathway have been associated in many cancer mutations (Dhillon *et al.*, 2007; Boutros *et al.*, 2008). Activated MEK1/2 has also been shown to up-regulate the expression of matrix metalloproteinases and to protect cancer cells from anoikis or detachment- induced apoptosis (Voisin *et al.*, 2008).

ERK signalling plays a role in several steps of tumour development, and also induces the expression of matrix metalloproteinases promoting the degradation of extracellular matrix proteins and consequent tumour invasion (Chakraborti *et al.*, 2003).

Furthermore, ERK1/2 signalling regulates both the activity and levels of Bcl-2 family proteins such as the pro-apoptotic protein BIM and the anti-apoptotic protein MCL-1, thereby promoting the survival of cancer cells (Balmanno *et al.*, 2009). Mutations in the epidermal growth factor receptor (EGFR), which activates the ERK pathway, occur frequently in lung and colorectal cancers (Hynes *et al.*, 2009, Nagahara *et al.*, 2005). The most common mutation of EGFR is an in-frame deletion in the tyrosine kinase domain, which results in activation of downstream signaling such as that mediated by the PI3K-Akt and Raf-MEK-ERK pathways (Fig 1.1) (Paez *et al.*, 2004). Gefitinib and erlotinib, both inhibitors of the tyrosine kinase activity of EGFR, are used to block the proliferation of non-small cell lung cancer cells (Zhu *et al.*, 2008).

#### **1.4.1.2. ERK**

Cell motility is a fundamental process that is required during normal embryonic development, wound repair, inflammatory response and tumour metastasis (Lauffenburger *et al.*, 1996). The ERK pathway plays an essential role in the induction of epithelial cell motility in response to hepatocyte growth factor (HGF) (Tanimura *et al.*, 1998). HGF-induced activation of the ERK pathway is linked to the expression of the matrix metalloproteinase (mmp)-9 gene, and MMP-9 activity is required for the induction of cell motility via the degradation of the extracellular matrix (Tanimura *et al.*, 2002). Elevated expression of MMPs is associated with

increased metastatic potential in many tumour cells, and inhibition of MMP activity results in the reduction of tumour invasion and metastasis (Reddy *et al.*, 2003). Transfection of a constitutive active form of MEK1 induces increased expression of MMP2/9 and confers metastatic potential to NIH3T3 cells (Welch *et al.*, 2000). Implication of the ERK pathway in the activation of the motility machinery of the cell has been reported, in which ERK1/2 phosphorylates and enhances the myosine light-chain kinase (MLCK) activity leading to increased MLC phosphorylation and enhanced cell migration (Klemke *et al.*, 1997).

Specific inhibition of the ERK pathway is expected to result in anti-metastatic as well as anti-angiogenic effects in tumour cell. Specific blockade of the ERK pathway has been shown to inhibit the disruption of cell-cell contact and motility required for the metastatic process in colon tumour cells (Sebolt-Leopold *et al.*, 1999) and to inhibit the invasiveness of tumour cells through the down-regulation of MMP-3/-9/-14 and CD44 (Tanimura *et al.*, 2003)

#### **1.4.1.3. Akt**

Akt delivers antiapoptotic signals via different proteins directly modulated by Akt phosphorylation. Bad (Bcl2 antagonist of cell death) is one of the first discovered targets of Akt phosphorylation. Bad is a proapoptotic member of the Bcl-2 family of proteins, able to bind Bcl-2 or Bcl- XL, blocking their antiapoptotic activities. Phosphorylation of Bad on S136 by Akt disrupts its interaction with Bcl- 2/Bcl-XL, localized on the outer mitochondrial membrane, sequestering Bad in the cytosol, through the interaction with 14-3-3 protein (Hirakawa *et al.*, 1988). In an analogous way, phosphorylation by Akt of proapoptotic Bax protein on S184 suppresses its

translocation to mitochondria, preventing Bax conformational change, a typical event that occurs after apoptotic induction. In addition, the caspase cascade is further inhibited by Akt phosphorylation of procaspase 9, inactivated through phosphorylation in S196, a residue that, however, is not conserved in other mammalian species (Crews *et al.*, 1993).

One of the best-conserved functions of Akt is its role in promoting cell growth. The predominant mechanism appears to be through activation of the mammalian target of rapamycin complex 1 (mTORC1), which is regulated by both nutrients and growth factor signalling. Akt-mediated cell proliferation and oncogenic transformation has been shown to be dependent on mTORC1 activation (Bononi *et al.*, 2011).

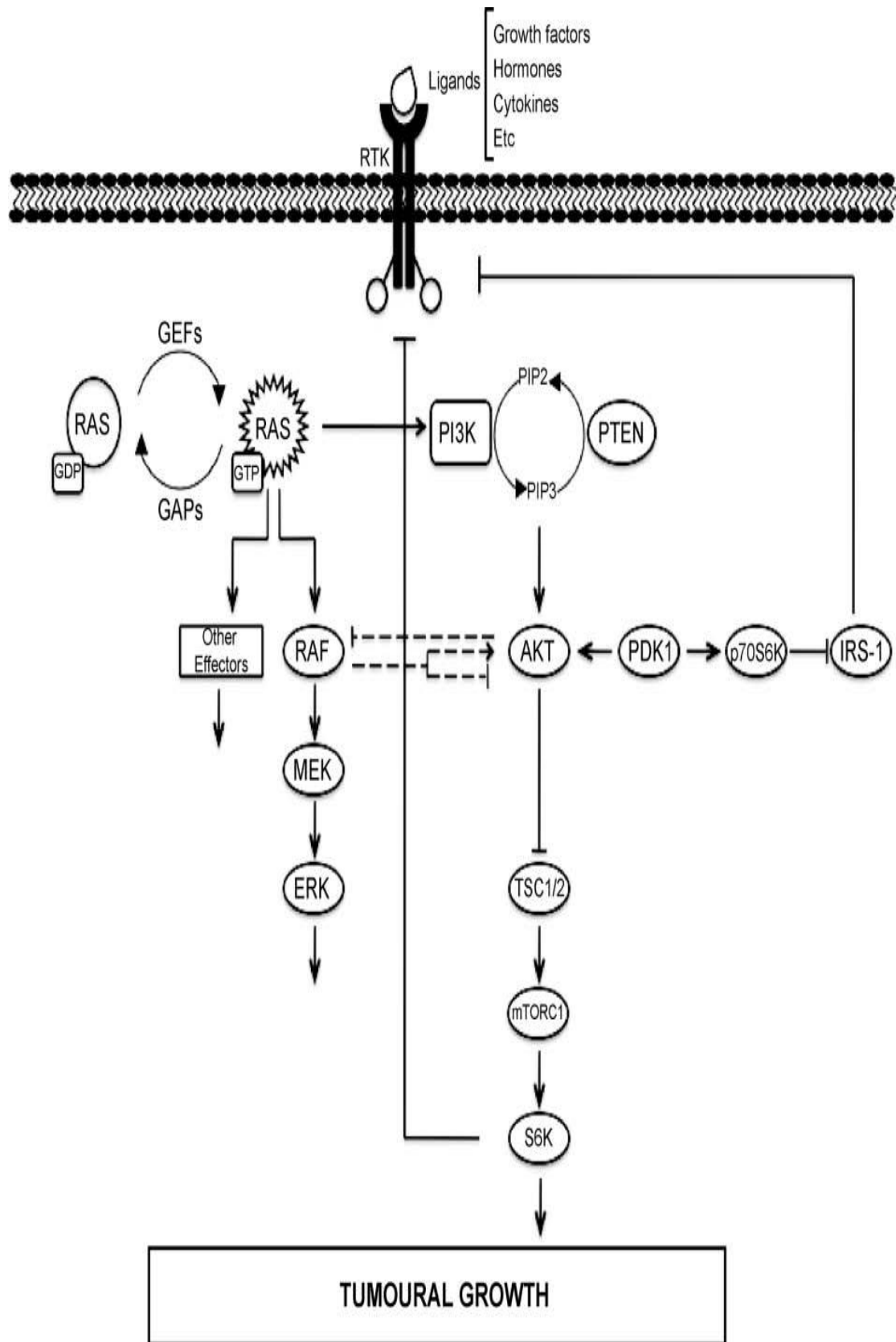


Figure 1.1: MAPK kinase signaling of tumour growth. (Figure modified from Hussam *et al.*, 2010).

## **1.4.2. Growth kinase signalling in gliomas**

### **1.4.2.1. ERK and gliomas.**

Malignant glioma tumours can be induced and maintained by aberrant signalling networks such as the Ras pathway. Although somatic oncogenic mutations of Ras genes are frequent in several cancer types, early investigations on gliomas reveal disappointing facts that the Ras mutations are nearly absent in malignant gliomas and that the BRAF mutations are present in a very small percentage in gliomas. Therefore, the observed deregulation of the Ras-RAF-ERK signalling pathway in gliomas is attributed to its upstream positive regulators, including, EGFR and PDGFR known to be highly active in the majority of malignant gliomas (Lo, 2010).

### **1.4.2.2. Akt and gliomas.**

Signalling through phosphatidylinositol 3-kinase (PtdIns3K)-Akt-mTOR is frequently activated in glioblastoma multiform (GBM), where this kinase network regulates survival. Inhibitors of these pathways induce minimal cell death in glioma. It has been shown that the dual PtdIns3K-mTOR inhibitor PI-103 induces autophagy in therapy-resistant, PTEN-mutant glioma, with blockade of mTOR complex 1 (mTORC1) and complex 2 (mTORC2) contributing independently to autophagy. Inhibition of autophagosome maturation synergizes with PI-103 to induce apoptosis through the Bax-dependent intrinsic mitochondrial pathway, indicating that PI-103 induces autophagy as a survival pathway in this setting (Fan, 2011).

## **1.5. Current treatment for brain malignant tumours**

### **1.5.1. Surgery**

Surgery can include gross total excision of the tumour using image guidance, awake craniotomy, and cortical mapping or may be restricted to biopsy alone, depending on the site of the lesion and the condition of the patient. The goal of surgery is to completely resect the tumour. However the infiltrating nature of gliomas and their ill-defined margins make this goal difficult. Therefore, most surgery attempts to reduce tumour bulk, alleviate raised intracranial pressure, obtain a diagnosis and removes hypoxic tissue resistant to chemotherapy. A study (Chang *et al*, 1983) from the RTOG (Radiation therapy and Oncology group) and eastern Cooperative oncology group showed an 18 month survival of 15% for biopsy alone, 25% for partial resection and 34% for total resection. A retrospective review (Simpson *et al*, 1993) of 3 RTOG trials showed an 11.3 months median survival for gross total excision compared to 6.6 months for biopsy alone. Whatever the nature of surgery, correct surgical planning is vital in minimizing morbidity from the procedure. Besides achieving maximum tumour resection it is also aimed at minimizing the risk of neurological deficits (Krishnam *et al*, 2004).

Many recent advances in surgical techniques have helped to achieve this aim but have not demonstrated any significant difference in survival (Whittle, 2002). These advances include pre-operative functional imaging, fusion of functional and anatomical imaging for per operative neuronavigation, intra operative functional mapping and use of intra operative MRI. Intra-operatively obtained functional information remains of crucial importance especially when operating on tumours that are located in or adjacent to functional cortical sites and subcortical pathways (Keles

*et al*, 2004). The corticospinal motor evoked potential (D-wave) has been used for pre-operative evaluation of the corticospinal tract in patients under general anaesthesia. A decrease of D wave amplitude of less than 30% may indicate postoperative preservation of motor function, including transient motor disturbance with subsequent complete recovery. This technique may allow maximal resection of brain tumours located around the motor cortex (Yamamoto *et al*, 2004). Magnetic source imaging (MSI) is useful in the surgical decision making for lesions adjacent to functionally important brain areas (Ganslandt *et al*, 2004) whilst use of intra-operative MRI has shown to be useful in maximizing the tumour resection (Nimsky *et al*, 2004). Furthermore, the integration of functional magnetic resonance imaging (fMRI) data into neuronavigation are a useful concept to assess the risk of a new motor defect after surgery. A lesion to activation distance of less than 5 mm is associated with a higher risk of neurological deterioration whereas a complete resection can be achieved safely with a lesion to activation distance of more than 10 mm (Krishnam *et al*, 2004). Diffusion tensor (DT) magnetic resonance imaging to track fibres is being used to help image guided tumour resection with decreased morbidity (Berman *et al*, 2004).

### **1.5.2. Radiotherapy**

Standard radiation treatment of glioma includes whole brain irradiation of 60 Gy with conventional external beam radiotherapy following surgery, in fractionated doses. The results of post-operative radiation therapy of malignant gliomas are disappointing, with mean survival time (MST) of 16-70 weeks and 2-year survival rates ranging from 8.5% to 25% in the literature. Only 10% of patients with glioblastoma and 44% of those with grade III gliomas will survive for more than 2 years following their

diagnosis (Burger *et al*, 1985). Interstitial brachytherapy and charged particle irradiation are being used mainly in lower grade glioma. The possibility of combining CT and MR Neuroimaging data together with stereotactic radiotherapy techniques enables the optimal development of the three-dimensional treatment plane (Rubino *et al*, 2004). Due to infiltrative nature of glioma, conventional radiotherapy is not able to deliver curative doses without damaging the normal brain tissue. Radio-immunotherapy is emerging as a novel technique because of the potential for more selectively irradiating tumour cells while sparing normal tissues. Therapeutic potential of monoclonal antibodies (MAB) labelled with the beta-emitters  $^{131}\text{I}$  and  $^{90}\text{Y}$  and the alpha-emitter  $^{211}\text{Y}$  is being investigated in brain tumours (Zalutsky, 2005)

### **1.5.3. Chemotherapy**

Surgery followed by standard radiotherapy with concomitant and adjuvant chemotherapy with temozolomide is the standard of care in patients with glioblastoma, however the prognosis remains poor with a median survival in the range of 12-15 months (Stupp *et al.*, 2005). Common genetic abnormalities in glioblastoma are associated with aberrant activation or suppression of cellular signal transduction pathways and resistance to radiation and chemotherapy. Special attention has been focused on targets such as epidermal growth factor receptor, vascular endothelial growth factor receptor, platelet-derived growth factor receptor, and on pathways such as the phosphatidylinositol-3kinase/Akt/mammalian target of rapamycin and Ras/Raf/mitogen-activated protein-kinase pathways.

Despite extensive efforts at defining biological markers as a basis for selecting therapies, most treatment decisions for glioblastoma patients are still based on age and

performance status (Weller and Stupp 2012). Currently, surgery followed by standard RT with concomitant and adjuvant chemotherapy with temozolomide is the standard of care in patients with GBM aged <70 years. However, the prognosis remains poor, with a median survival of 12-15 months (Stupp *et al.*, 2005). Clinical experience has revealed that gliomas sharing similar histomorphological criteria might indeed have different clinical courses and exhibit highly heterogenous responses to treatments (Tabatabai and Stupp, 2012). Overexpression, activation, and dysregulation of various membrane receptors, signalling pathways, and other factors may occur frequently in GBM (Kapoor *et al.*, 2003; Kitange *et al.*, 2003; Louis, 2006).

Mammalian target of rapamycin (mTOR) have been examined in preclinical and clinical trials for malignant glioma. The efficacy of these agents as monotherapies has been modest, at best; however, new multitargeted kinase inhibitors and combinations of single-targeted kinase inhibitors in combination with radiation and cytotoxic chemotherapy will likely play an increasing role in the management of GBM and several randomized.

#### **1.5.3.1. Current Standard Therapy for GBM**

Temozolomide given concomitantly and adjuvantly with RT after surgical resection represents the standard of care in patients with GBM. The epigenetic silencing of *MGMT* by promoter methylation is correlated with improved survival in patients treated with temozolomide. Although the prolonged exposure of cancer cells to temozolomide may represent a promising strategy to overcome resistance mediated by *MGMT*, at present, the clinical relevance of the use of a dose-dense temozolomide schedule remains to be proven (Groot *et al.*, 2007).

### **1.5.3.2. Targeted Therapies**

GBM is characterized by several aberrantly activated signalling pathways. Several growth factor receptors, such as epidermal growth factor receptor (EGFR), vascular endothelial growth factor receptor (VEGFR) and platelet-derived growth factor receptor (PDGFR), are overexpressed, amplified and/or mutated, leading to uncontrolled cell proliferation, angiogenesis, migration, survival and differentiation (Sanson *et al.*, 2004; Groot *et al.*, 2007) (Figure 1.2). The major challenge in the use of targeted therapies is the identification of the optimal therapeutic targets, and to select new agents which can translate to survival benefit for patients with GBM. Currently, the use of small molecule tyrosine kinases inhibitors (TKIs) and monoclonal antibodies against EGFR and VEGFR have been evaluated in phase II clinical trials as main anti-growth factor receptor strategies. Other potentially useful agents for the treatment of GBM are represented by the PDGFR-, mammalian target of rapamycin (mTOR) and integrin inhibitors.

### **1.5.3.3. EGFR Inhibitors**

Phosphorylation of the tyrosine kinase domain activates several signalling pathways, such as the phosphatidylinositol 3'-kinase (PI3K)/Akt/mTOR, and Ras/mitogen-activated protein kinase (MAPK) (Normanno *et al.*, 2006; Burgees *et al.*, 2008). Activation of EGFR pathways results in several biological processes, including cell proliferation, angiogenesis, migration, survival and differentiation.

#### **1.5.3.4. Mammalian Target of Rapamycin Inhibitors**

Overactivation of the PI3K/Akt/mTOR pathway seems to play an important role in gliomagenesis (Guertin *et al.*, 2007). Combined activation of Ras and Akt leads to the formation of GBM in mice (Hu *et al.*, 2007). In human GBM, Akt is activated in approximately 70% of these tumours, in association with loss of PTEN and/or activation of EGFR and PDGFR tyrosine kinases. Alterations of PTEN expression are present in 20-40% of GBM (Wang *et al.*, 1997; Zhou *et al.*, 1999), and have been associated with a worse prognosis, although conflicting results have been reported (Zhou *et al.*, 1999; Sano *et al.*, 1999; Ermoian *et al.*, 2002). There is emerging evidence suggesting that mTOR is a critical downstream component in PTEN/Akt signaling (Schmelzle *et al.*, 2000; Castedo *et al.*, 2002; Podsypanina *et al.*, 2001; Choe *et al.*, 2003), and pharmacological inactivation of mTOR reduces neoplastic proliferation and tumour size in PTEN-deficient mice (Rajasekhar *et al.*, 2003). These evidense has provided the rationale for clinical studies of mTOR inhibitors in GBM.

Although data strongly support the view of the PTEN/PI3K/AKT pathway as an important target for drugs, current clinical results on the use of mTOR inhibitors remain disappointing. A new generation of trials is seeking to define whether the combination of two or more targeted drugs together with RT and cytotoxic chemotherapy can overcome tumour resistance.

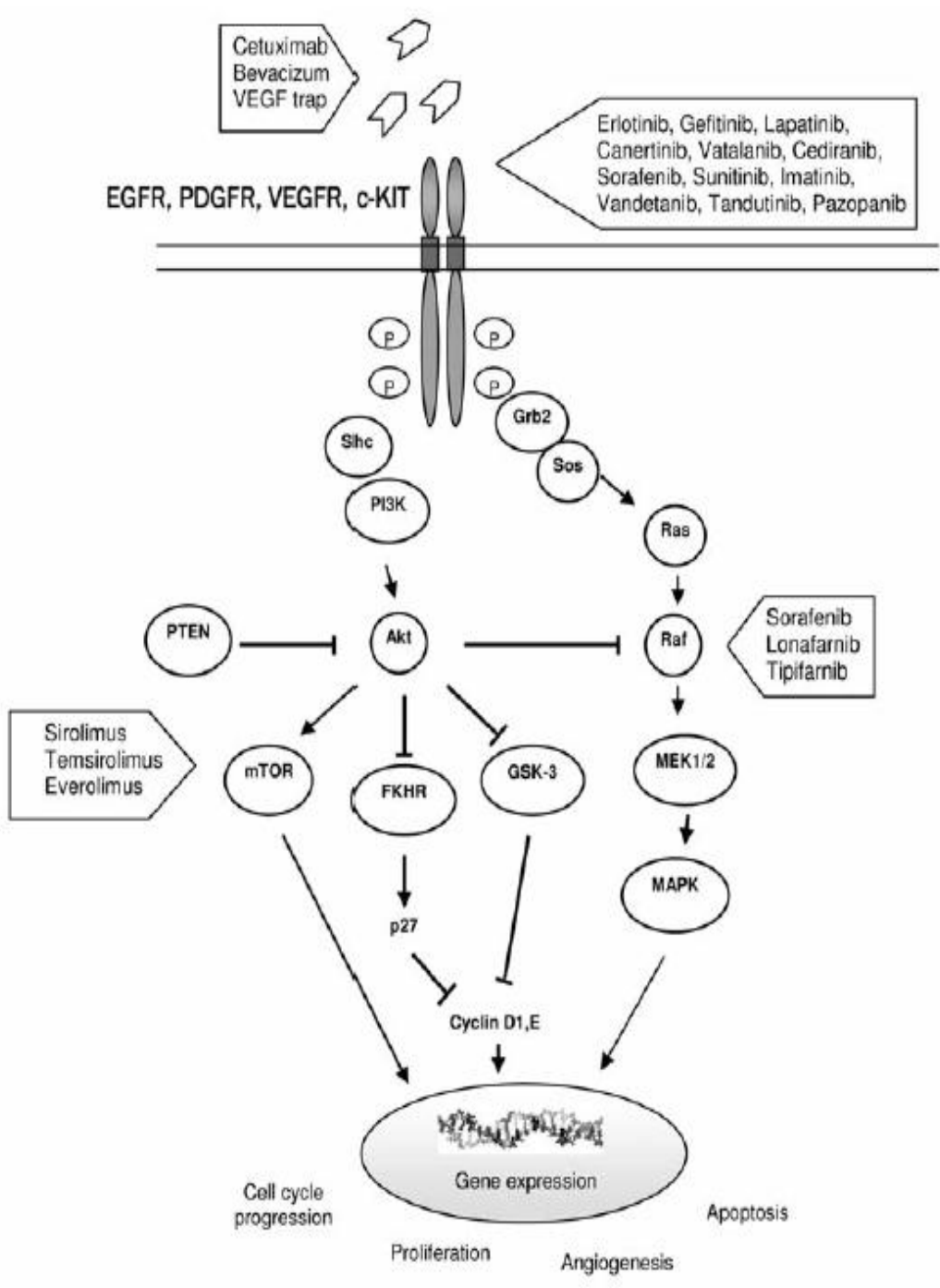


Figure 1.2: Schematic representation of main oncogenetic signaling pathways and site of action of molecular targeted therapies. (Taken from Minniti *et al.*, 2009).

## **1.6. Therapeutic approaches related to re-differentiation of cancer cells**

### **1.6.1. Cancer as maladaptive response to stress: a shift to a paradigm**

One of the main characteristics of pathological tissue is the re-expression of fetal characteristics. The physiologic significance of this rewind to foetal life remains largely unknown. However, this appears to be an evolutionary conserved mechanism related to stress response. Thus, return to foetal phenotype and cell dedifferentiation may be a prerequisite permissive state for regeneration after stress. De-differentiated cells have the ability to proliferate and/or grow and then to re-differentiate to specialized cells that comprise the regenerated structure or organ (Gurtner *et al.*, 2008). This mechanism appeared early in evolution and allowed living organisms to adapt to environmental stresses. In fact, salamanders have the ability to replace whole body parts or anurans can recover body parts at the embryonic stages through induction of cell dedifferentiation/re-differentiation processes (Pellettieri *et al.*, 2007). Mammals retain the ability to regenerate but in a more restrictive form. For instance, neonatal mouse heart displays a regenerative potential early after birth in which differentiation is not complete (Schafer *et al.*, 2008). This regenerative potential may be regained in adult life after stress-induced dedifferentiation and return to fetal phenotype. However, the ability of the cells to re-differentiate may be diminished upon intense and sustained stressful stimuli. This re-differentiation “deficit” may result in heart failure, cancer, and so forth (Tsonis *et al.*, 2000), while interventions which potentially could enhance endogenous re-differentiation may restore tissue integrity and function (Figure 1.3).

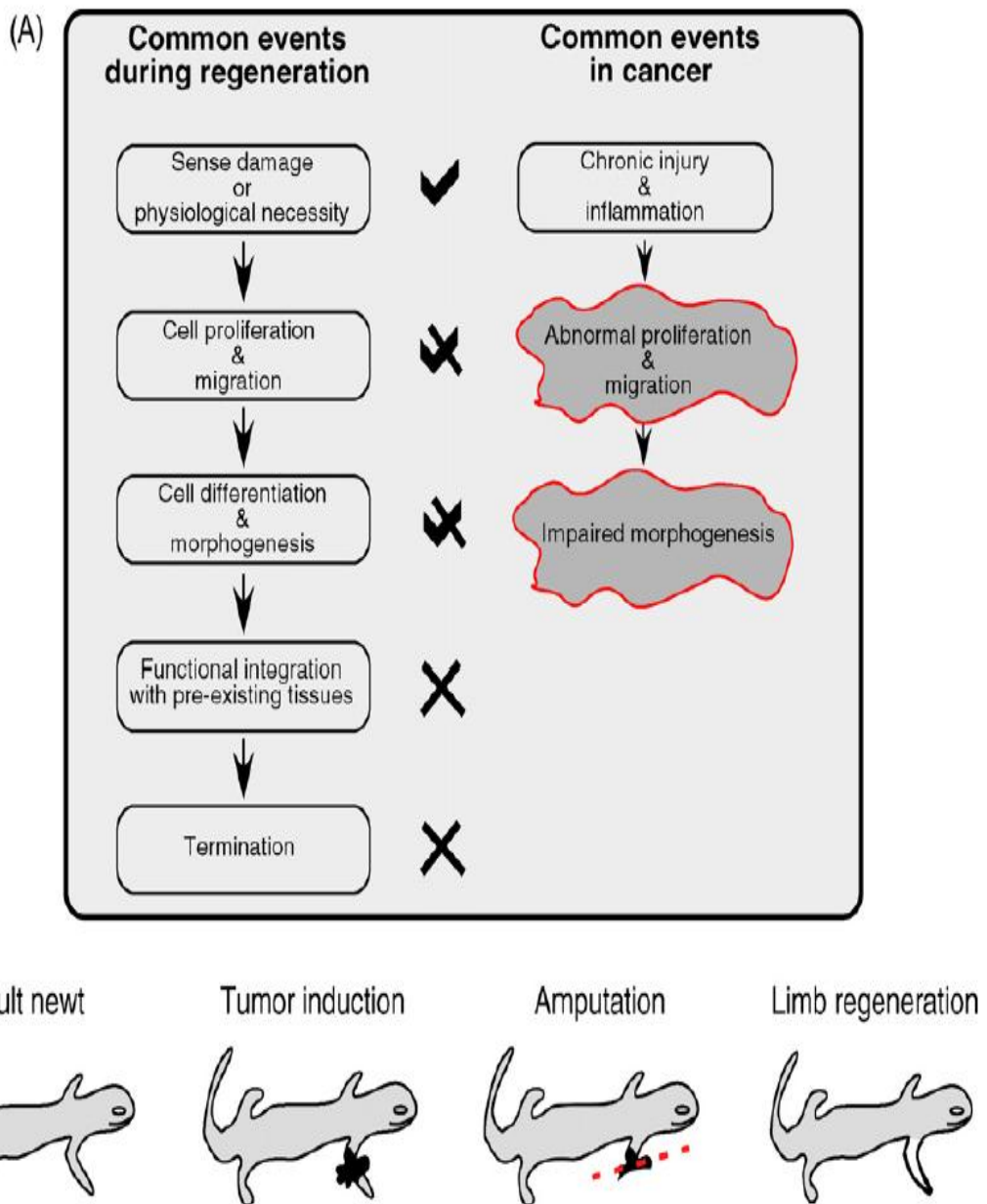
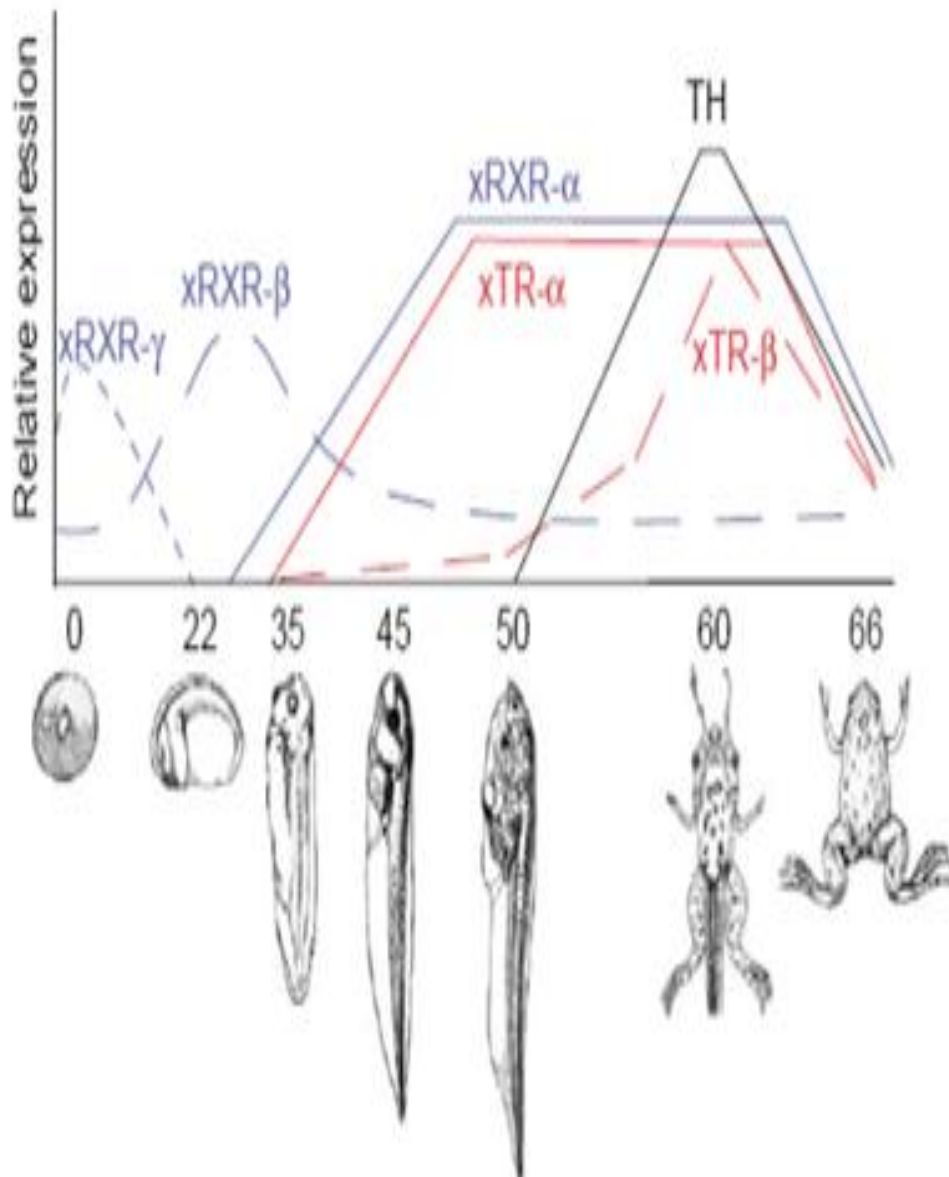


Figure 1.3: Links between regeneration and cancer. (A) Regenerative events and their corollaries in cancer. Importantly, the process of regeneration can be repeated without causing malignant transformation, while in cancer the regenerative process is incomplete such that chronic injury and inflammation leads to continuous proliferation. This suggests that characterizing signals at later stages of regeneration (especially those involved in termination) may help identify candidates able to stop abnormal proliferative responses to chronic injury. (B) Regeneration can correct malignant transformation, as in newt limbs where amputation through the site of induced tumours results in the regeneration of a normal limb without tumours. (Taken from Nestor *et al.*, 2009).

### **1.6.2. Thyroid hormone as novel cancer treatment**

Studies on the amphibian metamorphosis, which is one of the nature's paradigms of tissue and organ remodelling have revealed an evolutionary conserved mechanism of organ formation and repair entirely dependent on thyroid hormone (Sato *et al.*, 2007). Gudernatsch, almost 100 years ago, made the remarkable discovery that equine thyroid extracts could accelerate the metamorphosis of tadpole into juvenile frogs (Figure 1.4) (Gudernatsch, 1912). Since then, several studies, if not all, have shown that the morphological and functional changes of metamorphosis are the result of alterations in the transcription of specific sets of genes induced by TH (Berry *et al.*, 1998; Furlow *et al.*, 2004; Furlow and Neff, 2006; Shi *et al.*, 2001).



**Pre-metamorphosis period    metamorphosis period**

Figure 1.4: Amphibian metamorphosis is a nature’s paradigm of physiologic tissue remodeling in which a fine balance between cell proliferation, apoptosis and cell differentiation exists. This gene programming is dependent on TH hormone. The same molecule depending on the expression of TR receptors can have different biologic effects. Thus, un-liganded TR  $\alpha$ 1 receptor is associated with proliferating cells which are in undifferentiated state (pre-metamorphosis). Liganded TR  $\alpha$ 1 is associated with inhibition of proliferation and cell differentiation (metamorphosis period). (Slack *et al.*, 2007). These developmental mechanisms are evolutionary conserved in mammals and re-emerge in disease states. (Taken from Mourouzis *et al.*, 2011).

## 1.7. Thyroid hormone: metabolism and transport

The major biologically active TH is 3, 3', 5-triiodothyronine ( $T_3$ ), which is generated from thyroxine  $T_4$  by the deiodinating enzymes D1 and D2 (Bianco and Kim, 2006; Heuer, *et al.*, 2007; Visser *et al.*, 2007). The deiodinase D3 inactivates  $T_4$  to 3, 3', 5'-triiodothyronine ( $rT_3$ ) and  $T_3$  to 3, 3'-diiodothyronine ( $T_2$ ) (Figure 1.5) (Visser *et al.*, 2007). Enzymatic activity of D3 is especially high during fetal and neonatal development, suggesting that it might act as a scavenger to prevent a premature thyroid-hormone-induced differentiation of neural cells (Heuer, *et al.*, 2007).

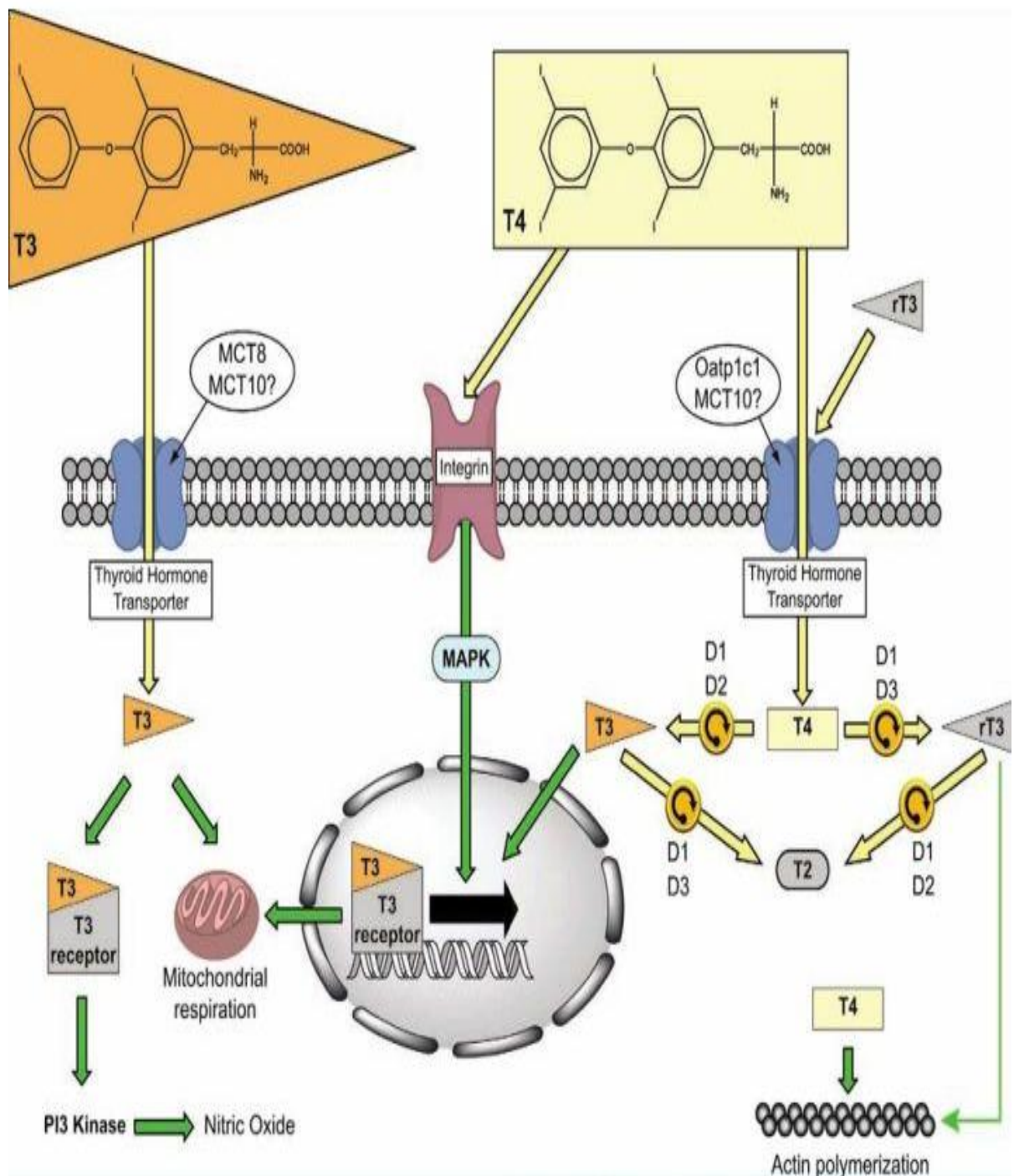


Figure 1.5: Diagram showing the mechanism of cellular action of Thyroid hormone. (Taken from American Society for Clinical Pathology, 2011).

Deiodinases are membrane – associated enzymes, the catalytic center of which is located intracellularly. Consequently, thyroid hormone has to enter the cells to be metabolized and to interact with its receptors (Heuer, *et al.*, 2007). TH metabolism and action require transport of the hormone from extracellular compartments (e.g. the bloodstream) across the plasma membrane. Based on their lipophilic nature, it was assumed previously that translocation of iodothyronines across the lipid bilayer of cell membranes occurred by diffusion. However, experimental evidence over the last three decades and clinical studies in recent years show clearly that TH traverses the cell membrane mainly through transporters (Hennemann *et al.*, 2001; Abe *et al.*, 2002; Jansen *et al.*, 2005; Friesema *et al.*, 2006; Heuer *et al.*, 2007; Visser *et al.*, 2007).

Several studies have demonstrated that TH uptake has different characteristics in different cell types, with regard to ligand specificity, energy (ATP) dependence, Na<sup>+</sup> dependence and interactions with a variety compounds (Hennemann *et al.*, 2001; Visser *et al.*, 2007). This suggested that TH uptake might be facilitated by different types of transporters and that was lately confirmed by the molecular identification of TH transporting proteins (Jansen *et al.*, 2005). These transporting proteins include the Na<sup>+</sup>taurocholate cotransporting polypeptide (Friesema *et al.*, 1999), fatty acid translocase (van der Putten *et al.*, 2003), multidrug resistance-associated proteins (Mitchell *et al.*, 2005), amino acid transporters (Taylor and Ritchie, 2007) and members of the organic anion transporting polypeptide (OATP) family (Hagenbuch, 2007) and monocarboxylate transporter (MCT) family (Visser *et al.*, 2007).

## **1.7.1. Thyroid hormone: cellular action**

### **1.7.1.1. Genomic action- thyroid hormone receptors**

In 1986, the Molecular cloning of cDNA for thyroid hormone receptors (TRs) led to the identification of two TR genes,  $\alpha$  and  $\beta$  located on human chromosomes 17 and 3, respectively (Weinberger *et al.*, 1986; Sap *et al.*, 1986). Since the first detection of thyroid receptors, five major TR isoforms, derived from alternative splicing of the primary transcripts of two TR genes have been identified (Cheng, 2003). The thyroid receptors belong to a large family of nuclear receptors including steroid hormone, retinoic acid, vitamin D and orphan receptors. TR $\alpha$ 1,  $\beta$ 1,  $\beta$ 2 and  $\beta$ 3 differ in the length and amino acid sequence at the terminal A/B domain, but bind thyroid hormone (T3) with high affinity to mediate gene regulatory activity (Cheng, 2003). On the other hand the fourth isoform, TR $\alpha$ 2, which differs from other isoforms in the C-terminus, does not bind T3 and the precise function has not been clarified. These receptors like the other nuclear receptors have an amino-terminal A/B domain, a central binding domain, and a carboxyl - terminal ligand binding domain while the amino- and carboxyl- terminal domains contain activations functions I and II respectively that are important for transcriptional activation (Cheng 2000; Yen, 2001; Harvey and Williams, 2002). The expressions of TR isoforms is tissue – dependent and is developmentally regulated (Cheng, 2000; Yen, 2001).

The transcriptional activity of TR depends not only on T3, but also on the type of thyroid hormone response elements (TREs) on the promoters of T3-target genes. The C-terminal region of the ligand binding domain contains multiple contact surfaces that are important for dimerization with its partners, the retinoid X receptor, and for interactions with co-receptors and co-activators (Cheng, 2000; Yen, 2001; McKenna

and O'Malley, 2002; Harvey and Williams, 2002). In the absence of T3, TRs via their interacting surfaces associate with co-repressors to act as silencers of transcription (Cheng, 2000; Yen, 2001; McKenna and O'Malley, 2002; Harvey and Williams, 2002).

### **1.7.1.2. Non genomic action of Thyroid hormone**

T4 can exert several of its non genomic actions without interaction of the hormone with the nuclear thyroid hormone receptor, TR $\beta$ 1, instead it is initiated its effect on the plasma membrane receptor via integrin  $\alpha\beta$ 3 (Davis *et al.*, 2006). The interaction of T4 with G-protein-coupled membrane receptor leads to a rapid serine phosphorylation of nuclear TRs. Davis *et al.*, (2000) proposed a model for cell surface mediated non-genomic actions of TH which involves mitogen activated protein kinases (MAPKs) and PI3-kinase signalling cascades. T4 binds on cell surface within a time period of 10-30 min, activates Ras, Raf1, MEK and PKC, resulting in tyrosine phosphorylation, activation and translocation of MAPKs, which in turn phosphorylate a serine residue in the second zinc finger of TR. The nuclear MAPKs/TR complex may also bind and phosphorylate p53 and regulate its transcriptional activity (Shih, *et al.*, 2001). In a parallel pathway, T4 –activated MEK phosphorylates tyrosine residues in STAT1 and STAT3 (signal transducers and activators of transcription) resulting in their nuclear translocation, further serine phosphorylation by MAPK and activation of gene transcription. Thus, non genomic actions of TH may influence gene transcription by at least three distinct pathways STATs, p53 and TRs.

T3 also exerts non genomic action via its cytosolic TR  $\alpha$ 1 receptor. This newly discovered non genomic mechanism is of physiologic relevance in acute response to stress and mediates TH reparative effect (Pantos *et al.*, 2011) (Figure 1.6).

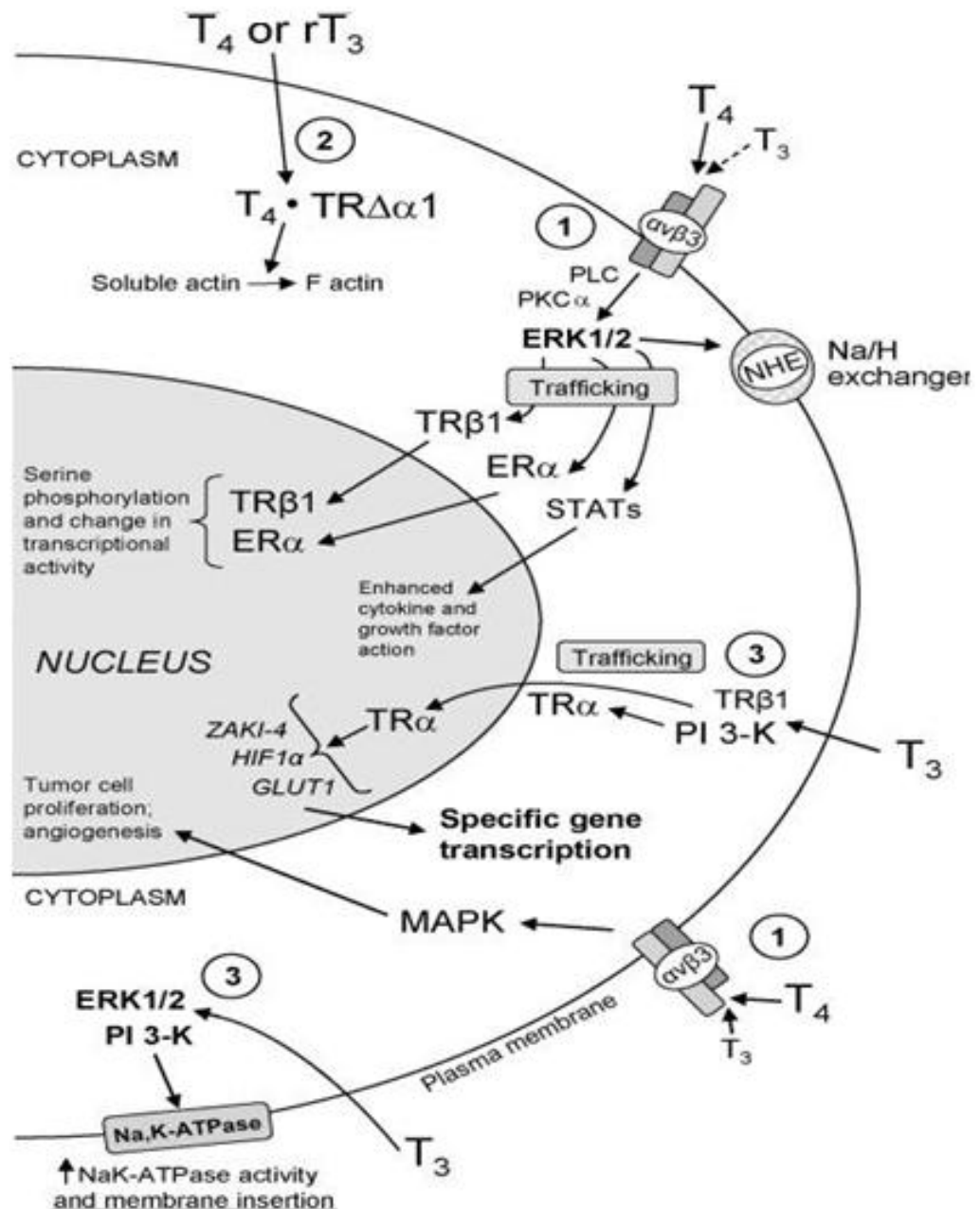


Figure 1.6: Schematic diagram showing the genomic and non genomic actions of TH (T<sub>4</sub>, T<sub>3</sub>). (Taken from Cheng *et al.*, 2010).

### **1.7.2. Novel thyroid hormone signaling**

Recent research has identified that TH regulate novel thyroid hormone signalling which may be relevant for tissue repair after injury. Thus, studies in cardiac cell based models and animal models of ischemic injury have shown that TH can up regulate important molecules involved in tissue differentiation which are of relevance in tissue repair (Figure 1.7).

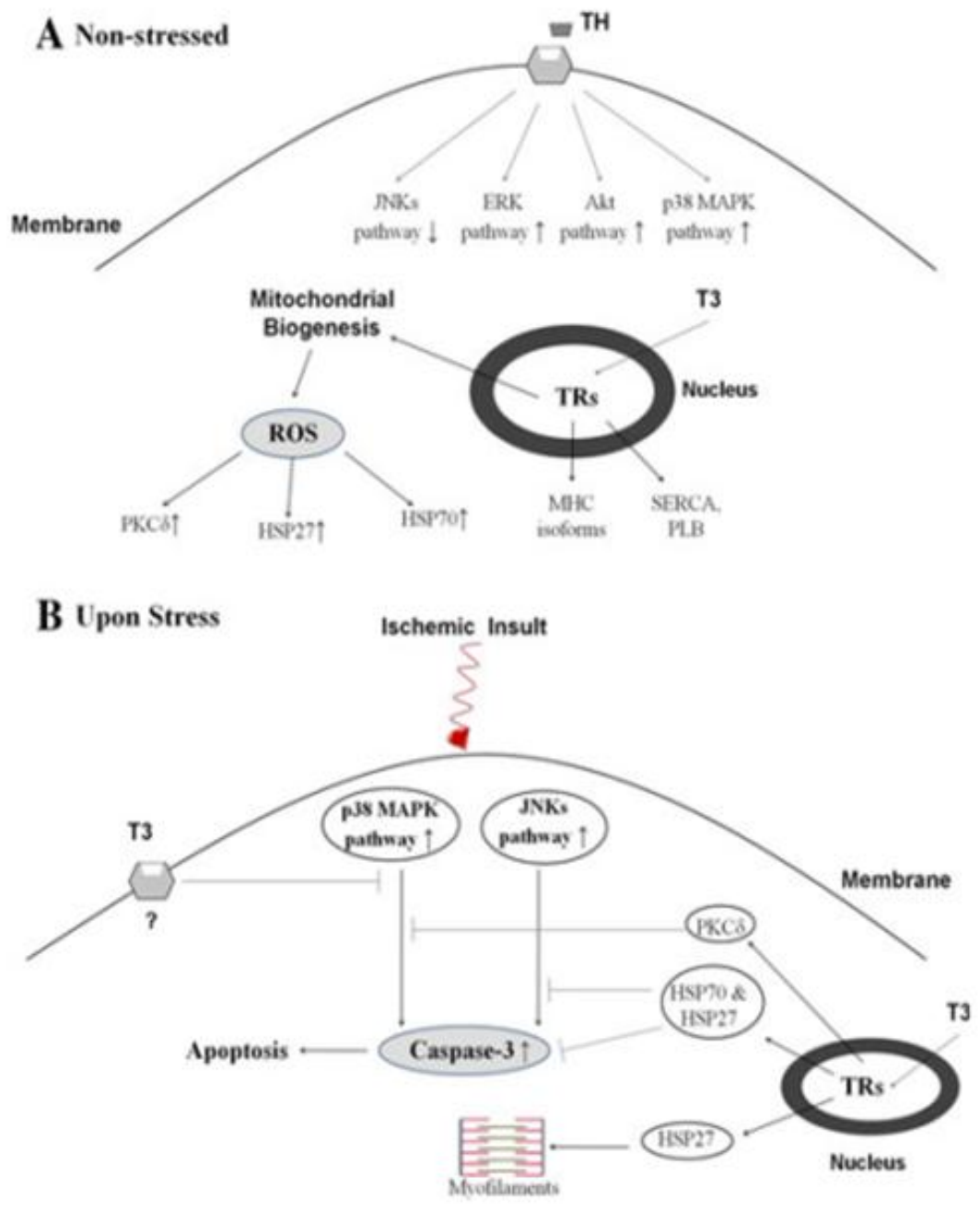


Figure 1.7: Schematic diagram showing how TH can alter cellular response to (A) non-stress and (B) stress by regulating novel intracellular signaling. (Taken from Pantos *et al.*, 2010).

### 1.7.3 Thyroid hormone and tissue differentiation

The role of TH as developmental signal has been demonstrated in several studies with *Xenopus laevis* to be an ideal system for ascertaining the developmental roles of TH and its receptors (Slack *et al.*, 2008). Interestingly, this system reveals that regulation of TH/TR axis can allow the same simple molecule TH to induce completely opposite morphological responses in distinct tissues. In this context (Figure 1.8), TR $\alpha$  seems to play an important physiological role due to its dual function (liganded vs unliganded state). Thus, at early developmental stages in which TH is low, TR $\alpha$  receptor is highly expressed and at its unliganded state acts as a repressor of TH positive regulated genes and prevents precocious metamorphosis (Sato *et al.*, 2007). At later stages, the rise in TH levels results in the conversion of the unliganded to the liganded TR $\alpha$  state and triggers cell differentiation and completes metamorphosis (Furlow and Neff, 2006). Similarly, in mammals, during fetal life, TR $\alpha$ 1 is increased while TH levels remain low and decrease after birth with the rising of the circulating TH (White *et al.*, 2001).

Based on this evidence, subsequent studies using mammal cell based-models have shown that this developmental programme has been conserved in mammals. Thus, in the embryonic heart derived cell line (H9c2), which has been used to model aspects of cardiac differentiation in vitro, TH was shown to be critical in this process (van der Heide *et al.*, 2007; van der Putten *et al.*, 2002). In fact, intracellular T4 and T3 increase during the progression of cell differentiation with a concomitant increase in the expression of TR $\alpha$ 1 and this response could be prevented by pharmacological inhibition of thyroid hormone binding to TR $\alpha$ 1 (Meischl *et al.*, 2008; Pantos *et al.*, 2008c; van der Heide *et al.*, 2007; van der Putten *et al.*, 2002). The potential role of

TR $\alpha$ 1 in cell differentiation/de-differentiation process has been further documented in transfection studies using neonatal cardiomyocytes (Figure 1.8). Thus, neonatal cardiac cells overexpressing TR $\alpha$ 1 and treated with TH were able to differentiate into adult cardiac cells (Kinugawa *et al.*, 2005). On the contrary, untreated cardiomyocytes remained undifferentiated and this response was characterized by cell growth with a foetal pattern of myosin heavy chain (MHC) isoform expression (Kinugawa *et al.*, 2005). This novel action was shown to be a unique feature of TR $\alpha$ 1 receptor. Along this line, TH was shown to stop proliferation and promote differentiation in fetal bovine cardiomyocytes (Figure 1.8 and 1.9). Interestingly, this unique effect was shown to be achieved in nearly normal T3 concentrations and is mediated via T3 action on cyclin D1 and p21 (Figure 1.10) (Chattergoon *et al.*, 2011).

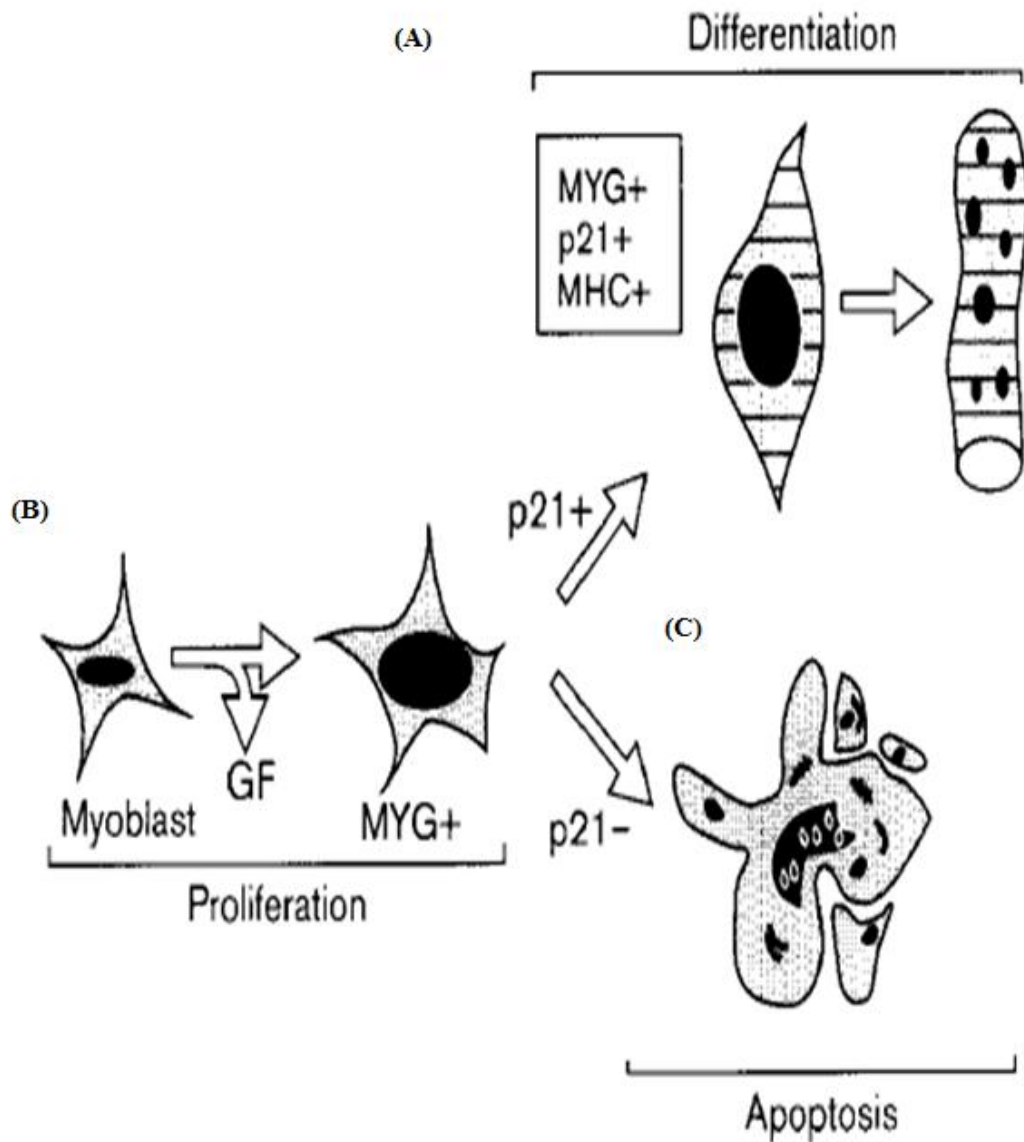


Figure 1.8: Cellular model of cardiac embryonic cell differentiation. (A) During fetal development, (B) cell proliferation and (C) apoptosis prevails. Apoptosis is a physiologic brake of growth. This process is inhibited during the transition to cell differentiation. Interestingly, in adult life, re-emergence of the fetal state occurs in disease. (Taken from Walsh *et al.*, 1997).

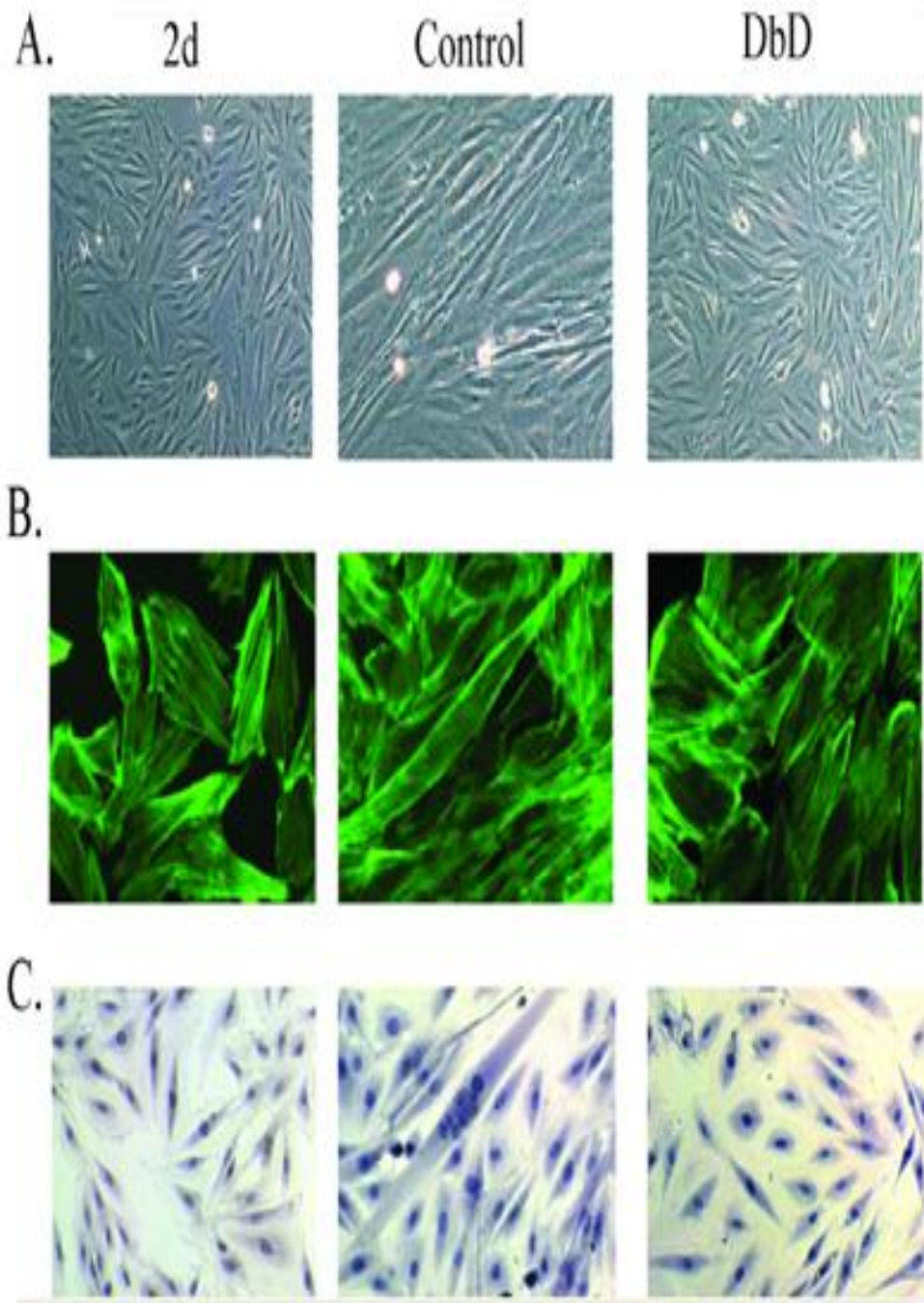


Figure 1.9: Cardiac myoblast differentiation is dependent on TH. Blockade of TR $\alpha$ 1 receptor by TR $\alpha$ 1 inhibitor (DbD) delays this process. (Taken from Pantos *et al*, 2008).

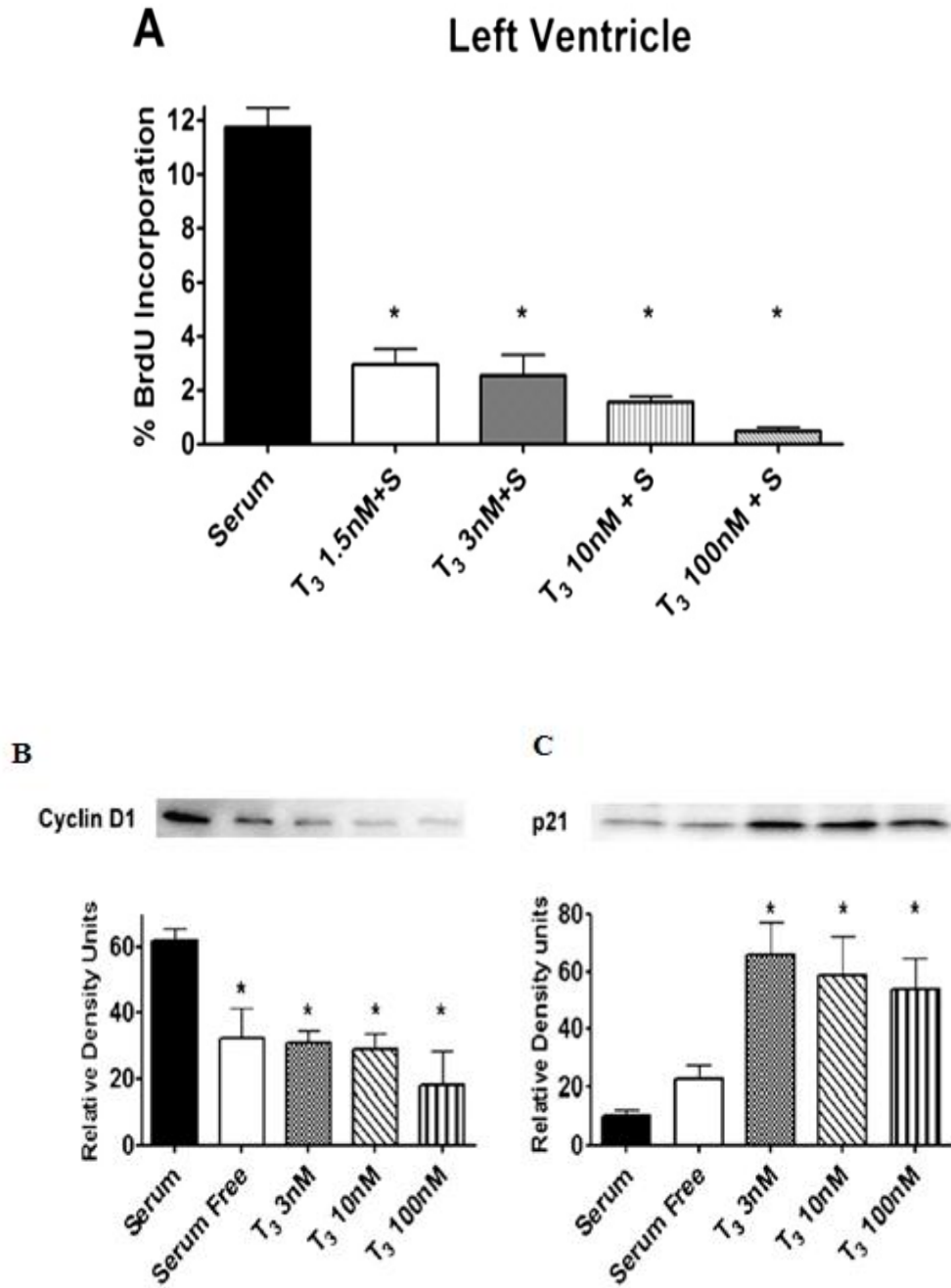


Figure 1.10: TH stops proliferation in (A) fetal bovine left ventricle cardiomyocytes. This effect is mediated via T<sub>3</sub> action on (B) cyclin D1 and (C) p21. (Taken from Chattergoon *et al.*, 2011).

#### **1.7.4. Thyroid hormone (TH) and brain development**

Thyroid hormone is essential for the proper development of numerous tissues, notably the brain. As an important target tissue of thyroid hormone action, the mammalian CNS is highly dependent on proper thyroid hormone supply. In rodents, it was found that deprivation of thyroid hormone during critical periods of brain development affects processes such as neuronal migration, outgrowth and differentiation, synaptogenesis, myelination and glial cell proliferation (Oppenheimer and Schwartz, 1997; Anderson *et al.*, 2003). Normal timing of oligodendrocyte development depends on thyroid hormone receptor alpha 1 (TR $\alpha$ 1) (Billon *et al.*, 2002) (Figure 1.11).

If thyroid hormone is to act in the brain, several transport processes have to take place. Firstly the hormone has to enter the brain and that occurs either via blood-brain barrier or the choroid plexus-cerebrospinal fluid (CSF) barrier (Heuer, *et al.*, 2007). The entry of T4 and T3 via the blood-brain barrier appears to be the preferred route for the distribution of thyroid hormone in the brain, whereas the uptake via choroid plexus –CSF barrier is thought to be necessary to provide circumventricular areas with sufficient amounts of thyroid hormone (Dratman, *et al.*, 1991). After passing one of these barriers, T4 has to be taken up by astrocytes for further activation and finally T3 has to enter neuronal cells, which not only express TRs but also participate in the inactivation of T4 and T3 by expressing D3 (Heuer, 2003).

In the brain, de-iodinase D2, an enzyme expressed in astrocytes, tancytes and in some sensory neurons, is responsible for converting T4 to T3 (Guadano-Ferraz, *et al.*, 1997; Guadano-Ferraz, *et al.*, 1999; Heuer, *et al.*, 2007). Inactivation of T4 and T3

can also take place within the brain is catalysed by the neuronally localized deiodinase D3 (Tu, *et al.*, 1999; Heuer, *et al.*, 2007)

Most remarkably, the activity of both D2 and D3 in the brain is profoundly affected by the thyroidal state of this tissue. In the presence of low levels of thyroid hormone, D2 activities are strongly upregulated and D3 activities are markedly decreased (Burmeister *et al.*, 1997; Friedrichsen, *et al.*, 2003). These alterations in local thyroid hormone metabolism have been suggested to represent a compensatory mechanism not only to cope with fluctuations in the circulating thyroid hormone levels but also to protect the brain from the detrimental effects of hypothyroidism as well as hyperthyroidism (Calvo *et al.*, 1990; Guadano-Ferraz *et al.*, 1999; Heuer *et al.*, 2007).

The local conversion of T4 to T3 by D2 in astrocytes was estimated to produce as much as 80% of the T3 bound to the nuclear receptors in the adult rat brain, indicating that astrocytes are critically involved in regulating the amount of T3 available for neuronal uptake (Heuer, 2003).

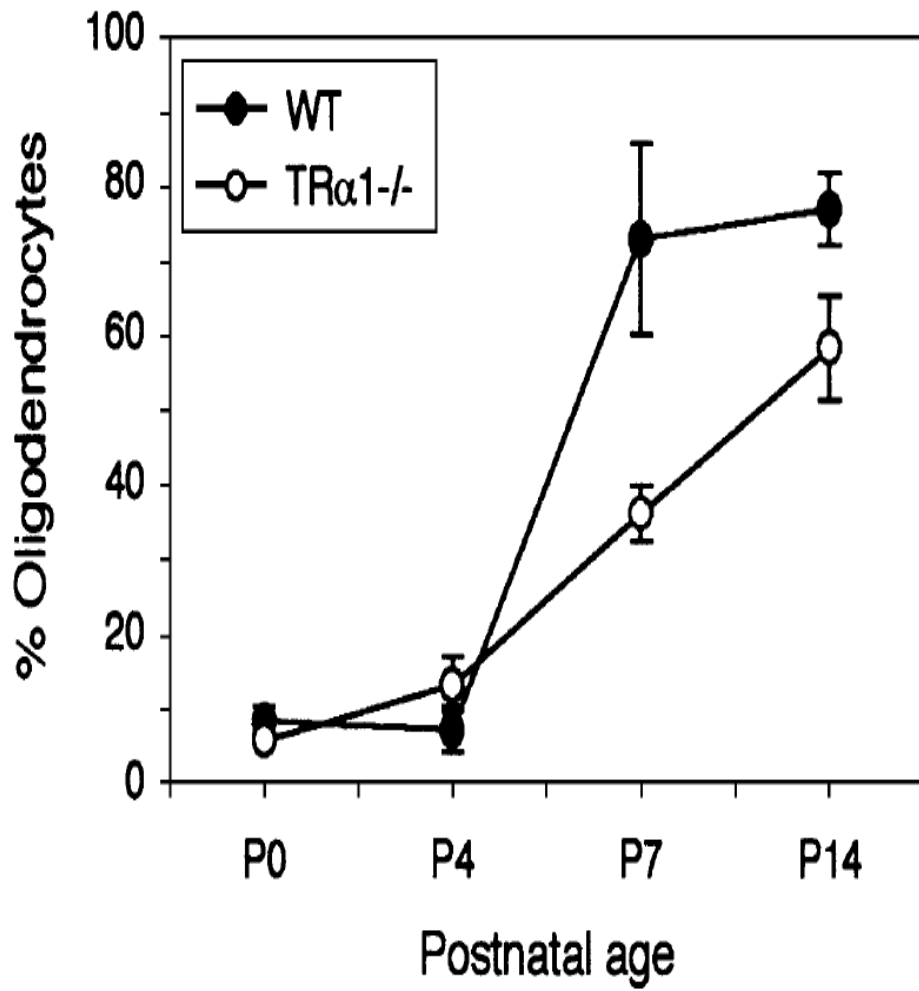


Figure 1.11: Oligodendrocyte development in the optic nerve is impaired in TR $\alpha$ 1<sup>-/-</sup> mice, but this only occurs at postnatal age of days 7 to 14. (Taken from Billon *et al.*, 2002).

### **1.7.5. Changes of thyroid hormone signalling in disease: a response of physiologic relevance**

It has long been recognized that circulating thyroid hormone in plasma are altered in acute and chronic illnesses (Pantos *et al.*, 2010). The physiological relevance of this response, known as euthyroid sick syndrome remains largely unknown. However, accumulating clinical evidence shows that low T3 levels in plasma are correlated with poor outcome of the disease (Koenig *et al.*, 2008).

### **1.7.6. Changes in thyroid hormone signalling in heart diseases**

The importance of TH in the cause and progression of the disease has mostly been studied in heart diseases. Thus, circulating T3 levels have been associated with the severity of cardiac dysfunction in heart failure patients and the recovery of cardiac function after myocardial infarction. Moreover, low T3 levels appear to increase mortality (Pantos *et al.*, 2010). Accordingly, in animal models of pathological growth and heart failure caused by ischemia, a distinct pattern of TR $\alpha$ 1 expression occurs. In fact, a re-expression of TR $\alpha$ 1 was shown to occur during the development of pathological growth. Interestingly, TH treatment converted the pathological growth to physiological growth and prevented heart failure (Pantos *et al.*, 2010).

### 1.7.7. Changes in thyroid hormone signalling in cancer

The interest for potential role of thyroid hormone signalling in cancer came from the recognition that TR $\alpha$ 1 is the cellular counterpart of the retroviral v-erbA which is involved in the neoplastic transformation leading to acute erythroleukemia and sarcomas (Sap, *et al.*, 1986; Thormeyer and Baniahmad, 1999). V-erbA itself has a weak oncogenic activity but augments the transformation activity of other oncoprotein (Cheng, 2003). V-erbA competes with TR for binding to TREs and interferes with the normal transcriptional activity of liganded-TR on several promoters (Yen *et al.*, 1994; Chen and Privalsky, 1993). Bearing that in mind, the v-erbA oncoprotein is thought to repress constitutively, through its dominant negative activity, a certain set of genes that prevent cellular transformation (Cheng, 2003).

Along this line, cyclin D1 and p53 were shown to physically interact with TR $\beta$ 1 (Cheng, 2003). p53 was shown to interact with TR $\beta$ 1 *in vitro* and in cultured cells, resulting in the repression of the transcriptional activity of TR $\beta$ 1 (Bhat, *et al.*, 1997). Cyclin D1 associates with C-terminal region of the ligand-binding domain of TR $\beta$ 1 *in vitro* and *in vivo* and acts to repress the transcriptional activity of TR $\beta$ 1,  $\alpha$ 1 and  $\beta$ 2 (Lin *et al.*, 2002).

Aberrant expression of TR has been found in breast cancer (Li *et al.*, 2002; Silva, *et al.*, 2002; Ferreira, 2006). Furthermore, in a study by Li *et al.* (2002), a variable degree of hypermethylation was observed in 11 cases of breast cancer. In addition, silencing of the TR $\beta$  gene by hypermethylation and concurrent reduction of TR $\beta$ 1 transcripts were demonstrated in several breast cancer cell lines (Cheng, 2003). Silva *et al.*, (2002) demonstrated alterations in mRNA and protein levels of TRs in 70 sporadic breast cancers. Truncated mRNA was found in six patients and in three

transcripts was found the same breaking point. Although there was no significant correlation between the TR $\beta$ 1 alterations and clinical features, there was a tendency toward association of mutations and onset of cancer in early age (Silva *et al.*, 2002; Cheng, 2003). Concluding from all these findings, it could be suggested that the TR $\beta$  gene may function as tumour suppressor in a subset of breast cancers (Cheng *et al.*, 2003).

In liver cancer, Lin *et al.*, (1999) showed that truncated TR $\alpha$ 1 and TR $\beta$ 1 cDNA was present in 53% of human haepatocellular carcinomas. Furthermore, somatic point mutations of TR $\alpha$ 1 and TR $\beta$ 1 were found in 65% and 76% of the haepatocellular carcinomas, respectively. Moreover, multiple point mutations were observed in mutated TRs (Lin *et al.*, 1999). Mutated TRs were observed in other studies of haepatocellular carcinomas also, demonstrating that these TRs have no normal T3 binding and transcriptional activities (Lin *et al.*, 1996; Lin *et al.*, 1997). However, in these studies it was not clear how the dominantly negative TR mutants led to haepatocellular carcinomas.

Aberrant expression of TR $\alpha$  and TR $\beta$  genes has found in renal cell carcinomas (Puzianowska – Kuznicka *et al.*, 2000). Puzianowska – Kuznicka *et al.* (2000) showed that the expression of both TR $\alpha$ 1 and TR $\alpha$ 2 mRNAs was reduced, whereas the TR $\beta$ 1 mRNA was over expressed in 30% and reduced significantly in 70% of tumours examined. In 22 cases of renal cells carcinomas, mutations of TR $\beta$ 1 were found in seven cases (32%), mutations of TR $\alpha$ 1 cDNAs in three cases (14%), and in two cases TR $\beta$ 1 cDNAs were mutated (Kamiya *et al.*, 2002). Furthermore, five TR $\beta$ 1 and three TR $\alpha$ 1 cDNAs had two to three mutations (Kamiya *et al.*, 2002). Most of these mutations were localized in the hormone binding domain that leads to loss of T3 binding activity and / or impairment in binding to TREs (Kamiya, *et al.*, 2002).

### 1.7.8. Thyroid hormone as potential treatment for cancer

The potential beneficial effect of TH was shown more than a century ago in patients with breast cancer treated with thyroid extracts. (Beatson *et al.*, 1896) However, primary hypothyroidism has also been associated with a reduced incidence of primary breast carcinoma (Cristofanilli *et al.*, 2005). Hypothyroidism though may have a dual effect on tumourigenesis; in animal models of induced tumour growth by haepatocarcinoma and breast cancer cells, tumour growth was slower in hypothyroid mice but was aggressive (undifferentiated) and invasive (increased metastasis). This was shown to be due to the decrease in cell proliferation, induction of cell dedifferentiation and changes in the extracellular matrix (Martinez-Iglesias 2009). Further to this controversial results, hypothyroidism has been shown to be a risk factor in patients with liver cancer (Reddy *et al.*, 2007) and in animals, T3 treatment induced rapid regression of carcinogen induced hepatic nodules and reduced the incidence of hepatocarcinoma and lung metastasis ( Ledda –Columbano *et al.*, 2003; Ledda –Columbano *et al.*, 1999; Perra *et al.*, 2008).

Recent studies have explored the potential role of thyroid hormone receptors in cancer. Thus, TRs are shown to control tumourigenesis through distinct mechanisms. Expression of TR $\beta$ 1 was shown to totally tumour formation by *ras*-transformed cells in nude mice, even under hypothyroid conditions. On the other hand, tumour formation was reduced in euthyroid mice inoculated with cells expressing *ras* oncogene and TR $\alpha$ 1, but all hypothyroid animals developed tumours, although tumour appearance was significantly delayed (Figure 1.12). These results are consistent with the ligand-dependent antitransforming activity of this receptor isoform and indicate that TR $\alpha$ 1 could only have tumour suppressor activity under euthyroid conditions. (in liganded state).

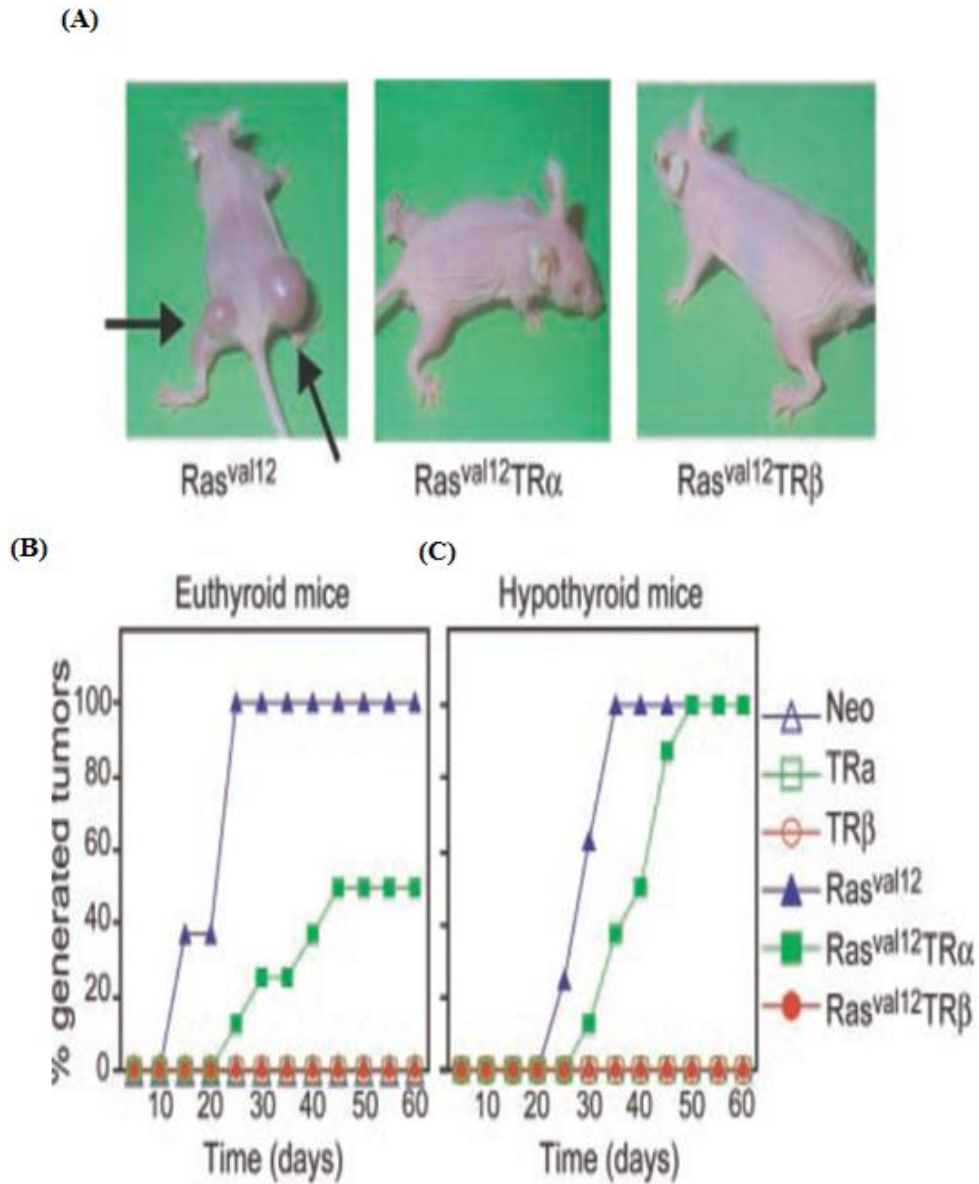


Figure 1.12: Overexpression of unliganded TR $\alpha$ 1 (in the case of induced hypothyroidism) increases cancer growth compared to liganded TR $\alpha$ 1 (as in euthyroid mice). (A) This pattern closely resembles that observed in pathologic cardiac growth,(B/C) indicating a potential role of TR $\alpha$ 1 in cancer and heart disease. (Taken from Garcia-Silva and Aranda, 2004).

### **1.7.8.1. Changes in thyroid hormone signalling in brain cancer**

Alterations in the expression of TRs in human brain tumours have been found mainly in pituitary tumours and meningiomas. (Margassi, *et al.*, 1993; Wang, *et al.*, 1995; Gonzalez-Sancho, *et al.*, 2003; Wang, *et al.*, 2003; Monden, *et al.*, 2006). Wang *et al.*, (1995) demonstrated that human TRs were differentially expressed in human pituitary tumour cells. Furthermore, reduced expression of TRs in thyrotropin – secreting pituitary tumours may also lead to a defective negative feedback of the thyroid hormone on thyrotropin production and this contribute to uncontrolled tumour growth (Gittoes *et al.*, 1998). Hwang *et al.*, (2008), compared TR expression between low grade (WHO grade II) and high grade (WHO grade III and IV) astrocytomas and showed that the frequency of either TR $\alpha$ 1 or TR $\alpha$ 2 expression was significantly decreased with the grade of malignancy. However, the frequency of TR $\beta$ 1 expression significantly increased with the grade of malignancy astrocytomas (Hwang, *et al.*, 2008).

### **1.7.9. Thyroid hormone treatment**

The potential effects of T3 on cell proliferation and differentiation were shown in neuro-2a cells transfected with TR $\beta$ 1. T3 (at concentrations ranging from 3 nM to 300 nM) blocked proliferation in G0/G1 and induced differentiation as indicated by increase in the number of perisomatal filopodia-like neuritis and achetylcholinesterase staining. This effect was evident after 24h and peaked at 48h. Interestingly, T3 had no effect on non transfected neuro-2a cells in which TR $\alpha$ 2 receptor expression was dominant inhibiting TR $\alpha$ 1 which was less expressed (Lebel *et al.*, 1994). Taken these data together, it appears that T3, even at low concentrations (which are of physiologic

and therapeutic relevance) can inhibit proliferation and differentiation via its genomic action. This effect may be lost in the case the expression of TRs is altered. The potential of T3 to induce cell necrosis has not been explored.

Contrary to its genomic effect, TH was shown rather to promote proliferation via a non genomic acute action (Davis *et al.*, 2006, Lin *et al.*, 2009). Interestingly, this action was shown to be initiated at the cellular membrane and thus, T4 was more potent growth inducer than T3. In fact, a proliferative effect was hardly seen with T3 at nearly physiologic concentrations (~1 nM). This effect was shown in several cell lines including C6, F98, GL261 and U87MG (Davis *et al.*, 2006; Lin *et al.*, 2009). These data probably point out that TH transient effect may proliferation which though may be avoided by low T3 concentrations.

## **1.8. Working hypothesis**

Based on the evidence above, it appears that the effects of TH on cell differentiation may be of relevance in cancer treatment. Preliminary experimental studies on brain malignances show a potential role of thyroid hormone as a novel treatment. This prompts for further studies in order to better understand the effects of TH on the balance of cell proliferation, cell differentiation and cell necrosis and the potential underlying mechanisms.

## 1.9. Aims of the study

The main aim of this study was to investigate the potential anti-cancer effects of thyroid hormone on glioma tumour cell lines.

The specific aims of the present study are:

- To confirm a TH differentiating action in an established model of cell differentiation / de-differentiation such as neonatal cardiomyocytes treated with growth factors
- To investigate the effects thyroid hormone on the morphology of glioma cells.
- To determine the effect thyroid hormone has on the cell growth of glioma cell lines.
- To determine the effects of thyroid hormone on proliferation of glioma cell lines.
- To determine the effects of thyroid hormone on apoptosis in glioma cell lines.
- To determine the effects of thyroid hormone on cell injury.
- To investigate the potential effect of thyroid hormone in relation to the degree of aggressiveness and altered expression of thyroid hormones.
- To investigate the pattern of growth kinase signalling which is potentially implicated in the thyroid hormone effect on glioma cell lines.
- To analyze the data and write up the PhD thesis.

# Chapter Two

## Materials and Methods

## Materials

1321N1: grade II astrocytomas

Acrylamide

Amphotericin B

Anti-mouse antibody

Anti-rabbit HRP antibody

Aprotinin

Ascorbic acid

BrdU: labelling reagent

Bromophenol blue

BSA: Bovine serum albumin

Cardiomyocytes

CO<sub>2</sub>: carbon dioxide

Digital camera (Axio Cam)

DMEM: Dulbeccos modified eagles medium

DMSO: freezing medium

DTT: Dithiothreitol

EDTA: Ethylenediaminetetraacetic acid

Ethanol

F10 medium

FBS: fetal bovine serum

Glycerol

Glysin

HEPES: 4-(2-hydroxyethyl)-1-piperazineethanesulfonic acid

Horse serum

KCl: potassium chloride

LDH: lactate dehydrogenase

Leupeptin

L-glutamine

Lumiglo reagent

MEM: essential minimum eagle medium

Mercaptoethanol

Mercaptoethanol

Methanol

MgCl<sub>2</sub>: Magnesium chloride

NaCl: Sodium chloride

Neubauer hematocytometer

Nitrocellulose membrane

NP-40: nonyl phenoxy polyethoxy ethanol

PBS: phosphate buffer solution

Penicillin

Peroxidase anti mouse IgG2a

PMSF: phenylmethylsulfonyl fluoride

SDS: sodium dodecyl sulfate

Sodium bicarbonate

Sodium pyruvate

Streptomycin

Transferrin/ selenium

Tris base

Tris-HCL

Trypsin

TUNNEL staining *in situ* cell death detection kit

U87-MG: grade IV glioblastomas

Zeiss microscope

$\beta$ -MHC: slow muscle myosin

## **2.1. Studies on cardiac cell-based models**

### **2.1.1. Cell culture**

Rats were handled in accordance with the Guide for the Care and Use of Laboratory Animals published by the US National Institutes of Health (NIH Publication No 85-23, revised 1996). Neonatal rat cardiomyocyte cultures were prepared as previously described (Detillieux *et al.*, 1999) with some slight modifications. Ventricles from Wistar rat pups (0-48 h after birth) were dissected, and the cells were dissociated in a spinner flask using a combination of collagenase (740 u/digestion Worthington Biochemicals, NJ), trypsin (370 u/digestion Worthington Biochemicals, NJ), Dnase I (2880 u/digestion Worthington Biochemicals, NJ). Myocytes were separated from non-muscle cells on a discontinuous Percoll gradient and plated at a density of 45000 cells/cm<sup>2</sup> for geometry-shape measurements, immunocytochemistry and protein content measurement. Cells were initially plated in F10 medium (Gibco) containing 10% Fetal Bovine Serum (Hyclone), 10% horse serum (Gibco) and antibiotics (100u/ml penicillin and streptomycin, Gibco) for the first 18-22 hours and then the culture medium was replaced with serum-free medium containing 10 µg/ml insulin, 10 µg/ml transferin/selenium, 0.2% BSA and 20 µg/ml ascorbic acid.

### **2.1.2. Measurement of Neonatal Cardiomyocytes Axes and Cell Size**

Images of neonatal cardiomyocytes were acquired using a digital camera (AxioCam MRC with AxioVision software) incorporated on a Zeiss microscope (Axiovert 25). Cells images were projected in a computer and a mouse was used to draw around the perimeter of each cell or to measure the major (a) and minor (b) axis. AlphaScan

Image analysis was used to calculate the planimetric area and the axes length. A sum of 100 to 200 cells from 5 different dishes was measured in each group.

### **2.1.3. Determination of cardiomyocyte growth (Cellular Protein Content)**

Total protein content of myocytes was measured as previously described (Lai *et al.*, 1996) with some modifications. Cells of all groups were plated at a density of 45000 cells/cm<sup>2</sup> and cultured for 5 days. The cells were washed twice with PBS and 200 µl Trypsin 0.25% was added to each well and incubated at 37<sup>0</sup>C until the cells detached. A solution of 10% FBS in PBS was added to each well to stop the reaction. The cells were harvested and a small fraction was used for determination of the cell number using a Neubauer hemacytometer. Cells were then collected by centrifugation and incubated with 100 µl lysis buffer (250mM Tris-HCL, 4% SDS, 10% glycerol pH 6.8) at 4<sup>0</sup>C overnight. This mixture was then warmed at 37<sup>0</sup>C, and protein concentration was determined using the DC protein assay (Bio-Rad) based on the Lowry method (Lowry *et al.*, 1953). Protein contents were normalized to the cell count. Twenty samples (dishes) from each group were used for this analysis.

### **2.1.4. Myosin Heavy Chain (MHC) Isoform Protein Analysis**

Cells (plated at a concentration of 100.000 cells/cm<sup>2</sup>) were washed twice with PBS, scraped into 100 µl lysis buffer (250 mM Tris-HCL, 4% SDS, 10 % glycerol pH 6.8) and boiled for 5 min at 100<sup>0</sup>C. Protein concentration was determined by the DC protein assay (Bio-Rad) based on the Lowry assay and the originally prepared samples were diluted 15 fold with Laemmli sample buffer containing 5% 2-mercaptoethanol. The composition and preparation of the gels was carried out as

previously described (Pantos *et al.*, 2008; Reiser *et al.*, 2006). The stacking and separating gels consisted of 4 and 8% acrylamide (wt/vol) respectively, with Acryl: bis-Acryl in the ratio of 50:1. The stacking and separating gels contained 5% (vol/vol) glycerol. The upper running buffer consisted of 0.1 M Tris (base), 150 mM glycine, 0.1% sodium dodecyl sulfate (SDS) and 2-mercaptoethanol at a final concentration of 10 mM. The lower running buffer consisted of 0.05 M Tris (base), 75 mM glycine and 0.05% SDS. The gels were run in Biorad Protean II xi electrophoresis unit at a constant voltage of 240 V for 21 h at 8 °C. The gels were fixed and silver-stained (Biorad silver stain kit). Gels were scanned and quantified using the AlphaScan Imaging Densitometer (Alpha Innotech Corporation, USA). Four samples (dishes) from each group were used for this analysis.

### **2.1.5. Immunocytochemistry**

Cardiomyocytes from all groups cultured in collagen-coated (collagen, Type I, Upstate) glass cover slides (Fisher Scientific), were fixed with 4% paraformaldehyde (Sigma) for 15 min at 4<sup>0</sup>C and permeabilised with 0.1 % Triton-X/PBS for 15 min at 4<sup>0</sup>C. Subsequently, the cells were incubated with fluorescent phallotoxin (Molecular Probes) in 1%BSA/PBS for 20 min at room temperature for staining of actin filaments. After each step, cells were washed three times with PBS. For immunocytochemical staining of myosin, cells were incubated with the slow-muscle myosin ( $\beta$ -MHC) antibody (Chemicon, dilution 1:1000) for 1.5 hour at room temperature and then treated with the goat anti-mouse IgG (Alexa-Fluor, Chemicon, dilution 1:1000) in 1%BSA/PBS at room temperature. After each step, cells were washed three times with PBS.

Slides were mounted and examined by fluorescence phase-contrast microscopy (Zeiss Axiovert).

### **2.1.6. Experimental protocol**

Cells were serum-starved for 24 hours before the initiation of the experimental protocol. These cells were remained undifferentiated. Further dedifferentiation was induced by the use of phenylephrine (PE), an  $\alpha$ 1 adrenergic agonist at a dose of 20  $\mu$ M for 5 days as previously described (Kinugawa *et al.*, 2001) T3, at 100 nM was used to differentiate undifferentiated and dedifferentiated cells. This dose is at the range of doses that have been previously used in this experimental setting (Kinugawa *et al.*, 2001; Gosteli-Peter *et al.*, 2003).

The following experimental studies were performed:

**Study 1.** Assessment of cell growth, cell morphology, myosin expression in neonatal cardiomyocytes which remained untreated for 5 days (control group, CONT, n=6) and cardiomyocytes dedifferentiated with phenylephrine (PE), an alpha adrenergic receptor agonist, 20  $\mu$ M for 5 days (PE group, n=6).

**Study 2.** Assessment of cell growth, cell morphology myosin expression in undifferentiated neonatal cardiomyocytes treated with T3 100 nM for 5 days (T3 group, n=6).

**Study 3.** Assessment of cell growth, cell morphology myosin expression in dedifferentiated cardiomyocytes treated with phenylephrine 20  $\mu$ M and T3 100 nM for 5 days (PE-T3 group, n=6).

## **2.2. Studies on Glioma cell lines**

### **2.2.1. Cell Culture**

Cell line 1321N1, an astrocytoma grade II, and U87MG a glioblastoma grade IV were used in this study. Glioma cell line U87MG was obtained from the American Type Culture Collection (ATCC) (Manassas, VA) and glioma cell line 1321N1 was obtained from the European Collection of Cell Culture (ECACC) (Salisbury, Wiltshire, UK). All cell lines were maintained in 150 cm<sup>2</sup> cell culture flasks (CORNING).

U87MG was maintained in Essential Minimum Eagle Medium (MEM) with Earle's salts supplemented with 10% fetal bovine serum (GIBCO), 1 mM sodium pyruvate, streptomycin and penicillin (5% v/v), 0.1 mM non-essential amino acids, 2 mM L-glutamine and amphotericin B (5% v/v).

1321N1 was maintained in Dulbecco's Modified Eagle's Medium (DMEM) with glucose and sodium bicarbonate supplemented with 10% FBS, 2 mM L-glutamine, 5% penicillin and streptomycin and 5% amphotericin B.

All cell lines were maintained in a 37° C humidified incubator with 5% CO<sub>2</sub>. For all experiments, each of the glioma cell lines were used between passages 20-30. Once cells were 70-80% confluent they were trypsinized using 1X (1x 2.5 g porcine trypsin per litre in Hanks' Balanced Salt solution, Sigma) Trypsin. Cells were settled for 24

hours in stripped medium (using charcoal FBS, GIBCO) before the initiation of treatment.

### **2.2.2. Subculture**

Once cells were 70- 80% confluent, they were trypsinized using 1X Trypsin and incubated at 37° C for 5-10 minutes. For the 150 cm<sup>2</sup> flasks, 3 mL of trypsin was added. After 5 min, the flasks were taken from the incubator and viewed under an inverted light microscope to see if the cells had detached. If not, the flasks were placed back into the incubator and checked again every few minutes until the cells had fully detached. Once detached, cell medium was added to neutralize the trypsin and prevent causing any damage to the cell membranes. For each 1 mL of trypsin, at least 1 mL of medium was added to the flask to neutralize the trypsin reaction.

To re-culture the cells, the cell suspension was added to new flasks containing fresh, warm medium at approximately  $2-4 \times 10^4$  cells/ cm<sup>2</sup> depending on the cell line. New flasks were then placed back into the incubator and left for 24 hours to attach. After 24 hours, the flasks were viewed under a light microscope to ensure they had attached healthily and were proliferating.

### **2.2.3. Cell freezing**

During cell freezing, the cells were trypsinized and counted as previously described above. The cells were then resuspended in cell freezing medium (medium + 0.5% DMSO) at a cell concentration of  $1 \times 10^6$  cells per mL, aliquoted in to cryovials, and put into a 'Mr Frosty' at room temperature. The 'Mr Frosty' was immersed in isopropanol, which cooled the cells, and placed in a -80° C freezer; this method caused the cells to be cooled at -1° C per minute. The cryovials were left overnight at

-80° C and then immersed in liquid nitrogen the following day, until required for sub-culture.

#### **2.2.4. Culturing cells from frozen**

Cryovials were taken from liquid nitrogen and quickly immersed in a 37° C bath to defrost. Once defrosted, the vials were wiped with a tissue, doused in 70% ethanol, and the cells were then placed in a 150 cm<sup>2</sup> flask containing warm fresh medium and placed into an incubator overnight. The following day, the medium was changed and fresh medium was added to remove as much of the cryoprotectant, DMSO, as possible.

#### **2.2.5. Cell Assays**

##### **2.2.5.1 Cell counting**

Once the cells were trypsinized and the trypsin was neutralized using cell media, 1 mL of cell/medium mix was taken from the flask and placed into a sterile Eppendorf tube. Using a haemocytometer (as displayed in figure 2.1), a cover slip was attached using a small amount of moisture, such as an exhaled breath, onto the slide. Approximately, 20 µL of the cell suspension was pipetted on to the slide and the slide viewed under a light microscope, under 20X magnification and the cells counted within the squares (figure 2.1). All cells were counted within a 4x4 grid (figure 2.1) and then a further two grids were counted to obtain an average.

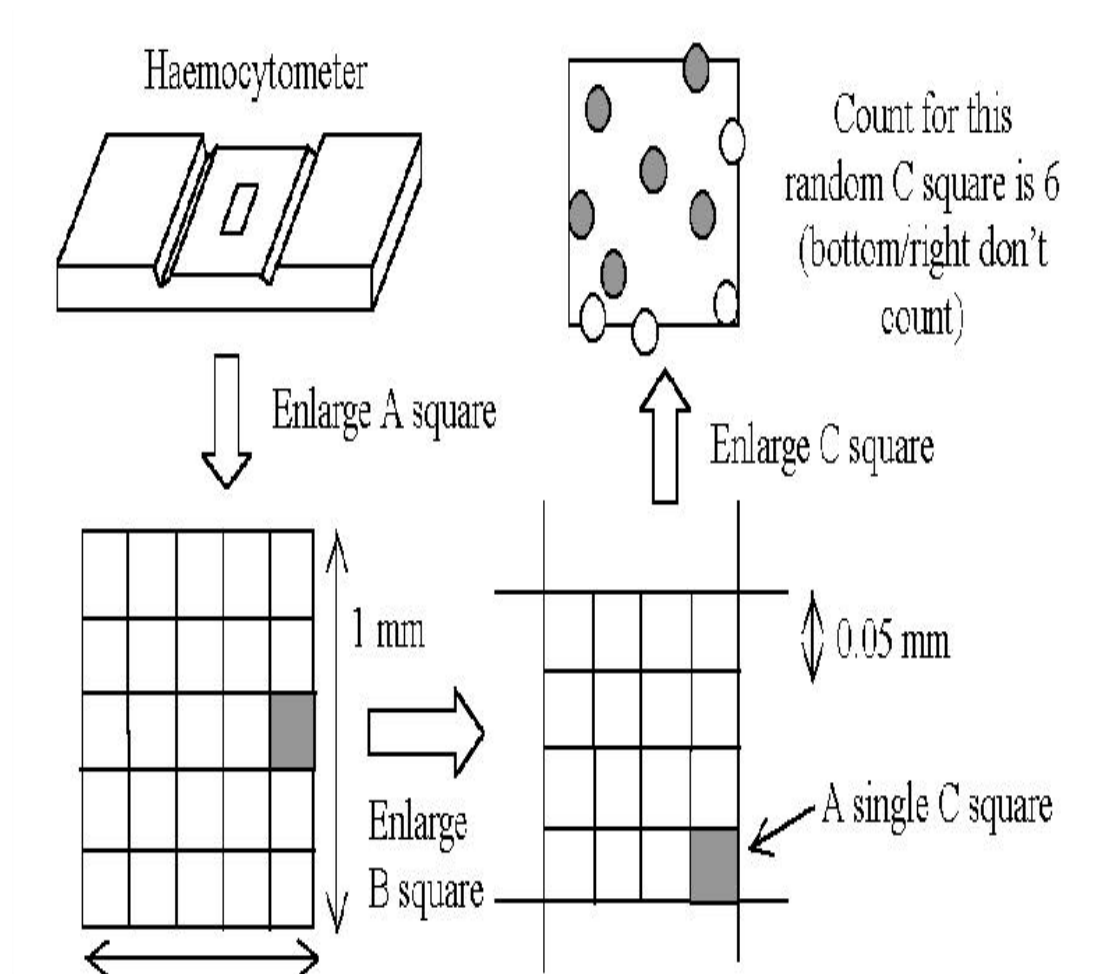


Figure 2.1: Diagram presenting the methods involved in cell counting using the Neubauer haemocytometer and cell cover attachment. (Taken from Power point presentation).

### 2.2.5.2. Cell morphology

Cell morphology was used to assess cell differentiation. Cells were fixed in paraformaldehyde solution, before being viewed with an inverted light microscope fitted with phase contrast optics. A scale (called a reticule) was built into one eyepiece of the light microscope, and was used to measure any planar dimension in a microscope field since the ocular can be turned in any direction and the cell can be repositioned with the stage manipulators. To measure the length of a cell the number

of ocular division spanned by the object had to be noted. Finally multiply by the conversion factor for the magnification used. Five random fields, each containing no more than 50 cells, were examined in each well and the total numbers of cells as well as the total number of projections that were greater than two cell body diameters in length were recorded. Data were derived from approximately 100 cells in each group. Cell morphology could not be reliably assessed at 96 hours due to more than 80% confluence.

### **2.2.5.3. Cell proliferation**

For determining cell proliferation, BrdU labelling reagent (RPN20 kit, GE Healthcare, Piscataway, NJ) was added to the medium. Cells were incubated for 30 minutes and then fixed using 4% paraformaldehyde for 15 minutes. Primary antibody (anti-BrdU monoclonal antibody, dilution 1:100) was applied for 1h at room temperature. Samples were washed  $3 \times 5$  minutes with PBS. Secondary antibody (peroxidase anti-mouse IgG2a) was then applied for 30 minutes at room temperature, followed by washing  $3 \times 5$  minutes. Finally, BrdU-immunostained cultures were visualized using DAB and photographs taken with a digital camera (Zeiss Axiovert) attached to an inverted microscope fitted with phase contrast optics. DAB has the ability to stain black the nucleus of the cells that are about to proliferate leaving the nucleus of the rest of the cells white. BrdU-positive nuclei were counted as a percentage of total nuclei. Proliferation data are derived from between 450 to 600 cells measured in each group.

#### **2.2.5.4. Cell apoptosis**

Apoptotic cell nuclei were assessed by TUNNEL staining using an *In Situ* Cell Death Detection Kit, according to a standard protocol based on the manufacturer's instructions (ROCHE, Cat. No. 11 684 795 910). Cell cultures were counterstained with Hoeschst 33358 (5 µg/ml) which stained the nuclei of all cells. Administration of doxorubicin known to induce apoptosis was used as a positive control in order to certify the selected method.

#### **2.2.5.5. Cell injury**

Cellular injury was assessed by LDH enzyme release in to the cultured medium. Culture medium was collected at the end of the experiment for the measurement of lactate dehydrogenase (LDH) activity (IU/L) using an ELISA kit (Quanticrom LDH Kit, DLDH-100, BioAssay Systems, USA). Measurements were performed with a Tecan Genios system (wavelength 565 nm). LDH release was expressed in each group as a percentage of the non-treated group.

#### **2.2.5.6. Molecular analysis**

After washing twice with PBS, the cells were scraped into 400 µl lysis buffer containing 20 mM HEPES, pH 7.9, 10 mM KCl, 1 mM EDTA, 10% glycerol, 0.2% NP-40, 0.5 mM DTT, 0.5 mM PMSF, 5 µg/ml aprotinin, 5 µg/ml leupeptin. A small quantity of total lysate was kept and the remainder centrifuged at 12000 g for 1 min at 4<sup>0</sup> C. The nuclear fraction was prepared by resuspension of the pellet in buffer containing 20 mM HEPES, pH 7.9, 0.42 M NaCl, 0.2 mM EDTA, 1.5 mM MgCl<sub>2</sub>, 25% glycerol, 0.5 mM DTT, 0.5 mM PMSF, 5 µg/ml aprotinin, 5 µg/ml leupeptin, and incubated with agitation for 1 hour at 4<sup>0</sup> C before centrifugation for 10 min at 12,000g.

The resulting supernatants were collected and used for protein analysis of the nuclear fraction. Protein concentrations were determined by the BSA assay method. After boiling for 5 min (with 4% SDS, 2% mercaptoethanol and 0.004% bromophenol blue) a quantity of 15 µg protein from nuclear or total fraction was separated on 7.5% SDS-PAGE using a Bio-Rad Mini-Protean gel apparatus. For Western blotting, proteins were transferred electrophoretically to a nitrocellulose membrane (Hybond ECL) at 100 V and 4° C, for 1.5 h using Towbin buffer (with 6.06 Tris, 28.8 Glycin, 400 ml Methanol and 1300 ml water). Filters were afterwards probed with specific antibodies. For Western blotting, membranes with total protein extracts were blocked with 5% non-fat milk in TBS-Tween for 60 min and then probed with specific antibodies against total and phospho-ERK (Cell Signaling Technology, dilution 1:1000) and total and phospho-Akt (Cell Signaling Technology, dilution 1:1000), overnight at 4° C. Filters were incubated with appropriate anti-rabbit HRP secondary antibody (Cell Signalling, 1:4000, 1h R.T.) and immunoreactivity was detected by enhanced chemiluminescence using Lumiglo reagents (New England Biolabs). Immunoblots were quantified using the FluorChem HD2 system (Alpha Innotech Corporation, 14743, Catalina Street, San Leandro, CA).

#### **2.2.5.7. Measurement of thyroid hormone receptors**

After Western blotting, filters were probed with specific antibodies against TRα1 (Abcam Rabbit polyclonal to TRα1, ab53729, dilution 1:1000, o/n at 4° C) and TRβ1 (Affinity Bioreagents, MA1-216, dilution 1:1000, o/n at 4° C). Filters were incubated with appropriate anti-mouse (Amersham) or anti-rabbit (Cell Signalling) HRP secondary antibodies. Immunoreactivity was detected by enhanced

chemiluminescence using Lumiglo reagents (New England Biolabs). Chemiluminescence was detected by the image analysis system FluorChem HD2 (AlphaInnotech Corporation, 14743, Catalina Street, San Leandro, CA) equipped with a CCD camera and analysis software. Five samples from each group were loaded on the same gel. Ponceau staining was used in order to normalize slight variations in protein loading.

#### **2.2.5.8. Construction of Growth Curves**

Growth curves provide important information when changes in cell number are to be used as a study end-point. A typical growth curve consists of the lag phase before the cells start to grow, the log phase of exponential growth and the plateau phase when contact-inhibited cells will cease growing. The lag period lasts usually around 12–24 hours and allows the cells to recover from trypsinization, reconstruct their cytoskeleton, secrete matrix to aid attachment, and spread out on the substrate, enabling them to reenter cell cycle. During the log phase the cell population doubles over a definable period, known as the *doubling time* and characteristic for each cell line. The rate of growing is calculated during the log phase of growth (Figure 2.2).

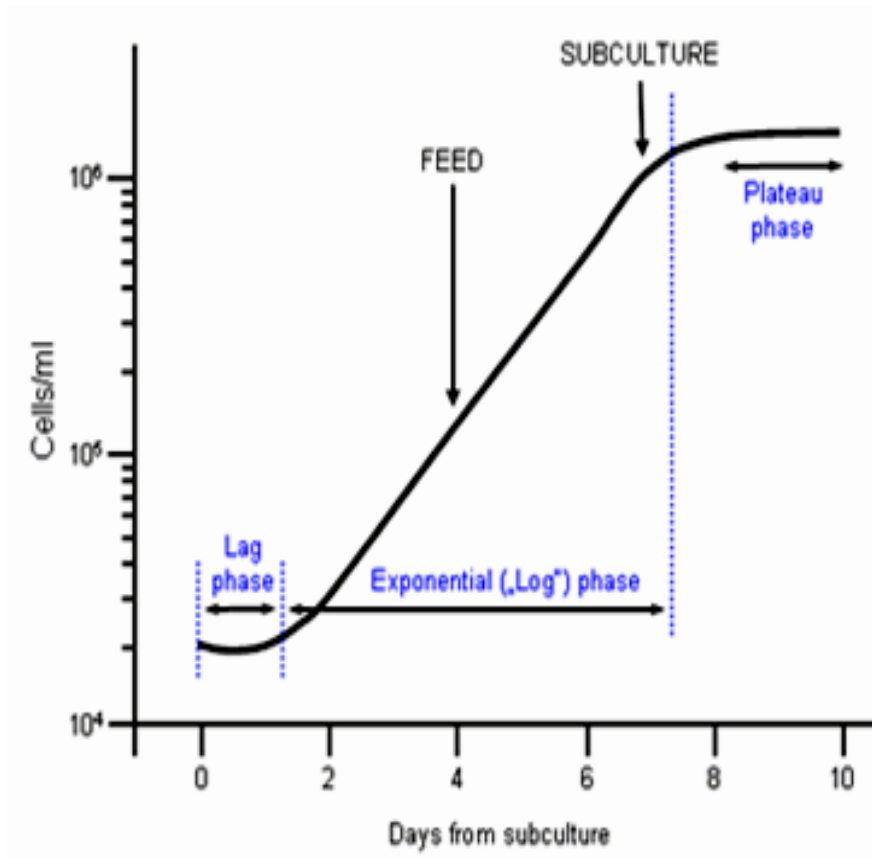


Figure 2.2: Time course changes in a typical growth curve. Note that maximal growth occurred after 7-8 days of culture. Typical of 10 such different experiments.

In order to construct the growth curves serum used in the culture medium for these experiments was stripped from steroid hormones in order to keep the untreated cells devoid of thyroid hormones. Then, population doubling time and saturation density were determined.

### **2.3. Experimental Protocols**

In the present study, T3 was used as chronic treatment since T4 acts on the cell membrane and has no genomic long acting effects. Cells deprived of T3 in medium were used as controls (0 nM, untreated). Two doses of T3 were used based on previous data (Lebel *et al.*, 1994; Aranda *et al.*, 2004). Thus, cells were treated with 1 nM which is a near physiologic dose and clinically relevant. A second dose of 500 nM was used as supraphysiological dose. The effects of T3 were assessed in two time points; 48 h and 96 h. This was based on the data obtained from the construction of growth curves and from previous studies showing that the effect of T3 on cell differentiation was peaked at 48h (Lebel *et al.*, 1994).

### **2.4. Experimental studies**

#### **Study 1. Morphological characteristics of glioma cell lines**

Two different cell lines (1321N1 and U87MG) were examined to determine the effect of T3 upon their morphology. After the cells had reached confluence, approximately 17000 cells/mm<sup>2</sup> cells were placed in a 35 mm petri dish and treated with T3 at doses of 0 nM, 1 nM and 500 nM for a period of 12, 24 and 48 hours. Cells were fixed, before being viewed under an inverted light microscope fitted with phase contrast optics. Five random fields, each containing no more than 50 cells, were examined for each of the doses. The number of projections and the ratio of cell length/width of each cell were recorded. Data were derived from approximately 100 cells in each group, n=8 repeats for each group.

## **Study 2. Cell count of glioma cell lines**

Two different cell lines (1321N1 and U87MG) were examined to determine the effect of T3 on the cell number. The cell lines were cultured until reaching a confluence level of 80%, and after trypsinisation approximately 17000/mm<sup>2</sup> cells of each cell line were placed in a 60mm petri dish and treated with T3 at doses of 0 nM, 1 nM and 500 nM for a period of 12, 24 and 48 hours (n=8 for each dose). Cell number was estimated using a light microscope and a Neubauer haemocytometer.

## **Study 3. Proliferation of glioma cell lines**

The two different cell lines (1321N1 and U87MG) were studied to examine the effect of T3 on the cell proliferation. After the cells had reached confluence, approximately 8500 cells /mm<sup>2</sup> were placed in a 60 mm petri dish (n=8 for each dose) and treated with T3 at the doses of 0 nM, 1 nM and 500 nM for a period of 12, 24 and 48 hours. A smaller density of cells were placed in the petri dish for proliferation experiments in order to better visualize and count the effects of BrdU labelling in photographs taken with a digital camera. For determining cell proliferation, BrdU labelling reagent (RPN20 kit, GE Healthcare, Piscataway, NJ) was used as described above. Proliferation data are derived from between 450 to 600 cells measured in each group.

## **Study 4. Levels of injury on glioma cell lines**

The two different cell lines (1321N1 and U87MG) were examined to determine the effect that T3 has on cell injury. When cells had reached confluence, approximately 17000 cells /mm<sup>2</sup> were placed in a 60 mm petri dish (n=8 for each dose) with T3 at doses of 0 nM, 1 nM and 500 nM for a period of 12, 24 and 48 hours.

Cellular injury was assessed by LDH enzyme release in the cultured medium. Culture medium (approximately 100  $\mu$ l, n=8 for each dose) was collected at the end of the experiment for the measurement of lactate dehydrogenase (LDH) activity (IU/L) using an ELISA kit (Quantichrom LDH Kit, DLDH-100, BioAssay Systems, USA). Measurements were performed with Tecan Genios system. LDH release was expressed in each group as percentage of the non-treated group.

### **Study 5. Levels of apoptosis in glioma cell lines**

The two different cell lines (1321N1 and U87MG) were examined to determine the effect that T3 has on cell apoptosis. When cells had reached the level of confluence, approximately 17000 cells /mm<sup>2</sup> were placed in a 60 mm petri dish (n=8 for each dose) and treated with T3 at doses of 0 nM, 1 nM and 500 nM a period of 12, 24 and 48 hours. After the treatment period apoptotic cell nuclei were assessed by the *In Situ* Cell Death Detection Kit, Fluorescein, according to the manufacturer's instructions (ROCHE, Cat. No. 11 684 795 910). Cell cultures were counterstained with Hoeschst 33358 (5 $\mu$ g/ml) which stained the nuclei of all cells.

### **Study 6. Molecular detection of kinase signalling in glioma cell lines**

The two different cell lines (1321N1 and U87MG) were examined to detect kinase signalling. When cells had reached confluence, 17000 cells /mm<sup>2</sup> were placed in a 60 mm petri dish (n=8 for each dose) treated with T3 at doses of 0 nM, 1 nM and 500 nM for a period of 12, 24 and 48 hours. Cell lysis and isolation of proteins, determination of protein concentration and western blotting analysis for

phosphorylated and total Akt and ERK was performed as described above. Data were obtained from n=8 samples for each group.

### **Study 7. Molecular detection of TR $\alpha$ 1 receptors in glioma cell lines**

Two different cell lines (1321N1 and U87MG) were examined for the presence of thyroid receptor TR $\alpha$ 1. Cell lysis and isolation of proteins, determination of protein concentration and western blotting analysis against TR $\alpha$ 1 was performed as described above.

### **2.5. Statistical analysis**

Values are presented as means +/- Standard Error of the Means (SEM). One-way analysis of variance (ANOVA) and Whitney- Mann tests were used for multiple comparisons between groups with the appropriate correction of Bonferroni or Dunnett T3. A two-tailed test with a *p* value less than 0.05 was considered significant.

# Chapter Three

## Results

### **3.1. Studies in cardiac cell based models**

#### **Study 1**

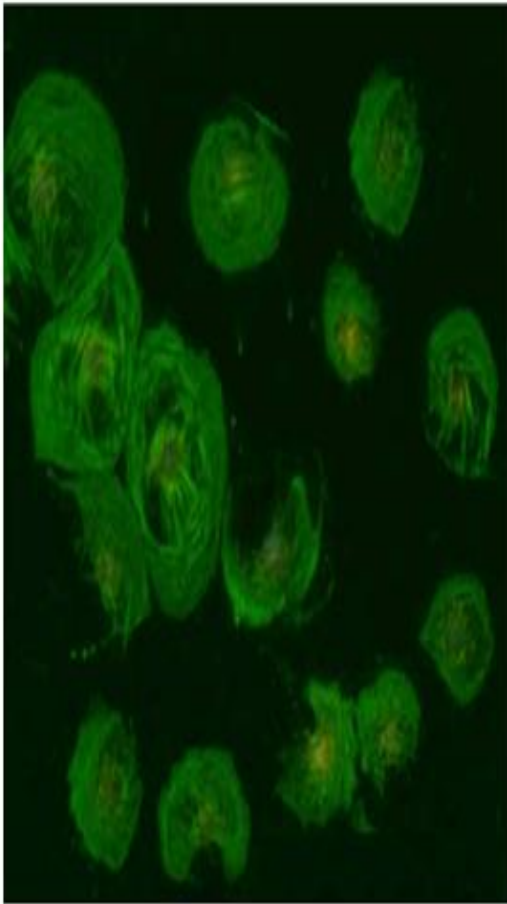
##### **3.1.1. Cell geometry, shape and $\alpha$ -myosin in untreated neonatal cells**

Figure 3.1(A) shows the cell geometry in non-treated cells. The results show that staining of actin cytoskeleton with phalloidin showed that non-treated cardiomyocytes remained undifferentiated with an almost circular shape with poorly organized cytoskeleton.  $\alpha$ -myosin which characterizes the adult phenotype was not detected.

##### **3.1.2. Effect of TH on cell geometry, shape and growth in the absence (non-treated) and presence (treated) of phenylephrine (PE)-treated cardiomyocytes**

Figure 3.1(B) shows the effect of PE treatment in cell geometry. The results show that PE treatment resulted in large cardiomyocytes with disoriented, dense myofibrils and cellular shape. PE increased cell growth as indicated by changes in total protein content and area. Total protein content (an index of hypertrophy) was increased 1.4 fold in PE-treated as compared to non-treated cardiomyocytes, ( $P<0.05$ ). Cell area was increased 1.3 ( $P<0.05$ ) fold more in PE-treated as compared to non-treated cardiomyocytes, ( $P<0.05$ ) (Figure 3.1).

(A) Non-treated



(B) PE-treated

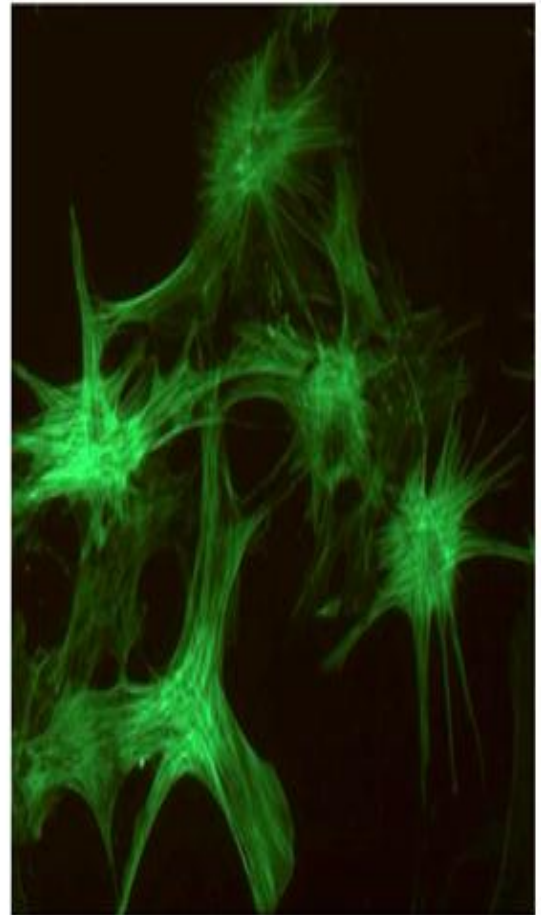


Figure 3.1: Images of (A) non-treated and (B) PE-treated neonatal cardiomyocytes for 5 days obtained by fluorescence microscopy after staining of actin cytoskeleton with phalloidin. Non-treated cardiomyocytes are of almost circular shape with poorly organized cytoskeleton, while PE treatment results in hypertrophied cardiomyocytes with disoriented, dense myofibrils and stellate shape. n=8, (20 x magnification).

### 3.1.3. Myosin heavy chain isoform expression in phenylephrine-treated neonatal cardiomyocytes

PE-treated cardiomyocytes exhibited a 30% increase in  $\beta$ -MHC expression,  $p < 0.05$ , as compared to non-treated cardiomyocytes.  $\alpha$ -MHC expression was not detected (Figure 3.2).

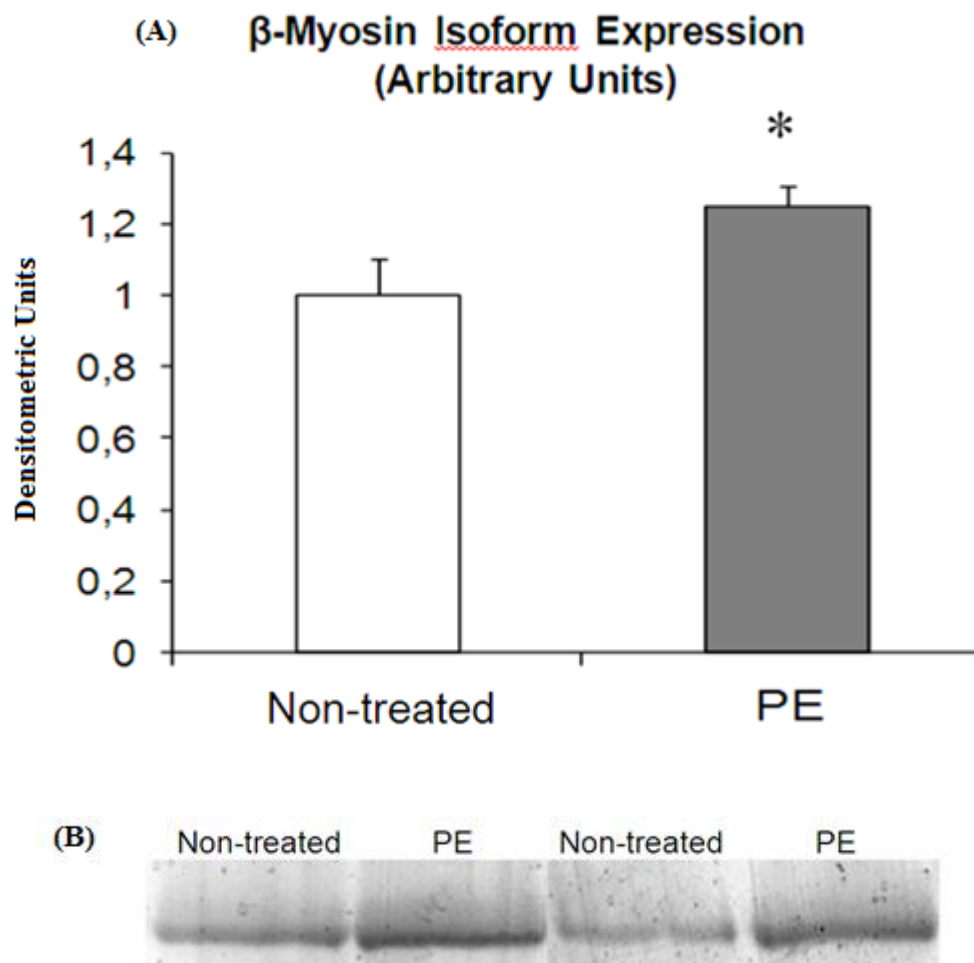
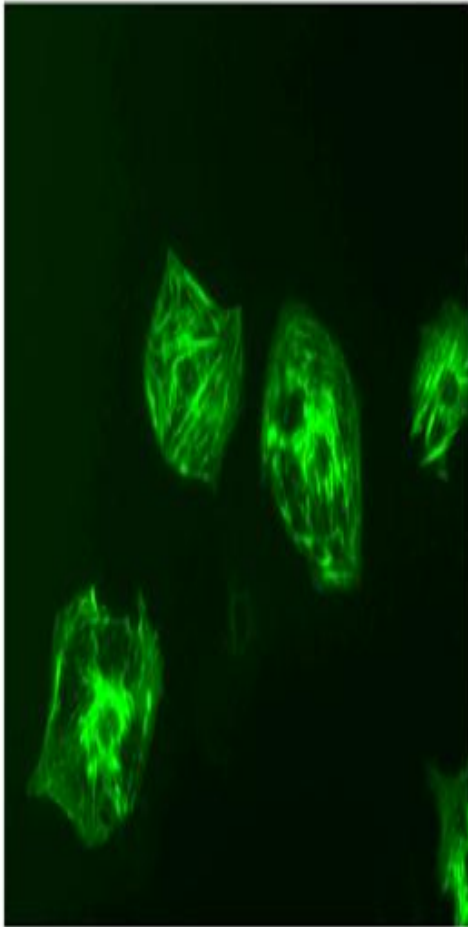


Figure 3.2: (B) Densitometric assessment and representative images of  $\beta$ -myosin heavy chain isoform expression in non-treated neonatal cardiomyocytes and cardiomyocytes treated with phenylephrine (PE, 20  $\mu$ M) for 5 days (A) Bar charts are means of optical ratios (arbitrary units), bar=SEM, n=8; \*  $P < 0.05$  for PE-treated vs non-treated.

(A) Non-treated



(B) PE-treated

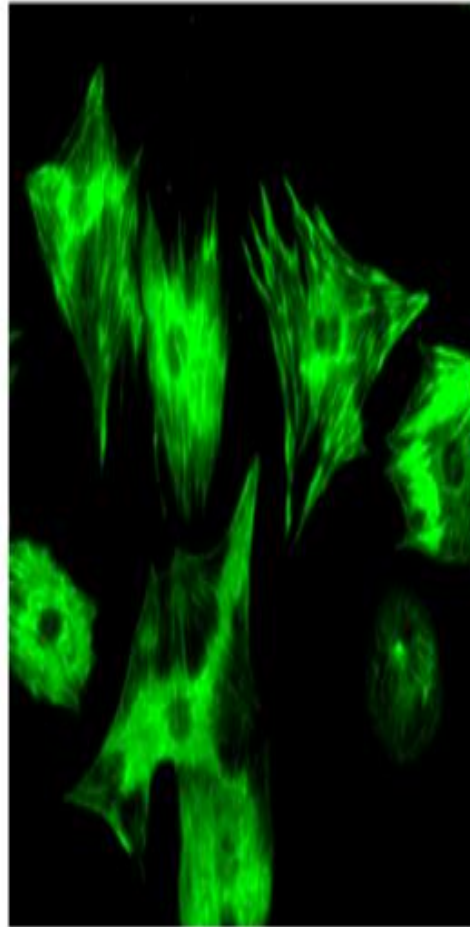


Figure 3.3: Images of (A) non-treated neonatal cardiomyocytes and (B) cardiomyocytes treated with phenylephrine (PE) for 5 days, obtained by fluorescence microscopy after staining for slow ( $\beta$ )-myosin with specific antibody. Immunostaining for  $\beta$ -myosin produced a stronger signal in PE-treated cardiomyocytes, as compared to non-treated; n=8, (20 x magnification).

### 3.1.4. Re-expression of TR $\alpha$ 1 in phenylephrine-treated neonatal cardiomyocytes

TR $\alpha$ 1 protein expression was found to increase 4.5 fold in PE-treated neonatal cardiomyocytes as compared to non-treated cardiomyocytes,  $P < 0.05$  (Figure 3.4).

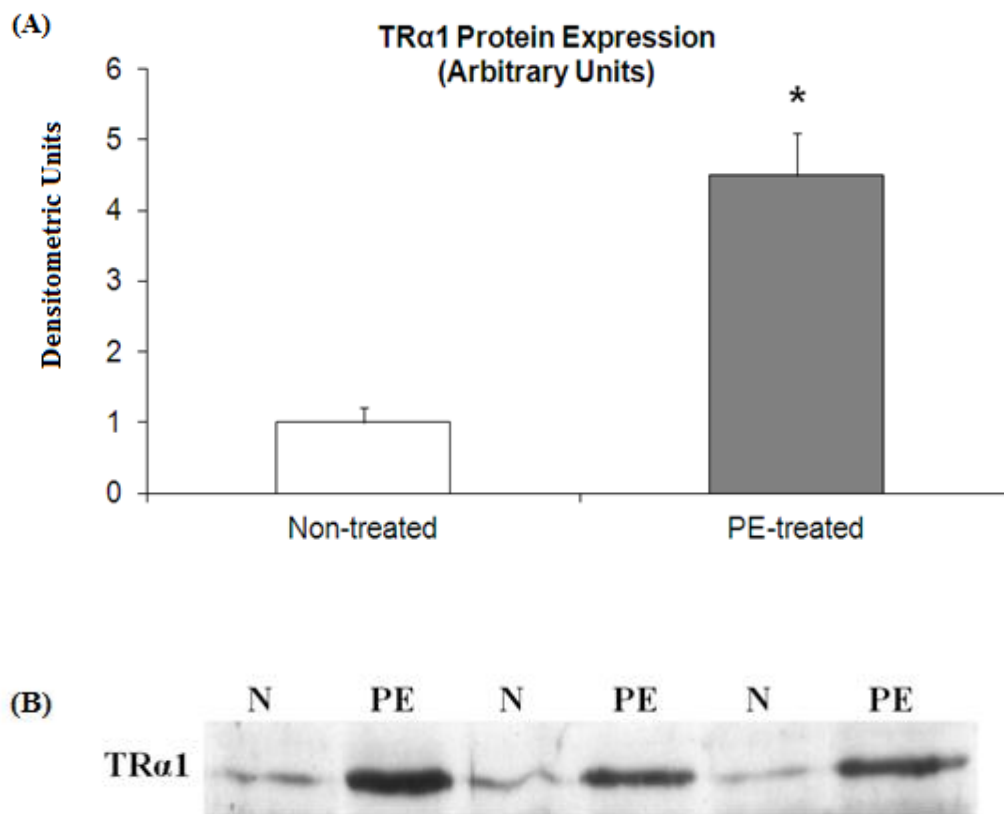


Figure 3.4: (A) Densitometric assessment in arbitrary units and (B) representative western blots of thyroid hormone receptor  $\alpha$ 1 (TR $\alpha$ 1) protein expression in non-treated neonatal cardiomyocytes and cardiomyocytes treated with phenylephrine (PE, 20  $\mu$ M) for 5 days (Bar charts in (A) are means of optical ratios or arbitrary units, bar=SEM, n=8); \*  $P < 0.05$  for PE-treated vs non-treated.

## Study 2

### 3.1.5. Cell geometry and shape in T<sub>3</sub>-treated undifferentiated cardiomyocytes

Administration of T<sub>3</sub> induced a significant increase in the major / minor axis ratio (Figure 3.5). The major/minor axis ratio was found to be  $2.2 \pm 0.14$  in T<sub>3</sub> treated cells as compared to  $1.5 \pm 0.04$  in non-treated cells,  $P < 0.05$  (Figure 3.6). This increase corresponded to a change in the cell shape from an almost circular to a more elongated form (Figure 3.5).

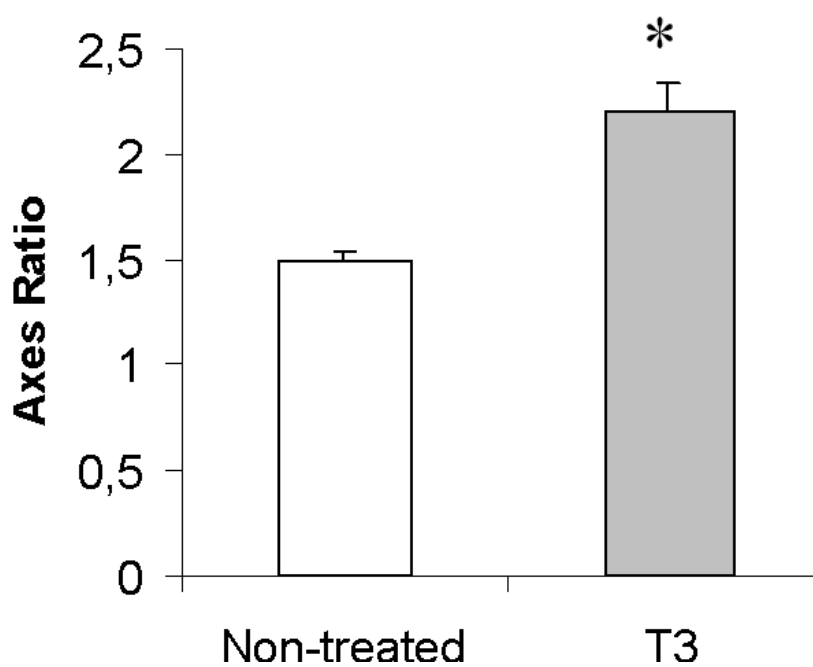
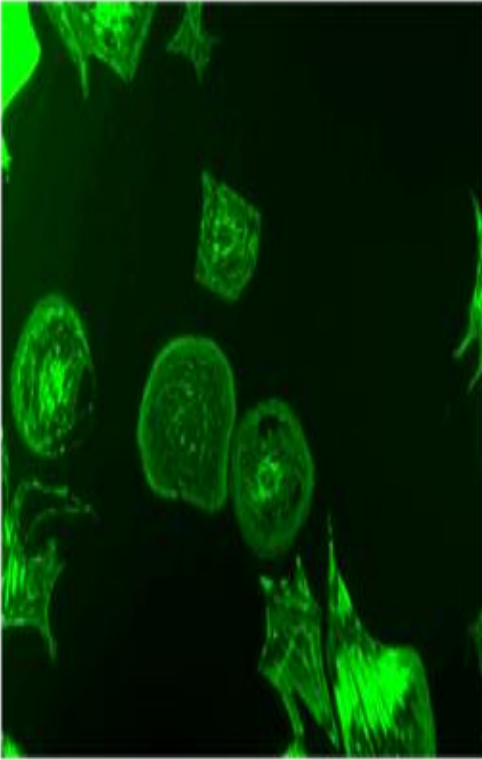


Figure 3.5: Cell shape determined by the ratio of major to minor cell axis in non-treated and T<sub>3</sub>-treated neonatal cardiomyocytes after 5 days\*.  $P < 0.05$  for T<sub>3</sub>-treated vs non-treated; (n=8).

(A) Non-treated



(B) T3-treated

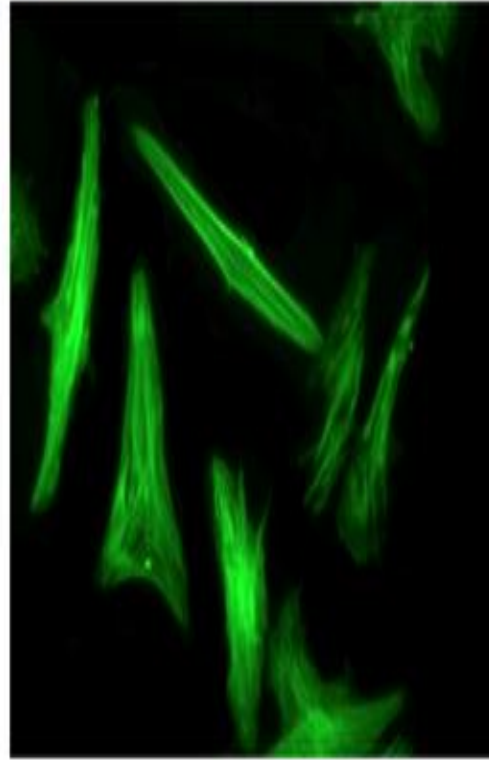


Figure 3.6: Images of (A) non-treated neonatal cardiomyocytes and (B) cardiomyocytes treated with T3 for 5 days, obtained by fluorescence microscopy after staining of actin cytoskeleton with phalloidin, n=8; (20 x magnification).

### **3.1.6. Cell area and protein synthesis in T<sub>3</sub>-treated undifferentiated cardiomyocytes**

The results presented in figure 3.7 show that the cell area was significantly increased ( $P < 0.05$ ) after 100 nM T<sub>3</sub> treatment. In fact, cell area was  $1.22 \pm 0.05$  fold more in T<sub>3</sub> treated as compared to non-treated cells.

Protein synthesis was also found to be significantly increased after T<sub>3</sub> treatment. In fact, protein content was  $1.3 \pm 0.06$  fold more in T<sub>3</sub> treated cells as compared to non-treated cells,  $P < 0.05$  (Figure 3.8).

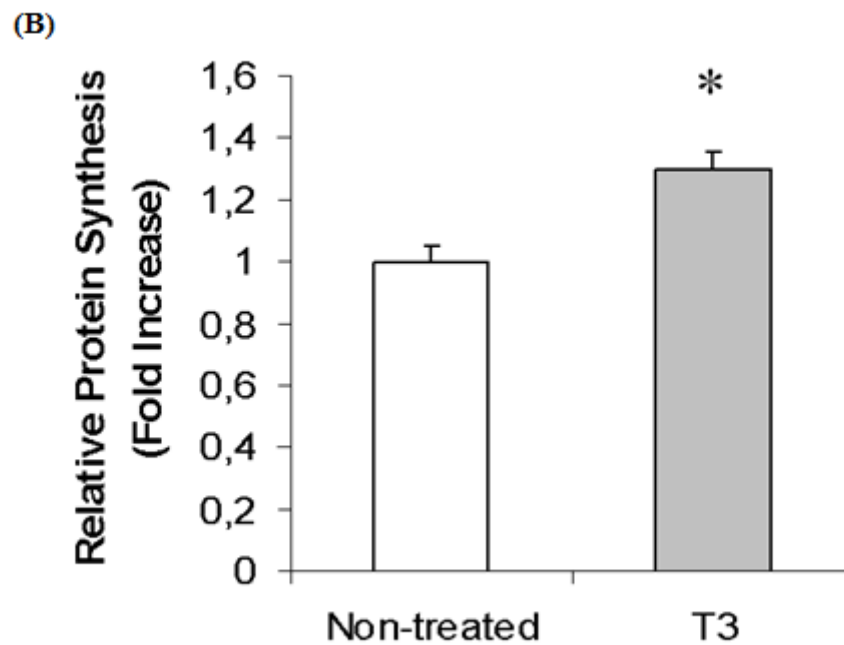
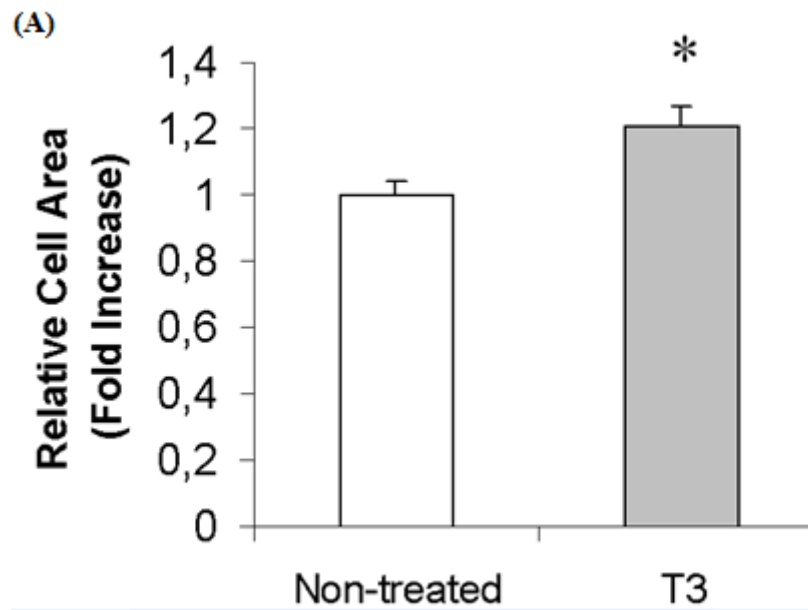


Figure 3.7-3.8: Cell area (A) and protein synthesis (B) in non-treated (open columns) and T<sub>3</sub>-treated (solid columns) neonatal cardiomyocytes after 5 days. Data are mean  $\pm$ SEM, \*  $P < 0.05$  for T<sub>3</sub>-treated vs non-treated,  $n=8$ .

### 3.1.7. Myosin heavy chain isoform expression in T<sub>3</sub>-treated undifferentiated cardiomyocytes

T<sub>3</sub> treatment resulted in a switch of the isoform expression of myosin from the  $\beta$ -isoform to the  $\alpha$ -isoform. T<sub>3</sub> cardiomyocytes expressed 100%  $\alpha$ -MHC and no signal was detected by immunostaining for  $\beta$ -MHC as compared to untreated cardiomyocytes expressing 100%  $\beta$ -MHC (Figure 3.9).

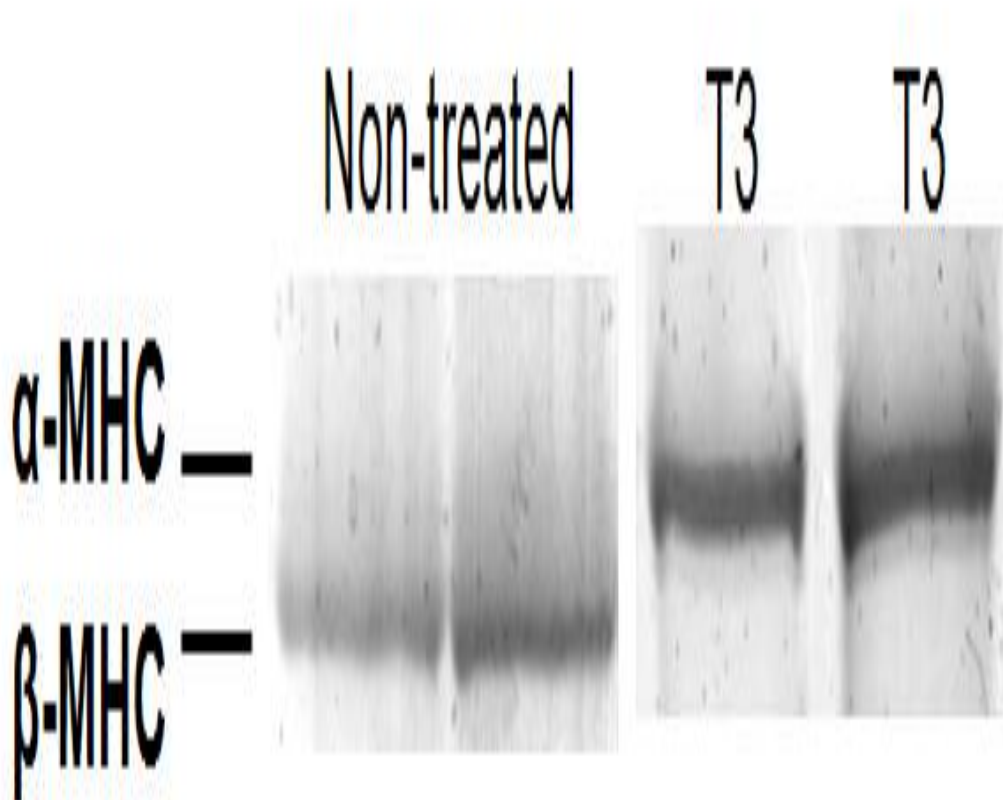


Figure 3.9: Image from electrophoresis showing myosin heavy chain isoform expression in non-treated neonatal cardiomyocytes and cardiomyocytes treated with T<sub>3</sub> (T<sub>3</sub>) for 5 days. T<sub>3</sub> treatment results in a switch of the isoform expression of myosin from the  $\beta$ -isoform to the  $\alpha$ -isoform, typical of 8 such different experiments.

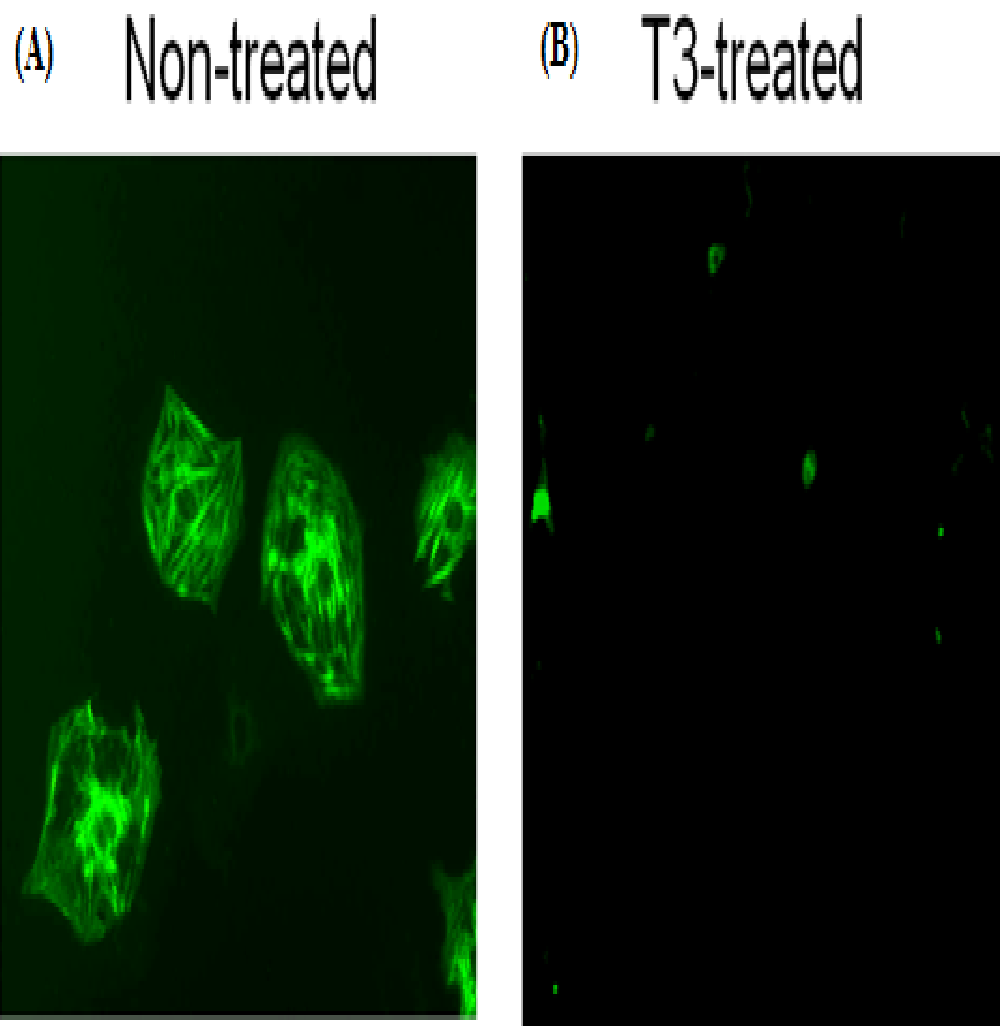


Figure 3.10: Images of (A) non-treated neonatal cardiomyocytes and (B) cardiomyocytes treated with T3 for 5 days, obtained by fluorescence microscopy after staining for slow ( $\beta$ )-myosin with specific antibody. The signal of  $\beta$ -myosin was almost undetectable in T3 cardiomyocytes. n=8; (20 x magnification).

## **Study 3**

### **3.1.8. Cell geometry and shape in T3-treated dedifferentiated cardiomyocytes**

PE-treated cardiomyocytes were large with disoriented, dense myofibrils and almost stellular shape. Morphologically, PE+T3-treated cells exhibited an elongated shape, with a filamentous actin pattern organized into orderly arrays resembling that of T3-treated cells (Figure 3.11).

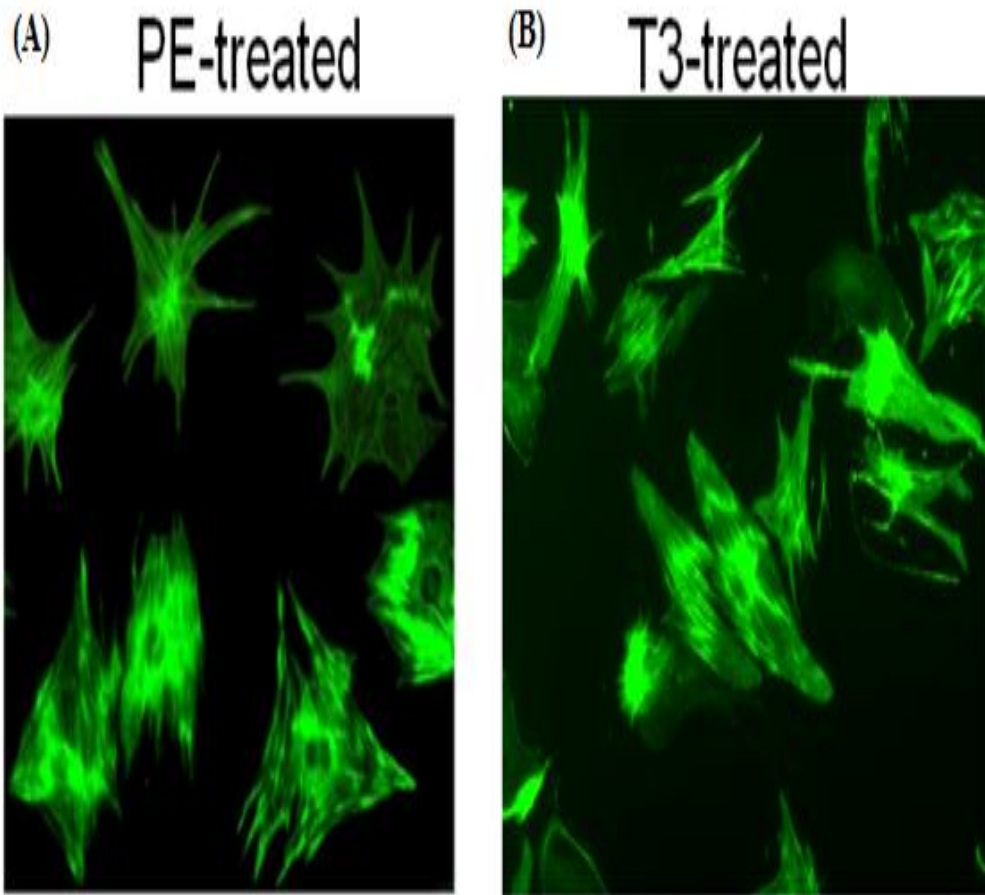


Figure 3.11: Images of (A) cardiomyocytes treated with phenylephrine (PE) and (B) cardiomyocytes treated with phenylephrine and T3 (PE+T3) for 5 days, obtained by fluorescence microscopy after staining of actin cytoskeleton with phalloidin. n=8, (20 x magnification).

### **3.1.9. Cell area and protein synthesis in T3 treated dedifferentiated cardiomyocytes**

T3 administration in PE-treated cardiomyocytes did not result in any change in cell area and protein synthesis.

### **3.1.10. Myosin isoform expression in T3 treated dedifferentiated cardiomyocytes**

PE-treated cardiomyocytes expressed 100%  $\beta$ -MHC. In contrast, T3 administration in PE-treated cardiomyocytes resulted in significantly reduced ( $P < 0.05$ ) amount of  $\beta$ -MHC (about 25% of the total myosin) and increased amount of  $\alpha$ -MHC (about 75% of the total myosin) (Figure 3.12).

The results presented in figure 3.12 also show that immunostaining for  $\beta$ -MHC resulted in a strong signal in PE-treated cardiomyocytes, while the signal was very weak in PE-T3 cardiomyocytes.

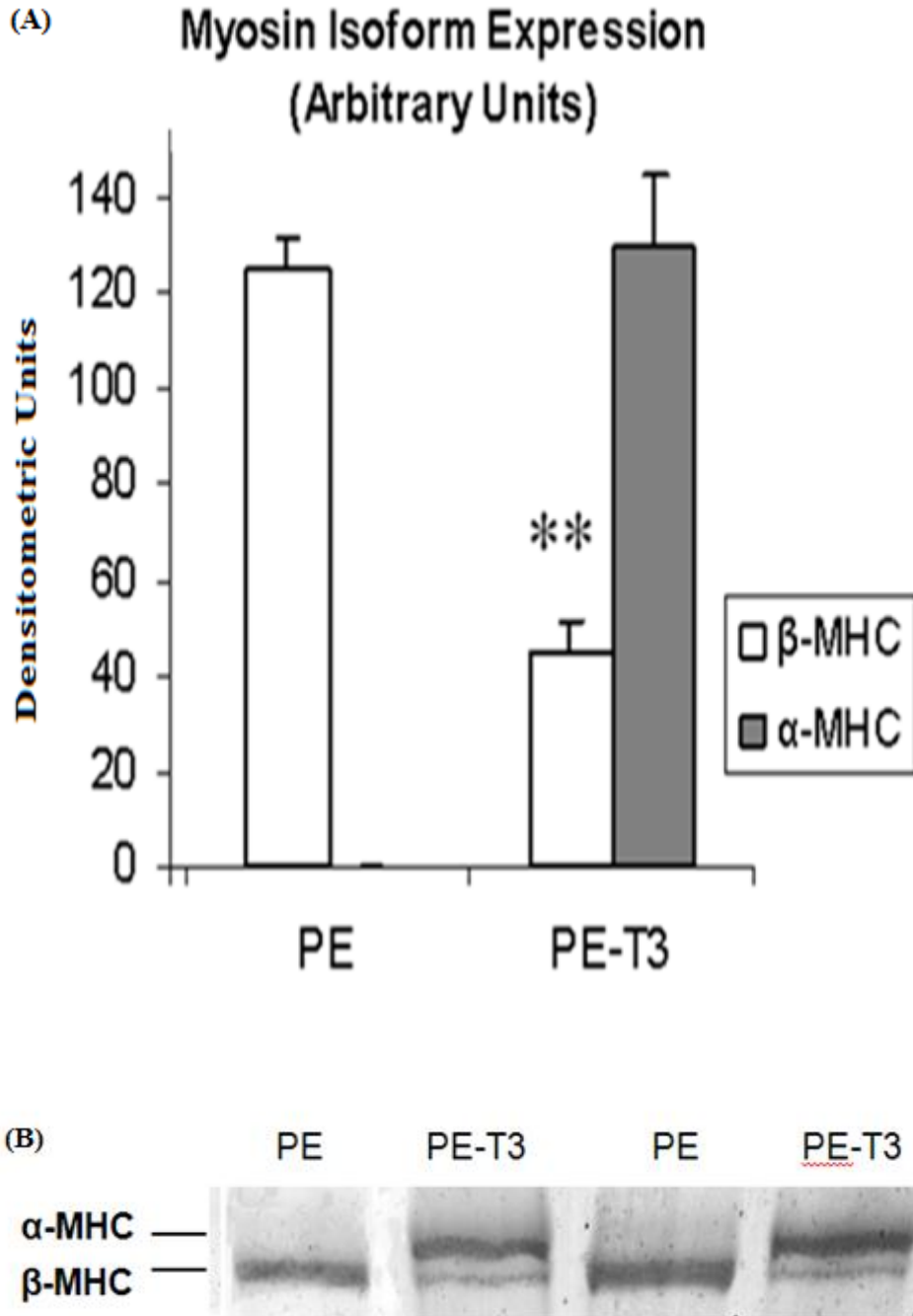


Figure 3.12: (A) Densitometric assessment in arbitrary units and (B) image of myosin heavy chain isoform expressions on cardiomyocytes treated with phenylephrine (PE) and cardiomyocytes treated with phenylephrine and T3 (PE-T3) for 5 days (Columns are means of optical ratios, bar=sem n=8); \*\*P<0.05 for PE+T3-treated vs PE.

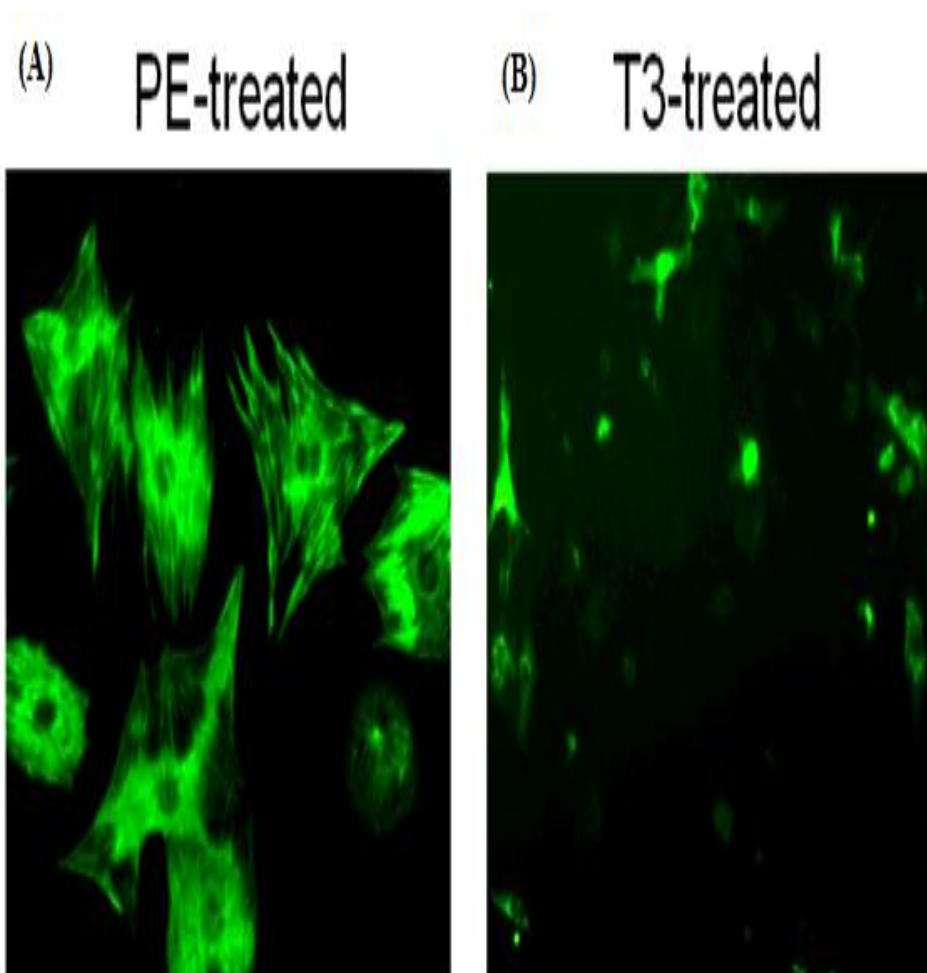


Figure 3.13: Images of (A) cardiomyocytes treated with phenylephrine (PE) and (B) cardiomyocytes treated with phenylephrine and T3 (PE+T3) for 5 days obtained by fluorescence microscopy after staining for slow ( $\beta$ )-myosin with specific antibody. Immunostaining for  $\beta$ -myosin produced a strong signal in PE-treated cardiomyocytes, while the signal of  $\beta$ -myosin was almost undetectable in PE-T3 cardiomyocytes. n=8, (20 x magnification).

## **3.2. Studies in Glioma cell lines**

### **3.2.1. Growth curves of 1321N1 and U87MG cell lines**

Growth curves of the non-treated groups in both cell lines (1321N1 and U87MG) were constructed to show the cell state (still multiplying and not having reached a confluent level) at the selected time points. Cells were counted within a 4x4 grid and then further two grids were counted to gain an average.

Figure 3.14 shows the growth curves of the two different cell lines between the non-treated groups. According to these data, cells reached the peak of growth after the period of 98 hours, while at 144 hours cells reached a confluent level and their number started to decrease indicating that after this point there was no more space to grow.

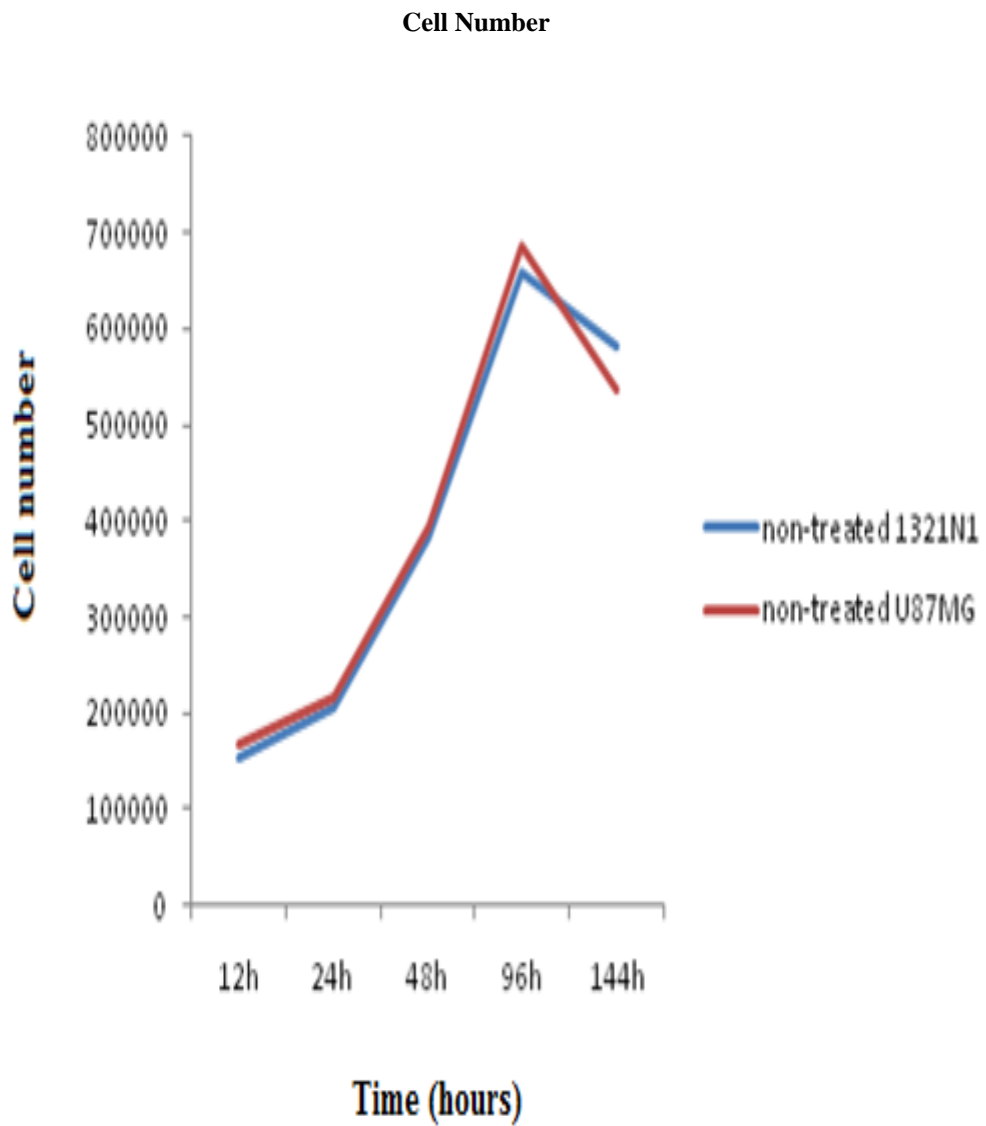


Figure 3.14: Time course growth curves showing the total number of 1321N1 and U87MG cells for the non-treated group over a period of 12, 24, 48, 96, and 144 hours. Data are mean of 8 experiments.

Generation of growth curves was necessary in evaluating the growth characteristics of each cell line under these conditions. From a growth curve, the population doubling time and saturation density can be determined. According to the data, cells reached the peak of growth after the period of 98 hours, while at 144 hours cells reached a confluent level and their number started to decrease indicating that after this point there was no more space to grow. Conclusions from these data were drawn indicating that the appropriate time-points to study the long-term effects of T3 were at 48 h and 96 h.

## **1321N1 Cell line**

### **3.2.2. Morphological characteristics of glioma cell lines**

#### **3.2.2.1. Cell morphology-2 days**

Figures 3.16-3.18 show typical images of 1321N1 cells following incubation with either no T3 (untreated group, image 3.15), 1 nM T3 (figure 3.16), and 500 nM T3 (figure 3.17). The results show that both 1 nM and 500 nM of T3 can induce the number of projections of the cells, but decreases the geometrical size of the cell compared to untreated cells. These images were analysed and the data are presented in figure 3.18.

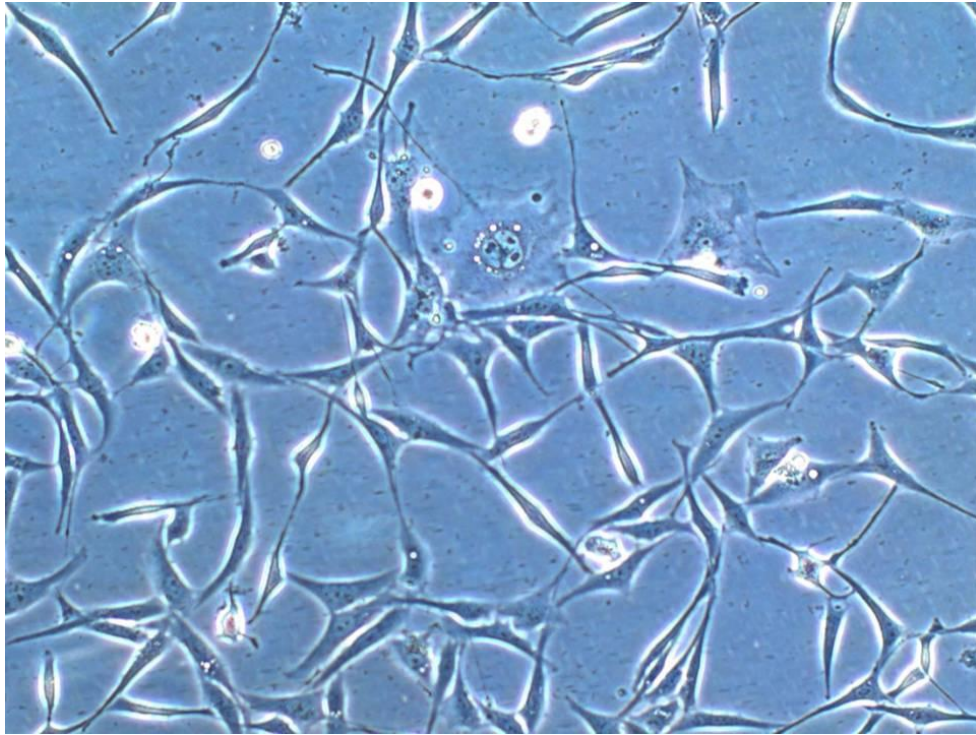


Figure 3.15: Image taken by phase-contrast optical microscopy. Characteristics such as cellular length, width, and number of projections in non-treated 1321N1 cell line after the period of 2 days are shown. This photograph is typical for  $n=8$  such different experiments (20 x magnification).

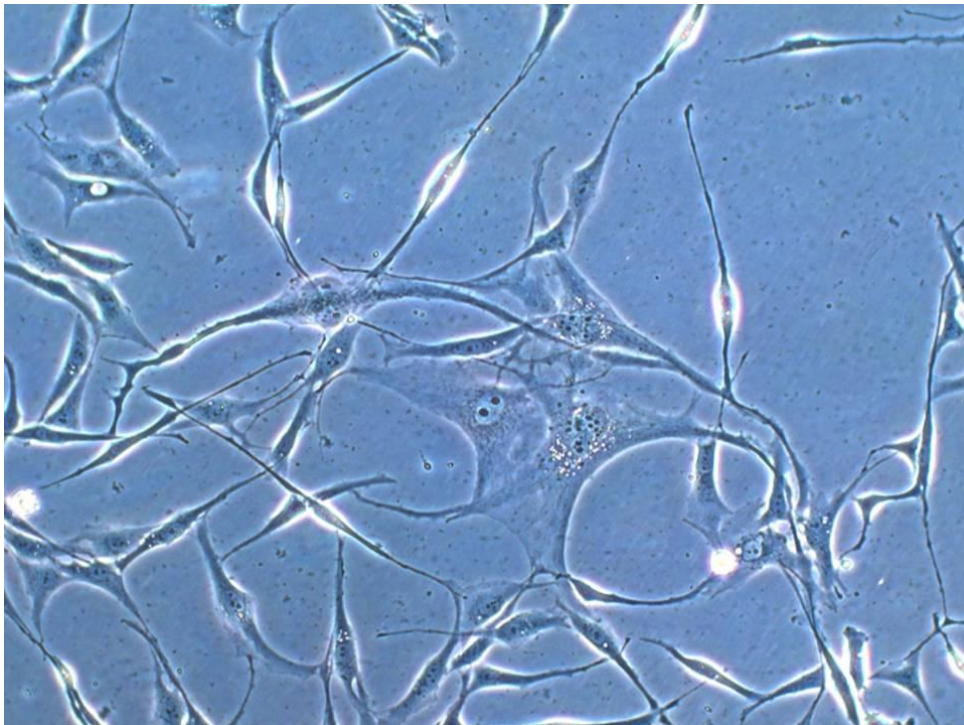


Figure 3.16: Image taken by phase-contrast optical microscopy. Characteristics such as cellular length, width, and number of projections in 1 nM T3-treated 1321N1 cells after the period of 2 days are shown. This photograph is typical for  $n=8$  such different experiments (20 x magnification).

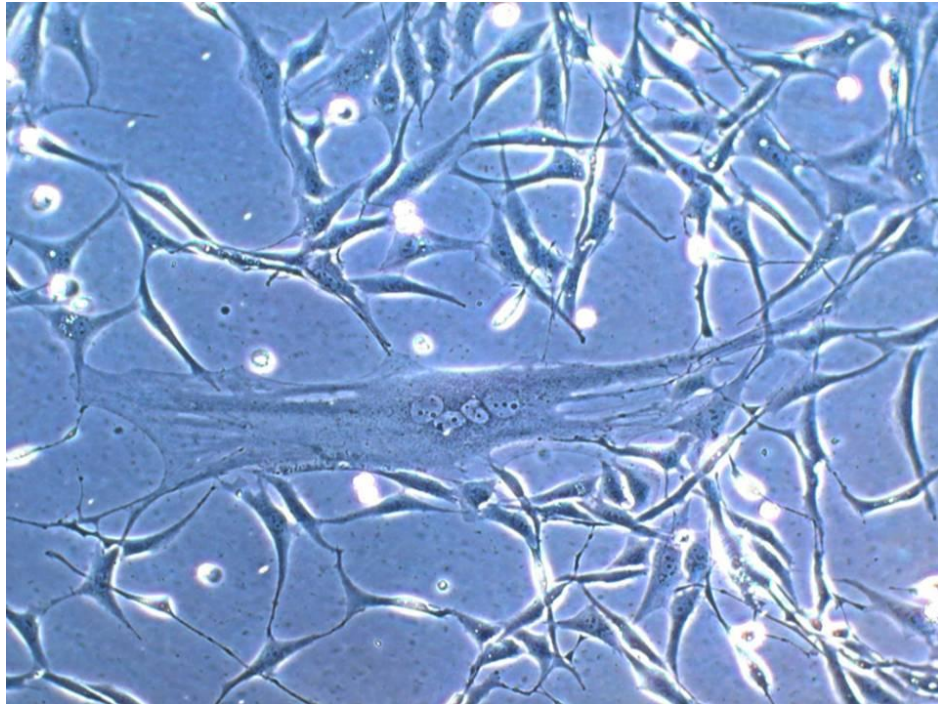


Figure 3.17: Image taken by phase-contrast optical microscopy. Characteristics such as cellular length, width, and number of projections in 500 nM T3-treated 1321N1 cells after the period of 2 days are shown. This photograph is typical for n=8 such different experiments (20 x magnification).

Figure 3.18 shows (A) the number of projections and (B) the shape of 1321N1 cells on 2 days following incubation with either 1 nM T3 or 500 nM T3 compared to the untreated group. The data show that treatment of 1321N1 glioma cells with 1 nM T3 can result in a significant ( $p < 0.05$ ) increase in cell projections, but no change in the shape of the cells. The ratio of total number of projections to total number of cells was  $1.04 \pm 0.14$  for non-treated vs  $1.9 \pm 0.11$  for 1 nM T3,  $p < 0.05$ , and  $2.0 \pm 0.14$  for 500 nM T3 treated cells,  $p < 0.05$  vs non-treated.

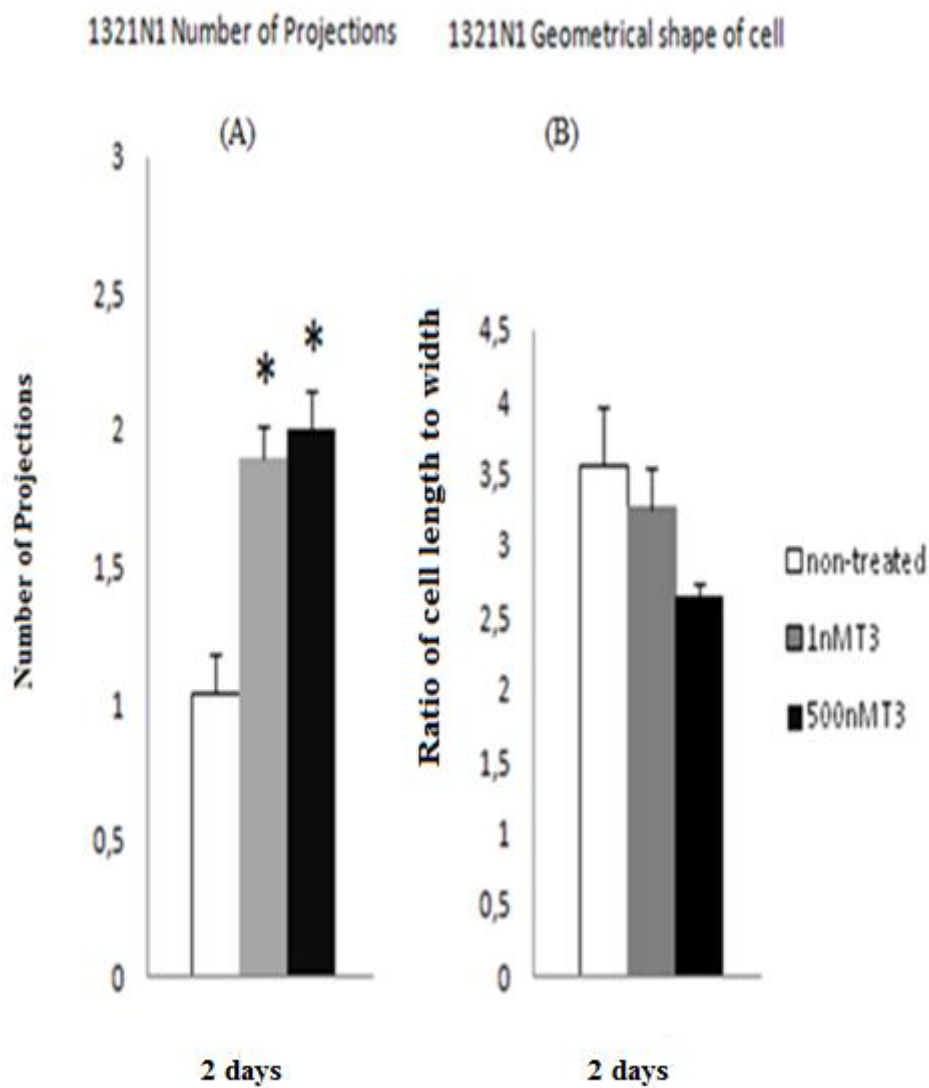


Figure 3.18: Bar charts showing changes in the number of projections (A) and ratio of cell length /width (B) of 1231N1 cell line after the period of 2 days. \*  $p < 0.05$  for treated vs non-treated cells,  $n=8$ , Data are mean  $\pm$ SEM.

### 3.2.2.2. Cell morphology-4 days

Figures 3.19-3.21 show typical images of 1321N1 cells following 4 days of incubation with either no T3 (untreated group, image 3.19), 1 nM T3 (image 3.20), or 500 nM T3 (image 3.21). Close observation of figures 3.20-3.22 shows the morphological difference of 1321N1 cell line over the period of 4 days between the non-treated group, and the groups treated with 1 nM and 500 nM T3 on the ratio of cell length /width and the number of projections. Cells were over confluent (over 80%) after the period of 4 days and no quantitative data could be obtained regarding the measurement of number of projections and the ratio of cell length /width.

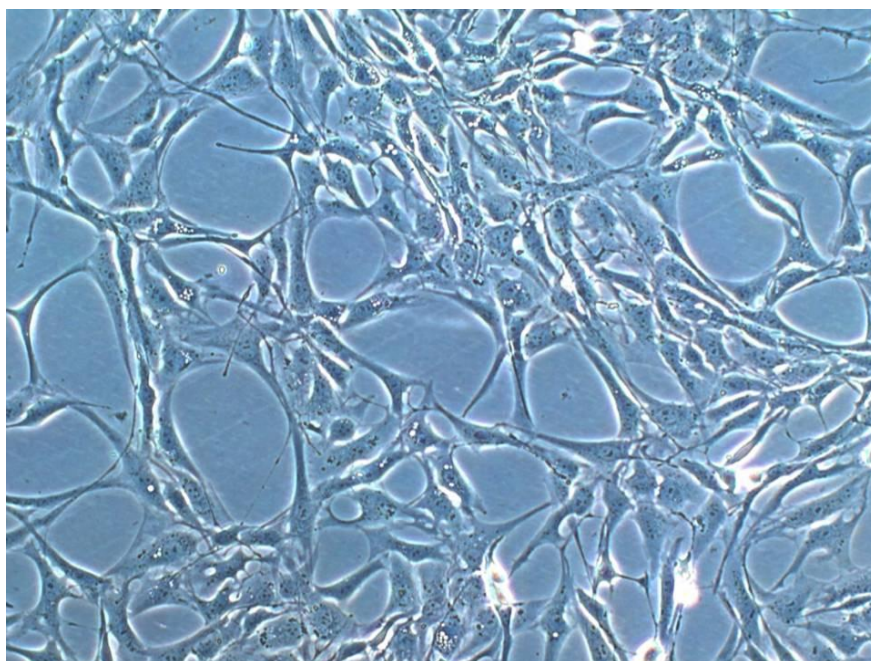


Figure 3.19: Image taken by phase-contrast optical microscopy. In this and subsequent figures of images characteristics such as cellular length, width, and number of projections in non-treated 1321N1 cells after the period of 4 days are shown for comparison. This photograph is typical for n=8 such different experiments (20 x magnification).

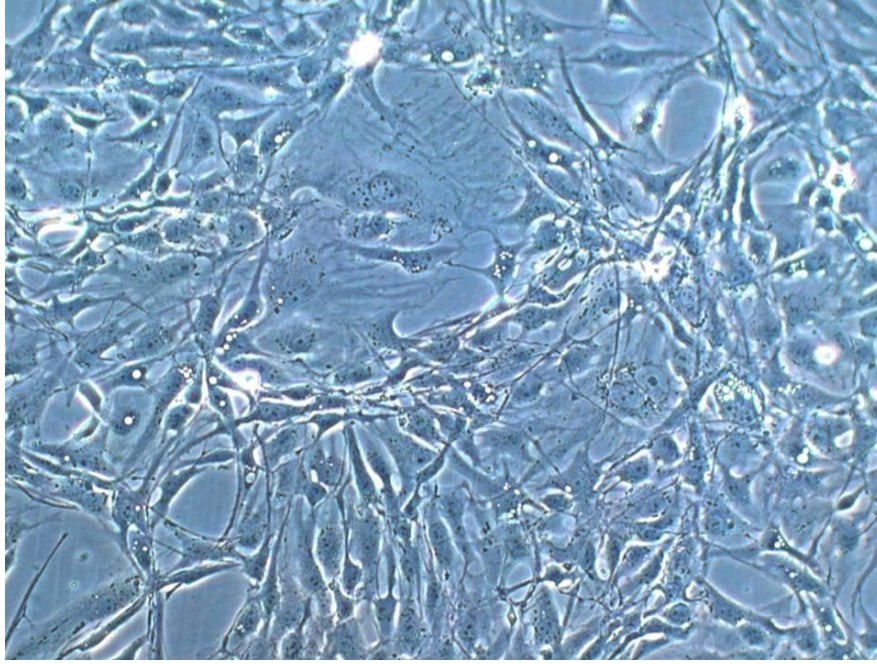


Figure 3.20: Image taken by phase-contrast optical microscopy. Characteristics such as cellular length, width, and number of projections in 1 nM T3-treated 1321N1 cells after the period of 4 days are shown. This photograph is typical for  $n=8$  such different experiments (20 x magnification).

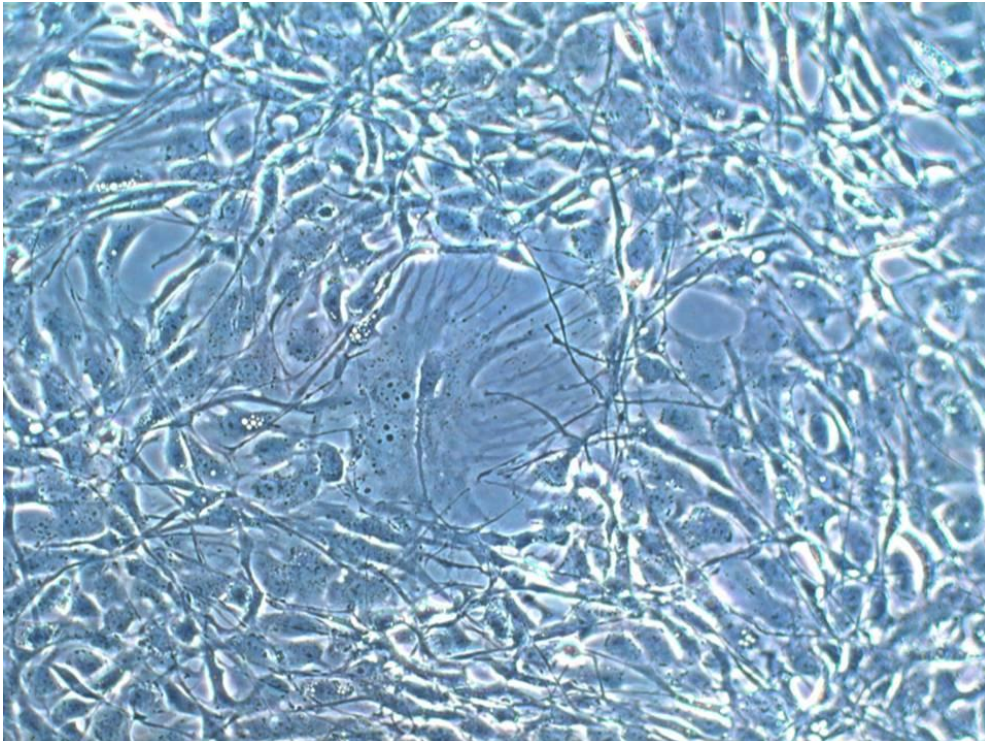


Figure 3.21: Image taken by phase-contrast optical microscopy. Characteristics such as cellular length, width, and number of projections in 500 nM T3-treated 1321N1 cells after the period of 4 days are shown. This photograph is typical for  $n=8$  such different experiments (20 x magnification).

### **3.2.3. Cell count of glioma cell lines**

#### **3.2.3.1. Total cell number count 2 days**

Figure 3.22 shows the numbers of untreated and treated 1321N1 glioma cells following incubation with either 1 nM T3 or 500 nM T3 for 2 days. The results show that there was a significant increase ( $p < 0.05$ ) on the total number of the cells in both treatment groups (1 nM and 500 nM) in comparison with the non-treated group. Total number of cells were found to be  $207183 \pm 2145$  for non-treated vs  $232366 \pm 2390$  for 1 nM T3,  $p < 0.05$ , and  $241283 \pm 2818$  for 500 nM T3 treated cells,  $p < 0.05$  vs non-treated.

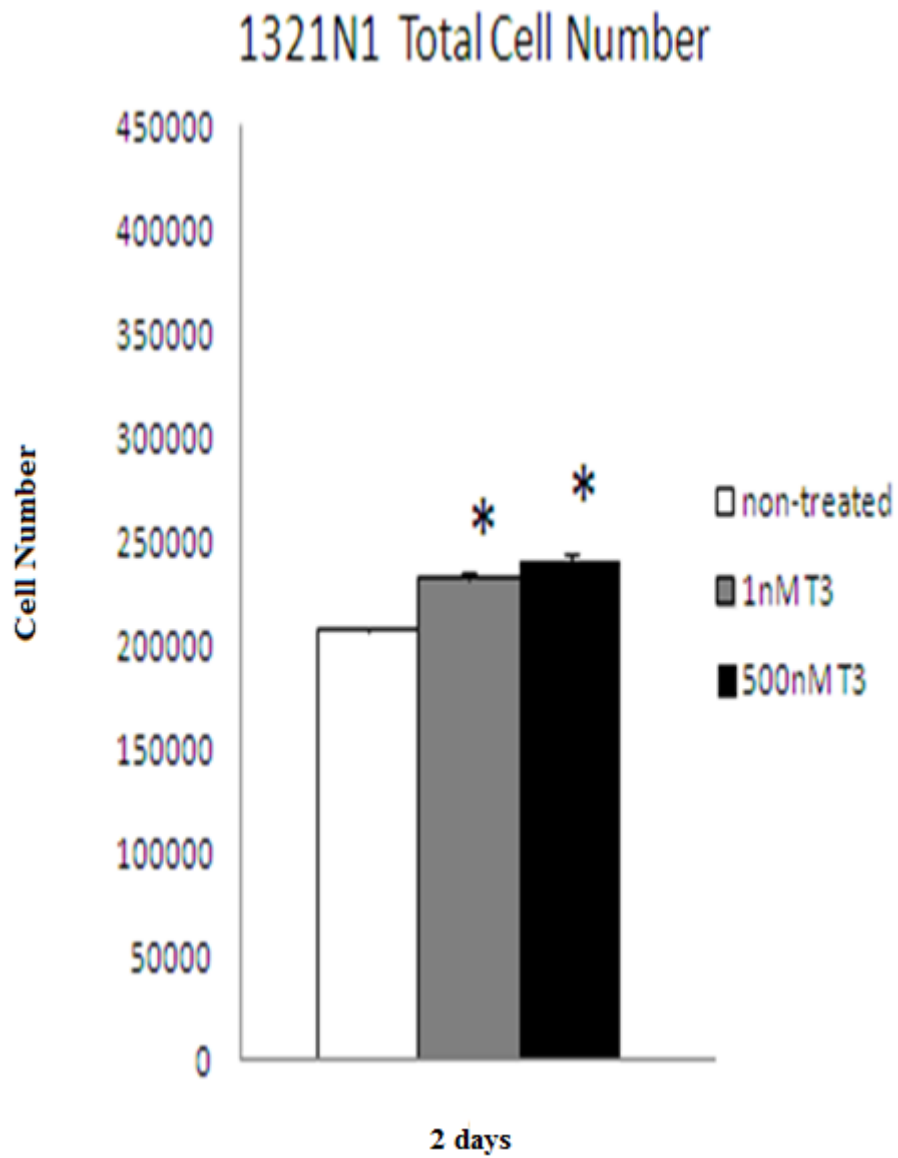


Figure 3.22: Bar chart showing the total number of 1321N1 cells between the untreated and treated cells with either 1 nM or 500 nM T3 over a period of 2 days. Data are mean  $\pm$ SEM,  $n=8$ ;  $p<0.05$  for treated cells compared to untreated cells.

### **3.2.3.2. Total cell count 4 days**

Figure 3.23 shows the numbers of untreated and treated 1321N1 glioma cells following incubation with either 1 nM T3 or 500 nM T3 for 4 days. The results show no significant differences ( $p>0.05$ ) in the total number of the 1321N1 cells between the non-treated, 1 nM and 500 nM T3 treatment groups for the period of 4 days.

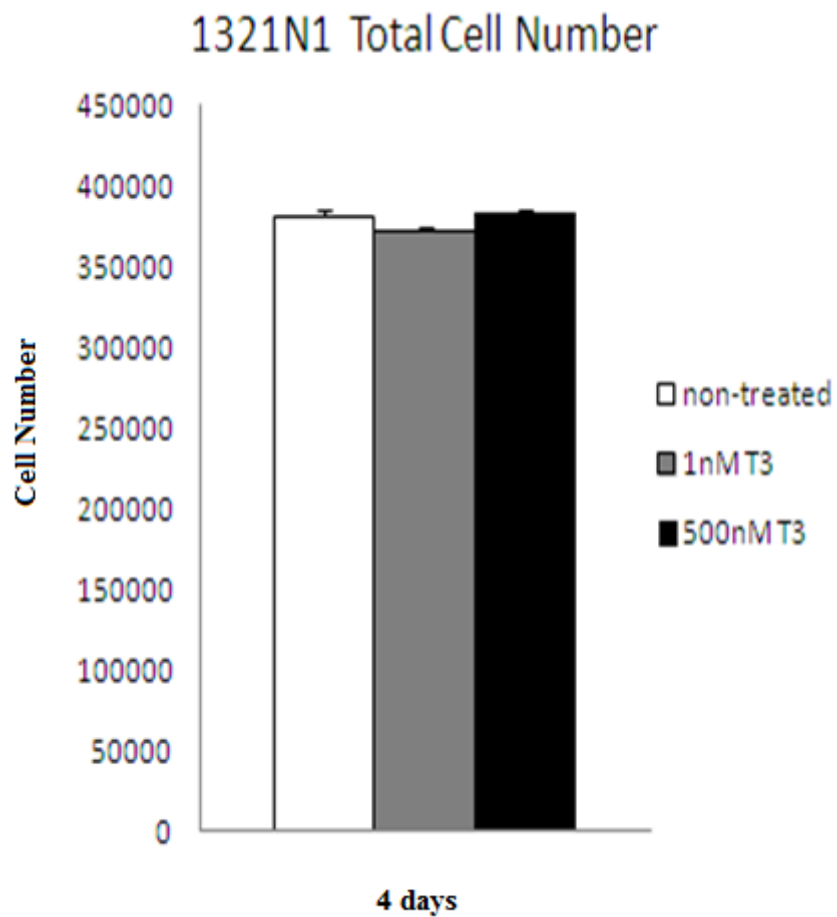


Figure 3.23: Bar chart showing the total number of 1321N1 cells between the untreated and treated cells with either 1 nM or 500 nM T3 over a period of 4 days. Data are mean  $\pm$ SEM, n=8; Note that there was no significant differences between the data in either of the three groups.

### 3.2.4. Cell proliferation of glioma cell lines

#### 3.2.4.1. Cell proliferation-2 days

Figures 3.24-3.26 show the nucleus of 1321N1 cells following incubation with either no T3 (untreated group, figure 3.24), 1 nM T3 (figure 3.25), and 500 nM T3 (figure 3.26). The results show that either 1 nM or 500 nM of T3 can induce cell proliferation in comparison with the untreated group.

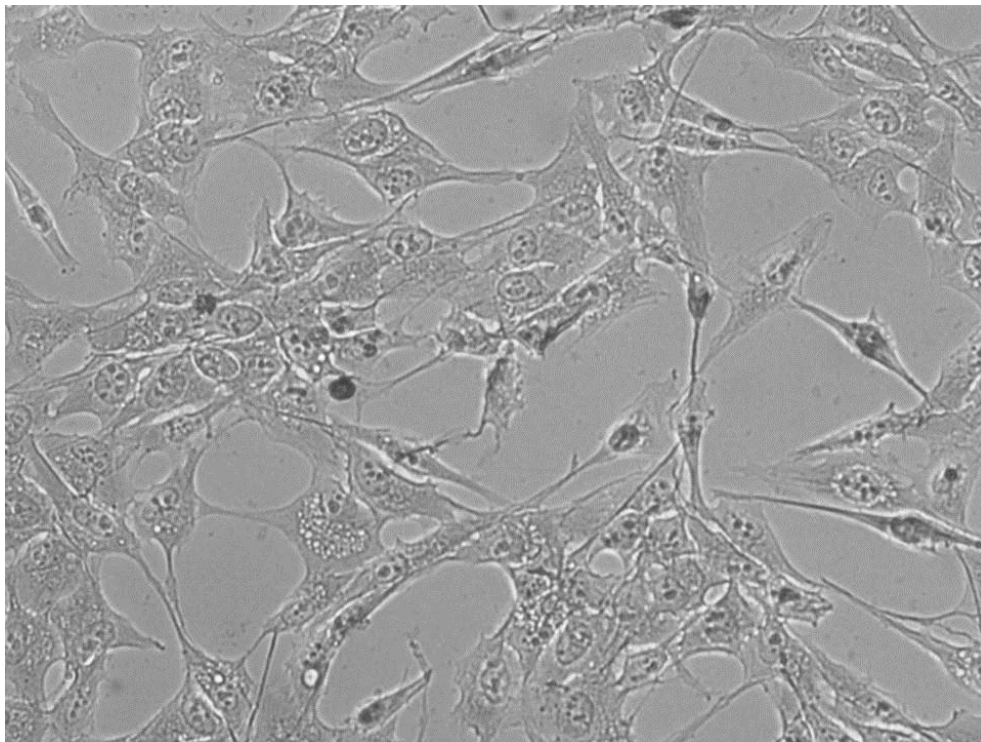


Figure 3.24: A typical photograph showing the proliferation of the 1321N1 cells on the non-treated group. The nuclei that were stained black represent the cells that are replicating their DNA. This photograph is typical for n=8 such different experiments (20 x magnification).

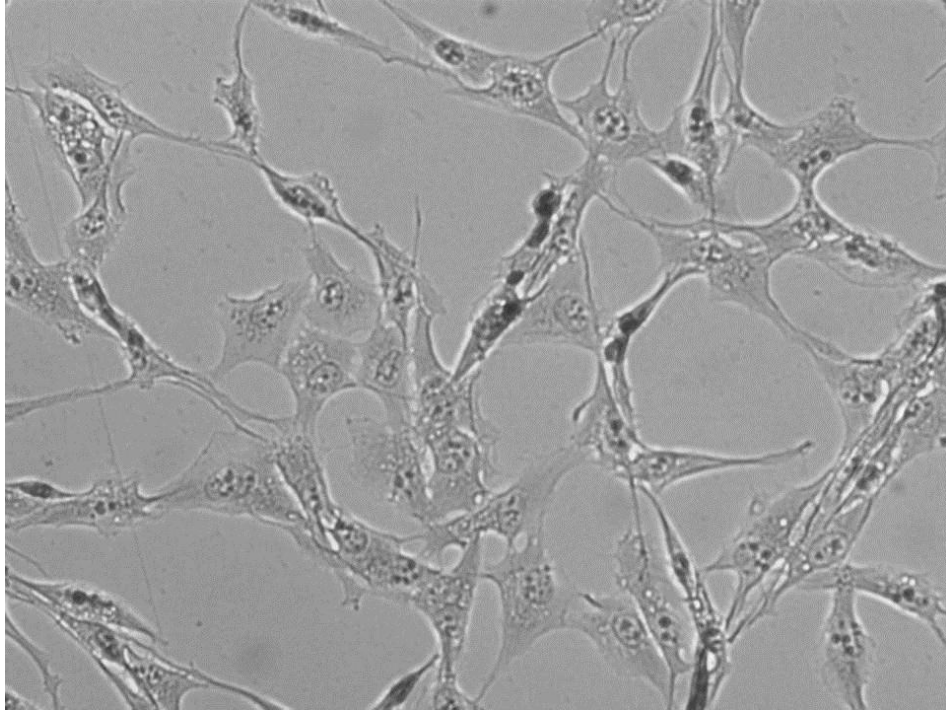


Figure 3.25: A typical photograph showing the proliferation of the 1321N1 cells on the 1nM T3 treated group. The nuclei that were stained black represent the cells that are replicating their DNA. This photograph is typical for  $n=8$  such different experiments (20 x magnification).

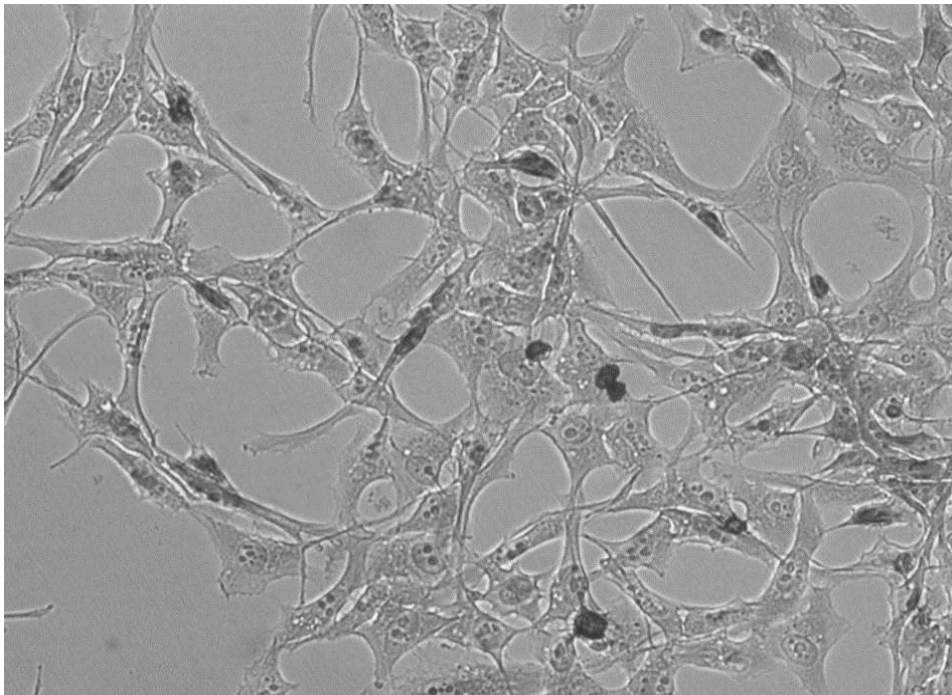


Figure 3.26: A typical photograph showing the proliferation of the 1321N1 cells on the 500nM T3 treated group. The nuclei that were stained black represent the cells that are replicating their DNA. This photograph is typical for  $n=8$  such different experiments (20 x magnification).

Figure 3.27 shows the proliferation percentage of 1321N1 glioma cells in untreated group and groups treated with either 1 nM or 500 nM T3 over a period of 2 days. The results have demonstrated a significant increase ( $p < 0.05$ ) in cell proliferation in both treatment groups (1 nM and 500 nM) in comparison with the non-treated group. The ratio was  $23.6 \pm 3\%$  in non-treated vs  $30.5 \pm 3\%$  in 1 nM T3,  $p < 0.05$ , and  $31.6 \pm 2\%$  in 500 nM T3 treated cells,  $p < 0.05$  vs non-treated.

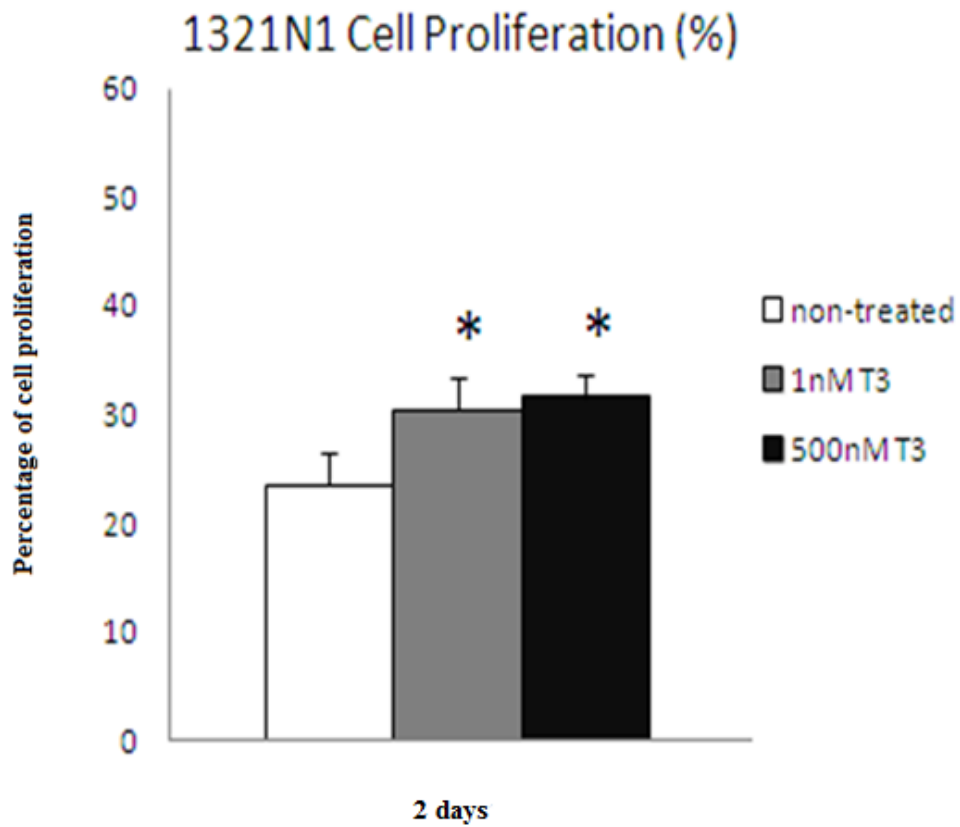


Figure 3.27: Bar chart showing the percentages of cell proliferation of the 1321N1 cell line for untreated group and groups treated with either 1 nM T3 or 500 nM T3 for 2 days. Data are mean  $\pm$  SEM, n=8; \*p<0.05 for untreated cells compare to treated cells with 1 nM T3 or 500 nM T3.

#### 3.2.4.2. Cell proliferation-4 days

Figures 3.28-3.30 show the nucleus of 1321N1 cells following incubation with either no T3 (untreated group, figure 3.28), 1 nM T3 (figure 3.29), and 500 nM T3 (figure 3.30). The results show no significant differences ( $p>0.05$ ) between the groups after the period of 4 days.

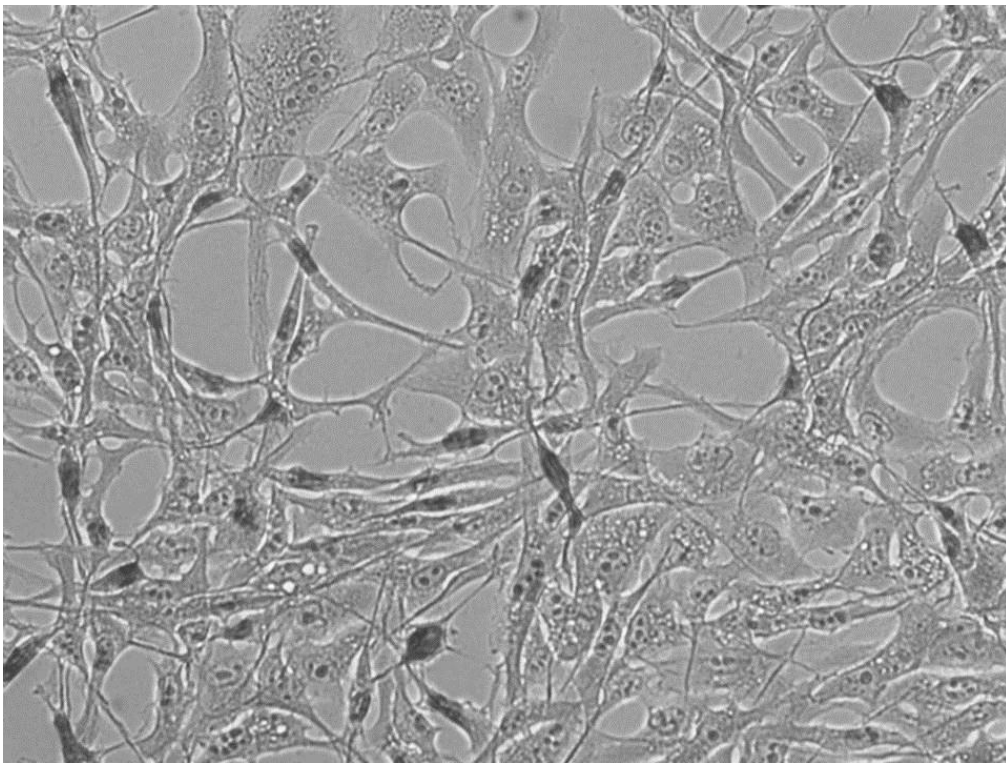


Figure 3.28: A typical photograph showing the proliferation of the 1321N1 cells on the non-treated group. The nuclei that were stained black represent the cells that are replicating their DNA. This photograph is typical for  $n=8$  such different experiments (20 x magnification).

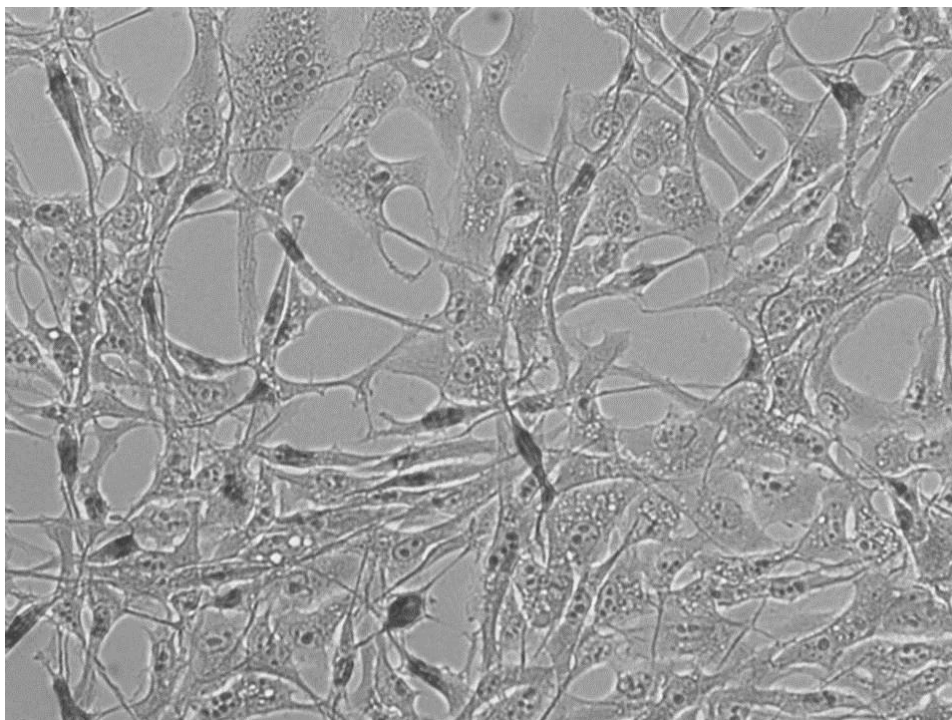


Figure 3.29: A typical photograph showing the proliferation of the 1321N1 cells on the 1 nM T3 treated group. The nuclei that were stained black represent the cells that are replicating their DNA. This photograph is typical for n=8 such different experiments (20 x magnification).

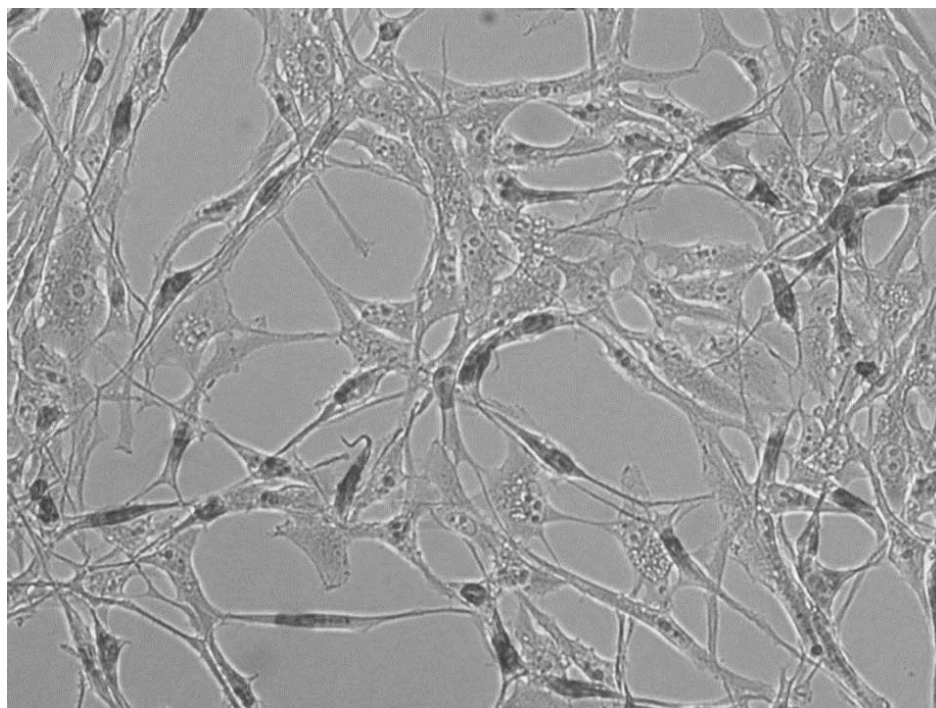


Figure 3.30: A typical photograph showing the proliferation of the 1321N1 cells on the 500 nM T3 treated group. The nuclei that were stained black represent the cells that are replicating their DNA. This photograph is typical for n=8 such different experiments (20 x magnification).

Figure 3.31 shows the proliferation percentage of 1321N1 glioma cells in untreated group and groups treated with either 1 nM or 500 nM T3 over a period of 4 days. The results show no significant difference ( $p>0.05$ ) between the non-treated and the T3 treated groups on the 1321N1 cell line. The ratio was  $45.2 \pm 5\%$  in non-treated vs  $40 \pm 6\%$  in 1 nM T3,  $p>0.05$ , and  $43.8 \pm 5\%$  in 500 nM T3 treated cells,  $p>0.05$  vs non treated.

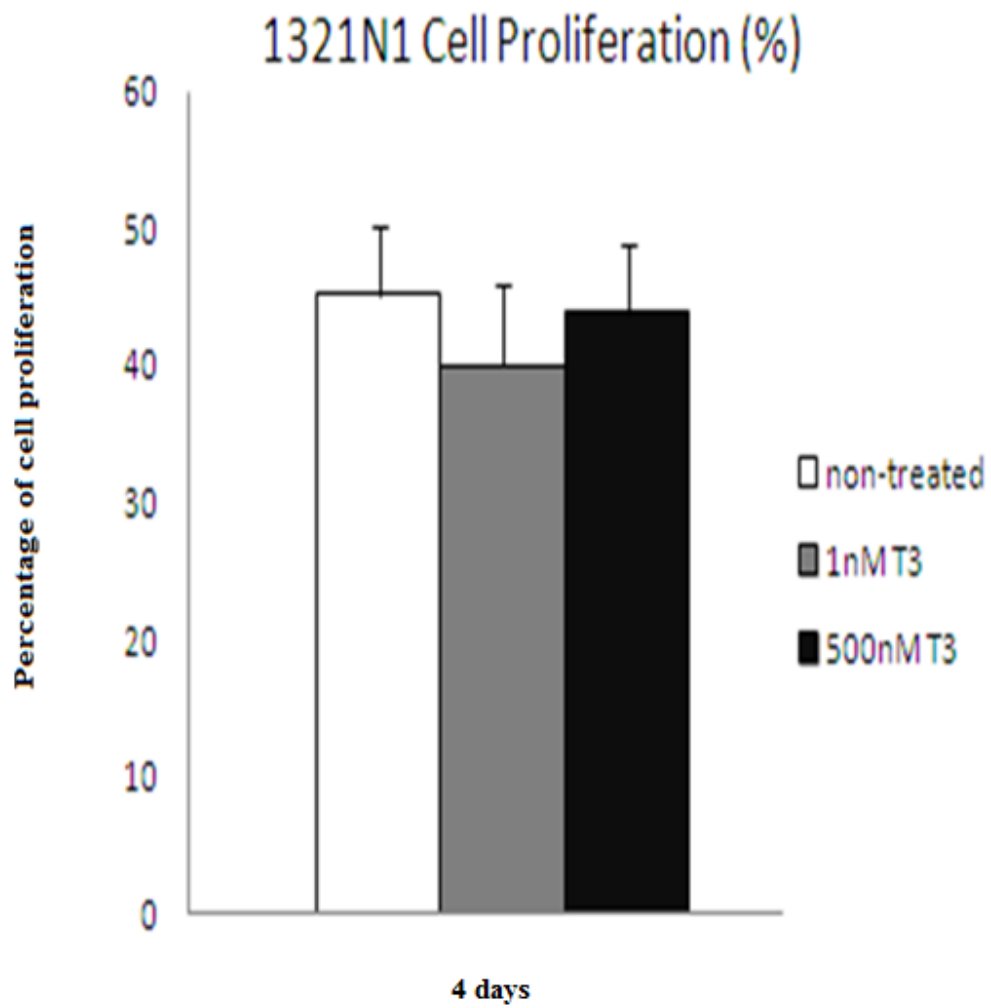


Figure 3.31: Bar chart showing the percentage of cell proliferation of the 1321N1 cell line for untreated group and groups treated with either 1 nM T3 or 500 nM T3 for 4 days. Data are mean  $\pm$ SEM, n=8. Note that there was no significant difference in the percentage of cell proliferation between the groups.

### **3.2.5. Levels of injury on glioma cell lines**

#### **3.2.5.1. Cell necrosis-2 days**

Figure 3.32 shows the percentage of LDH levels in the culture medium for untreated and treated 1321N1 cells incubated with either 1 nM or 500 nM for 2 days. The results show no significant difference ( $p>0.05$ ) in the LDH levels between the three groups of the 1321N1 cell line for the 2 day treatment with T3. The ratio was  $100 \pm 2.3\%$  for non-treated vs  $103.2 \pm 4.2\%$  for 1 nM T3,  $p>0.05$ , and  $100.2 \pm 4.1\%$  for 500 nM T3 treated cells,  $p>0.05$  vs non-treated. These results indicated that no injury seems to take place in the cells following T3 treatment.

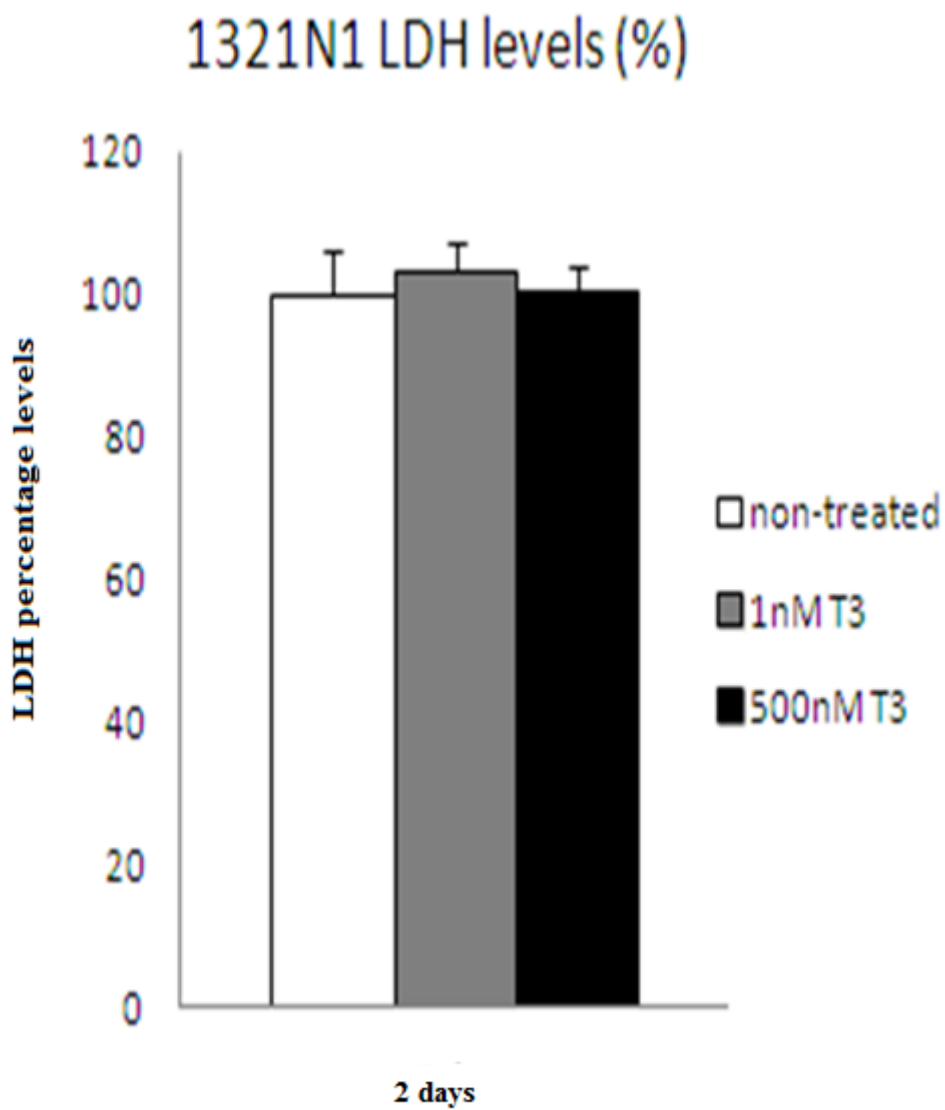


Figure 3.32: Bar charts showing the LDH release in culture medium in the three groups (non-treated, 1 nM, and 500 nM) of the 1321N1 cell line. The results are expressed as the percentage of the non-treated group, in comparison with the two treatment groups. Data are mean  $\pm$ SEM, n=8; Note that there is no significant difference between the untreated and the 1 nM and 500 nM treatment groups.

### 3.2.5.2. Cell necrosis-4 days

Figure 3.33 shows the percentage of LDH levels in the culture medium for untreated and treated 1321N1 cells incubated with either 1 nM or 500 nM for 4 days. The results show no significant difference ( $p>0.05$ ) in the LDH levels between the three groups of the 1321N1 cell line for the 4 day treatment with T3. The ratio was  $100 \pm 5.2$  for non-treated vs  $103.8 \pm 5.1\%$  for 1 nM T3,  $p>0.05$ , and  $108.2 \pm 4\%$  for 500 nM T3 treated cells,  $p>0.05$  vs non-treated. The results clearly show that T3 has no effect on 1321N1 cells even after 4 days of treatment.

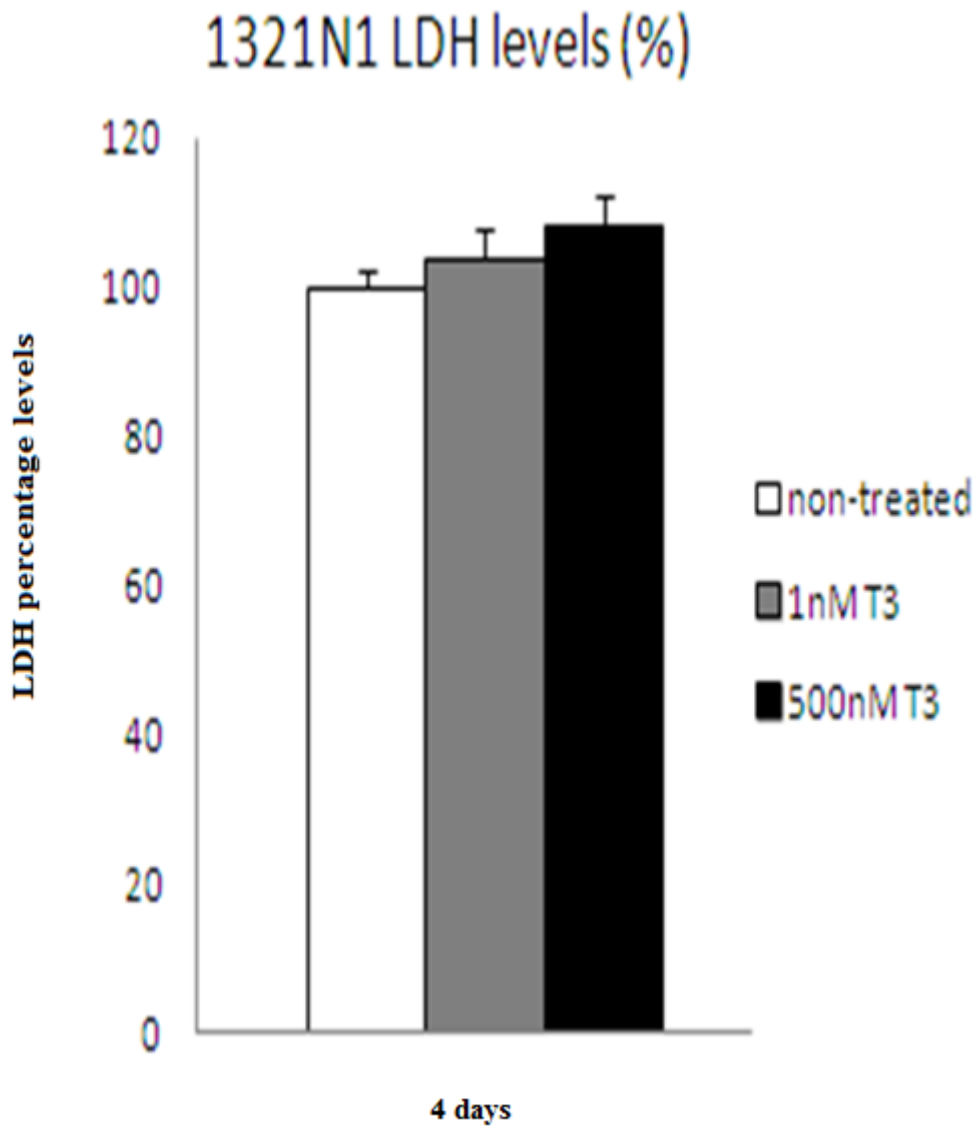


Figure 3.33. Bar charts showing the LDH release in culture medium in the three groups (non-treated, 1 nM, and 500 nM) of the 1321N1 cell line. The results are expressed as the percentage of the non-treated group, in comparison with the two treatment groups. Data are mean  $\pm$ SEM, n=8; Note that there is no significant difference between the untreated and the 1 nM and 500 nM treatment groups.

### **3.2.6. Levels of apoptosis on glioma cell lines**

#### **3.2.6.1. Cell apoptosis-2 days**

The images in figures 3.34-3.35 show the nucleus of 1321N1 cells following treatment with 10  $\mu$ l doxorubicin. Administration of doxorubicin is known to induce apoptosis and this drug was used as a positive control in order to certify the selected method. Apoptotic cell nuclei were assessed by TUNNEL staining using the In Situ Cell Death Detection Kit.

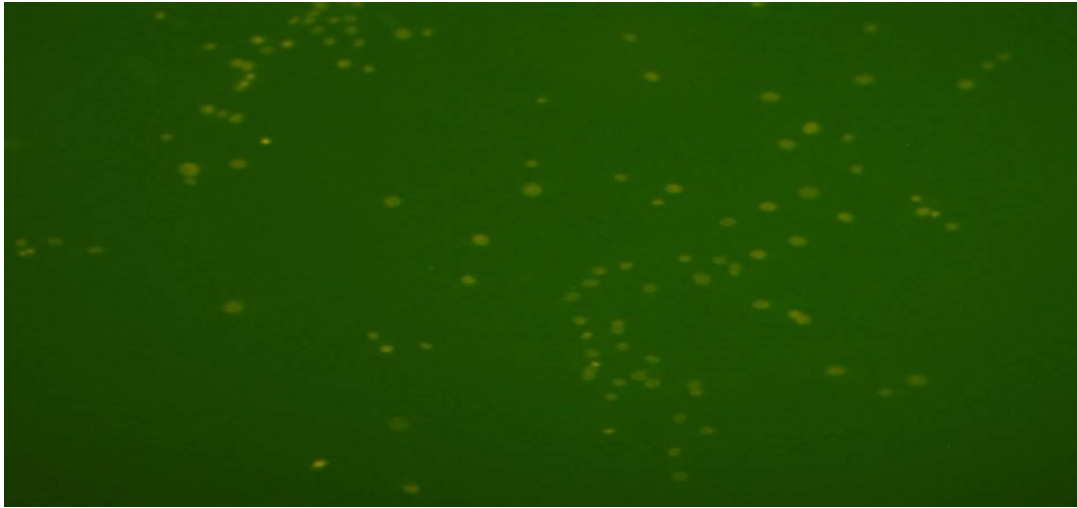


Figure 3.34: Image showing the apoptotic nuclei of the 1321N1 cells that were treated with doxorubicin. . The image was taken by fluorescence microscopy with a special filter for fluorescein detection. This photograph is typical for n=8 such different experiments (10 x magnification).

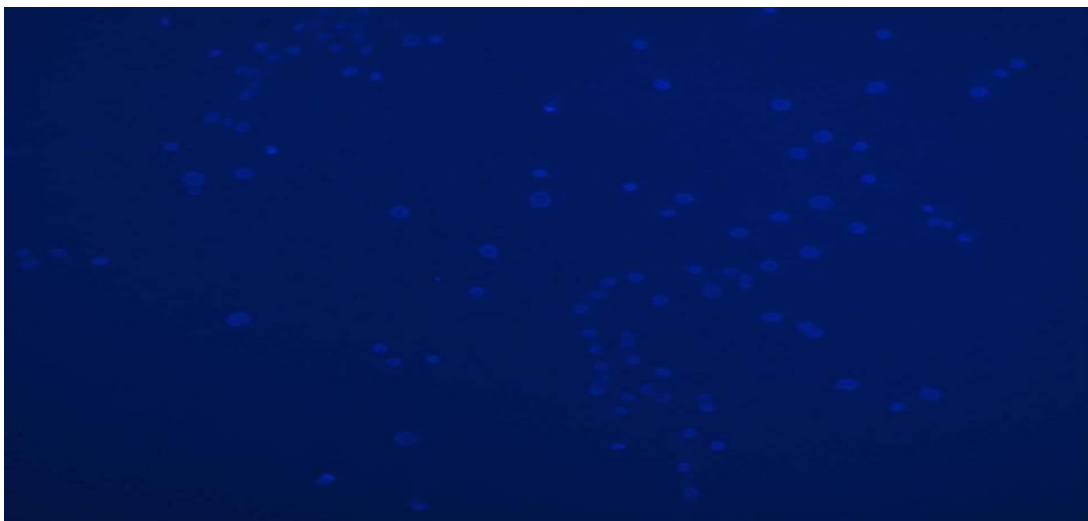


Figure 3.35: Image showing all the nuclei of the 1321N1 cells that were treated with doxorubicin after counterstained with Hoeschst 33358. The image was taken by fluorescence microscopy with a special filter for Hoeschst 33358. This photograph is typical for n=8 such different experiments (10 x magnification).

The images in figures 3.36-3.37 show the stained nucleus of 1321N1 cell line for the untreated cells over the period of 2 days. As shown on the images, there was no apoptotic cells on the untreated group of the 1321N1 cell line, in comparison with the

total number of cells stained on the figure 3.37. After the period of 2 days the cells were stained, and were viewed with a fluorescence microscope.

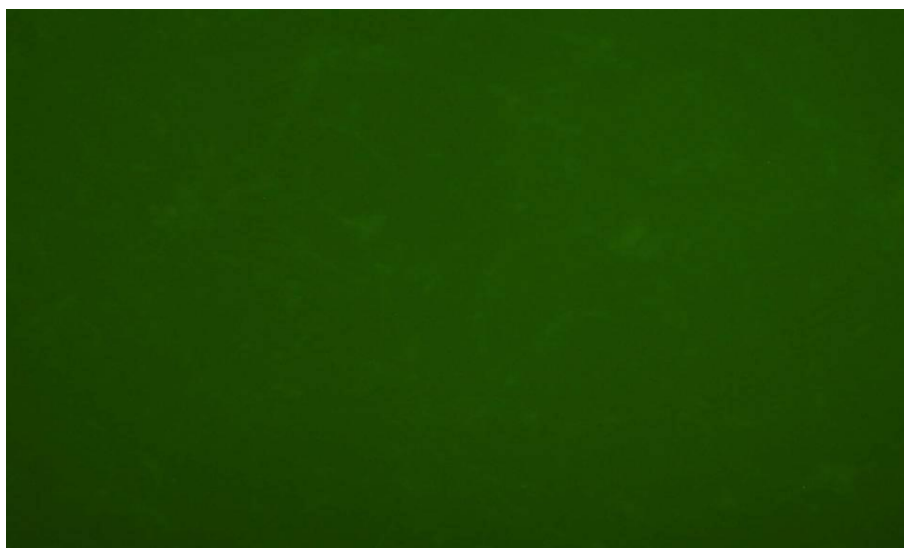


Figure 3.36: Image showing non-treated 1321N1 cells after staining for TUNNEL. No apoptotic cells were detected. This photograph is typical for n=8 such different experiments (10 x magnification).

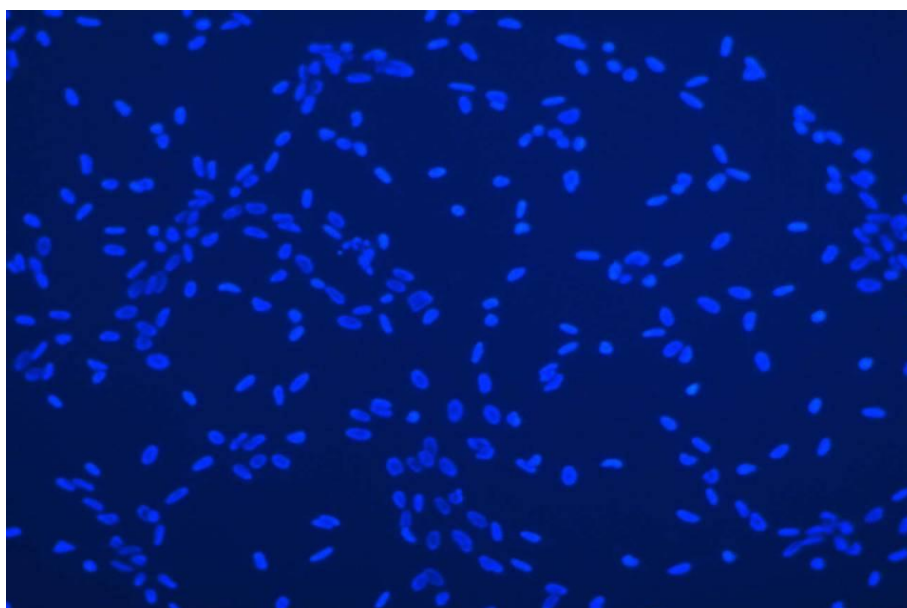


Figure 3.37: Image showing the total number of cells of the 1321N1 cell line on the non-treated group after staining with Hoeschst 33358. This photograph is typical for n=8 such different experiments (10 x magnification).

The images in figures 3.38-3.39 show the stained nucleus of 1321N1 cell line for the 1 nM T3 treated cells over the period of 2 days. As shown on the images, there was no apoptotic cells on 1 nM T3 group of the 1321N1 cell line, in comparison with the total

number of cells stained on the figure 3.39. After the period of 2 days the cells were stained, and were viewed with a fluorescence microscope.

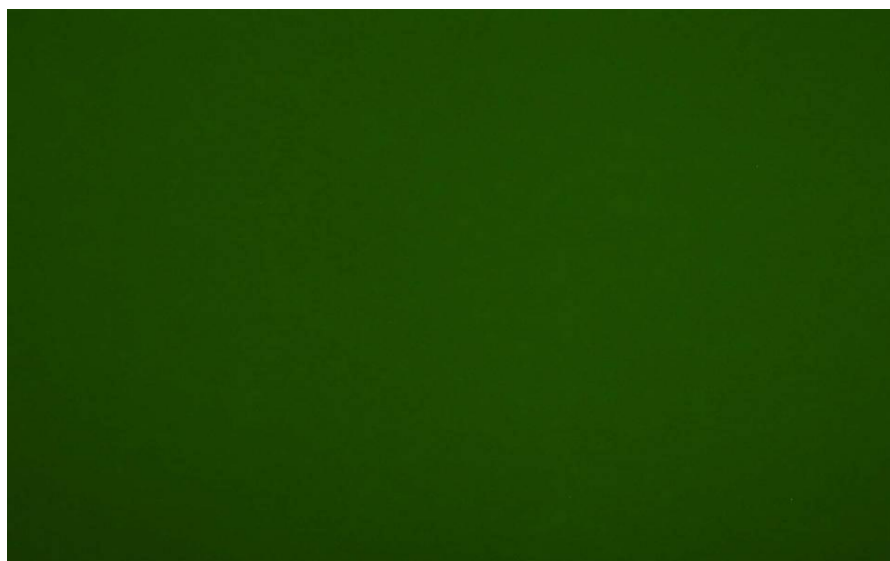


Figure 3.38: Image showing 1321N1 cells treated with 1 nM T3 after staining for TUNNEL. No apoptotic cells were detected. This photograph is typical for n=8 such different experiments (10 x magnification).

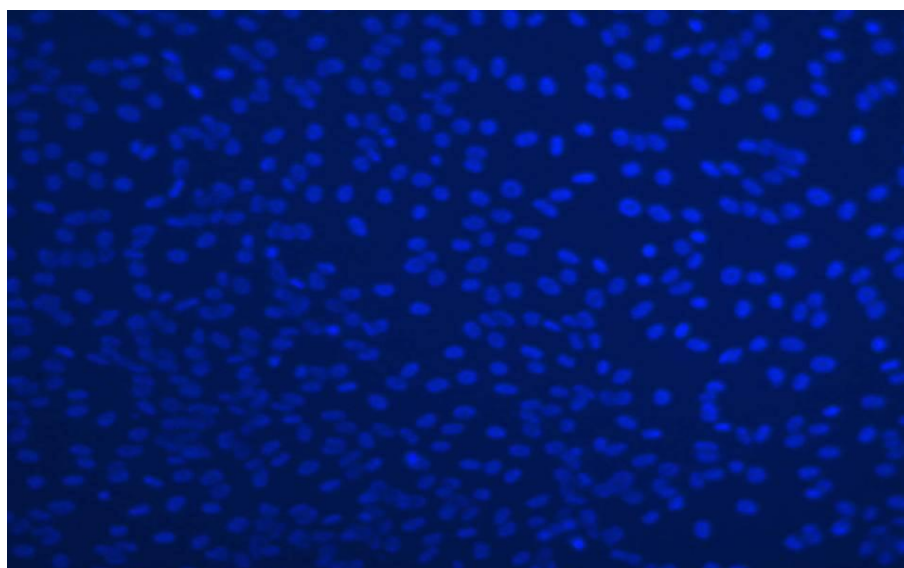


Figure 3.39: Image showing the total number of 1321N1 cells treated with 1 nM T3 after staining with Hoeschst 33358. This photograph is typical for n=8 such different experiments (10 x magnification).

The images in figures 3.40-3.41 show the stained nucleus of 1321N1 cell line for the 500 nM T3 treated cells over the period of 2 days. As shown on the images there was no apoptotic cells on 500 nM T3 group of the 1321N1 cell line, in comparison with

the total number of cells stained on the figure 3.41. After the period of 2 days the cells were stained, and were viewed with a fluorescence microscope.



Figure 3.40: Image showing 1321N1 cells treated with 500 nM T3 after staining for TUNNEL. No apoptotic cells were detected. This photograph is typical for n=8 such different experiments (10 x magnification).

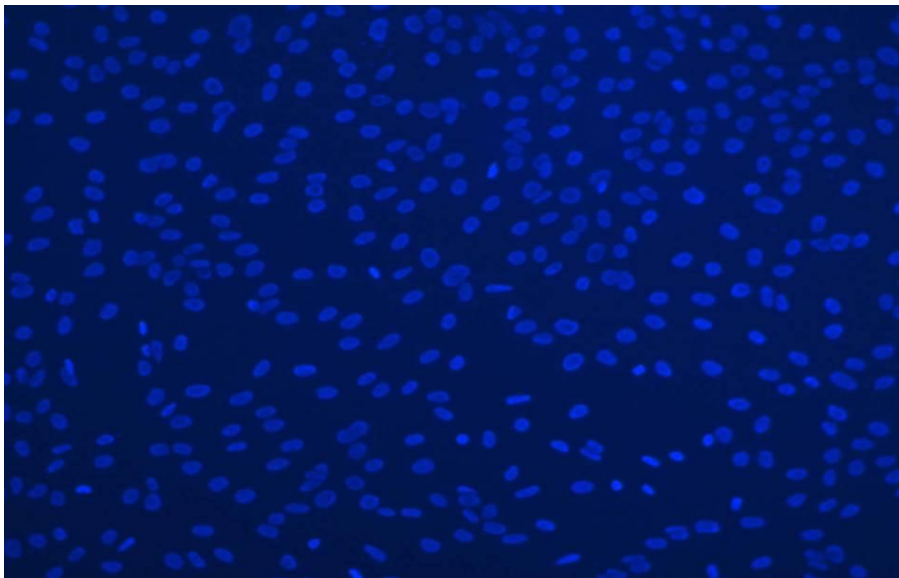


Figure 3.41: Image showing the total number of 1321N1 cells treated with 500 nM T3 after staining with Hoeschst 33358. This photograph is typical for n=8 such different experiments (10 x magnification).

### 3.2.6.2. Cell apoptosis 4 days

The images in figures 3.42-3.43 show the nucleus of 1321N1 cells following treatment with 10  $\mu$ l doxorubicin. Administration of doxorubicin is known to induce apoptosis and was used as a positive control in order to certify the selected method. Apoptotic cell nuclei were assessed by TUNNEL staining using the In Situ Cell Death Detection Kit.



Figure 3.42: Image showing the apoptotic nuclei of the 1321N1 cells that were treated with doxorubicin. . The image was taken by fluorescence microscopy with a special filter for fluorescein detection. This photograph is typical for n=8 such different experiments (10 x magnification).

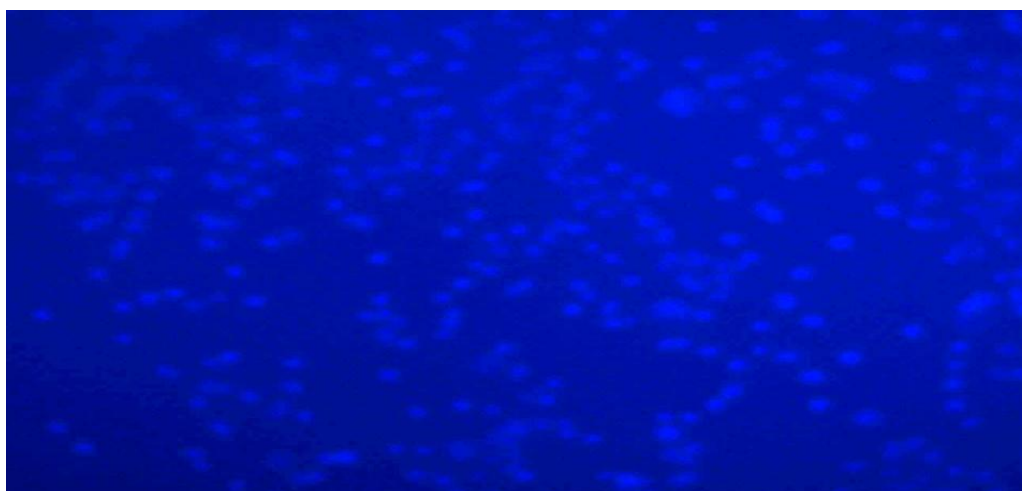


Figure 3.43: Image showing all the nuclei of the 1321N1 cells that were treated with doxorubicin after counterstained with Hoeschst 33358. The image was taken by fluorescence microscopy with a special filter for Hoeschst 33358. This photograph is typical for n=8 such different experiments (10 x magnification).

The images in figures 3.44-3.45 show the stained nucleus of 1321N1 cell line for the untreated cells over the period of 4 days. As shown on the images, there was no apoptotic cells on the untreated group of the 1321N1 cell line, in comparison with the total number of cells stained on the figure 3.31. After the period of 4 days the cells were stained, and were viewed with a flurescence microscope.



Figure 3.44: Image showing non-treated 1321N1 cells after staining for TUNNEL. No apoptotic cells were detected. This photograph is typical for n=8 such different experiments (10 x magnification).

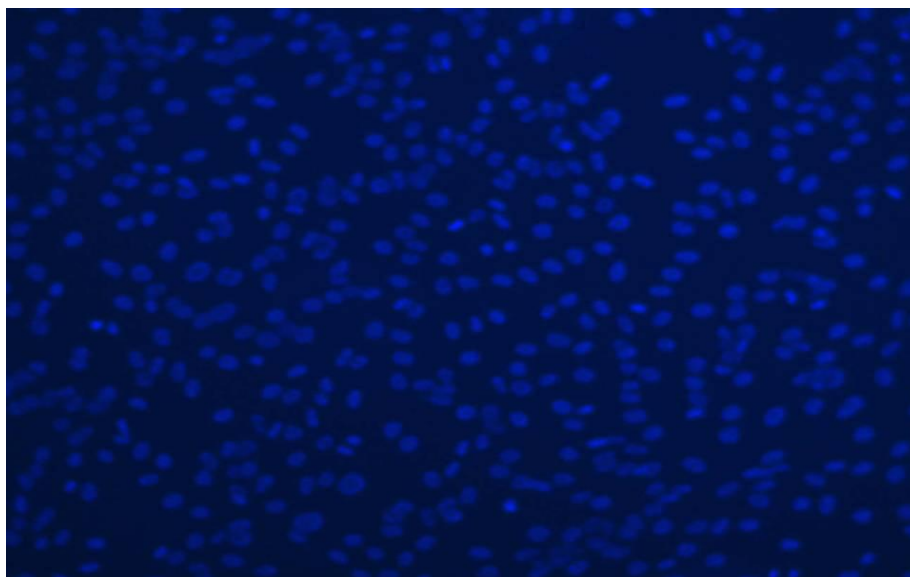


Figure 3.45: Image showing the total number of cells of the 1321N1 cell line on the non-treated group after staining with Hoeschst 33358. This photograph is typical for n=8 such different experiments (10 x magnification).

The images in figures 3.46-3.47 show the stained nucleus of 1321N1 cell line for the 1 nM T3 treated cells over the period of 4 days. As shown on the images, there was no apoptotic cells on 1 nM T3 group of the 1321N1 cell line, in comparison with the total number of cells stained on the figure 3.47. After the period of 4 days the cells were stained, and were viewed with a fluorescence microscope.

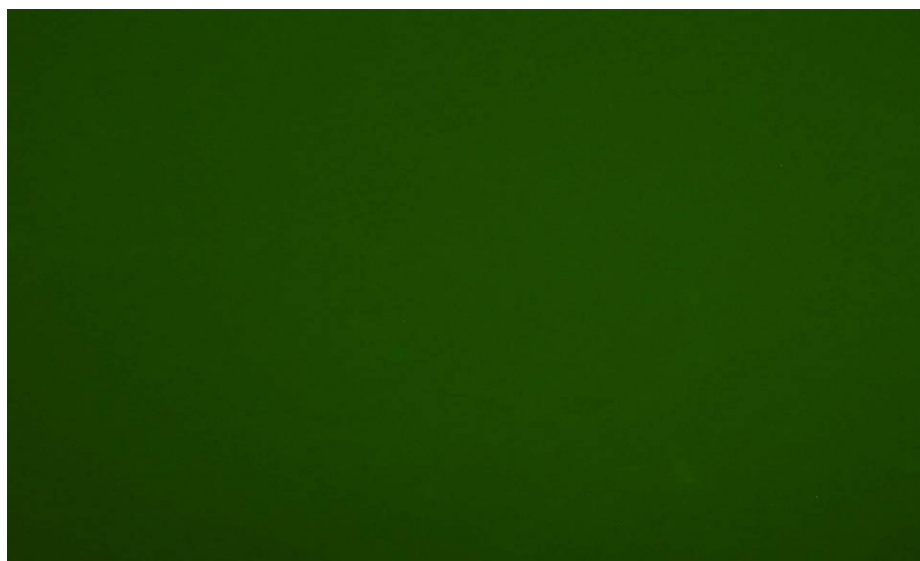


Figure 3.46: Image showing 1321N1 cells treated with 1 nM T3 after staining for TUNNEL. No apoptotic cells were detected. This photograph is typical for n=8 such different experiments (10 x magnification).

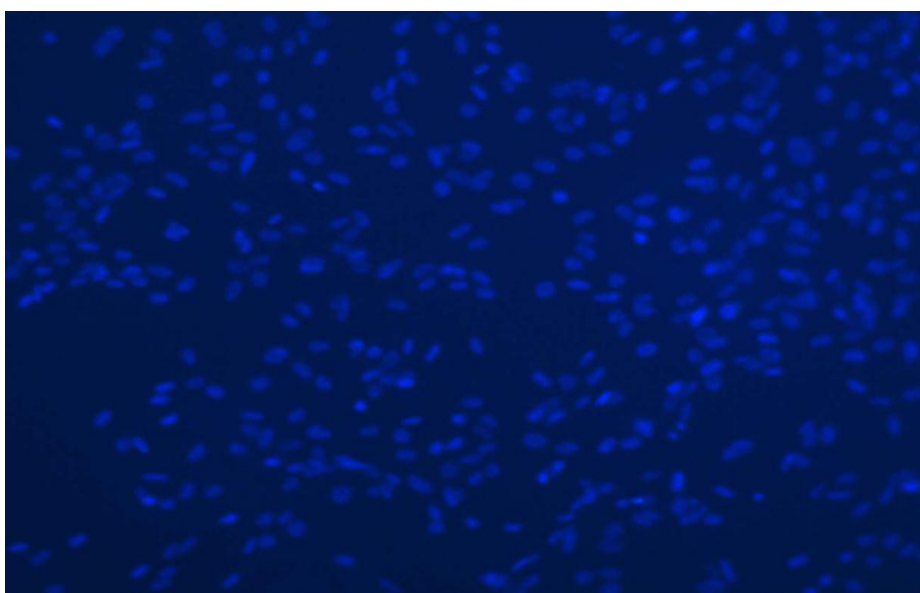


Figure 3.47: Image showing the total number of 1321N1 cells treated with 1 nM T3 after staining with Hoeschst 33358. This photograph is typical for n=8 such different experiments (10 x magnification).

The images in figures 3.48-3.49 show the stained nucleus of 1321N1 cell line for the 500 nM T3 treated cells over the period of 4 days. As shown on the images, there was no apoptotic cells on 500 nM T3 group of the 1321N1 cell line, in comparison with the total number of cells stained on the figure 3.49. After the period of 4 days the cells were stained, and were viewed with a fluorescence microscope.

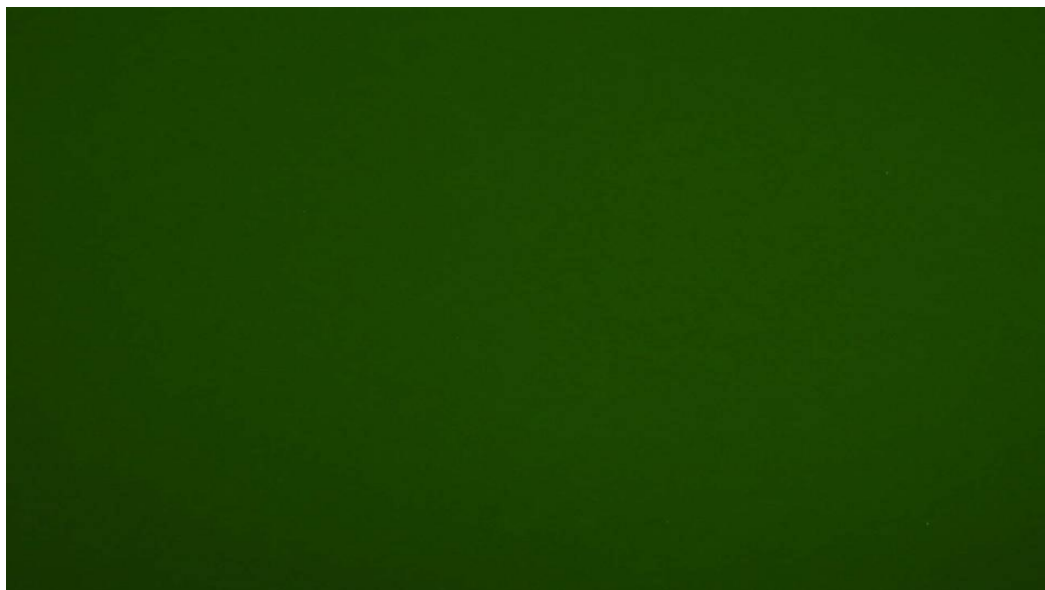


Figure 3.48: Image showing 1321N1 cells treated with 500 nM T3 after staining for TUNNEL. No apoptotic cells were detected. This photograph is typical for n=8 such different experiments (10 x magnification).

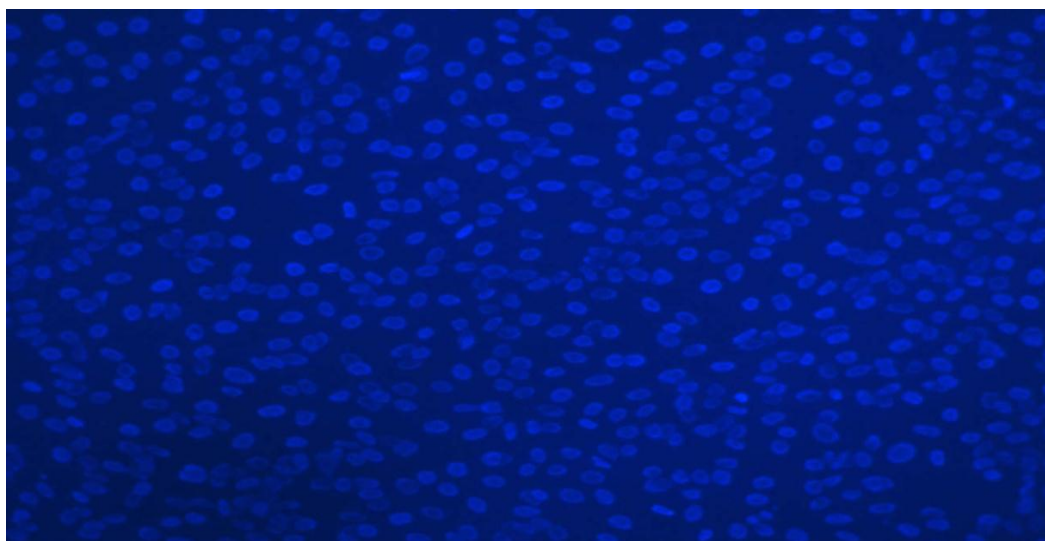


Figure 3.49: Image showing the total number of 1321N1 cells treated with 500 nM T3 after staining with Hoeschst 33358. This photograph is typical for n=8 such different experiments (10 x magnification).

### **3.2.7. Molecular detection of kinase signalling in glioma cell lines**

#### **3.2.7.1. Kinase signaling activation-2 days**

Figure 3.50 shows the analysis of the density of the Western blotting protein (B) and (A) the average of the optical density (arbitrary units) as obtained from the Western blotting experiment. The results show that after 2 days the ratio of p44 and p42 phospho-ERK to total ERK in 1321N1 cells was increased by 2.0 fold in the 1 nM T3-treated cultures ( $p>0.05$ ) and by 2.6 fold in 500 nM T3-treated cells ( $p<0.05$ ) as compared to non-treated cells. Although there was a dose dependent increase in p44 and p42, the value was only significant on the 500 nM dose in comparison with the control group.

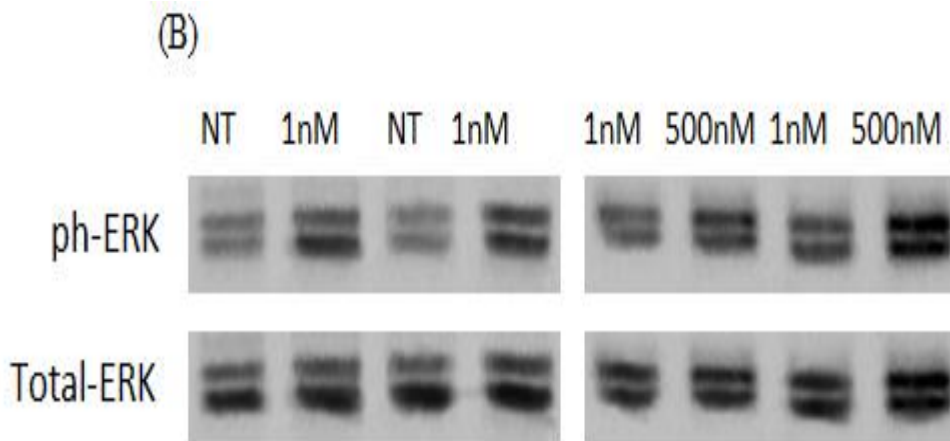
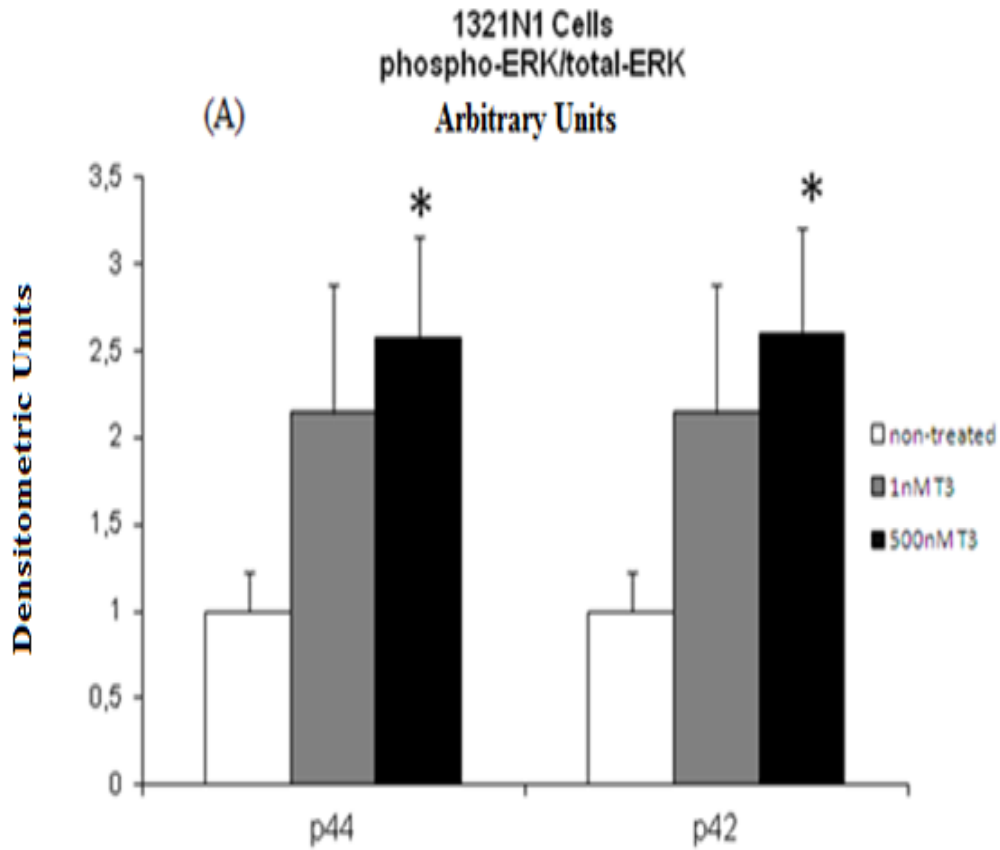


Figure 3.50: Bar charts in (A) show the ratio of phosphorylated to total p44 and p42 ERKs in non-treated cells and after 1 nM and 500 nM treatment with T3 for 2 days. (The bars are the average of the optical density (arbitrary units),  $\pm$ SEM)  $n=8$ . NT= non-treated,  $*p<0.05$  vs non-treated. Figure (B) shows representative western blot of p44 and p42 phospho-ERK and total ERK.

Figure 3.51 shows the analysis of the density of the Western blotting protein (B) and (A) the average of the optical density as obtained from the Western blotting experiment. The results show that the ratio of phospho-Akt to total Akt was found to be 1.4 and 1.5 fold higher both in 1 nM and 500 nM T3 treated cells, as compared to non-treated cells,  $p < 0.05$  after the 2 day treatment period.

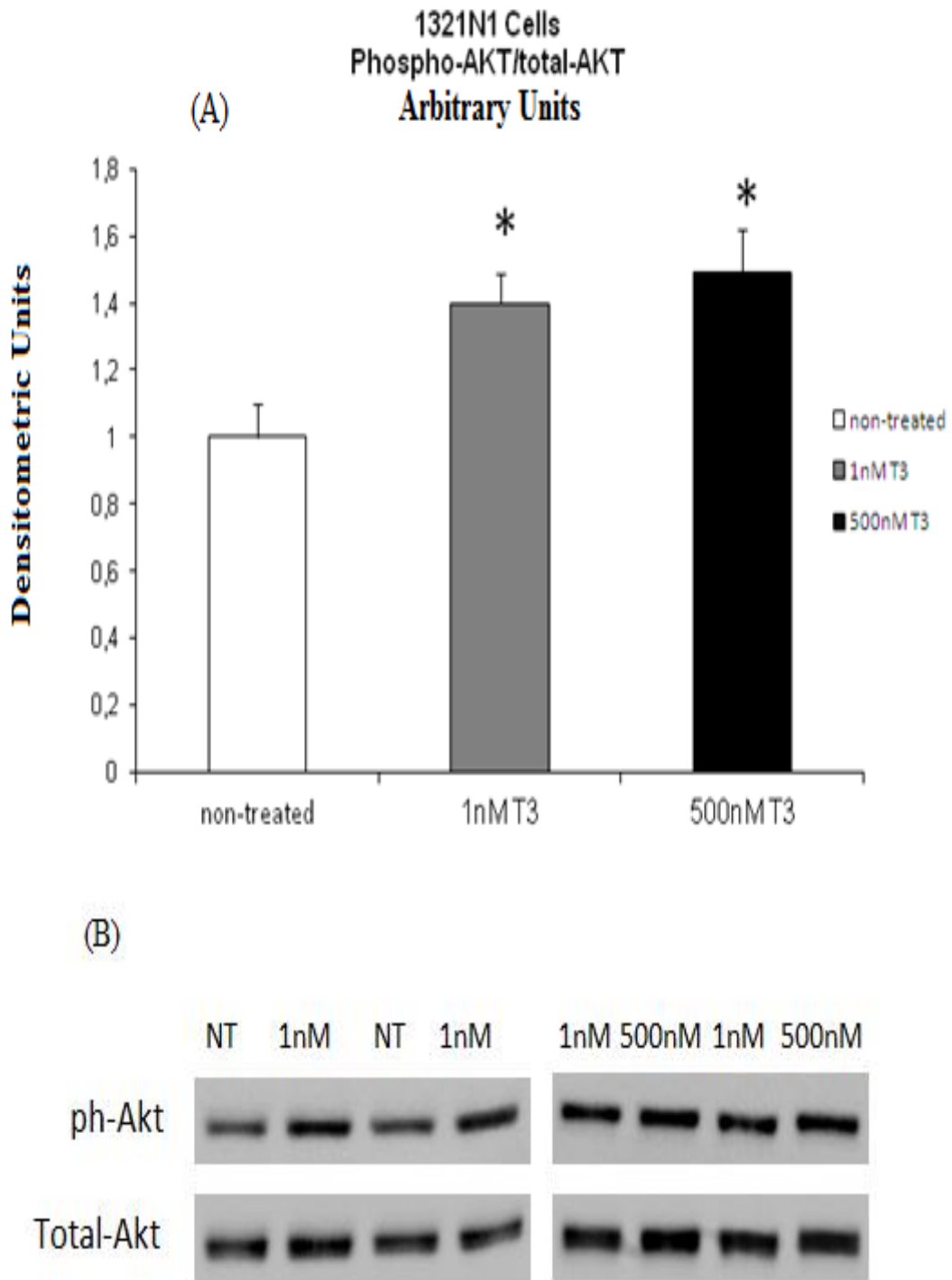


Figure 3.51: Bar charts in (A) show the ratio of phosphorylated to total AKT in non-treated cells and after 1nM and 500nM treatment with T3 for 2 days. (The bars are the average of the optical density (arbitrary units),  $\pm$ SEM, n=8). NT=non-treated, \* p<0.05 vs non-treated. Figure (B) shows representatives of western blot of the AKT protein.

### **3.2.7.2. Kinase signaling activation-4 days**

Figure 3.52 shows the analysis of the density of the Western blotting protein (B) and (A) the average of the optical density as obtained from the Western blotting experiment. The results show that there were no differences in the ratio of p44 and p42 phospho-ERK to total ERK between the groups after the 4 day treatment period.

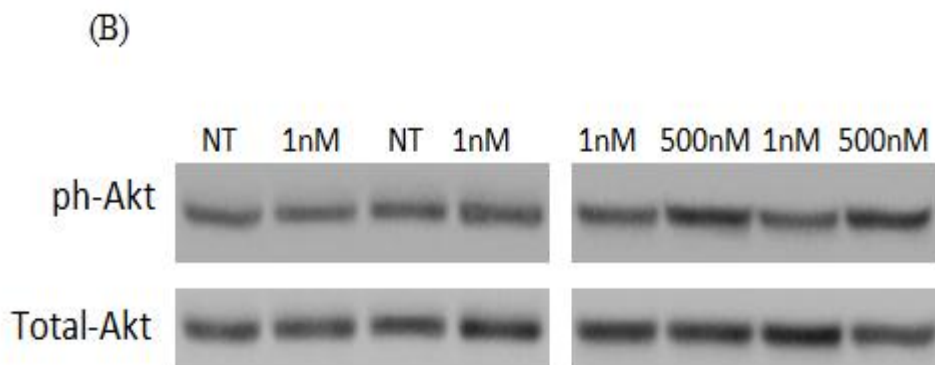
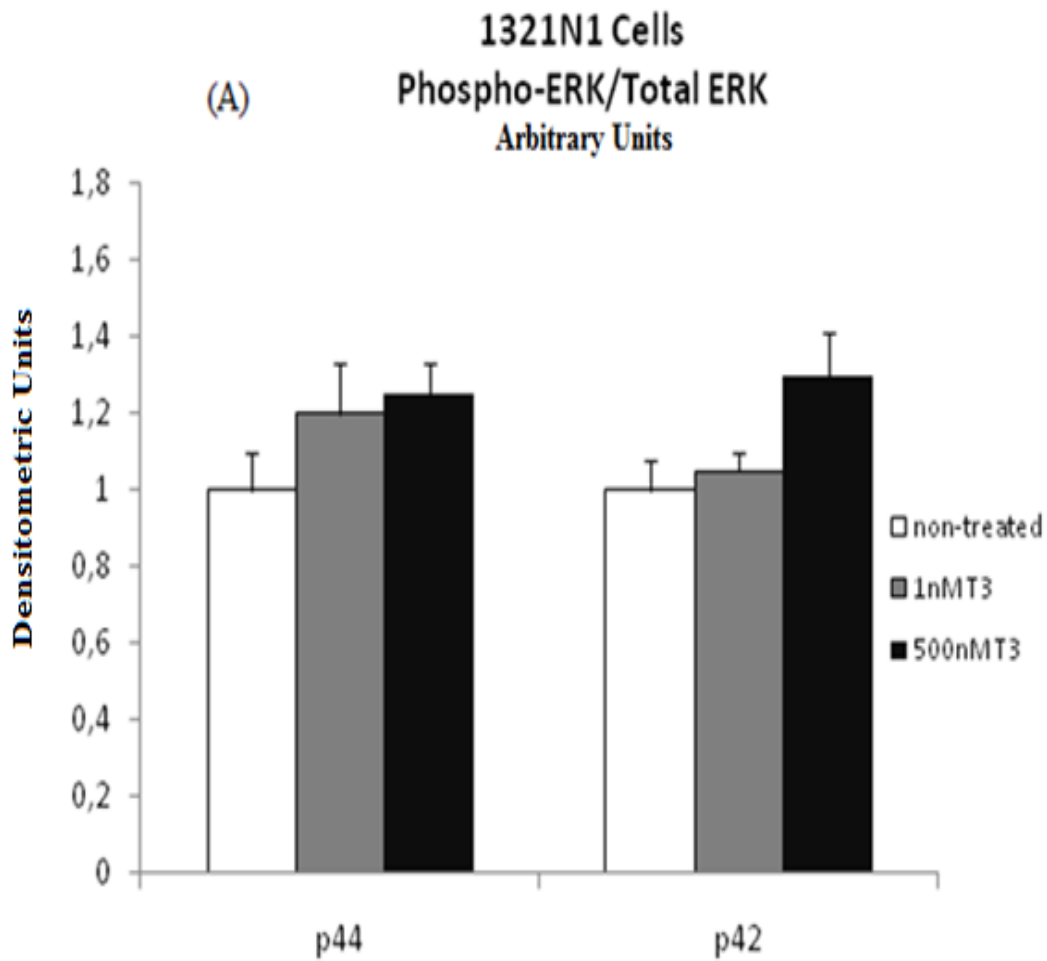


Figure 3.52: Bar charts in (A) show the ratio of phosphorylated to total p44 and p42 ERKs in non-treated cells and after 1 nM and 500 nM treatment with T3 for 4 days. (The bars are the average of the optical density (arbitrary units), bar=SEM, n=8). NT=non-treated. Figure (B) shows representative western blot of p44 and p42 phospho-ERK and total ERK.

Figure 3.53 shows the analysis of the density of the Western blotting protein (B) and (A) the average of the optical density as obtained from the Western blotting experiment. The results show that the ratio of phospho-Akt to total Akt was found to be 1.4 fold higher in 500 nM T3 treated cells as compared to non-treated and 1 nM T3 treated cells ( $p < 0.05$ ) after the 4 day treatment period.

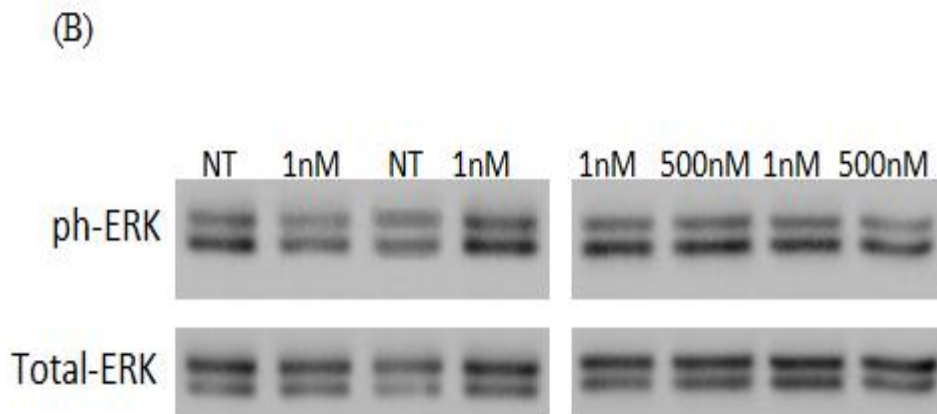
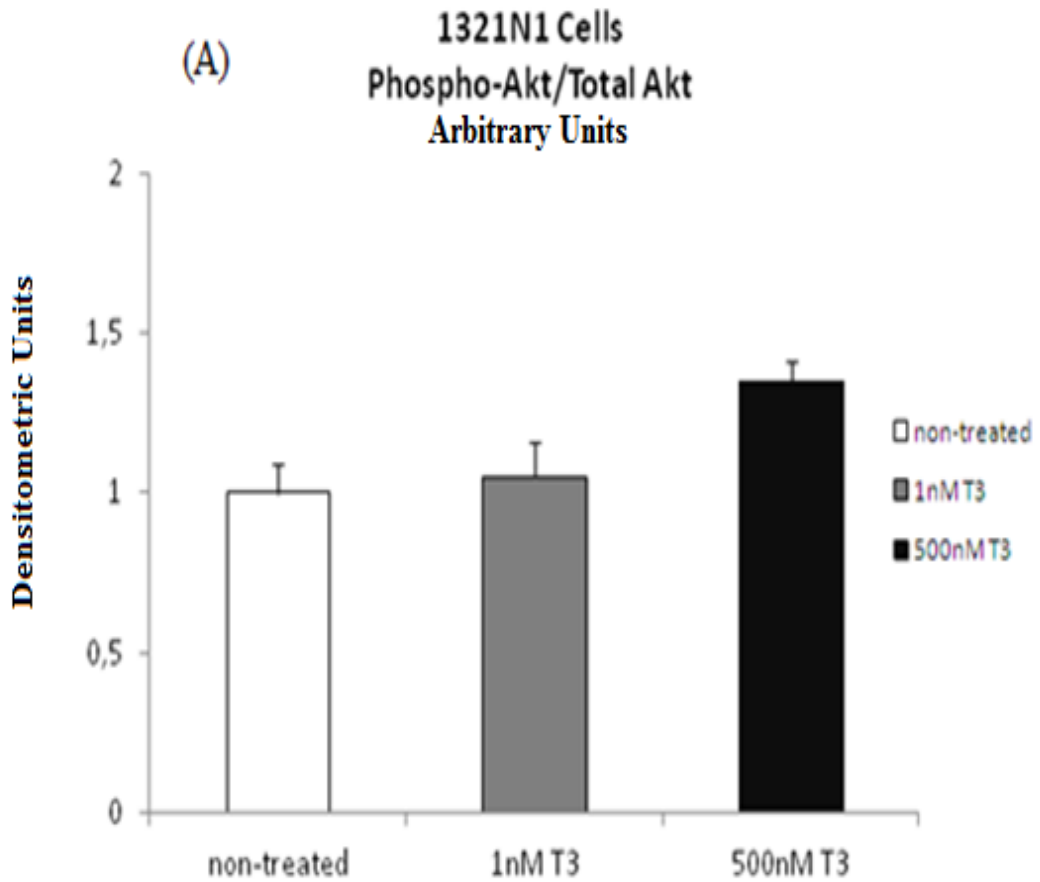


Figure 3.53: Bar charts in (A) show the ratio of phosphorylated to total AKT in non-treated cells and after 1 nM and 500 nM treatment with T3 for 4 days. (The bars are the average of the optical density (arbitrary units), bar=SEM, n=8). NT=non-treated. Figure (B) shows representatives of western blot of the AKT protein.

## U87MG Cell line

### 3.3.1. Morphological characteristics of glioma cell lines

#### 3.3.1.1. Cell morphology 2 days

Figures 3.54-3.56 show typical images of U87-MG cells following incubation with either no T3 (untreated group, image in fig 3.54), 1 nM T3 (image in figure 3.55), and 500 nM T3 (image in figure 3.56). The results show that both 1 nM and 500 nM of T3 can induce growth effects on the number of projections of the cells, but show no changes in the ratio of cell length /width compared to untreated cells. These images were analysed and the data are presented in figure 3.57.

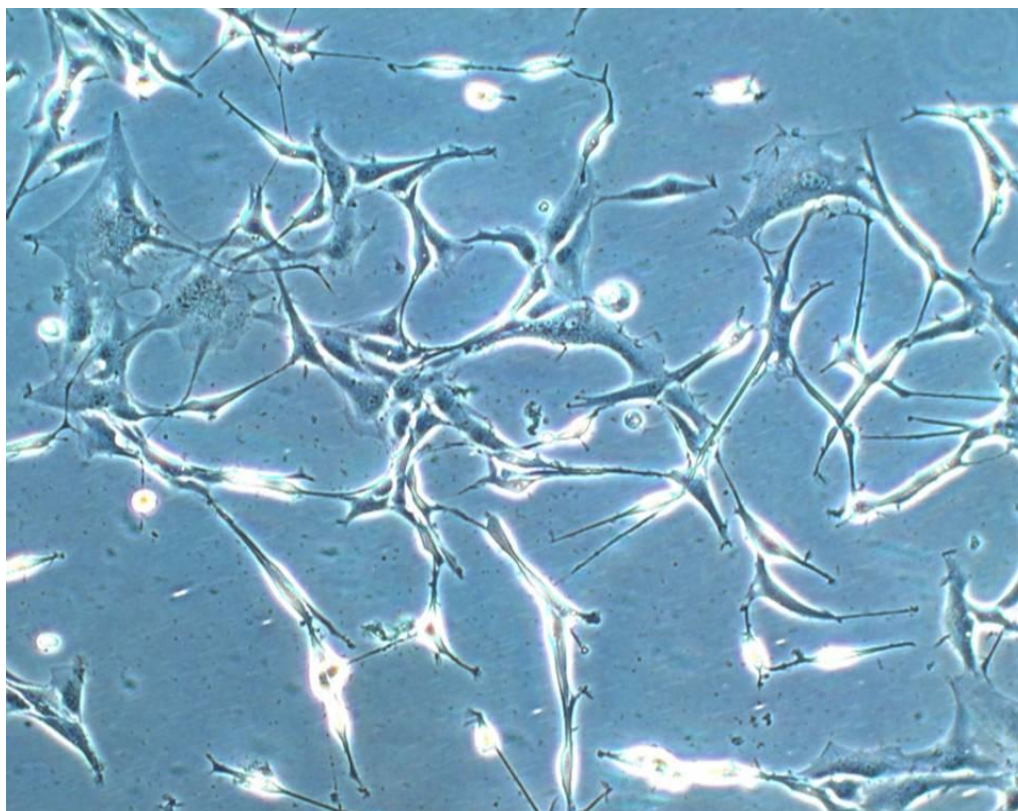


Figure 3.54: Image taken by phase-contrast optical microscopy. In this and subsequent image the data show characteristics such as cellular length, width, and number of projections in non-treated U87-MG cell line after the period of 2 days are shown for comparison. This photograph is typical for n=8 such different experiments (20 x magnification).

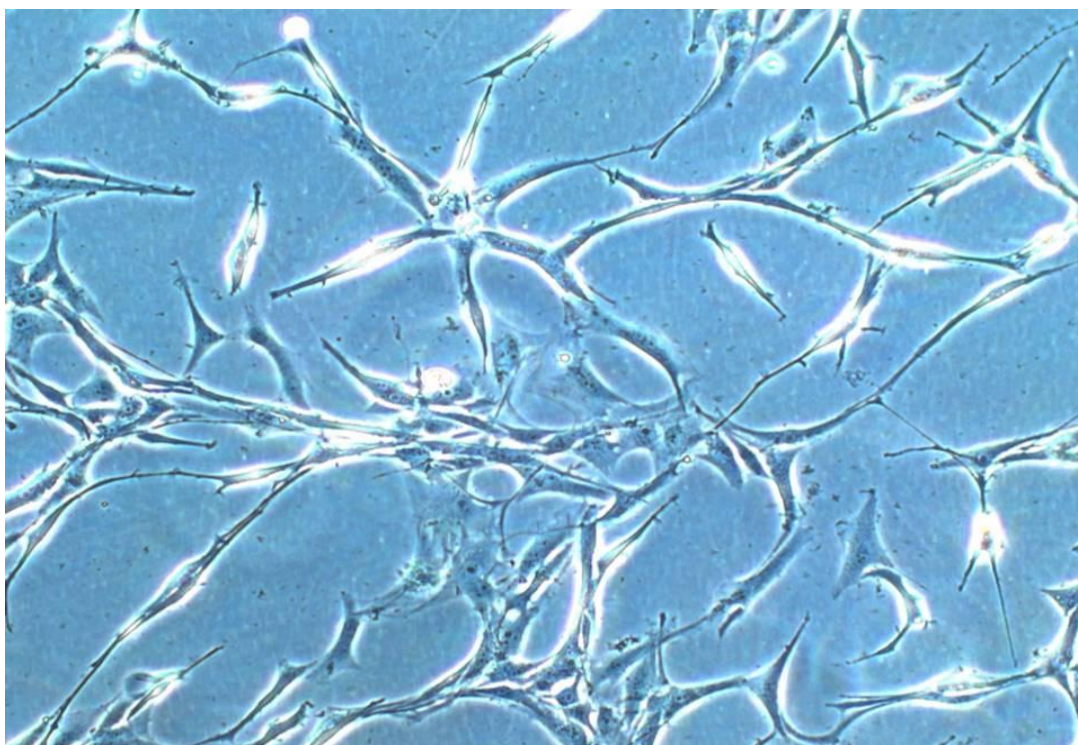


Figure 3.55: Image taken by phase-contrast optical microscopy. Characteristics such as cellular length, width, and number of projections in 1 nM T3-treated U87-MG cells after the period of 2 days are shown. This photograph is typical for  $n=8$  such different experiments (20 x magnification).

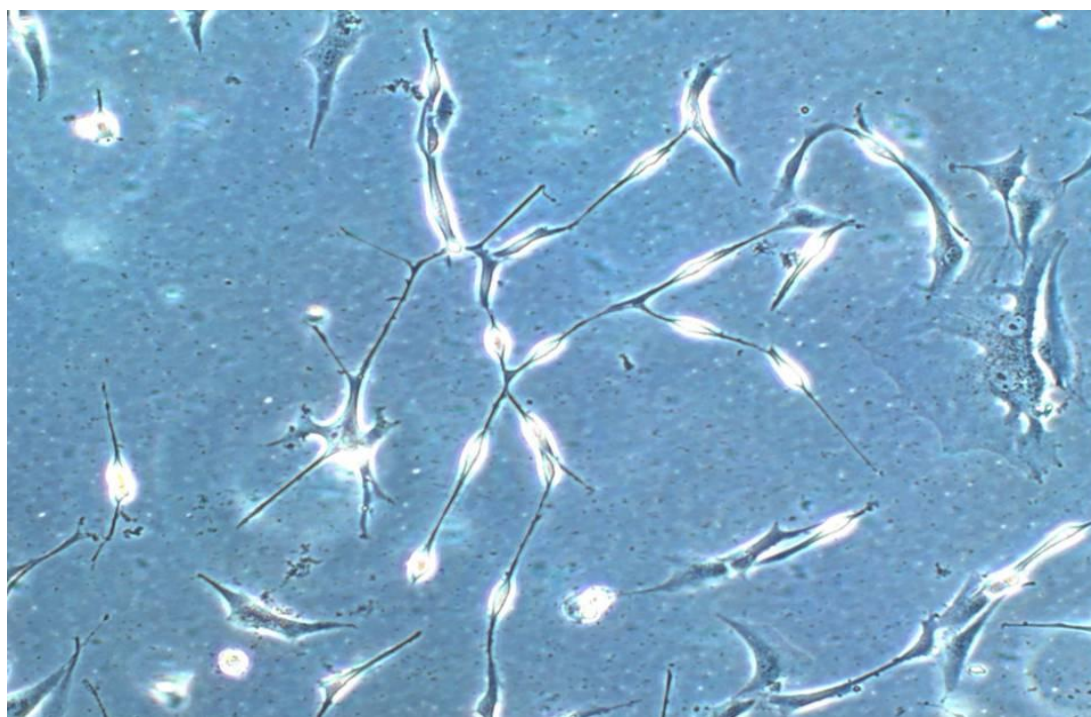


Figure 3.56: Image taken by phase-contrast optical microscopy. Characteristics such as cellular length, width, and number of projections in 500 nM T3-treated U87-MG cells after the period of 2 days are shown. This photograph is typical for  $n=8$  such different experiments (20 x magnification).

Figure 3.57 shows (A) the number of projections and (B) the ratio of cell length /width of U87-MG cells on 2 days following incubation with either 1 nM T3 or 500 nM T3 compared to untreated group. The results shown that treatment of U87-MG glioma cells with 1 nM T3 can result in a significant ( $p < 0.05$ ) increase in cell projections but no change in the geometry of the cells. The ratio of total number of projections to total number of cells was  $1.16 \pm 0.14\%$  for non treated vs  $1.83 \pm 0.19\%$  for 1 nM T3,  $p < 0.05$ , and  $2.0 \pm 0.19\%$  for 500 nM, T3 treated cells,  $p < 0.05$  vs for non-treated.

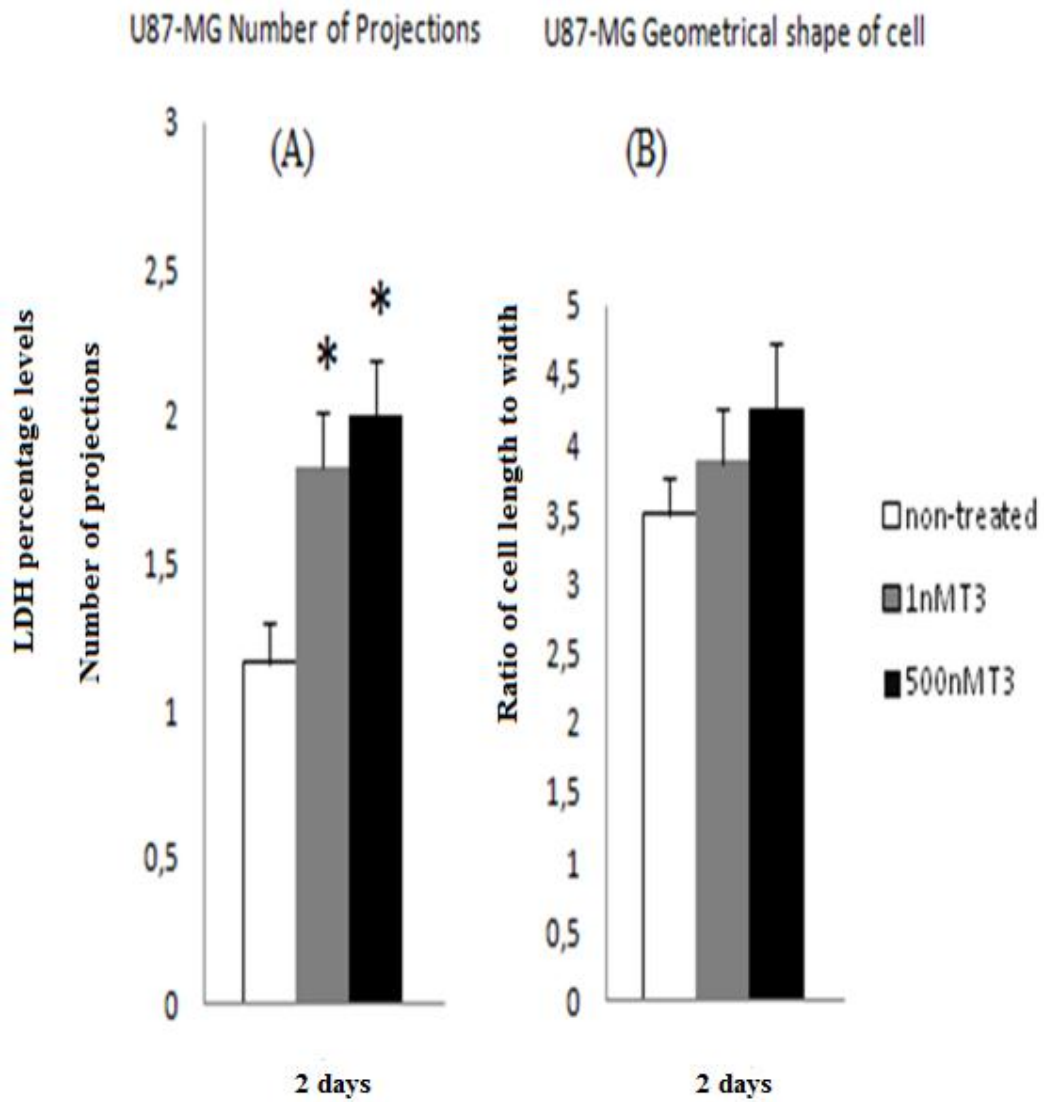


Figure 3.57: Bar charts showing changes on the number of projections (A) and the ratio of cell length /width (B) of the geometrical shape of U87-MG cell line after the period of 2 days. Data are mean±SEM \*  $p < 0.05$  vs non-treated,  $n=8$ .

### 3.3.1.2. Cell morphology-4 days

Figures 3.58-3.60 show typical images of U87-MG cells following 4 days of incubation with either no T3 (untreated group, image in figure 3.58), 1 nM T3 (image in figure 3.59), and 500 nM T3 (image in figure 3.60). Close observation of figures 3.44-3.46 shows the morphological differences of U87-MG cell line over the period of 4 days between the non-treated group and the groups treated with 1 nM and 500 nM T3 on both the ratio of length /width of the cell, and the number of projections. The cells were over confluent (over 80%) after the period of 4 days and no quantitative data could be obtained regarding the measurement of number of projections and the ratio of cell length /width.

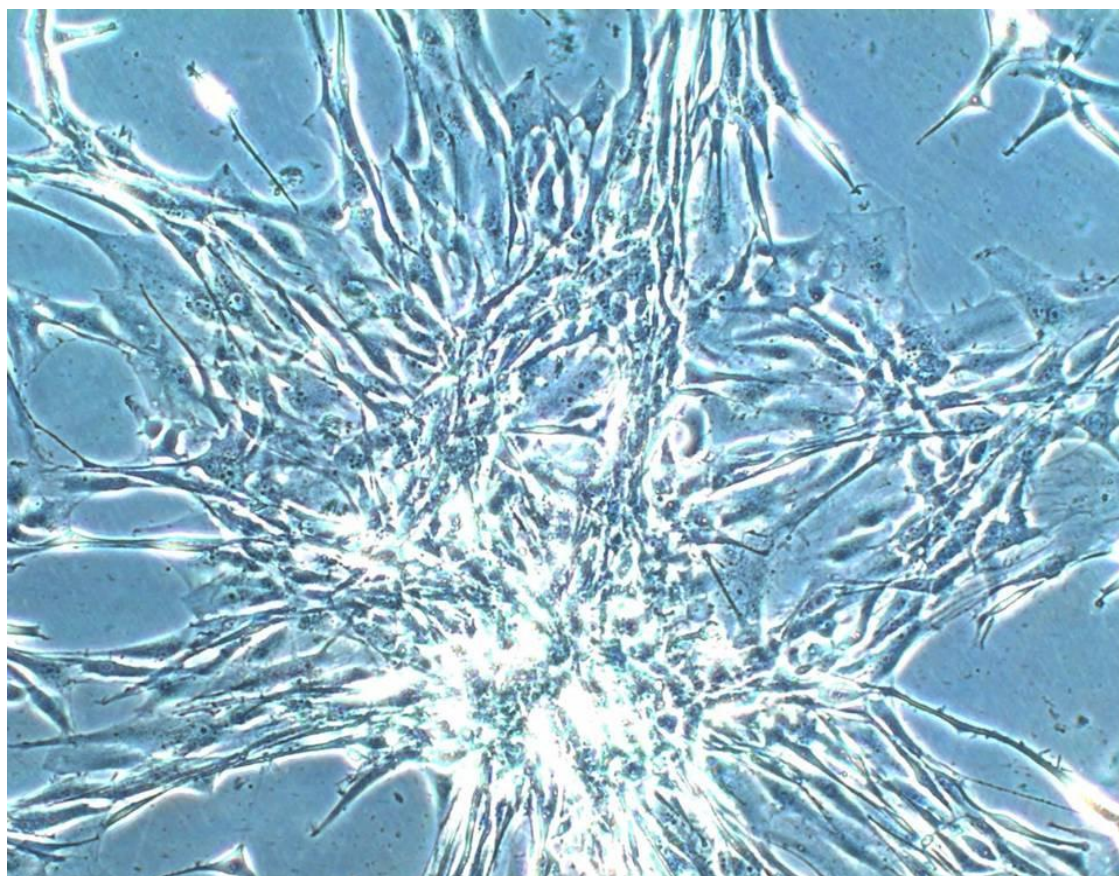


Figure 3.58: Image taken by phase-contrast optical microscopy. Characteristics such as cellular length, width, and number of projections in non-treated U87-MG cell line after the period of 2 days are shown. This photograph is typical for n=8 such different experiments (20 x magnification).

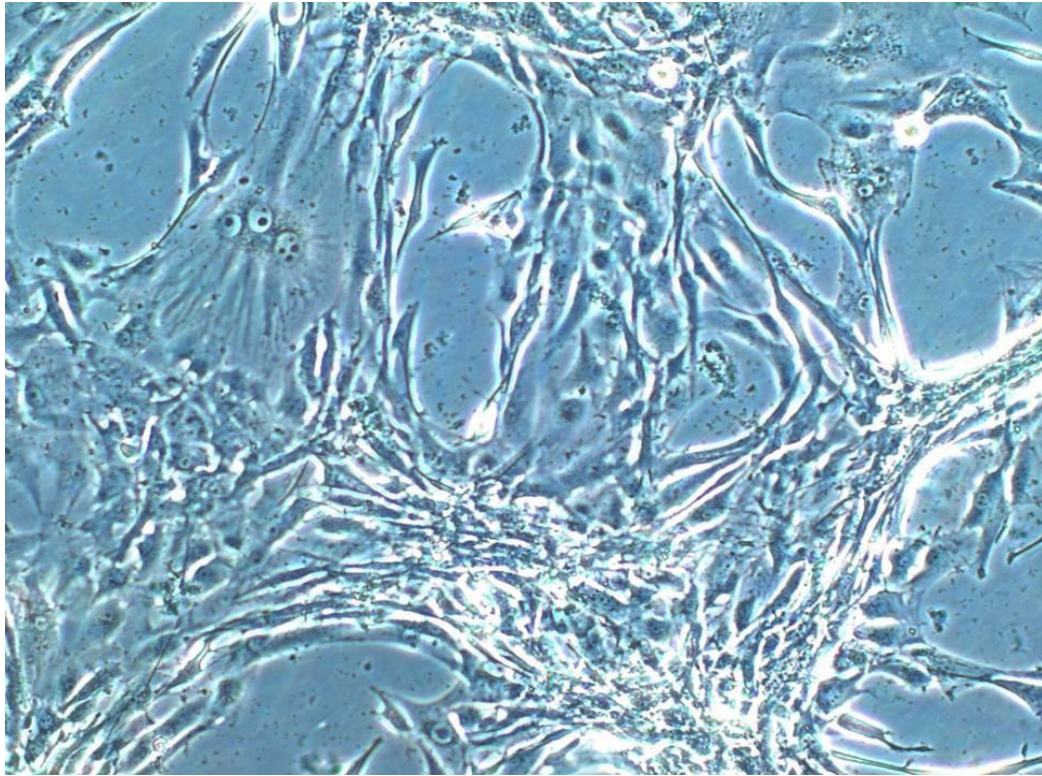


Figure 3.59: Image taken by phase-contrast optical microscopy. Characteristics such as cellular length, width, and number of projections in 1 nM T3-treated U87-MG cells after the period of 2 days are shown. This photograph is typical for n=8 such different experiments (20 x magnification).

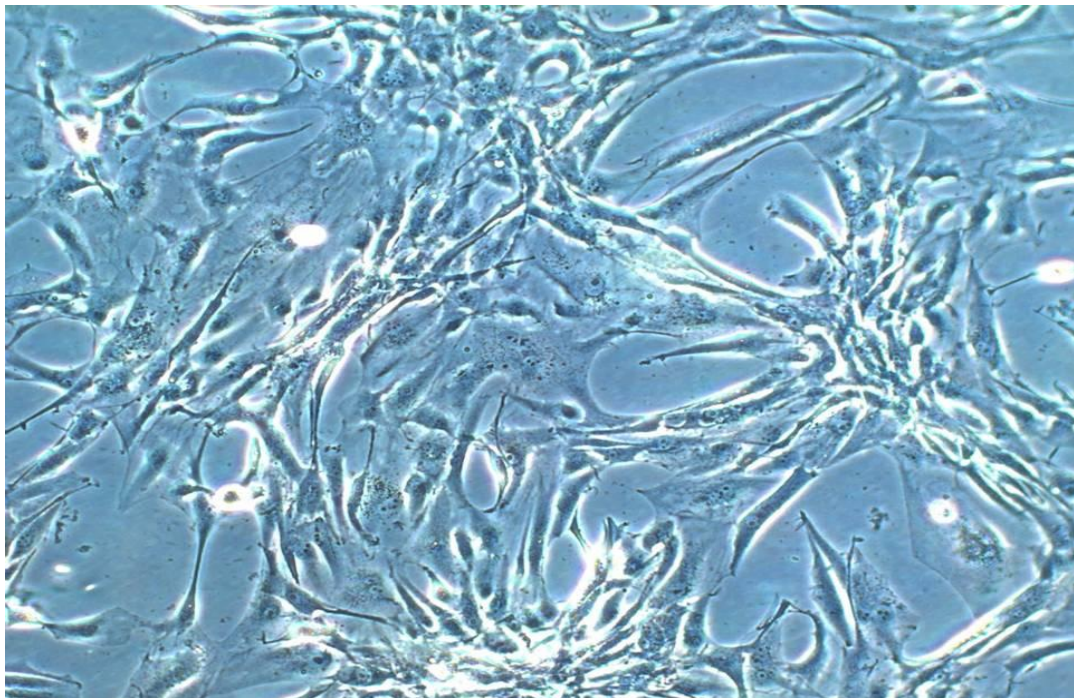


Figure 3.60: Image taken by phase-contrast optical microscopy. Characteristics such as cellular length, width, and number of projections in 500 nM T3-treated U87-MG cells after the period of 2 days are shown. This photograph is typical for n=8 such different experiments (20 x magnification).

### **3.3.2. Cell count of glioma cell lines**

#### **3.3.2.1. Total cell number count 2 days**

Figure 3.61 shows the numbers of untreated and treated U87-MG glioma cells following incubation with either 1 nM T3 or 500 nM T3 for 2 days. The results show that there was a significant decrease ( $p < 0.05$ ) on the total number of the cells in both treatment groups (1 nM and 500 nM) in comparison with the non-treated group. The ratio of total number of cells was  $211300 \pm 3000$  for non-treated vs  $186166 \pm 3122$  for 1 nM T3,  $p < 0.05$ , and  $18000 \pm 1833$  for 500 nM T3 treated cells,  $p < 0.05$  vs non-treated after a period of 2 days of treatment.

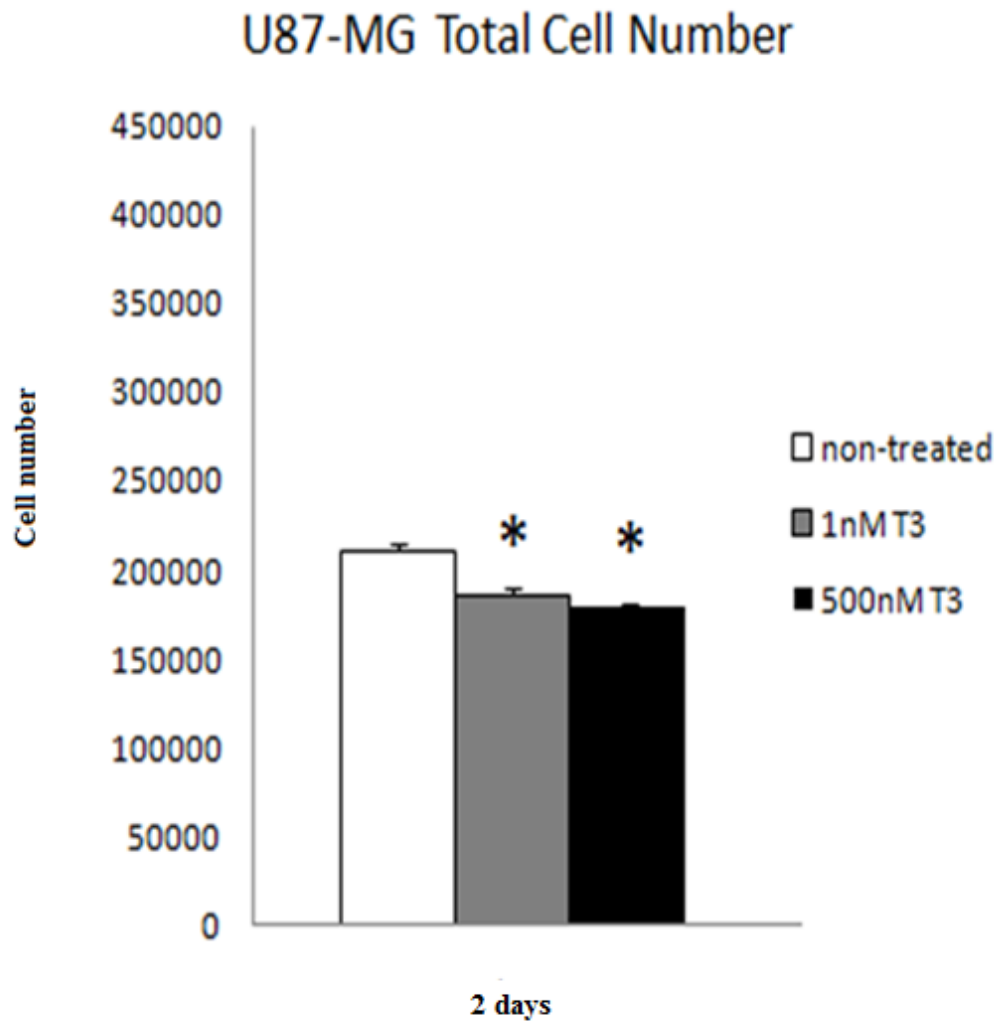


Figure 3.61: Bar charts showing the total number of U87-MG cells between the untreated and treated cells with either 1 nM or 500 nM T3 over a period of 2 days. Data are mean  $\pm$ SEM, n=8;  $p < 0.05$  for treated cells compared to untreated cells.

### **3.3.2.2. Total cell count 4 days**

Figure 3.62 shows the numbers of untreated and treated U87-MG glioma cells following incubation with either 1 nM T3 or 500 nM T3 for 4 days. The results show there was a significant decrease ( $p < 0.05$ ) in the total number of the cells in both treatment groups (1 nM and 500 nM) in comparison with the non-treated group. The ratio of total number of cells was  $396866 \pm 5791$  for non-treated vs  $331133 \pm 11652$  for 1 nM T3,  $p < 0.05$ , and  $310216 \pm 7090$  for 500 nM T3 treated cells,  $p < 0.05$  vs non-treated after the period of 4 day treatment.

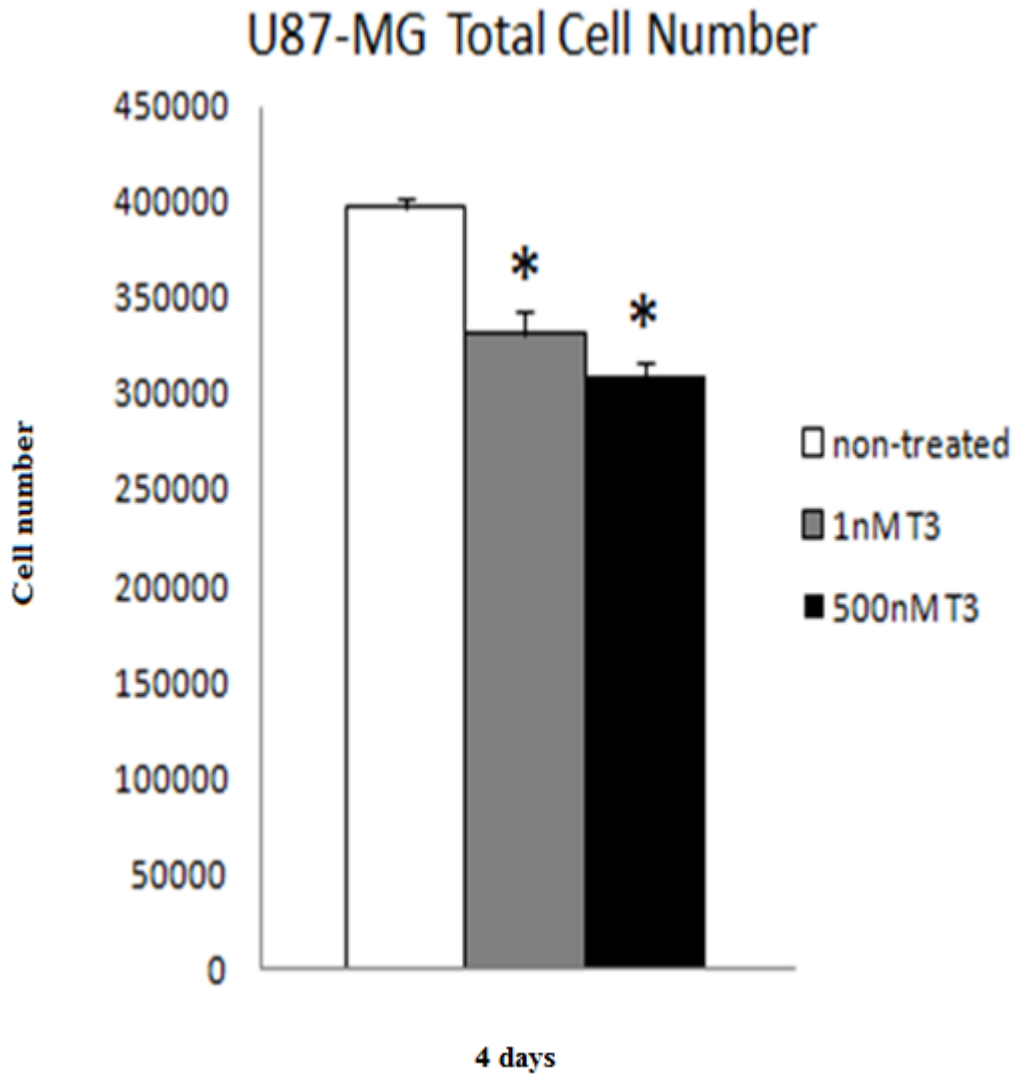


Figure 3.62: Bar charts showing the total number of U87-MG cells between the untreated and treated cells with either 1 nM or 500 nM T3 over a period of 4 days. Data are mean  $\pm$ SEM, n=8; \*p<0.05 for treated cells compared to untreated cells.

### 3.3.3. Proliferation of glioma cell lines

#### 3.3.3.1. Cell proliferation 2 days

Figures 3.63-3.65 show the nucleus of U87-MG cells following incubation with either no T3 (untreated group, figure 3.63), 1 nM T3 (image in figure 3.64), and 500 nM T3 (image in figure 3.65). The results show that either 1 nM or 500 nM of T3 can significantly ( $p < 0.05$ ) decrease cell proliferation in comparison with the untreated group.

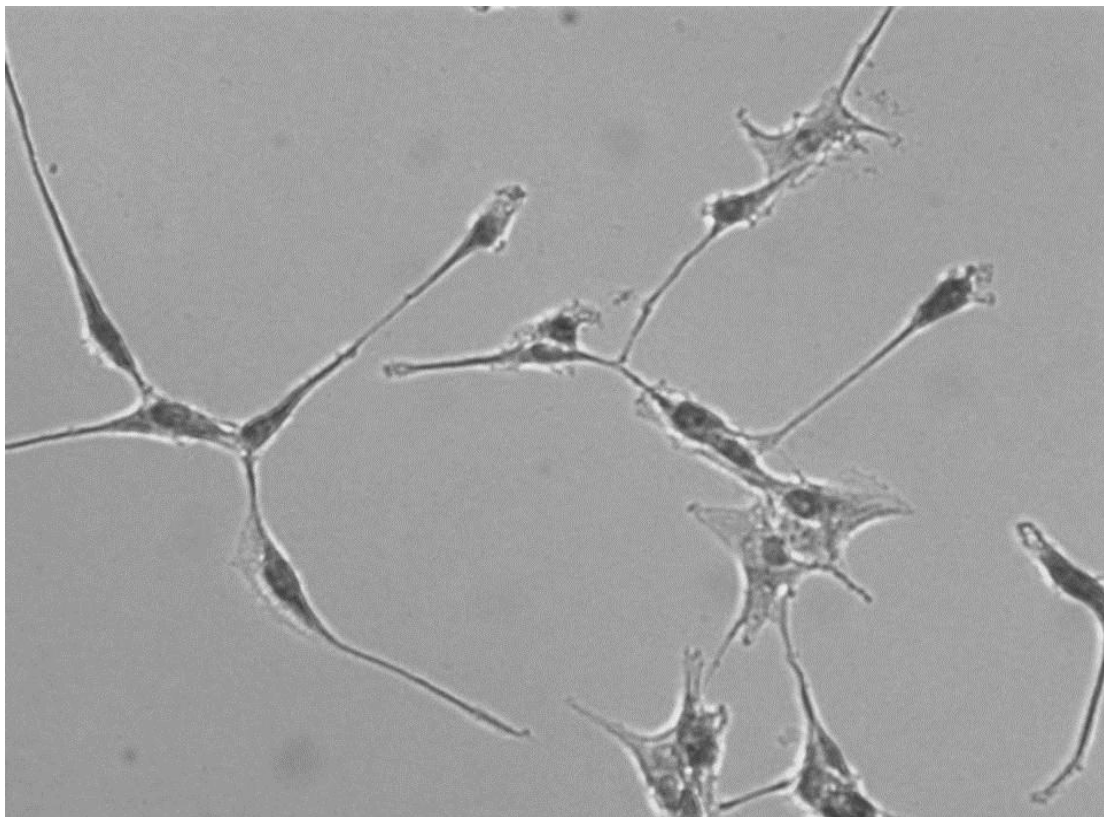


Figure 3.63: A photograph showing the proliferation of the U87-MG cells on the non-treated group. The nuclei that were stained black represent the cells that are replicating their DNA. This photograph is typical for  $n=8$  such different experiments (20 x magnification).

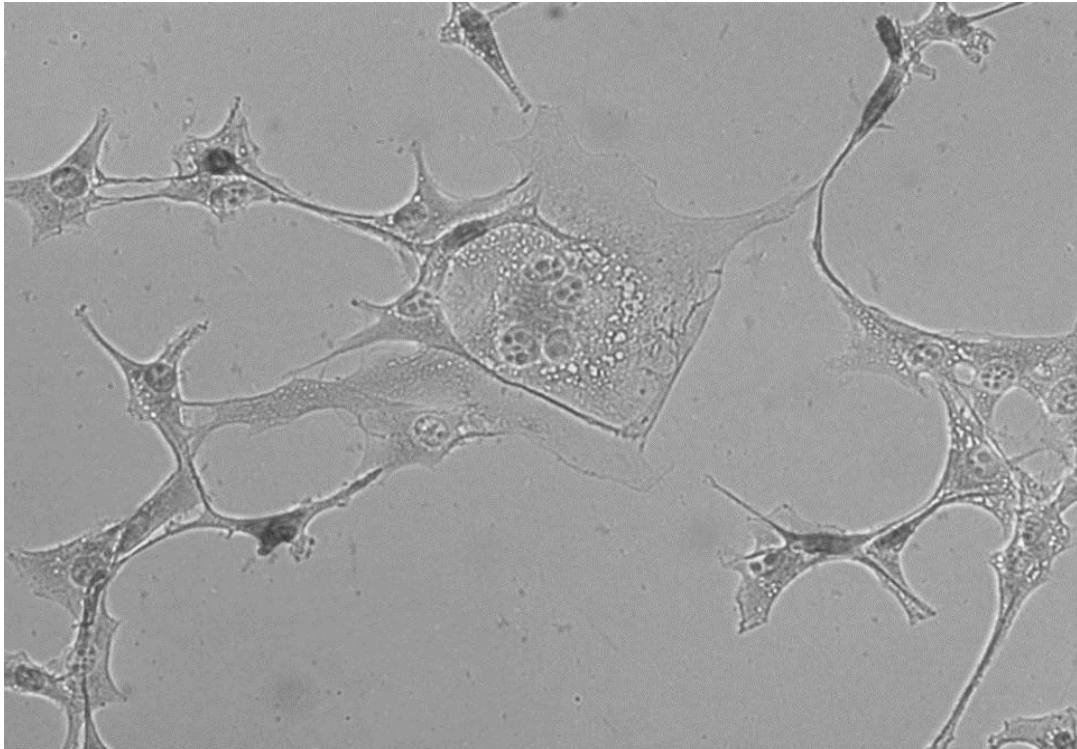


Figure 3.64: A photograph showing the proliferation of the U87-MG cells on the 1 nM T3 treated group. The nuclei that were stained black represent the cells that are replicating their DNA. This photograph is typical for n=8 such different experiments (20 x magnification).

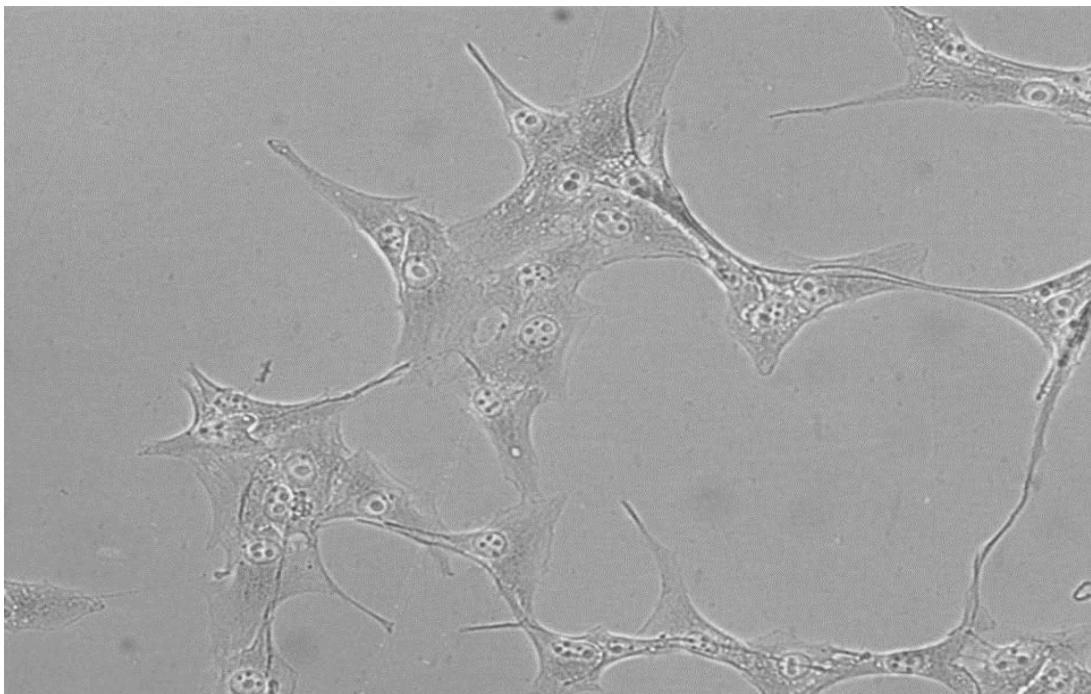


Figure 3.65: A photograph showing the proliferation of the U87-MG cells on the 500 nM treated group. The nuclei that were stained black represent the cells that are replicating their DNA. This photograph is typical for n=8 such different experiments (20 x magnification).

Figure 3.66 shows the proliferation percentage of U87-MG glioma cells in untreated group and groups treated with either 1 nM or 500 nM T3 over a period of 2 days. The results show that there was a significant decrease ( $p < 0.05$ ) in cell proliferation in both the treatment groups in comparison with the non-treated group on the 2 day treatment. The ratio was  $48 \pm 5\%$  in non treated vs  $23.6 \pm 4\%$  in 1 nM T3,  $p < 0.05$ , and  $22 \pm 4\%$  in 500 nM T3 treated cells,  $p < 0.05$  vs non treated.

## U87-MG Cell Proliferation (%)

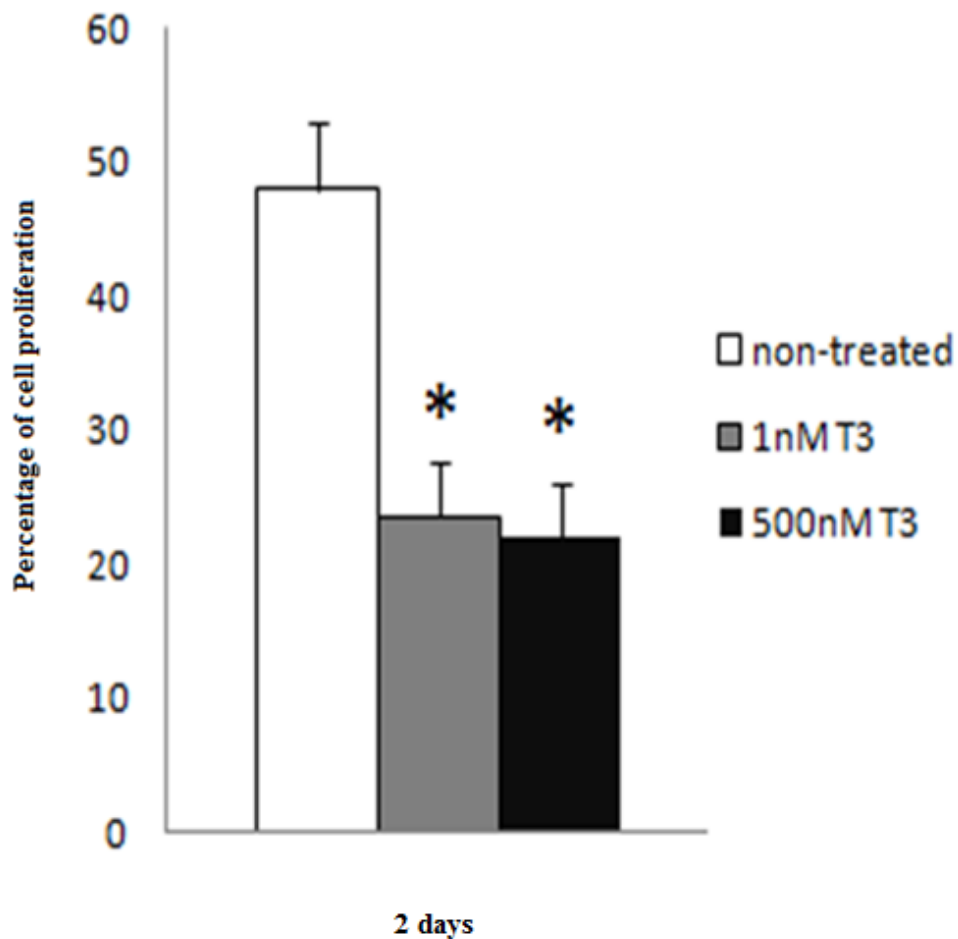


Figure 3.66: Bar charts showing the percentages of cell proliferation of the U87-MG cell line for untreated group and groups treated with either 1 nM T3 or 500 nM T3 for 2 days. Data are mean  $\pm$  SEM n=8; \* p<0.05 for untreated cells compare to treated cells with 1 nM T3 or 500 nM T3.

### 3.3.3.2. Cell proliferation 4 days

Figures 3.67-3.69 show the nucleus of U87-MG cells following incubation with either no T3 (untreated group, figure 3.67), 1 nM T3 (image in figure 3.68), and 500 nM T3 (image in figure 3.69). The results show that 1 nM or 500 nM of T3 can decrease cell proliferation in comparison with the untreated group.

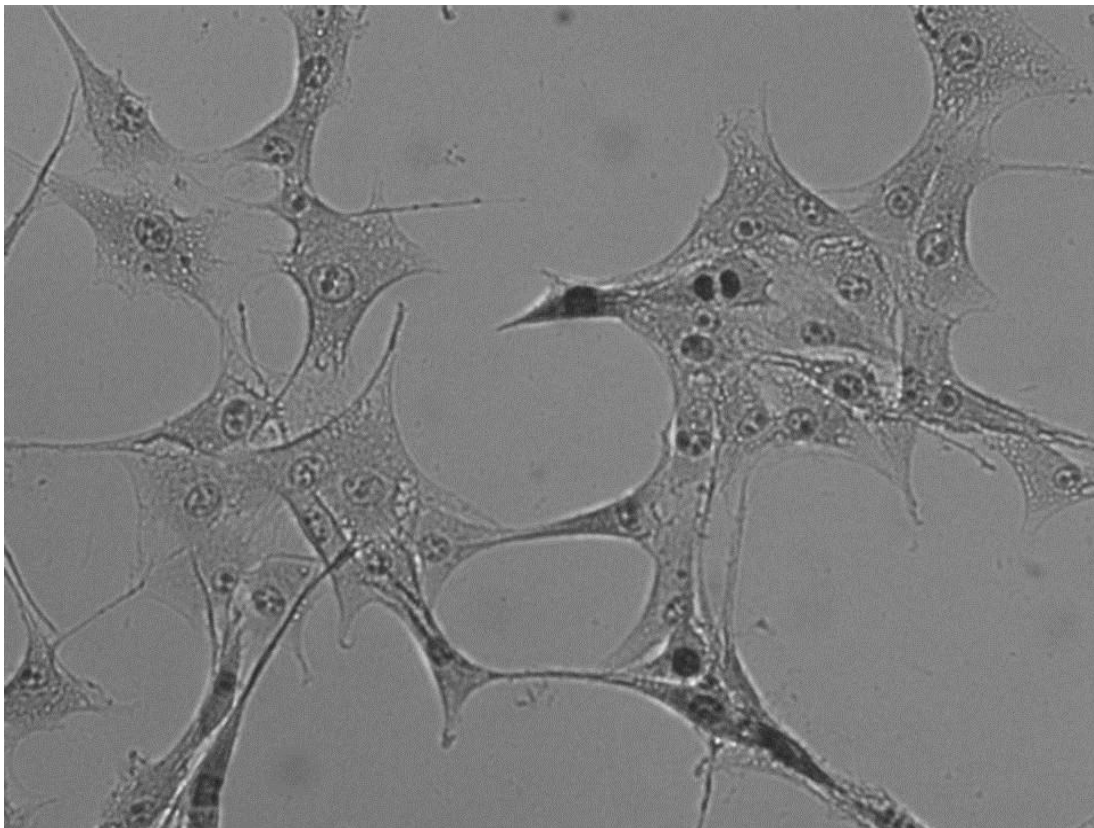


Figure 3.67: A photograph showing the proliferation of the U87-MG cells on the non-treated group. The nuclei that were stained black represent the cells that are replicating their DNA. This photograph is typical for n=8 such different experiments (20 x magnification).

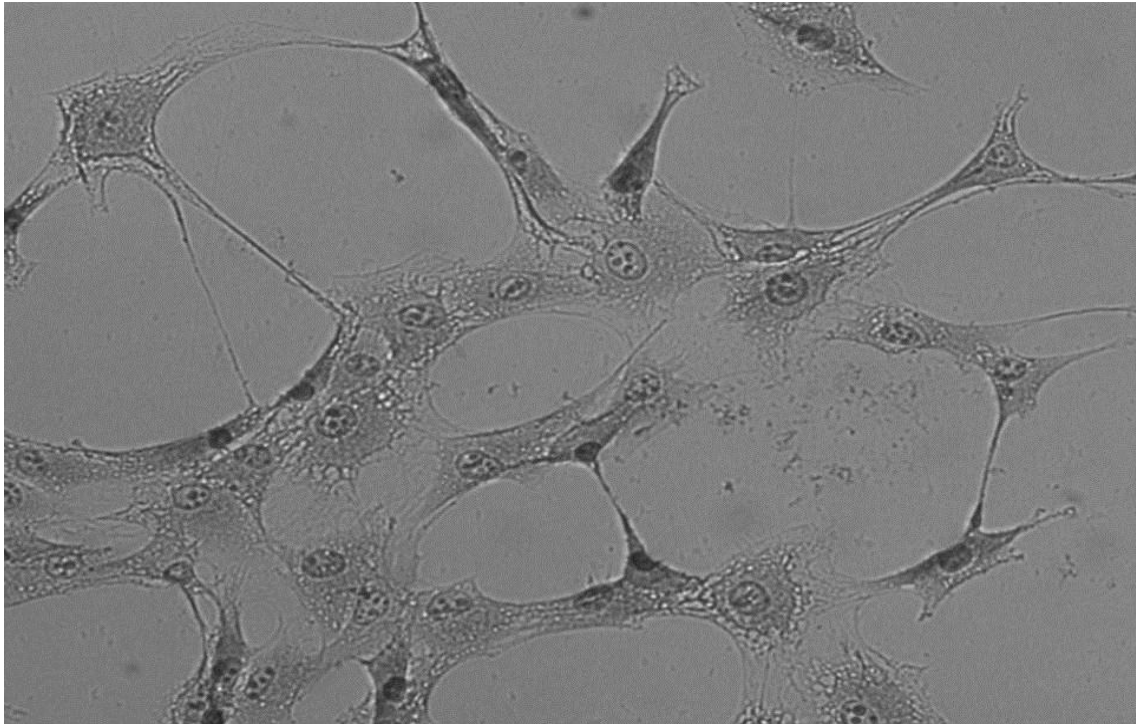


Figure 3.68: A photograph showing the proliferation of the U87-MG cells on the 1 nM T3 treated group. The nuclei that were stained black represent the cells that are replicating their DNA. This photograph is typical for n=8 such different experiments (20 x magnification).

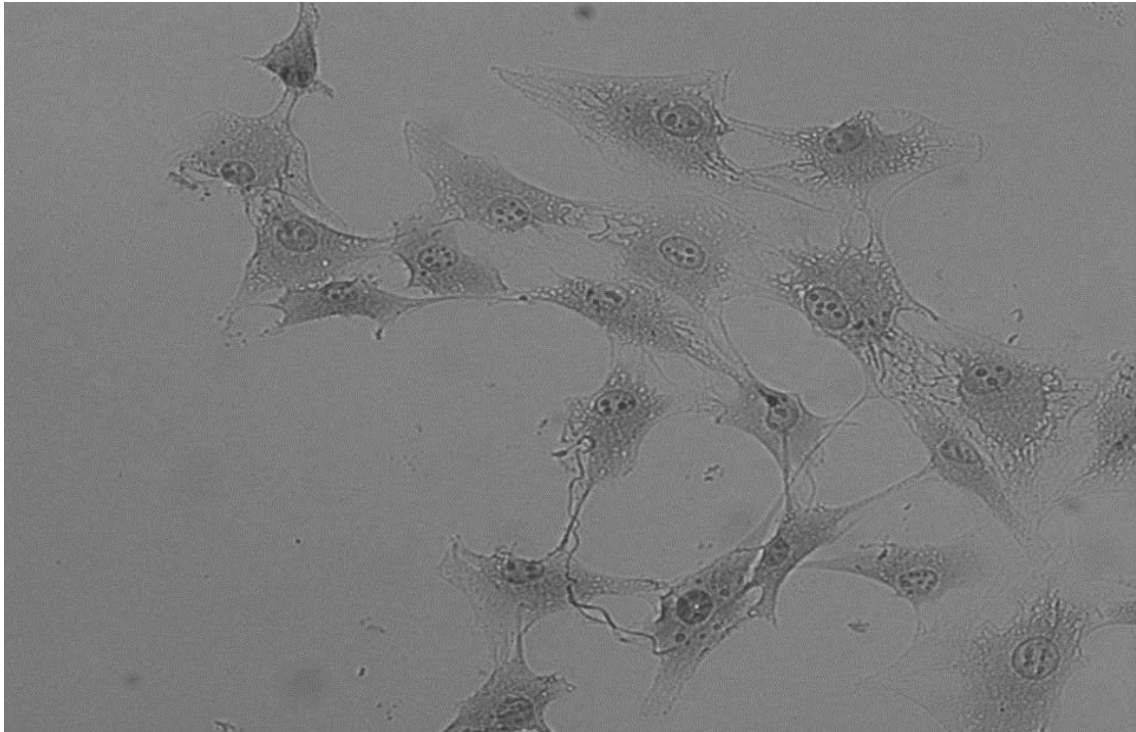


Figure 3.69: A photograph showing the proliferation of the U87-MG cells on the 500 nM T3 treated group. The nuclei that were stained black represent the cells that are replicating their DNA. This photograph is typical for n=8 such different experiments (20 x magnification).

Figure 3.70 shows the proliferation percentage of U87-MG glioma cells in untreated group and groups treated with either 1 nM or 500 nM T3 over a period of 4 days. The results show that there was a significant decrease ( $p < 0.05$ ) in cell proliferation in both the treatment groups in comparison with the non-treated group on the 4 day treatment.

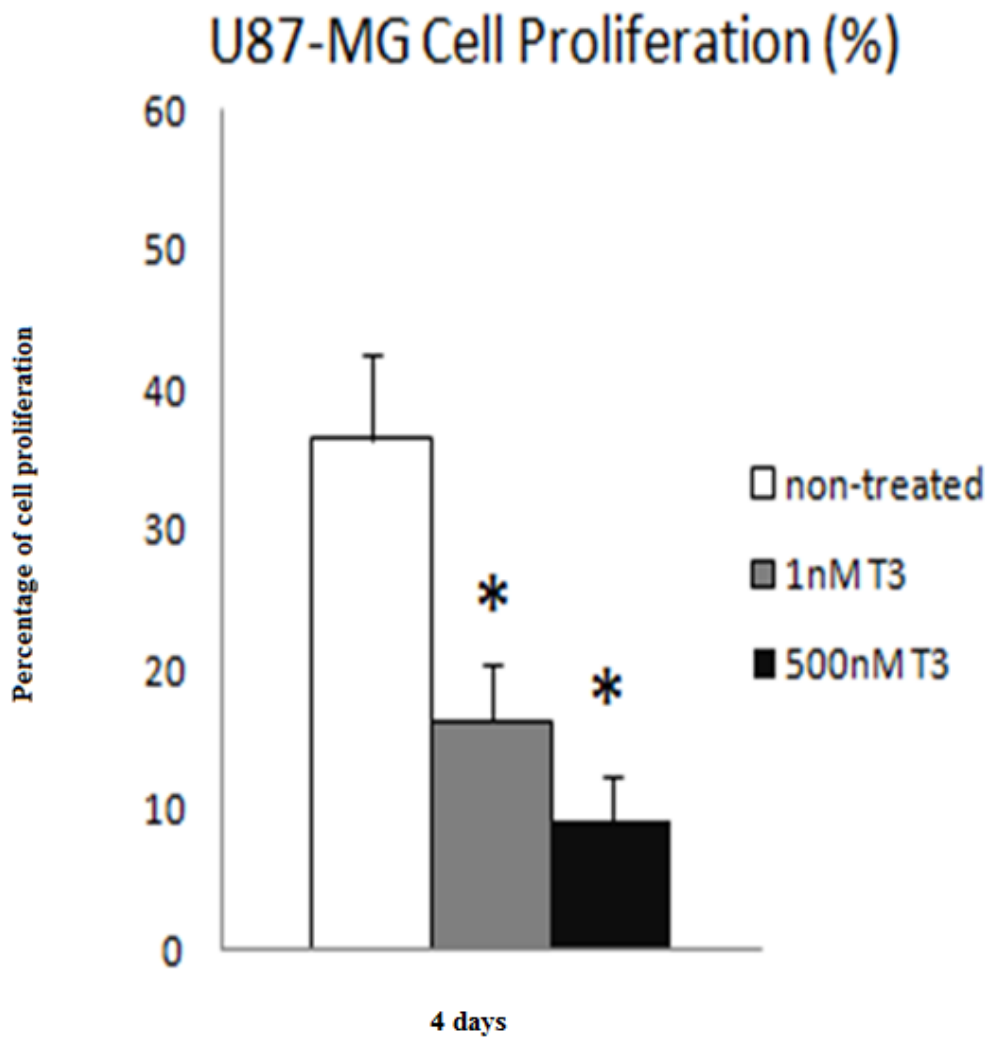


Figure 3.70: Bar charts showing the percentages of cell proliferation of the U87-MG cell line for untreated group and groups treated with either 1 nM T3 or 500 nM T3 for 2 days. Data are mean  $\pm$  SEM, n=8;\* p<0.05 for untreated cells compare to treated cells with 1 nM T3 or 500 nM T3.

### **3.3.4. Levels of injury on glioma cell lines**

#### **3.3.4.1. Cell necrosis 2 days**

Figure 3.71 shows the percentage of LDH levels in the culture medium for either untreated or treated U87-MG cells with either 1 nM or 500 nM incubated for 2 days. The results show that there was no significant difference ( $p>0.05$ ) between the non-treated group and the 1 nM T3 treated group for the period of 2 days, but the 500 nM T3 group showed a significant increase ( $p<0.05$ ) of LDH levels in comparison to the non-treated and 1nM T3 groups. The ratio was  $100 \pm 2\%$  for non-treated vs  $102.6 \pm 3.1\%$  for 1 nM T3,  $p>0.05$ , and  $120 \pm 7.2\%$  for 500 nM T3 treated cells,  $p<0.05$  vs non-treated and 1 nM.

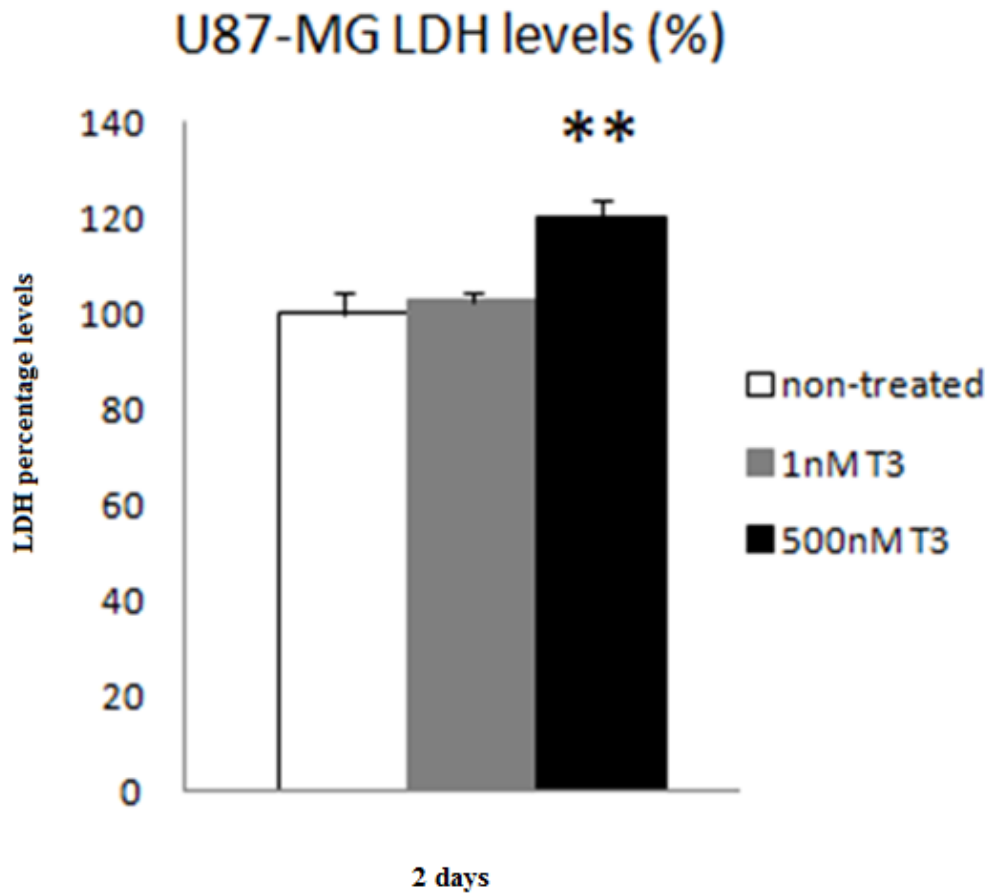


Figure 3.71: Bar charts showing the LDH release in culture medium in the three groups (non-treated, 1 nM, and 500 nM) of the U87-MG cell line. The results are expressed as the percentage of the non-treated group, in comparison with the two treatment groups. Data are mean  $\pm$ SEM, n=8; \*p<0.05 for 500 nM T3 treated cells compared with either non-treated or 1 nM T3 treated cells. Note that there is no significant difference between the untreated and the 1 nM treatment group.

#### **3.3.4.2. Cell necrosis 4 days**

Figure 3.72 shows the percentage of LDH levels in the culture medium for untreated and treated U87-MG cells with either 1 nM or 500 nM incubated for 4 days. The results show that there was no significant difference ( $p>0.05$ ) between the control group and the 1 nM T3 treated group for the period of 4 days, but the 500 nM T3 group showed a significant increase ( $p<0.05$ ) of LDH levels in comparison to the non-treated and 1 nM T3 groups. The ratio was  $100 \pm 3.2\%$  for non-treated vs  $104 \pm 3.1\%$  for 1 nM T3,  $p>0.05$ , and  $121 \pm 6.96\%$  for 500 nM T3 treated cells,  $p<0.05$  vs non-treated and 1 nM.

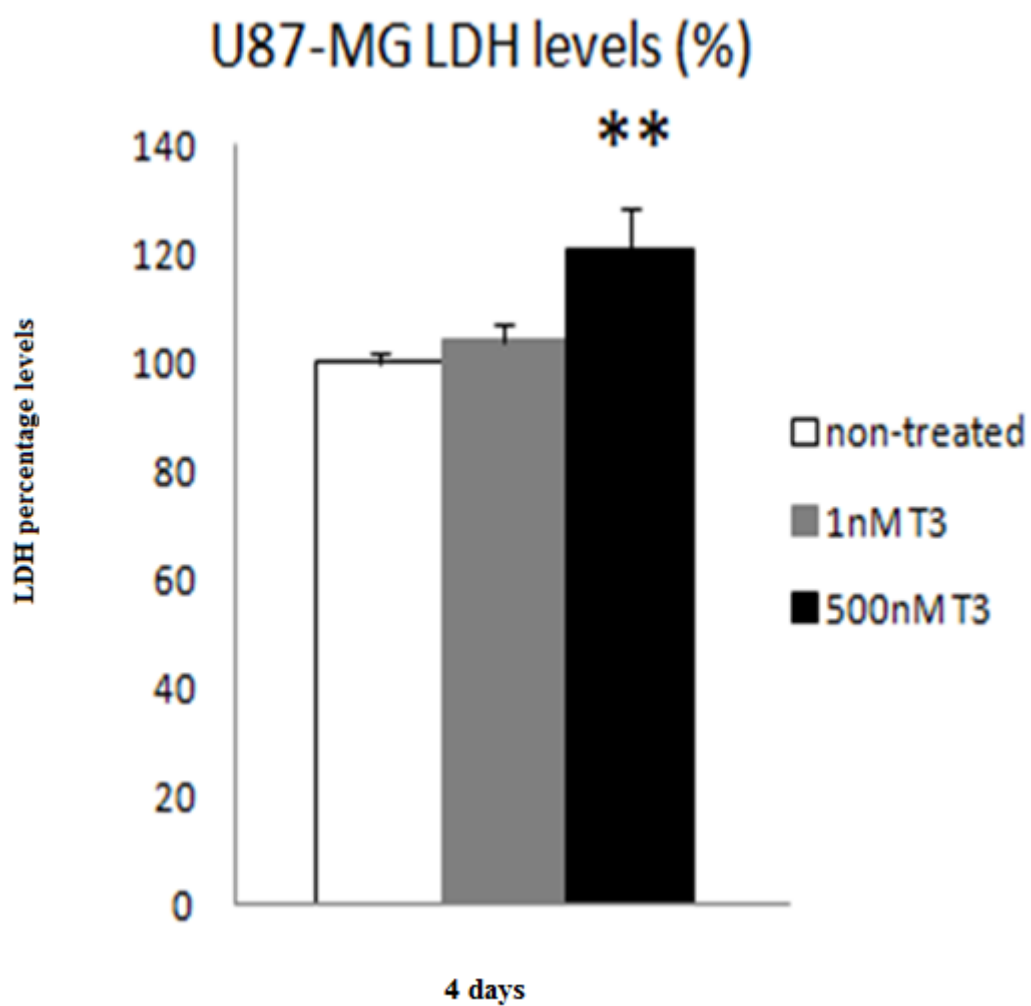


Figure 3.72: Bar charts showing the LDH release in culture medium in the three groups (non-treated, 1 nM, and 500 nM) of the U87-MG cell line. The results are expressed as the percentage of the non-treated group, in comparison with the two treatment groups. Data are mean  $\pm$ SEM, n=8; \*\*p<0.05 for 500 nM treated cells compared to non-treated or 1 nM T3 treated cells.

### **3.3.5. Levels of apoptosis on glioma cell lines**

#### **3.3.5.1. Cell apoptosis 2 days**

The images in figures 3.73-3.74 show the nuclei of U87-MG cells following treatment with 10  $\mu$ l doxorubicin. Administration of doxorubicin is known to induce apoptosis and was used as a positive control in order to certify the selected method. Apoptotic cell nuclei were assessed by TUNNEL staining using the In Situ Cell Death Detection Kit.

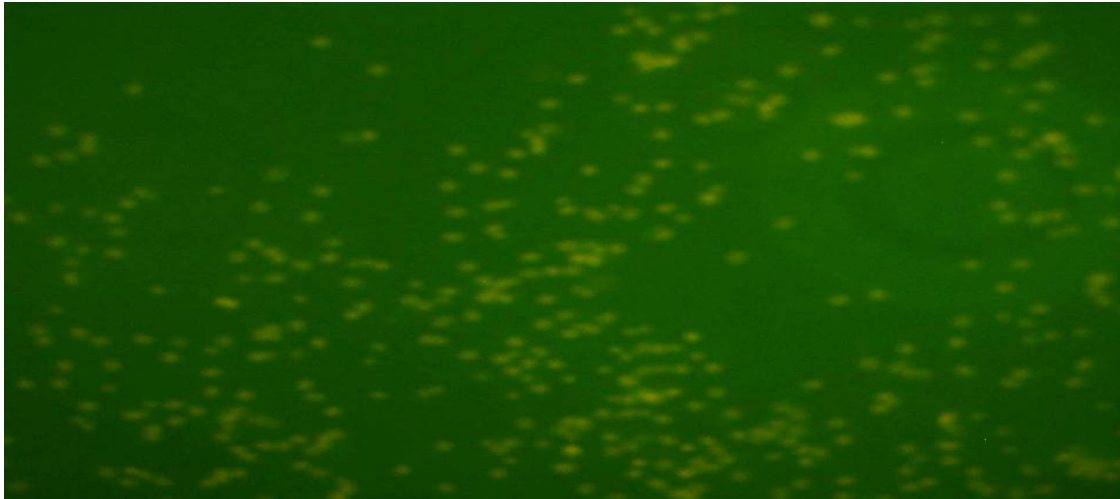


Figure 3.73: Image showing the apoptotic nuclei of the U87-MG cells that were treated with doxorubicin. . Image was taken by phase-contrast fluorescence microscopy with a special filter for fluorescein detection. This photograph is typical for n=8 such different experiments (10 x magnification).

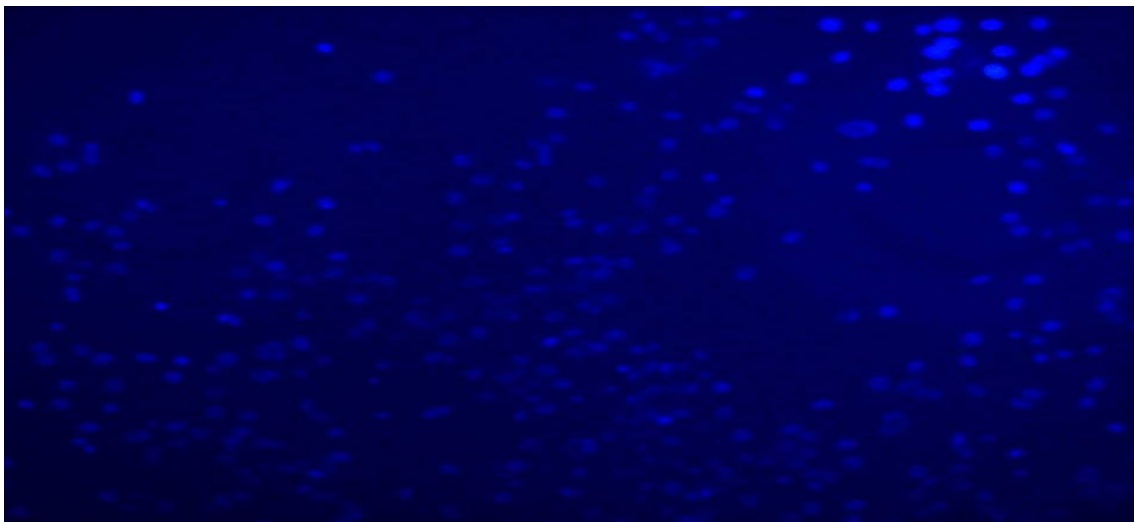


Figure 3.74: Image showing all the nuclei of the U87-MG cells that were treated with doxorubicin after counterstained with Hoeschst 33358. Image was taken by phase-contrast fluorescence microscopy with a special filter for Hoeschst 33358. This photograph is typical for n=8 such different experiments (10 x magnification).

The images in figures 3.75-3.76 show the stained nucleus of U87-MG cell line for the untreated cells over the period of 2 days. As shown on the images there was no apoptotic cells on the untreated group of the U87-MG cell line, in comparison with the total number of cells stained on the figure 3.76. After the period of 2 days the cells were stained, and subsequently viewed with a fluorescence microscope.



Figure 3.75: Image showing non-treated U87-MG cells after staining for TUNNEL. No apoptotic cells were detected. This photograph is typical for n=8 such different experiments (10 x magnification).

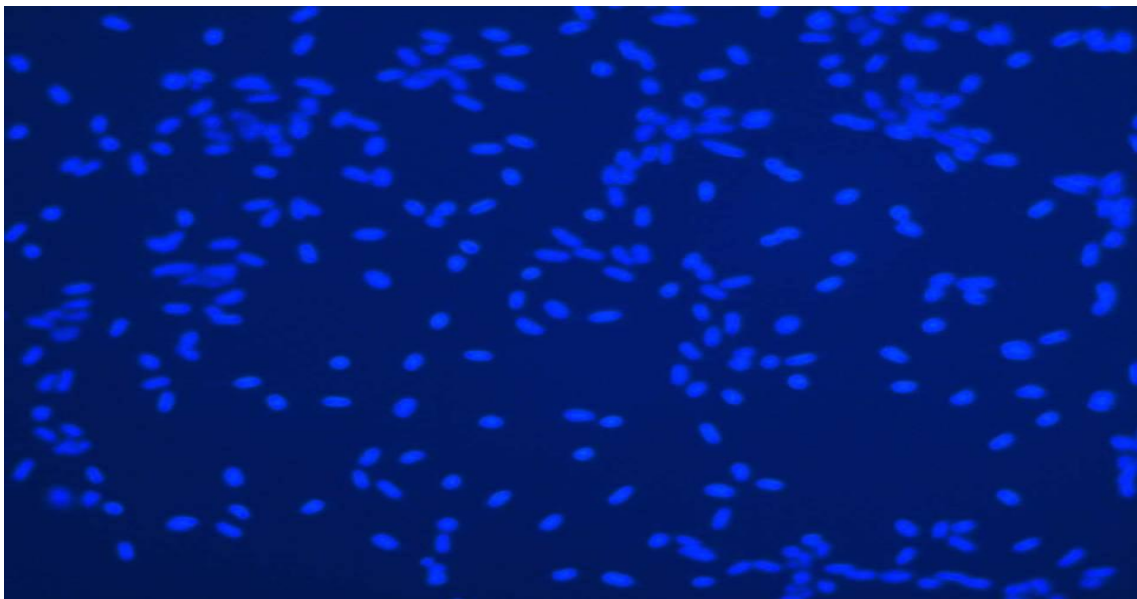


Figure 3.76: Image showing the total number of cells of the U87-MG cell line on the non-treated group after staining with Hoeschst 33358. This photograph is typical for n=8 such different experiments (10 x magnification).

The images in figures 3.77-3.78 show the stained nucleus of U87-MG cell line for the 1 nM T3 treated cells over the period of 2 days. As shown on the images there was no apoptotic cells on 1 nM T3 group of the U87-MG cell line, in comparison with the total number of cells stained on the figure 3.78. After the period of 2 days the cells were stained, and subsequently viewed with a fluorescence microscope.

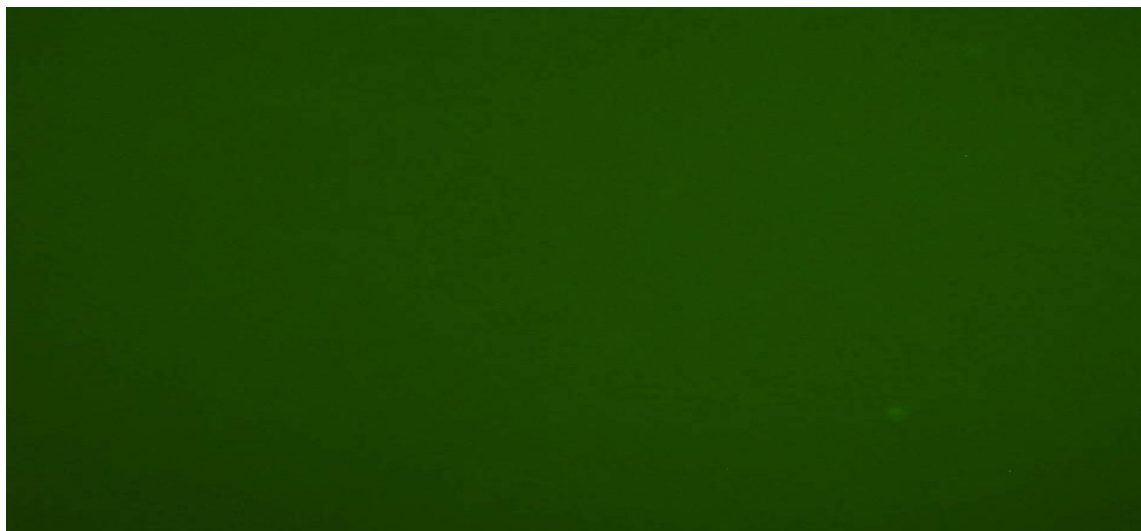


Figure 3.77: Image showing U87-MG cells treated with 1nM T3 after staining for TUNNEL. No apoptotic cells were detected. This photograph is typical for n=8 such different experiments (10 x magnification).

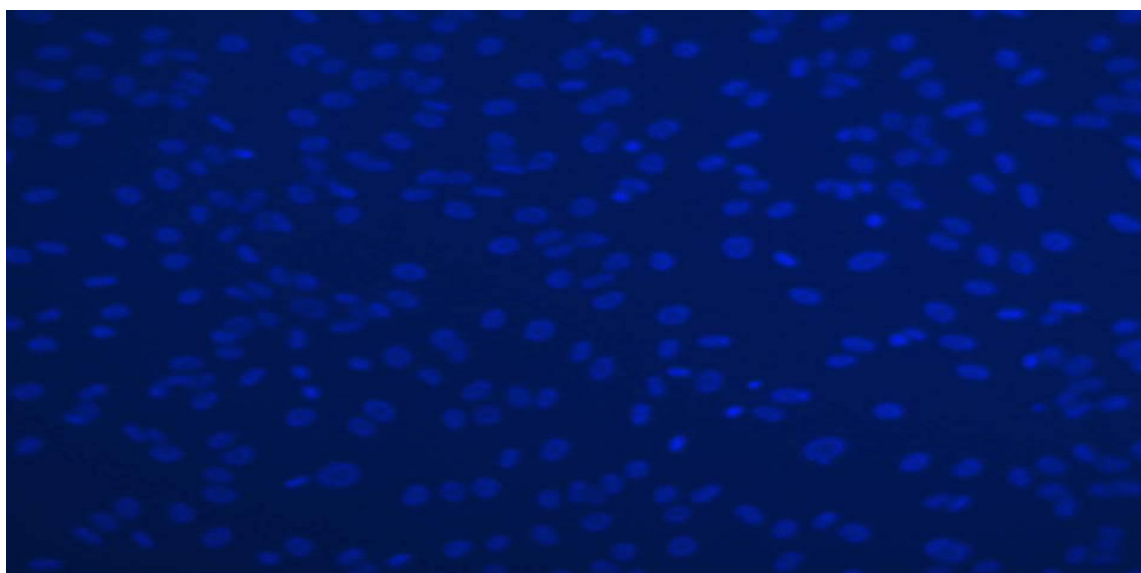


Figure 3.78: Image showing the total number of U87-MG cells treated with 1nM T3 after staining with Hoeschst 33358. This photograph is typical for n=8 such different experiments (10 x magnification).

The images in figures 3.79-3.80 show the stained nucleus of U87-MG cell line for the 500 nM T3 treated cells over the period of 2 days. As shown on the images there was no apoptotic cells on 500 nM T3 group of the U87-MG cell line, in comparison with the total number of cells stained on the figure 3.80. After the period of 2 days the cells were stained, and subsequently viewed with a fluorescence microscope.

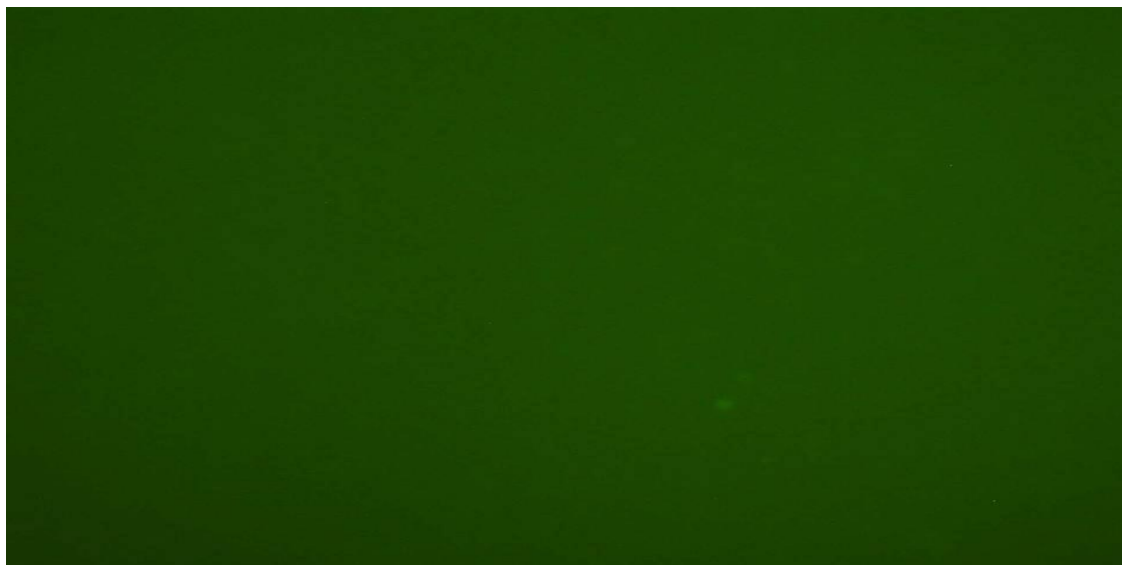


Figure 3.79: Image showing U87-MG cells treated with 500 nM T3 after staining for TUNNEL. No apoptotic cells were detected. This photograph is typical for n=8 such different experiments (10 x magnification).

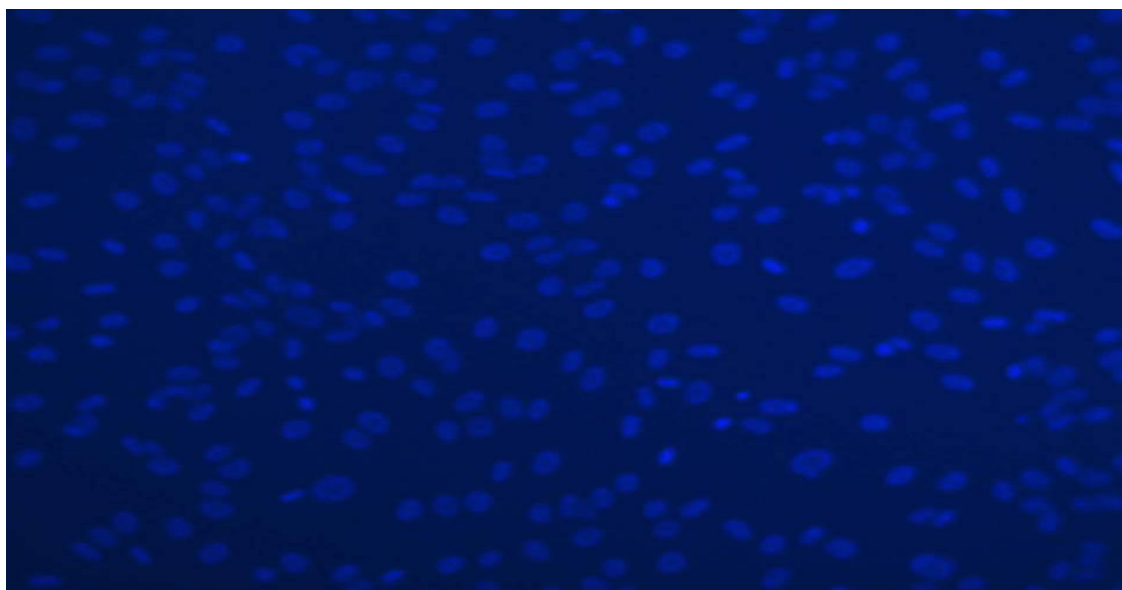


Figure 3.80: Image showing the total number of U87-MG cells treated with 500 nM T3 after staining with Hoeschst 33358. This photograph is typical for n=8 such different experiments (10 x magnification).

### 3.3.5.2. Cell apoptosis 4 days

The images in figures 3.81-3.82 show the nuclei of U87-MG cells following treatment with 10  $\mu$ l doxorubicin. Administration of doxorubicin is known to induce apoptosis and was used as a positive control in order to certify the selected method. Apoptotic cell nuclei were assessed by TUNNEL staining using the In Situ Cell Death Detection Kit.

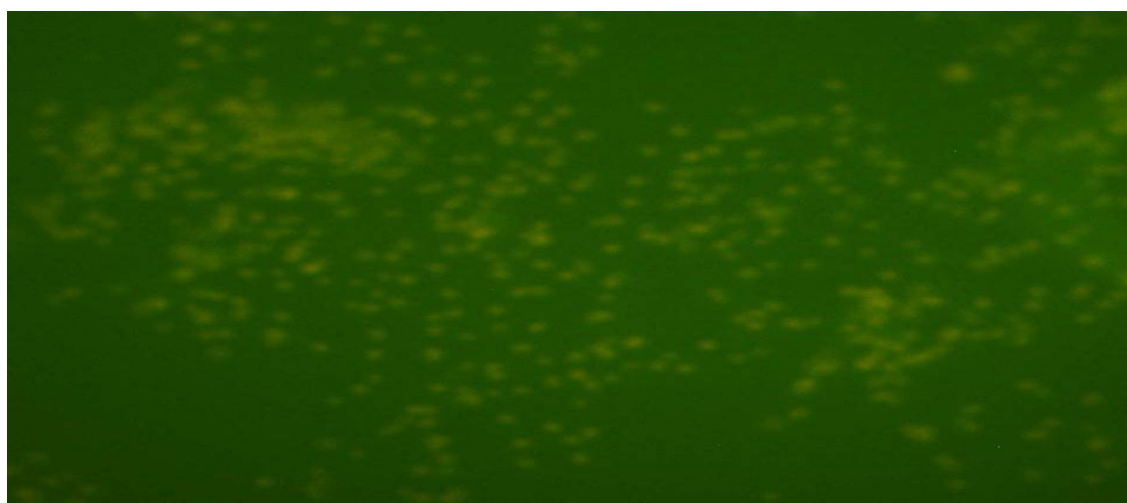


Figure 3.81: Image showing the apoptotic nuclei of the U87-MG cells that were treated with doxorubicin. . Image was taken by phase-contrast fluorescence microscopy with a special filter for fluorescein detection. This photograph is typical for n=8 such different experiments (10 x magnification).



Figure 3.82: Image showing all the nuclei of the U87-MG cells that were treated with doxorubicin after counterstained with Hoeschst 33358. Image was taken by phase-contrast fluorescence microscopy with a special filter for Hoeschst 33358. This photograph is typical for n=8 such different experiments (10 x magnification).

The images in figures 3.83-3.84 show the stained nuclei of U87-MG cell line for the untreated cells over the period of 4 days. As shown on the images there was no apoptotic cells on the untreated group of the U87-MG cell line, in comparison with the total number of cells stained on the figure 3.84. After the period of 4 days the cells were stained, and subsequently viewed with a fluorescence microscope.



Figure 3.83: Image showing non-treated U87-MG cells after staining for TUNNEL. No apoptotic cells were detected. This photograph is typical for n=8 such different experiments (10 x magnification).

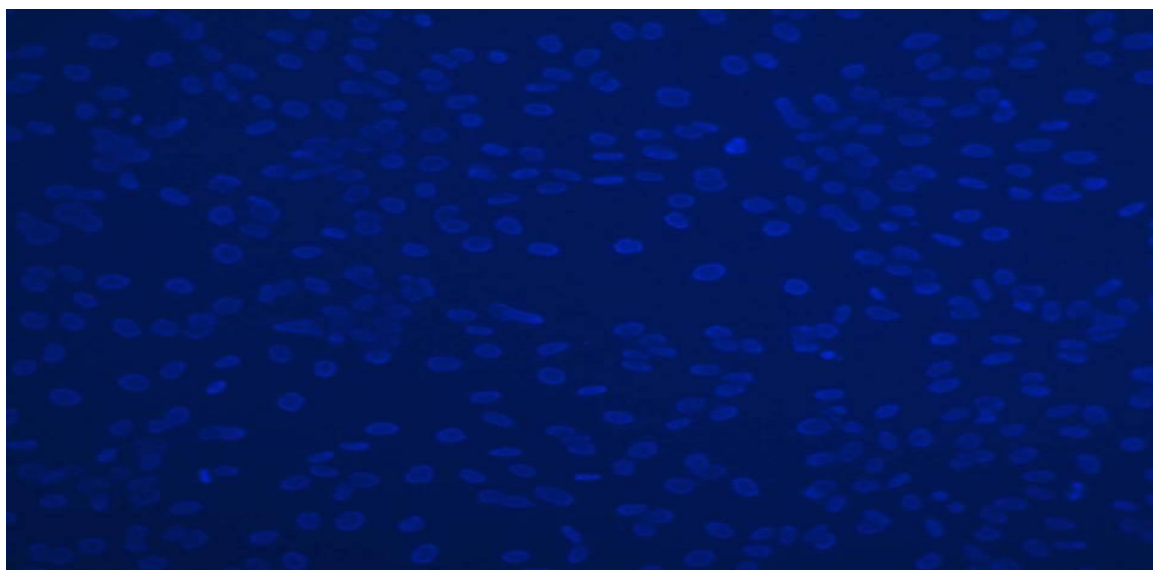


Figure 3.84: Image showing the total number of cells of the U87-MG cell line on the non-treated group after staining with Hoeschst 33358. This photograph is typical for n=8 such different experiments (10 x magnification).

The images in figures 3.85-3.86 show the stained nuclei of U87-MG cell line for the 1 nM T3 treated cells over the period of 4 days. As shown on the images there was no apoptotic cells on 1 nM T3 group of the U87-MG cell line, in comparison with the total number of cells stained on the figure 3.86. After the period of 4 days the cells were stained, and subsequently viewed with a fluorescence microscope.

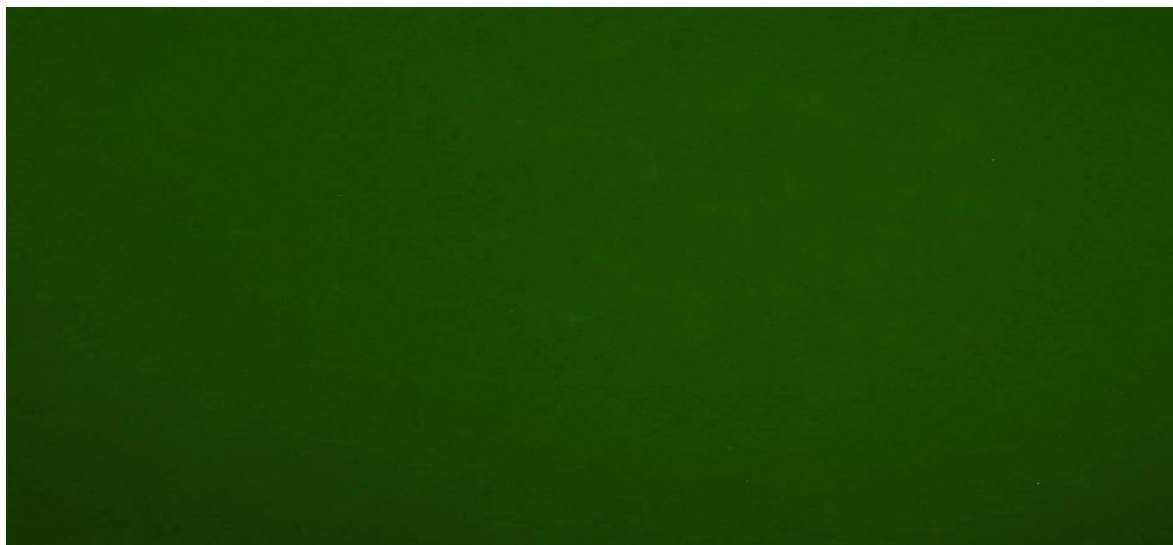


Figure 3.85: Image showing U87-MG cells treated with 1 nM T3 after staining for TUNNEL. No apoptotic cells were detected. This photograph is typical for n=8 such different experiments (10 x magnification).



Figure 3.86: Image showing the total number of U87-MG cells treated with 1 nM T3 after staining with Hoeschst 33358. This photograph is typical for n=8 such different experiments (10 x magnification).

The images in figures 3.87-3.88 show the stained nuclei of U87-MG cell line for the 500 nM T3 treated cells over the period of 4 days. As shown on the images there was no apoptotic cells on 500 nM T3 group of the U87-MG cell line, in comparison with the total number of cells stained on the figure 3.88. After the period of 4 days the cells were stained, and subsequently viewed with a fluorescence microscope.

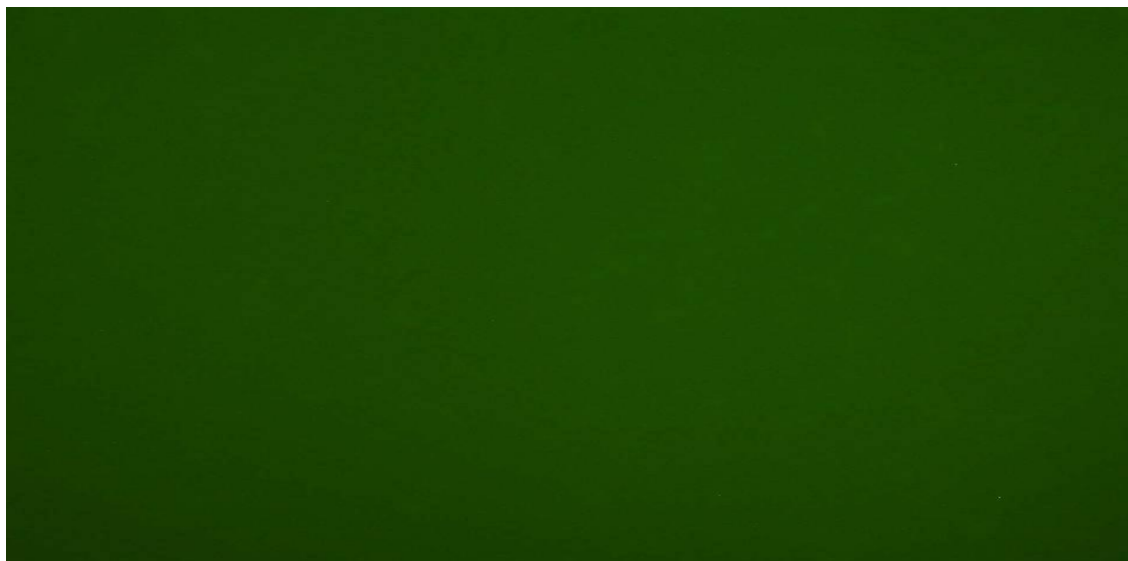


Figure 3.87: Image showing U87-MG cells treated with 500 nM T3 after staining for TUNNEL. No apoptotic cells were detected. This photograph is typical for n=8 such different experiments (10 x magnification).

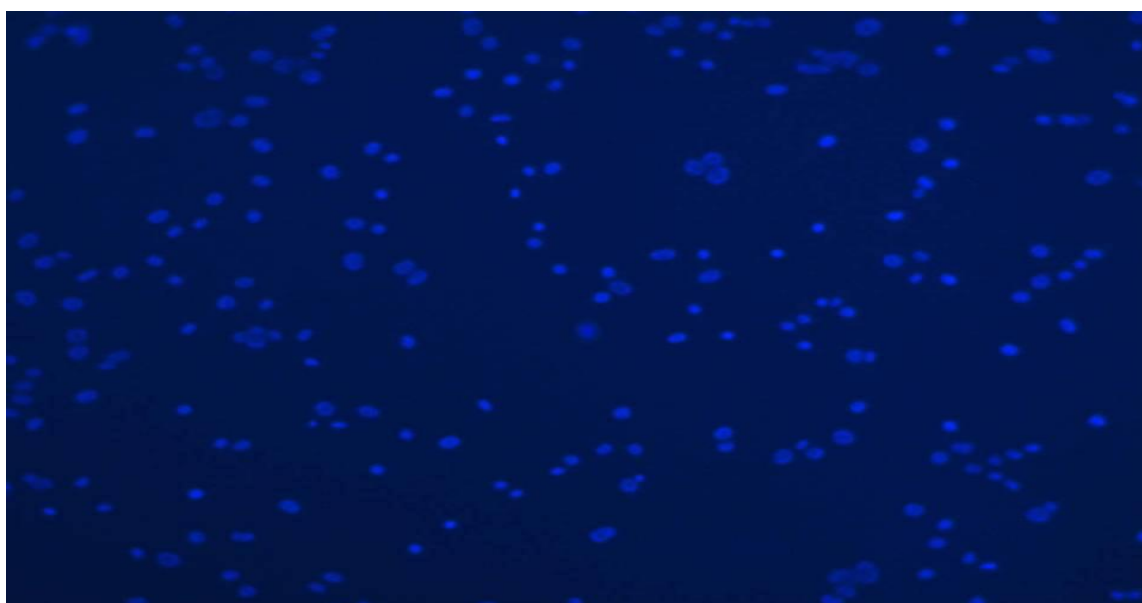


Figure 3.88: Image showing the total number of U87-MG cells treated with 500 nM T3 after staining with Hoeschst 33358. This photograph is typical for n=8 such different experiments (10 x magnification).

### **3.3.6. Molecular detection of kinase signalling in glioma cell lines**

#### **3.3.6.1. Kinase signalling activation 2 days**

Figure 3.89 shows the analysis of the density of the Western blotting protein (B) and (A) the average of the optical density (arbitrary units) as obtained from the Western blotting experiment for U87-MG cells. The results show no significant differences in the ratio of p44 and p42 phospho-ERK to total ERK after the 2 days of treatment.

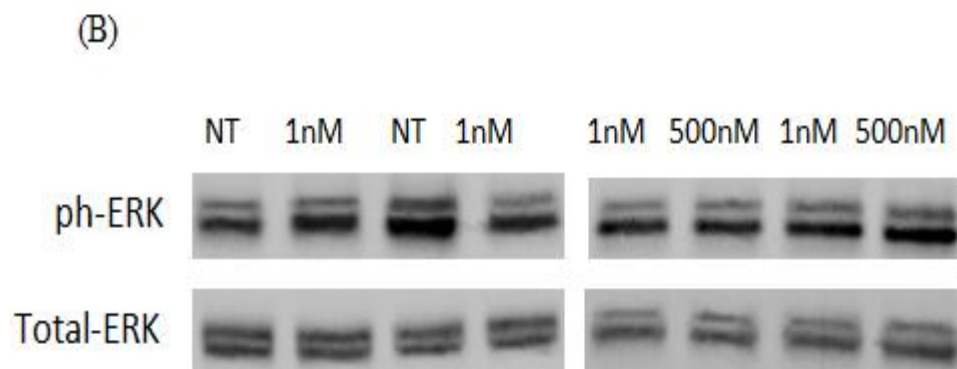
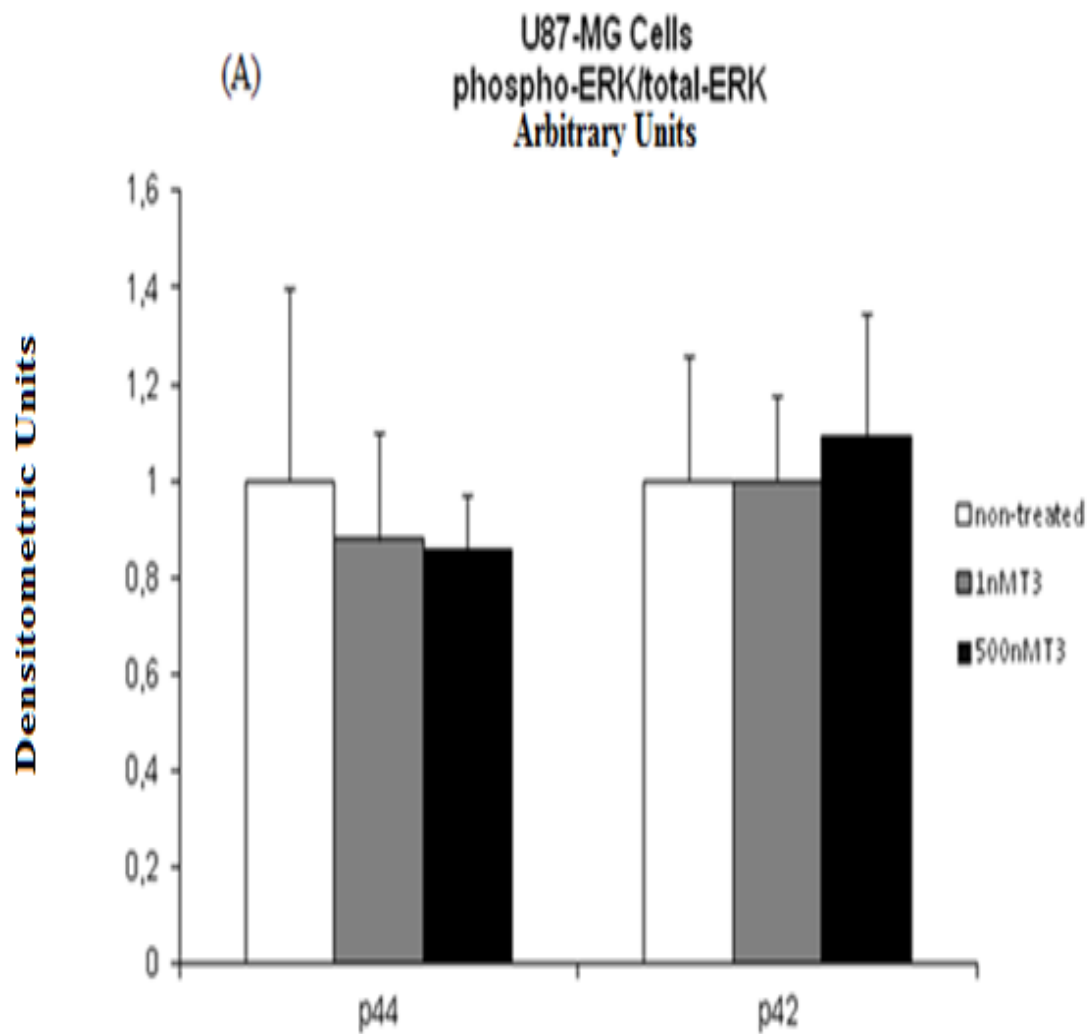


Figure 3.89: (A) Bar charts showing the ratio of phosphorylated to total p44 and p42 ERKs in non-treated cells and after 1 nM and 500 nM treatment with T3 for 2 days. (The bars are the average of the optical density (arbitrary units),  $\pm$ SEM, n=8). NT= non-treated. (B) Representative samples of Western blot of phosphor and total ERK protein.

Figure 3.90 shows the analysis of the density of the Western blotting protein (B) and (A) the average of the optical density as obtained from the Western blotting experiment. The results show that the ratio of phospho-Akt to total Akt after 2 days in culture was found to be reduced in 1 nM and 500 nM T3 treated cells as compared to the non-treated group. However, this decrease was not statistically significant.

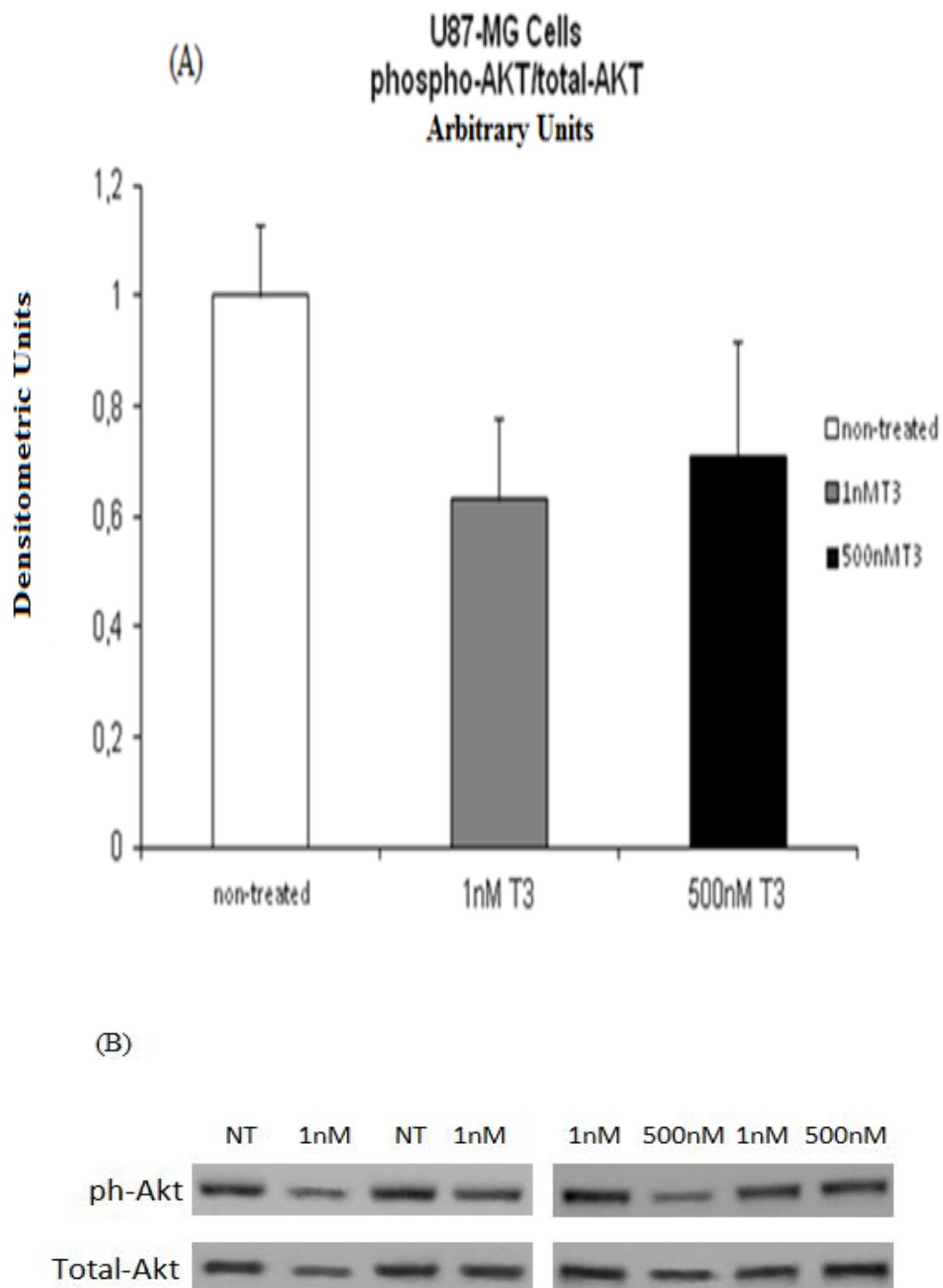


Figure 3.90: (A) Bar charts showing the ratio of phosphorylated to total AKT in non-treated cells and after 1 nM and 500 nM treatment with T3 for 2 days. (The bars are the average of the optical density (arbitrary units),  $\pm$ SEM, n=8). NT=non-treated. (B) Representative samples of Western blot of phospho and total AKT protein.

### **3.3.6.2. Kinase signalling activation 4 days**

Figure 3.91 shows the analysis of the density of the Western blotting protein (B) and (A) the average of the optical density as obtained from the Western blotting experiment in U87-MG cells. The results show no changes in the ratio of p44 and p42 phospho-ERK to total ERK between the groups after the 4 day treatment period.

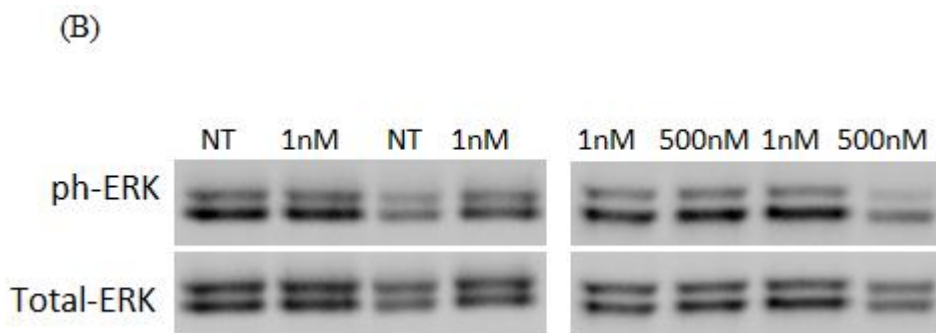
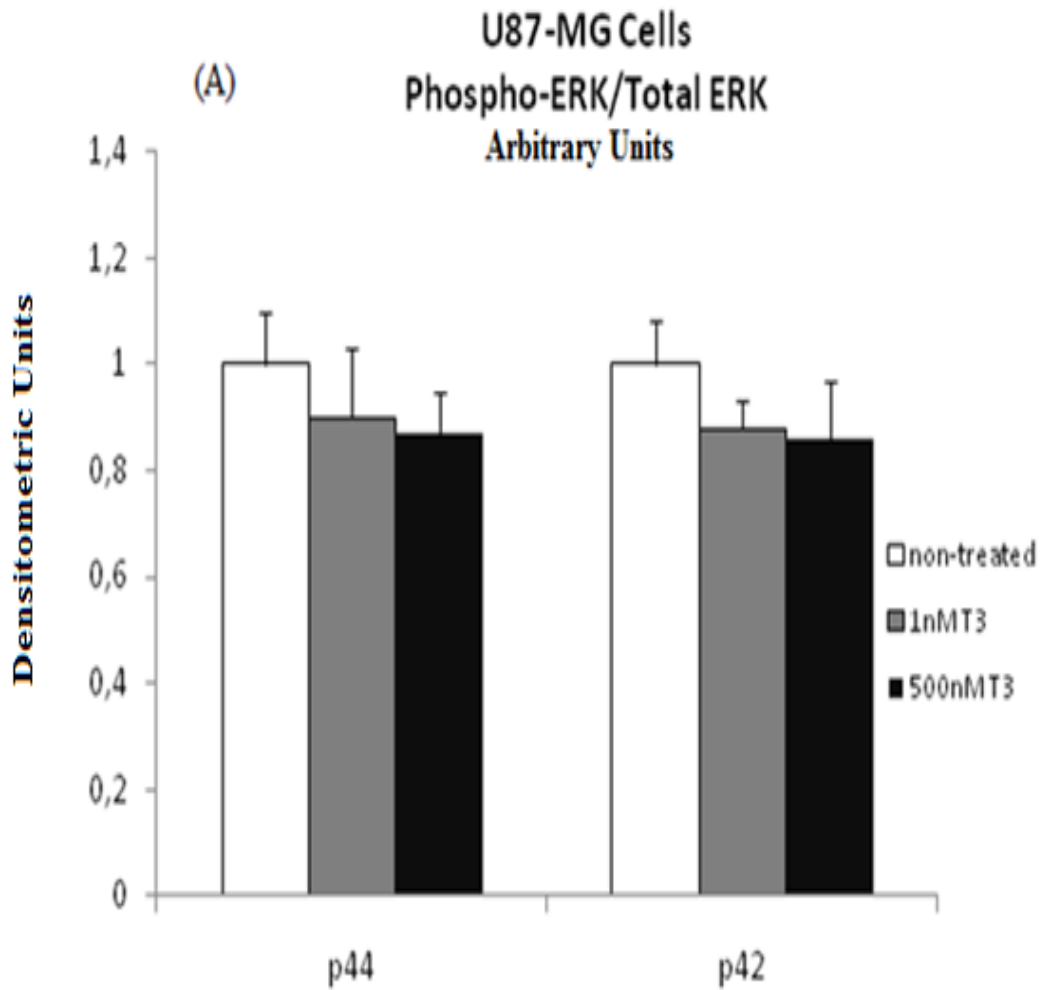


Figure 3.91: (A) Bar charts showing the ratio of phosphorylated to total p44 and p42 ERKs in non-treated cells and after 1nM and 500nM treatment with T3 for 4 days. (The bars are the average of the optical density (arbitrary units),  $\pm$ SEM, n=8). NT= non-treated. (B) Representative example of Western blot of phosphor and total ERK protein.

Figure 3.92 shows the analysis of the density of the Western blotting protein (B) and (A) the average of the optical density as obtained from the Western blotting experiment. The results show that the ratio of phospho-Akt to total Akt was decreased by 1.5 fold in 500 nM T3 treated cells as compared to non treated and 1 nM, T3 treated cells, ( $p < 0.05$ ).

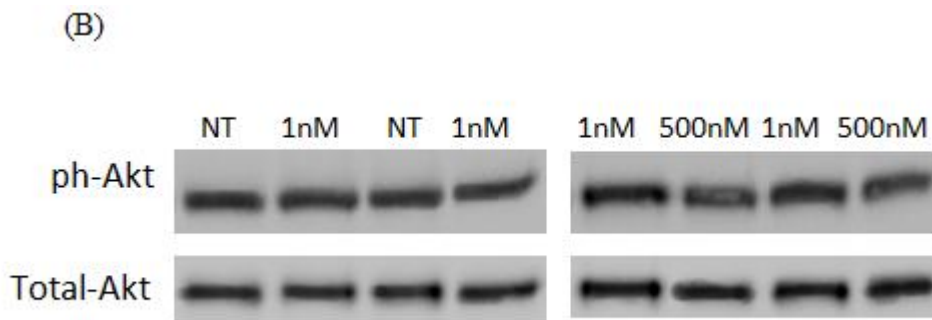
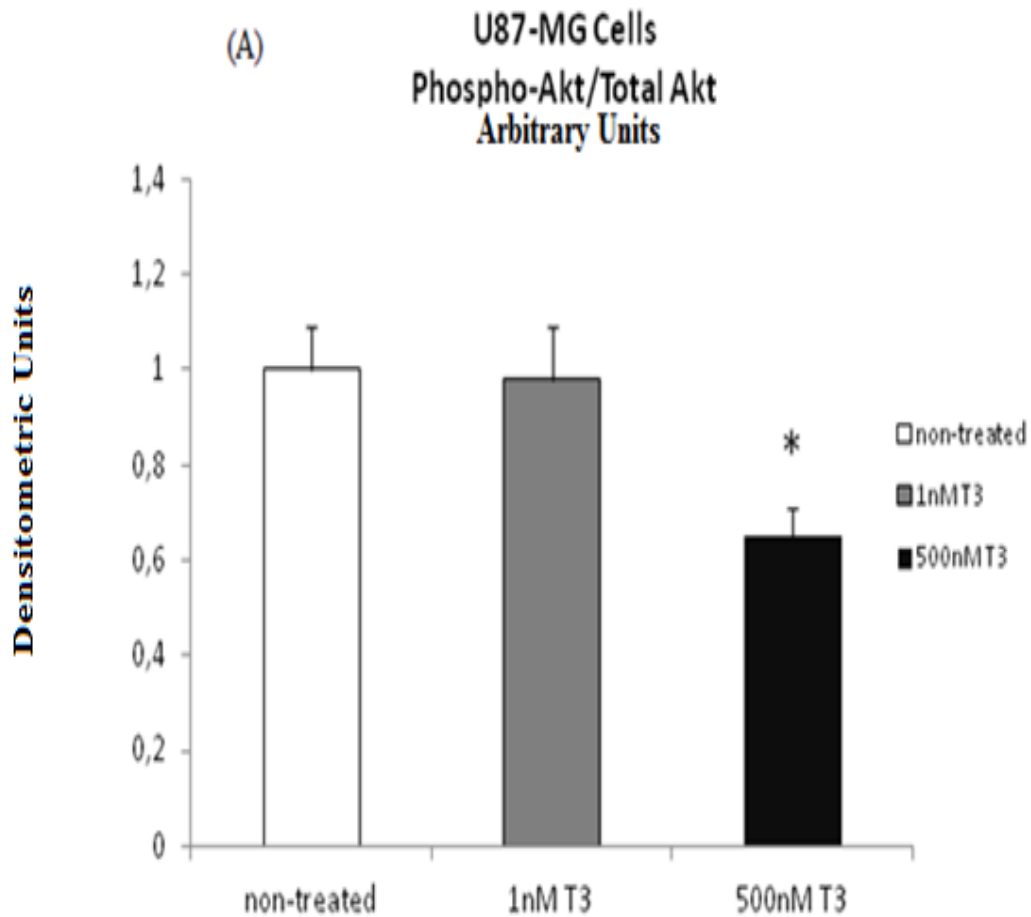
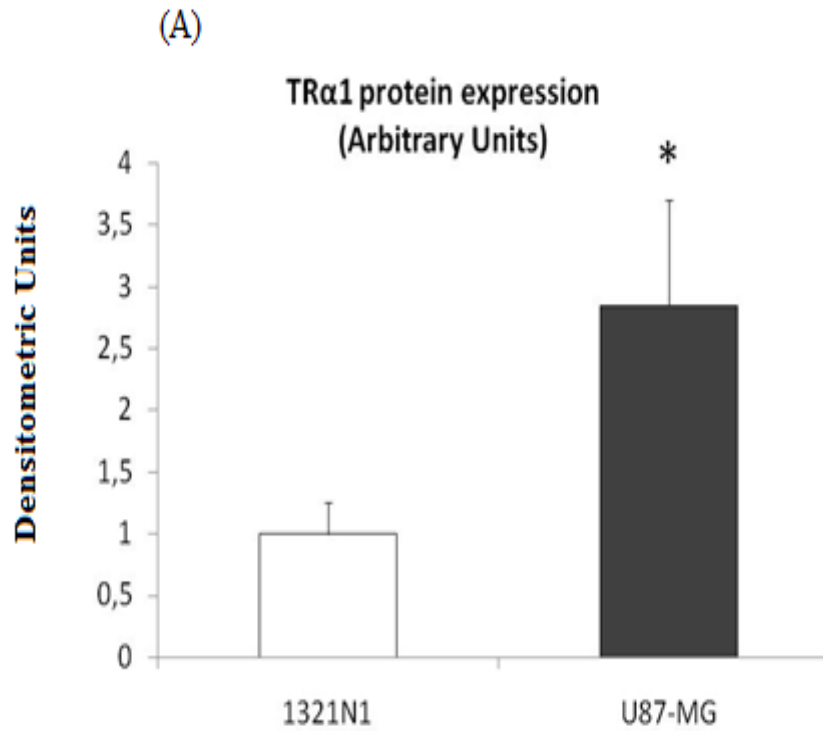


Figure 3.92: (A) Bar charts showing the ratio of phosphorylated to total AKT in non-treated cells and after 1 nM and 500 nM treatment with T3 for 4 days. (The bars are the average of the optical density (arbitrary units),  $\pm$ SEM,  $n=8$ ;  $*p<0.05$  for 500 nM T3 treated cells compared with either non-treated or 1 nM T3 treated cells). NT=non-treated. (B) Representative example of Western blot of phosphor and total Akt protein.

### **3.3.7. Molecular detection of TR $\alpha$ 1 receptors in glioma cell lines**

#### **3.3.7.1. Thyroid hormone receptors expression**

Figure 3.93 shows (B) the protein expression of the TR $\alpha$ 1 Thyroid hormone receptor between the cell lines 1321N1 and U87-MG after the treatment period of 4 days, and (A) the average of the optical density as obtained from the Western blotting experiment. As shown in the results, there was a 2.9 fold increase in the expression of TR $\alpha$ 1 receptor for U87MG cells as compared to 1321N1,  $p < 0.05$ . TR $\beta$ 1 receptor was undetectable in both cell lines.



(B)

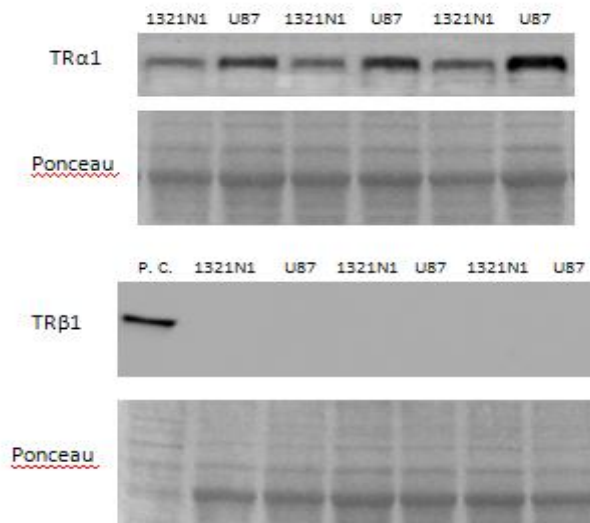


Figure 3.93: (A) Bar charts showing the TR $\alpha$ 1 and TR $\beta$ 1 protein expressions between the two cell lines 1321N1 and U87 (the bars are average of the optical density (arbitrary units),  $\pm$ SEM, n=8). \*  $p < 0.05$  for U87-MG vs 1321N1. (B) Representative example of Western blot protein.

# Chapter Four

## Discussion

## 4.1. Discussion

It is now well recognized that thyroid hormone (TH) may have a critical role in the pathogenesis and the progression of the diseases due to its regulatory action on cell differentiation, proliferation and cell survival (Mourouzis *et al.*, 2011). TH has regenerative/reparative action under pathological conditions (Pantos *et al.*, 2010; Pantos *et al.*, 2011; Shulga *et al.*, 2009). This unique effect could potentially be of therapeutic value in cancer therapy (Kress *et al.*, 2009).

Experimental and clinical studies provide a growing body of evidence that TH signalling may be altered in heart failure with important physiological and therapeutic consequences (Pantos *et al.*, 2008). Similarly, alterations in TH signalling have been observed in malignancies (Aranda *et al.*, 2009; Gonzalez-Sancho *et al.*, 2003) and hypothyroidism is shown to enhance tumour invasiveness and metastasis development (Garcia-Silva *et al.*, 2004; Martinez-Iglesias *et al.*, 2009). Furthermore, in 1896, thyroxine (horse thyroid extract) was the first successful hormonal product to be used against a fulminating breast cancer (Beatson *et al.*, 1896). Similar results were thereafter reported for a series of patients with breast cancer in 1954 (Loeser *et al.*, 1954). However, until now, the potential of TH as cancer therapy has not been adequately explored.

This thesis first explored the potential effects of thyroid hormone to differentiate undifferentiated and/ or dedifferentiated cells due to growth stimuli in an established model of neonatal cardiomyocytes.

These cells in a serum free environment remained undifferentiated. Then, the response of those cells to physiologic and pathologic growth stimuli was assessed. Cell size and shape, cytoskeleton organization and the pattern of myosin expression

were used as index of cell differentiation / dedifferentiation as previously described (Kinugawa *et al.*, 2005).

#### **4.2. T3 has the ability to differentiate neonatal cardiomyocytes**

Non-treated cardiomyocytes remained undifferentiated with an almost circular shape with poorly organized cytoskeleton and did not express  $\alpha$ -myosin which characterizes the adult phenotype. Addition of T3 promoted cell differentiation with cells to have an elongated shape, with a filamentous actin pattern organized into orderly arrays. Those cells expressed 100%  $\alpha$ -MHC and no signal was detected by immunostaining for  $\beta$ -MHC as compared to untreated cardiomyocytes expressing 100%  $\beta$ -MHC. These data clearly show that T3 is critical for the maturation of the myocytes during development and are in accordance with other studies.

Thus, TH was shown to be critical in the maturation of embryonic heart-derived cells (H9c2), (van der Heide *et al.*, 2007; van der Putten *et al.*, 2002). In fact, intracellular T4 and T3 levels increase during the progression of cell differentiation with a concomitant increase in the expression of TR $\alpha$ 1 and this response could be prevented by pharmacological inhibition of thyroid hormone binding to TR $\alpha$ 1 (Meischl *et al.*, 2008; Pantos *et al.*, 2008c; van der Heide *et al.*, 2007; van der Putten *et al.*, 2002). Furthermore, TH was shown to stop proliferation and promote differentiation in fetal bovine cardiomyocytes. Interestingly, this unique effect was shown to be achieved in nearly normal T3 concentrations and is mediated via T3 action on cyclin D1 and p21. (Chattergoon *et al.*, 2011).

### **4.3. Phenylephrine (PE) induce dedifferentiation in neonatal cells**

In this model, PE, an alpha adrenergic receptor, agonist was shown to further dedifferentiate the neonatal cardiomyocytes. In fact, PE treatment resulted in large cardiomyocytes with disoriented, dense myofibrils and stellular shape. PE-treated cardiomyocytes exhibited a 30% fold increase in  $\beta$ -MHC expression,  $p < 0.05$ , as compared to non-treated cardiomyocytes.  $\alpha$ -MHC expression was not detected. Interestingly, these cardiomyocytes were found to re-express TR $\alpha$ 1 as this occurs during foetal life (White *et al.*, 2001). Previous studies failed to show this effect since the authors measured only the total mRNA and not the expression of the protein in the nucleus (Kinugawa *et al.*, 2005).

### **4.4. T3 differentiates dedifferentiated cells**

Morphologically, PE-T3-treated cells exhibited an elongated shape, with a filamentous actin pattern organized into orderly arrays resembling that of T3-treated cells. T3 administration in PE-treated cardiomyocytes resulted in significantly reduced amount of  $\beta$ -MHC (about 25% of the total myosin) and increased amount of  $\alpha$ -MHC (about 75% of the total myosin). These data reveal that T3 can reverse stress-induced dedifferentiation and this effect may be of physiological and therapeutic relevance. In fact, TH treatment early after coronary ligation in animals could favorably remodel the viable, non ischemic myocardium. TH accelerated the development of cardiac hypertrophy characterized by an adult pattern of MHC isoform expression. This response caused an early normalization of wall stress which is known to be a critical determinant of oxygen consumption and myocardial performance (Pantos *et al.*, 2008). TH either early or late after myocardial infarction could reshape the heart from spherical to the elipsoid shape (Pantos *et al.*, 2008; Pantos *et al.*, 2009).

After showing that thyroid hormone has a unique ability to promote cell differentiation in heart cells, the present study further explored whether this can be of relevance in glioma tumour cells

Gliomas represent the most common primary brain tumour and are among the most aggressive of cancers. Patients with glioma typically relapse within a year of initial diagnosis (Ohgaki *et al.*, 2009). Although neurosurgical resection, radiation and chemotherapy provide clear benefit, prognosis remains disappointing. TH levels are shown to be low in patients with gliomas but the relevance of this response to the pathophysiology of the disease remains largely unknown (Nauman *et al.*, 2004).

#### **4.5. Glioma cell line models**

Cell models of glioma tumours are available for decades but the extent to which these models recapitulate the human disease remains debatable (Jacobs *et al.*, 2011). Two different glioma cell lines, the 1321N1, an astrocytoma grade II, and U87MG, a glioblastoma grade IV cell line were used in this study. Both cell lines are shown to express Akt (Koul *et al.*, 2006; Toll *et al.*, 2011) which is a frequent finding in gliomas (Pollack *et al.*, 2010).

U87 MG is the most commonly studied brain cancer cell line and is highly cytogenetically aberrant as genomic decoding has recently revealed (Clark *et al.*, 2010). This cell line is PTEN deficient and resistant to conventional therapy (Premkumar *et al.*, 2012) PTEN is a well studied tumour suppressor gene that is mutated or deleted in various cancers including glioma (Parson *et al.*, 2008) and the lack of it is implicated in resistance to chemotherapy and radiation (Hanahan *et al.*,

2011). Here, it should be noted that the longest survival of patient with glioma was shown to be associated with a molecular profile including PTEN tumour suppressor gene positive and Akt negative (Sperduto and Chakravarti, 2009)

#### **4.6. Thyroid hormone (TH) and brain tumours**

Thyroid hormone is essential for the proper development of numerous tissues, notably the brain. The entry of T4 and T3 via the blood-brain barrier appears to be the preferred route for the distribution of thyroid hormone in the brain, whereas the uptake via choroid plexus–CSF barrier is thought to be necessary to provide circumventricular areas with sufficient amounts of thyroid hormone (Dratman, *et al.*, 1991). After passing these barriers, T4 has to be taken up by astrocytes for further activation and finally T3 has to enter neuronal cells, which not only express TRs but also participate in the inactivation of T4 and T3 by expressing D3 (Heuer, 2003).

The action of T3 in relation to brain tumours has not been adequately explored. Preliminary experimental studies provide evidence showing that acute, short-term TH treatment may increase cell proliferation and survival via its non genomic action (Davis *et al.*, 2006; Lin *et al.*, 2009; Lin *et al.*, 2008). However, this effect may not be sustained and long-term TH treatment appears to suppress cell proliferation in neuroblastoma cells (Garcia-Silva *et al.*, 2004). Most of those studies have looked at the effect of thyroid hormone on cell proliferation and not on cell differentiation and induction of cell necrosis. Furthermore, there are no data regarding potential changes in thyroid hormone receptors in experimental glioma cell lines.

T3 was used as chronic treatment since T4 acts on the cell membrane and has no genomic long acting effects. Cells deprived of T3 in medium were used as controls (0 nM, untreated). Two doses of T3 were used based on previous data (Lebel *et al.*, 1994; Aranda *et al.*, 2004). Thus, cells were treated with 1 nM which is a near physiologic dose and clinically relevant. A second dose of 500 nM was used as supraphysiological dose. The effects of T3 were assessed in two time points; 48 h and 96h. This was based on the data obtained from the construction of growth curves and from previous studies showing that the effect of T3 on cell differentiation was peaked at 48h (Lebel *et al.*, 1994). The effect of T3 on cell proliferation was assessed by BrdU labeling (Garcia –Silva *et al.*, 2004). Cell differentiation was assessed by morphology studies (Lebel *et al.*, 2004). Apoptosis was assessed by TUNNEL staining and cellular necrosis was measured by LDH release (Tamura *et al.*, 2000).

#### **4.7. T3 effect on glioma cell differentiation**

T3 at concentration of 1 nM and 500 nM resulted in cell re-differentiation in both cell lines studied as indicated by the morphological changes and the marked increase in the number of perisomatal filopodia like neurites. This finding is in accordance with previous reports showing a transforming effect of T3 in neuroblastoma cells (Garcia-Silva *et al.*, 2004). A series of genes related to neuroblastoma cell differentiation are shown to be responsive to TH (Bebo *et al.*, 2011). It is of note that this unique effect of TH has also been shown in other cancer cells and may be of physiological and therapeutic relevance (Perra *et al.*, 2009).

#### **4.8. T3 effect on cell growth and survival**

T3 at concentration of 1 nM had a differential effect on cell growth between the two cell lines as indicated by the total cell number count. Thus, in 1321N1, T3 treatment significantly increased total cell number at 2 days which declined thereafter. On the contrary, in the U87MG cell line, total cell number was markedly decreased both at 2 and 4 days with T3 incubation. Changes in cell numbers may reflect alterations in cell proliferation and /or cell injury (cell necrosis and / or apoptosis). In order to address this issue we measured cell proliferation using BrdU labelling reagent added to the medium and LDH release in medium for cell necrosis and TUNNEL staining using the In Situ Cell Death Detection Kit for cell apoptosis. The results showed that T3 had no effect cell injury but had a differential effect on cell proliferation. In fact, in 1321N1, T3 treatment resulted in increased cell proliferation at two days which declined thereafter and in the U87MG cell line, T3 markedly suppressed cell proliferation which was evident both at two and four days. Taken together, these data clearly show that near physiological T3 concentrations can reduce glioma growth in the more aggressive type via its effect on cell proliferation (Pantos *et al.*, 2012).

T3 at the higher concentration had also a differential effect on cell growth between the two cell lines as indicated by the total cell number count. Thus, in 1321N1, T3 treatment significantly increased total cell number at 2 days which declined thereafter. This was due to T3 effect on cell proliferation: T3 treatment resulted in increased cell proliferation at two days which declined thereafter. In U87MG cell line, total cell number was markedly decreased both at 2 and 4 days with T3 incubation. This was found to be due to the effect of T3 both on cell proliferation and cell survival. In fact, T3 at high concentration not only inhibited cell proliferation but also caused a marked

increase in cell injury in the form of cell necrosis as indicated by the LDH release. Similar result has not been previously reported since there is no study which has investigated potential effect of T3 on glioma cell survival.

#### **4.9. Molecular aspects of T3 action on glioma tumours**

##### **4.9.1. The potential role of TR receptors**

The potential underlying mechanisms of TH on glioma cell growth are not fully understood. Long-term TH effects are mediated via thyroid hormone receptors (TRs). TRs are transcription factors which regulate important genes related to cell differentiation, proliferation and survival (Kress *et al.*, 2009). It is now recognized that TRs are altered in pathological conditions with important physiological consequences. Thus, it has previously been shown that TRs can change under pathological conditions such as myocardial ischaemia or in cardiac cells exposed to growth stimuli (Pantos *et al.*, 2011; Pantos *et al.*, 2008). Similarly, there is increasing evidence that alterations in TRs are common events in cancer (Pantos *et al.*, 2010). The evidence demonstrating that the mutated TR could be involved in carcinogenesis came from the discovery that TR $\alpha$ 1 is the cellular counterpart of the retroviral v-erbA that is involved in the neoplastic transformation leading to acute erythroleukemia and sarcomas (Sap, *et al.*, 1986; Thormeyer and Baniahmad, 1999). It was shown that V-erbA itself has a weak oncogenic activity but it augments the transformation activity of other oncoproteins (Cheng, 2003). V-erbA competes with TR for binding to TREs and interferes with the normal transcriptional activity of liganded-TR on several promoters (Yen *et al.*, 1994; Chen and Privalsky, 1993). V-erbA oncoprotein is

thought to repress constitutively, through its dominant negative activity, a certain set of genes that prevent cellular transformation (Cheng, 2003).

Further evidence, which involves the mutated TRs in carcinogenesis, comes from from the identification that cyclin D1, a known oncogene product, and p53, a known suppressor can physically interact with TR $\beta$ 1 (Cheng, 2003). It was found that p53 interacts with TR $\beta$ 1 *in vitro* and in cultured cells an interaction that results in repression of the transcriptional activity of TR $\beta$ 1 (Bhat, *et al.*, 1997). Cyclin D1 associates with C-terminal region of the ligand-binding domain of TR $\beta$ 1 *in vitro* and *in vivo* and acts to repress the transcriptional activity of TR $\beta$ 1,  $\alpha$ 1 and  $\beta$ 2 (Lin *et al.*, 2002).

TR receptors are shown to have a tumour suppressor effect. Thus, mice expressing a dominant negative TR $\beta$  mutant present in some patients with thyroid hormone resistance syndrome spontaneously develop metastatic carcinoma (Suzuki *et al.*, 2002). Expression of TR $\beta$ 1 was shown to abolish totally tumour formation by *ras* – transformed cells in nude mice, even under hypothyroid conditions and block to a significant extent fibroblast transformation by *ras* in the absence of exogenously added ligand. On the other hand, tumour formation is reduced in euthyroid mice inoculated with cells expressing *ras* oncogene and TR $\alpha$ 1, but all hypothyroid animals develop tumours. Thus, TR $\alpha$ 1 has a ligand –dependent antitransforming activity (Garcia-Silva *et al.*, 2004).

On the basis of this evidence, the present study explored whether altered TR expression in these two cell lines could possibly underlie the differential T3 effect on cell proliferation. Interestingly, TR $\alpha$ 1 was found to be over expressed in U87MG cell line compared to 1321N1, while TR $\beta$ 1 receptor was undetectable in both cell lines. This finding may indicate a potential implication of TR $\alpha$ 1 receptor in T3 action on

glioma cell tumours. In fact, T3 was shown to have no effect on neuro-2a cells in which TR $\alpha$ 2 receptor expression was dominant and inhibited TR $\alpha$ 1 which was hardly expressed (Lebel *et al.*, 1994).

TR $\alpha$ 1 receptor has a unique dual mode of function depending on thyroid hormone availability. Thus, TR $\alpha$ 1 in its un-liganded state (aporeceptor) instead of being inactive exerts repressive or inducible effect on the transcription of T3 inducible or repressive genes by recruiting co-repressor complexes with histone deacetylase (Zhang *et al.*, 2000). This is of important physiological relevance during development with TR $\alpha$ 1 to be over-expressed at early embryonic stages when TH is low, resulting in cell proliferation and declines thereafter with the rise of TH resulting in cell differentiation (Mourouzis *et al.*, 2011). This foetal pattern of TR $\alpha$ 1 expression re-emerges under pathological conditions and may lead to pathological hypertrophy (Pantos *et al.*, 2011; Pantos *et al.*, 2008) or promote cell cancer proliferation (Garcia-Silva *et al.*, 2004). The addition of TH prevents pathological growth and stops cancer cell proliferation by converting the un-liganded TR $\alpha$ 1 to liganded receptor (Pantos *et al.*, 2011, Pantos *et al.*, 2008; Garcia-Silva *et al.*, 2004) (Figure 4.1). This ligand dependent antitransforming activity of thyroid hormone receptor is unique for the TR $\alpha$ 1. In fact, over-expression of TR  $\beta$ 1 was shown to abolish tumour formation by ras –transformed cells in nude mice, even under hypothyroid condition (Garcia-Silva *et al.*, 2004).

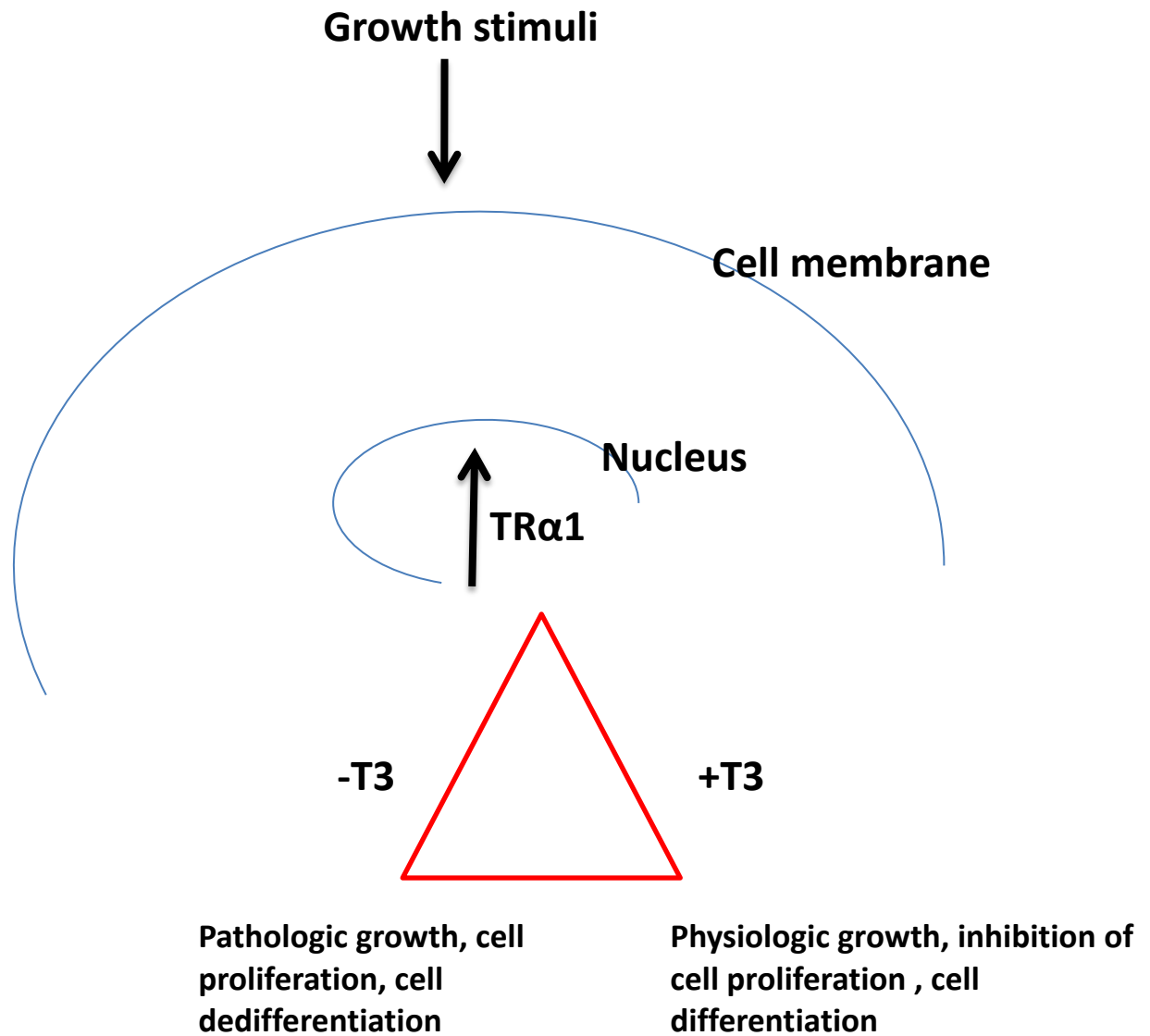


Figure 4.1. A schematic diagram showing the role of TR $\alpha$ 1 in the response of the cell to growth stimuli. The present study and previous reports provide evidence that T3 can convert pathological growth to physiologic growth and re-differentiate cardiomyocytes or cancer cells (Taken from a Power point presentation).

#### **4.9.2. TR $\alpha$ 1: a common player in pathological cardiac growth and cancer**

An interesting finding of this study was that TR $\alpha$ 1 receptor was found to be re-expressed both in pathologic growth induced by (PE) and glioma tumour cells. This probably indicates that a common mechanism which returns the cells to fetal phenotype in response to stress may exist (Pantos *et al.*, 2011). More importantly, the fact that the addition of thyroid hormone could reverse this response probably indicates that TR $\alpha$ 1 is a critical molecular switch that regulates the process of cell differentiation /dedifferentiation in response to stress. TR $\alpha$ 1 may be pharmacologically targeted and novel treatments for cancer and heart failure may emerge (Pantos *et al.*, 2011). However, this issue merits further investigation in future studies.

#### **4.9.3. The potential role of growth signalling**

Complex signaling pathways are implicated in cell growth and survival. Interestingly, growth and cell response to injury share common pathways. Akt and ERK are the most studied kinase signalling in cell growth and survival (Chappell *et al.*, 2011; Hers *et al.*, 2011; Lo *et al.*, 2011).

Akt deliver antiapoptotic signals via different proteins directly modulated by Akt phosphorylation. Bad is one of the first discovered targets of Akt phosphorylation. Bad is a proapoptotic member of the Bcl-2 family of proteins, able to bind Bcl-2 or Bcl-XL, blocking their antiapoptotic activities. Phosphorylation of Bad on S136 by Akt disrupts its interaction with Bcl-2/Bcl-XL, localized on the outer mitochondrial membrane, sequestering Bad in the cytosol through the interaction with 14-3-3 protein. In an analogous way, phosphorylation of proapoptotic Bax protein by Akt on S184 suppresses its translocation to mitochondria, preventing Bax conformational change, a typical event that occurs after apoptotic induction. In addition, the caspase

cascade is further inhibited by Akt phosphorylation of pro-caspase 9, inactivated through phosphorylation in S196, a residue that, however, is not conserved in other mammalian species.

One of the best-conserved functions of Akt is its role in promoting cell growth. The predominant mechanism appears to be through activation of the mammalian target of rapamycin complex 1 (mTORC1), which is regulated by both nutrients and growth factor signalling. Akt-mediated cell proliferation and oncogenic transformation has been shown to be dependent on mTORC1 activation (reviewed by Bononi *et al.*, 2011).

The ERK signalling pathway plays a role in several steps of tumour development. The phosphorylation by ERK of proteins such as myosin light chain kinase, calpain, focal adhesion kinase, and paxillin promotes cancer cell migration. The ERK pathway also induces the expression of matrix metalloproteinases and thereby promotes the degradation of extracellular matrix proteins and consequent tumour invasion. Furthermore, ERK1/2 signaling regulates the activities and levels of Bcl-2 family proteins such as the pro-apoptotic protein BIM and the anti-apoptotic protein MCL-1, thereby promoting the survival of cancer cells. The ERK signalling pathway is therefore considered a prominent therapeutic target for the development of chemotherapeutic drugs, with sorafenib, a Raf inhibitor, being one of the most efficient drugs available (Tanimura *et al.*, 2002; Welch *et al.*, 2000).

Akt and ERK have been associated with glioma tumour aggressiveness (Pollack *et al.*, 2010; Fanand *et al.*, 2011; Robinson *et al.*, 2011). The present study showed that T3 treatment in glioma cell lines could induce distinct changes in Akt and ERK activation (assessed by measuring the phosphorylated levels of these kinases). Thus, T3, at 1 nM, significantly increased p-Akt levels in 1321N1 and not in U87MG cell

line while had no effect on ERK activation in either cell line. With the higher concentration, T3 increased both Akt and ERK activation in 1321N1 without any effect on ERK activation in U87MG. However, T3 at this dose resulted in marked decrease of Akt activation and this finding may offer an explanation of the observed increased cell injury with the use of this dose. Interestingly, progesterone, at high dose, was also shown to induce cell injury in neuroblastoma by suppressing Akt activation (Atif *et al.*, 2011). Similarly, tamoxifen induced apoptosis of rat C6 glioma by suppressing Akt phosphorylation in a time dependent manner (Feng and Huang 2010). Taken together, it appears that hormones may induce cell injury in gliomas by targeting the Akt pathway. Akt remains an important target to induce apoptosis in glioma cells. In fact, although therapies targeting pro-apoptotic pathways can also increase cell injury, cells that lack PTEN and overexpress Akt such as U87 remain resistant to those treatments (Premkumar *et al.*, 2012).

Tables 4.1 and 4.2 summarize the major findings of this study employing 1321N1 and U87-MG glioma cell lines for the period of 2 and 4 days of treatment with T3. The results show that following 2 days of treatment, T3 can affect cell differentiation in both the cell lines as well as the cell number of the cells showing an increase on both doses on the 1321N1 cells in comparison with the reduction of cell number on the U87-MG cells. The changes on the cell number come as a result of cell proliferation which is increased in both doses on the 1321N1 cells, and decreased in both doses on the U87-MG cells. The Akt pathway plays an important role for the changes happen to both cell lines after the 2 days treatment period.

The results following the 4 days treatment period show that T3 can affect cell differentiation in both the cell lines but show a reduction on the cell number and cell proliferation in both doses only in the U87-MG cells. Cell necrosis is increased only

on the 500 nM dose in the U87-MG cells. The ERK pathway plays an important role for the changes happen to the U87-MG cells.

The results for the effect of TH treatment on cardiomyocytes are summarized in Table 4.3. The data show that both PE and TH treatments can result in significant increase in cell geometry, cell growth, cell protein synthesis and the expression of TR $\alpha$ 1 receptor in comparison with the non-treated cells.

**Table. 4.1. Summary of main results after 2 days T3 treatment**

	1321N1 Cell line		U87 Cell line	
	<i>1nM T3</i>	<i>500nM T3</i>	<i>1nM T3</i>	<i>500nM T3</i>
<b>Cell differentiation</b>	+	+	+	+
<b>Cell number</b>	Increased	Increased	Reduced	Reduced
<b>Cell proliferation</b>	+	+	-	-
<b>Apoptosis</b>	ND	ND	ND	ND
<b>Necrosis</b>	No change	No change	No change	+
<b>Phospho-Akt levels</b>	Increased	Increased	No change	No change
<b>Phospho-ERK levels</b>	No change	Increased	No change	No change

**“+” represents induction, “-” represents inhibition, ND represents not detected**

**Table.4.2. Summary of main results after 4 days T3 treatment**

	1321N1 Cell line		U87 Cell line	
	<i>1nM T3</i>	<i>500nM T3</i>	<i>1nM T3</i>	<i>500nM T3</i>
<b>Cell differentiation</b>	+	+	+	+
<b>Cell number</b>	No change	No change	Reduced	Reduced
<b>Cell proliferation</b>	No change	No change	-	-
<b>Apoptosis</b>	ND	ND	ND	ND
<b>Necrosis</b>	No change	No change	No change	+
<b>Phospho-Akt levels</b>	No change	No change	No change	No change
<b>Phospho-ERK levels</b>	No change	No change	No change	Decreased

**“+” represents induction, “-” represents inhibition, ND represents not detected**

**Table 4.3. Summary of main results on cardiomyocyte cells after PE and T3 treatment**

	<b>Non-treated</b>	<b>PE</b>	<b>T3</b>
<b>Cell growth</b>	ND	Increased	Increased
<b>Cell area</b>	ND	Increased	Increased
<b>Protein synthesis</b>	Reduced	ND	Increased
<b><math>\alpha</math>-MHC</b>	ND	ND	Increased
<b><math>\beta</math>-MHC</b>	Increased	Increased	ND
<b>TR<math>\alpha</math>1</b>	Reduced	Increased	Increased

**ND represents not detected**

#### **4.10. Conclusion**

Tables 4.1, 4.2 and 4.3 summarize the major findings of this study. The results show that T3 may reverse pathological growth in cardiac cells and re-differentiate glioma tumour cells due to its unique regulatory action on cell differentiation. In cardiomyocytes T3 has the ability to differentiate neonatal cells and PE induces dedifferentiation on those cells. In gliomas, T3 effect on cell proliferation appears to be dependent on the type of tumour cell line with aggressive tumours to be more sensitive to thyroid hormone treatment. TR $\alpha$ 1 receptor may, at least in part, be implicated in this response.

#### **4.11. Clinical and therapeutic relevance –future directions**

These preliminary results may be the basis of further investigation to better clarify the effects of T3 on glioma treatment. It appears that physiological doses may be sufficient to control growth in glioma tumours. In fact, it has been shown that T3 levels are low in patients with glioma (Nauman *et al.*, 2004) and thus, T3 replacement therapy may be of value. This has to be tested in small clinical trials. A beneficial effect of the combination treatment with radiotherapy and thyroid hormone has been previously reported (Morales *et al.*, 1988).

#### **4.12. Scope for future studies**

1. Investigating the cellular mechanisms of contraction of the cardiomyocytes by measuring intracellular free  $\text{Ca}^{2+}$  concentrations, L-type  $\text{Ca}^{2+}$  channel activities and contraction using established physiological methods as fluorometry, patch clamp and video edge techniques. These experiments can be done in the absence and presence of TH and the cardiomyocytes will be stimulated electrically.

2. Investigating the possible effects of T3 on other glioma cell lines with different grades and different levels of aggressiveness. The experiments will involve measuring cell growth, cell geometry, cell proliferation, cell injury, and the expressions of TR $\alpha$ 1 and other kinases.

3. Investigating the effects of different growth factors on differentiated and dedifferentiated glioma cell lines, measuring the same parameters as described in this thesis.

4. Investigating the effects of T3 on a clinical level on patients with glioma and to see the effects in comparison with radiotherapy.

5. Investigating if patients with glioma tumours express TR $\alpha$ 1 receptor.

6. Investigating the effect of T3 and T4 treatments on primary glioma taken from patients. These experiments will involve tissue culture, cell geometry and expression of TH receptors and a number of kinases similar to these shown in this thesis.

## **Publication**

Part of the results of this thesis has been published in Journal of thyroid research with the title:

### **Cell type dependent thyroid hormone effects on glioma tumour cell lines**

**Liappas, A., Mourouzis, I., Zisakis, A., Economou, K., Lea, R., W., Pantos, C. 2011.**

Journal of Thyroid Research Volume 2011 (2011), Article ID 856050, 8 pagesdoi:10.4061/2011/856050

## **Research Article**

### **Cell-Type-Dependent Thyroid Hormone Effects on Glioma Tumor Cell Lines**

Liappas Alexandros,<sup>1,2</sup> Mourouzis Iordanis,<sup>1</sup> Zisakis Athanasios,<sup>1</sup> Economou Konstantinos,<sup>1</sup> Lea Robert-William,<sup>2</sup> and Pantos Constantinos<sup>1</sup>

<sup>1</sup>Department of Pharmacology, University of Athens, 75 Mikras Asias Avenue, 11527 Goudi, Athens, Greece<sup>2</sup>School of Pharmacy and Biomedical Sciences, University of Central Lancashire, Preston PR1 2HE, Lancashire, UK

Received 5 August 2011; Revised 24 September 2011; Accepted 24 September 2011

Academic Editor: Fausto Bogazzi

Copyright © 2011 Liappas Alexandros et al. This is an open access article distributed under the Creative Commons Attribution License, which permits unrestricted use,

distribution, and reproduction in any medium, provided the original work is properly cited.

## Abstract

*Purpose.* The present study investigated the potential effects of long-term T3 treatment on glioma tumor cell lines. Thyroid hormone action on cell growth, differentiation and survival during development may be of therapeutic relevance. *Methods and Results* 1321N1 cell line, an astrocytoma grade II, and U87MG, a glioblastoma grade IV, were exposed for 2 and 4 days in medium deprived of T3 and in medium containing 1 nM T3. T3 promoted re-differentiation in both cell lines. However, T3 increased cell proliferation in 1321N1 (2 days) which declined thereafter (4 days) while in U87MG resulted in suppression of cell proliferation. At the molecular level, a 2.9 fold increase in the expression of TR $\alpha$ 1 receptor was observed in U87MG versus 1321N1,  $P < 0.05$ . TR $\beta$ 1 receptor was undetectable. These changes corresponded to a distinct pattern of T3-induced kinase signaling activation; T3 had no effect on ERK activation in both cell lines but significantly increased phospho-Akt levels in 1321N1. *Conclusion.* In conclusion, T3 can re-differentiate glioma tumor cells, whereas its effect on cell proliferation appears to be dependent on the type of tumor cell line with aggressive tumors being more sensitive to T3. TR $\alpha$ 1 receptor may, at least in part, be implicated in this response.

## References

Abe, T. (2002). Thyroid hormone transporters: recent advances. *Trends Endocrinol. Metab*; **13**(5):215-220.

Abo-Zenah, H. A., Shoeb, S. A., Sabry, A. A., and Ismail, H. A. (2008). Relating circulating thyroid hormone concentrations to serum interleukins-6 and 10 in association with non-thyroidal illnesses including chronic renal insufficiency. *BMC Endocr Disord*; **8**(1): 1-7.

Abohashem-Aly, A. A., Meng, X., Li, J., Sadaria, M. R., Ao, L., Wennergren, J. (2011). DITPA, A Thyroid Hormone Analog, Reduces Infarct Size and Attenuates the Inflammatory Response Following Myocardial Ischemia. *J Surg Res*. **18**(10): 252-257.

Ali, N., Marcou, Y., Plowman, P., N. (2000). The optimal management of brain metastases. *Int J Clin Pract*; **54**(4):209-211.

Alkemade, A., Visser, T., J., Fliers, E. (2008). Thyroid hormone signaling in the hypothalamus. *Current Opinion in Endocrinology, Diabetes and Obesity*; **15**(5): 453-458.

American Cancer Society. (2007). *Cancer Facts and Figures*. Atlanta Ga.

Aminoff, M., J. (2004). Nervous System. In: Current Medical Diagnosis and Treatment. Chapter 24. Edited by Tierney, L., M., Jr., McPhee, S., J., Papadakis, M., A. 43<sup>rd</sup> International Edition. Lange Medical Books/ McGraw Hill; pp: 333-356.

Anderson, G., W., Schoonover, C., M., Jones, S., A. (2003). Control of thyroid hormone action in the developing rat brain. *Thyroid*; **13**(11):1039-1056.

Anversa, P., and Kajstura, J. (1998). Ventricular myocytes are not terminally differentiated in the adult mammalian heart. *Circ Res*; **83**(1): 1-14.

Aranda, A., Martínez-Iglesias, O., Ruiz-Llorente, L., García-Carpizo, V., Zambrano, A. (2009). Thyroid receptor: roles in cancer. *Trends Endocrinol Metab*; **20**(7):318-324.

Armstrong, T., S., Gilbert, M., R. (2000). Metastatic brain tumours: diagnosis, treatment, and nursing interventions. *Clin J Oncol Nurs*; **4**(5):217-225.

Aronen, H., J., Perkio, J. (2002). Dynamic susceptibility contrast MRI of gliomas. *Neuroimaging Clin N Am*; **12**(4):501–523.

Atif, F., Sayeed, I., Yousuf, S., Ishrat, T., Hua, F., Wang, J., Brat, D., J., Stein, D., G. (2011). Progesterone Inhibits the Growth of Human Neuroblastoma: In Vitro and In Vivo Evidence. *Mol Med*. **9**(1):34-46.

Avgeropoulos, N., G., Batchelor, T., T. (1999). New treatment strategies for malignant glioma. *The Oncologist*. **4**(3): 209-224.

Balmano, K., Cook, S., J. (2009). Tumour cell survival signalling by the ERK1/2 pathway. *Cell Death Differ*; **16**(3):368-377.

Barth, J. D., Jansen, H., Kromhout, D., Reiber, J. H., Birkenhager, J. C., Arntzenius, A. C. (1987). Progression and regression of human coronary atherosclerosis. The role of lipoproteins, lipases and thyroid hormones in coronary lesion growth. *Atherosclerosis*; **68**(1-2): 51-58.

Baxter, J. D., and Webb, P. (2009). Thyroid hormone mimetics: potential applications in atherosclerosis, obesity and type 2 diabetes. *Nat Rev Drug Discov*; **8**(4): 308-320.

Beatson, G. (1896). On the treatment of inoperable cases of carcinoma of the mamma: suggestions for a new method of treatment with illustrative cases. *Lancet*; **2**: 104-107.

Bedo, G., Pascualand, A., Aranda, A. (2011). Early Thyroid Hormone-induced Gene Expression Changes in N2a-beta Neuroblastoma Cells. *J Mol Neurosc*; **3**: 56-59.

Belakavadi, M., Saunders, J., Weisleder, N., Raghava, P. S., Fondell, J. D. (2010). Repression of cardiac phospholamban gene expression is mediated by thyroid hormone receptor- $\alpha$ 1 and involves targeted covalent histone modifications. *Endocrinology*; **151**(6): 2946-2956.

Benjamin, R., Capparella, J., Brown, A. (2003). Classification of glioblastoma multiforme in adults by molecular genetics. *Cancer J*; **9**(2):82-90.

Berry, D. L., Rose, C. S., Remo, B. F., Brown, D. D. (1998). The expression pattern of thyroid hormone response genes in remodeling tadpole tissues defines distinct growth and resorption gene expression programs. *Dev Biol*; **203**(1): 24-35.

Berman, J., I., Berger, M., S., Mukherjee, P., Henry, R., G. (2004). Diffusion-tensor imaging-guided tracking of fibers of the pyramidal tract combined with intraoperative cortical stimulation mapping in patients with gliomas. *J Neurosurg*; **101**(1):66-72.

Bhat, M., K., Yu, C., Yap, N., Zhan, Q., Hayashi, Y., Seth, P., Cheng, S. (1997). Tumour suppressor p53 is a negative regulator in thyroid hormone receptor signaling pathways. *J. Biol.Chem*; **272**(46):28989-28993.

Bianco, A. C., Salvatore, D., Gereben, B., Berry, M. J., Larsen, P. R. (2002). Biochemistry, cellular and molecular biology, and physiological roles of the iodothyronine selenodeiodinases. *Endocr Rev*; **23**(1): 38-89.

Bianco, A. C., Kim, B. W. (2006). Deiodinases: implications of the local control of thyroid hormone action. *J Clin Invest*; **116**(10): 2571-2579.

Billon, N., Jolicoeur, C., Tokumoto, Y., Vennstrom, B., Raff, M. (2002). Normal timing of oligodendrocyte development depends on thyroid hormone receptor alpha 1 (TR $\alpha$ 1). *The EMBO Journal*; **21**(23):6452-6460.

Black, P., M. (1991): Brain tumour. Part 2. *N Engl J Med*; **324**:1555–1564.

Black, P., M. (1991): Brain tumours. Part 1. *N Engl J Med*; **324**: 1471–1476.

Bondy, M.,L., Spitz, M.,R., Halabi, S., Fueger, J.,J., Schantz, S.,P., Sample, D., Hsu, T., C. (1993). Association between family history of cancer and mutagen sensitivity in upper aerodigestive tract cancer patients. *Cancer Epidemiol Biomarkers Prev*; **2**(2):103-106.

Bononi, A., Agnoletto, C., De Marchi, E., Marchi, S., Patergnani, S., Bonora, M., Giorgi, C., Missiroli, S., Poletti, F., Rimessi, A., Pinton, P. (2011). Protein kinases and phosphatases in the control of cell fate. *Enzyme Res*:**3**: 290-298.

Boutros, T., Chevet, E., Metrakos, P. (2008). Mitogen-activated protein (MAP) kinase/MAP kinase phosphatase regulation: roles in cell growth, death, and cancer. *Pharmacol Rev*; **60**(3):261-310.

Bouzaffour, M., Rampon, C., Ramauge, M., Courtin, F., Vrizz, S. (2010). Implication of type 3 deiodinase induction in zebrafish fin regeneration. *Gen Comp Endocrinol*; **168**(1): 88-94.

Brandes, A., A., Vastola, F., Basso, U., Pasetto, L., M., Ermani, M., Berti, F., Rotilio, A., Amistà, P., Scienza, R., Monfardini, S. (2002). Temozolomide in glioblastoma multiforme of the elderly. *Tumori*; **88**(1): 69-70.

Bronnegard, M., Topping, O., Boos, J., Sylven, C., Marcus, C., Wallin, G. (1994). Expression of thyrotropin receptor and thyroid hormone receptor messenger ribonucleic acid in normal, hyperplastic, and neoplastic human thyroid tissue. *J. Clin. Endocrinol. Metab*; **79**(2):384-389.

Burger, P., C., Vogel, F., S., Green, S., B., Strike., T., A. (1985). Glioblastoma multiforme and anaplastic astrocytoma. Pathologic criteria and prognostic implications. *Cancer*; **56**(5):1106-1111.

Burmeister, L., A., Pachucki, J., St Germain, D., L. (1997). Thyroid hormones inhibit 2-iodothyronine deiodinase in the rat cerebral cortex by both pre- and posttranslational mechanisms. *Endocrinology*; **138**(12):5231-5237.

Buss, S. J., Riffel, J. H., Malekar, P., Hagenmueller, M., Asel, C., Zhang, M., (2011). Chronic Akt blockade aggravates pathological hypertrophy and inhibits physiological hypertrophy. *Am J Physiol Heart Circ Physiol*: **5**(4):26-48.

Calvo, R., Obregon, M., J., Ruiz de Ona, C. (1990). Congenital hypothyroidism, as studied in rats. Crucial role of maternal thyroxine but not of 3,5,3'-triiodothyronine in the protection of the fetal brain. *The Journal of Clinical Investigation*; **86**(3):889-899.

Cardis E, Varsier N, Bowman JD, Deltour I, Figuerola J, Mann S, Moissonnier M, Taki M, Vecchia P, Villegas R, Vrijheid M, Wake K, Wiart J.(2011). Estimation of RF energy absorbed in the brain from mobile phones in the Interphone Study. *Occup Environ Med*;**68**(9):686-693.

Carlson, D., J., Strait, K., A., Schwartz., H., L., et al., (1996). Thyroid hormone receptor isoform content in cultured type 1 and type 2 astrocytes. *Endocrinology*; **137**(3):911-917.

Caruthers, B. (2001). High-Grade astrocytoma in the adult: Part 2. Diagnostics and Treatment. *Surg Technol*; **33**(3):24-35.

Cavenee, W., K, Nagane, M. (2000). Astrocytic tumours: World Health Organisation classification of tumours: pathology and genetics: tumours of the nervous system. Lyon: LARC press, **23**: 35-77

Chablais, F., Veit, J., Rainer, G., Jazwinska, A. (2011). The zebrafish heart regenerates after cryoinjury-induced myocardial infarction. BMC Dev Biol; **11**: 21-44.

Chattergoon, N. N., Giraud, G. D., Louey, S., Stork, P., Fowden, A. L., Thornburg, K. L. (2011). Thyroid hormone drives fetal cardiomyocyte maturation. FASEB J: **46**(2): 156-167.

Chen, Y. F., Kobayashi, S., Chen, J., Redetzke, R. A., Said, S., Liang, Q. (2008). Short term triiodo-l-thyronine treatment inhibits cardiac myocyte apoptosis in border area after myocardial infarction in rats. J Mol Cell Cardiol; **44**(1): 180-187.

Chakraborti, S., Mandal, M., Das, S., Mandal, A., Chakraborti, T. (2003). Regulation of matrix metalloproteinases: an overview. Mol Cell Biochem; **253**(1-2):269-285.

Chamberlain, M., C., Kormanik, P., A. (1998). Practical guidelines for the treatment of malignant gliomas. West J Med; **168**(2):114-120.

Chang, S., D., Adler, J., R. (2000). Current treatment of patients with multiple brain metastases. *Neurosurg Focus*; **9**(2): 1-5.

Chappell, W., H., Steelman, L., S., Long, J., M., Kempf, R., C., Abrams, S., L., Franklin, R., A., Basecke, J., Stivala, F., Donia, M., Fagone, P., Malaponte, G., Mazzarino, M., C., Nicoletti, F., Libra, M., Maksimovic-Ivanic, D., Mijatovic, S., Montalto, G., Cervello, M., Laidler, P., Milella, M., Tafuri, A., Bonati, A., Evangelisti, C., Cocco, L., Martelli, A., M., McCubrey, J., A. (2011). Ras/Raf/MEK/ERK and PI3K/PTEN/Akt/mTOR inhibitors: rationale and importance to inhibiting these pathways in human health. *Oncotarget*; **2**(3):135-164.

Chassande, O. (2003). "Do unliganded thyroid hormone receptors have physiological functions?" *Journal of Molecular Endocrinology*; **31**(1): 9–20.

Chen, H., W., Privalsky, M., L., (1993). The erbA oncogene represses the actions of both retinoid X and retinoid A receptors but does so distinct mechanisms. *Mol. Cell. Biol*; **13**(10):5970-5980.

Cheng, S., Y. (2000). Multiple mechanisms for regulation of the transcriptional activity of the thyroid hormone receptors. *Rev. Endocr. Metab. Disord*; **1**(2): 9-18.

Cheng, S., Y. (2003). Thyroid hormone receptor mutations in cancer. *Molecular and cellular Endocrinology*; **213**(1):23-30.

Choucair, A., K., Levin, V., A., Gutin, P., H. (1986). Development of multiple lesions during radiation therapy and chemotherapy in patients with gliomas. *J Neurosurg*; **65**(5):654–658.

Coghlan, C., Hoffman, J. (2006). Leonardo da Vinci's flights of the mind must continue: cardiac architecture and the fundamental relation of form and function revisited. *Eur J Cardiothorac Surg*; **29**(1): 4-17.

Colombo, F., Barzon, L., Franchin, E. (2005). Combined HSV-TK/IL-2 gene therapy in patients with recurrent glioblastoma multiforme: biological and clinical results. *Cancer Gene Ther*; **12**(10): 835–848.

Columbano, A., Pibiri, M., Deidda, M., Cossu, C., Scanlan, T., S., Chiellini, G., Muntoni, S., Ledda-Columbano, G., M. (2006). The thyroid hormone receptor-beta agonist GC-1 induces cell proliferation in rat liver and pancreas. *Endocrinology*; **147**(7):3211-3218.

Combs, S., E., Widmer, V., Thilmann, C. (2005). Stereotactic radiosurgery (SRS). Treatment option for recurrent glioblastoma multiforme (GBM). *Cancer*; **104**(10):2168–2173.

Crews, C., M., Erikson, R., L. (1993). Extracellular signals and reversible protein phosphorylation: what to Mek of it all. *Cell*; **74**(2):215-217.

Davis, F., B., Tang, H., Y., Shih, et al. (2006). Acting via a cell surface receptor thyroid hormone is a growth factor for glioma cells. *Cancer Res*; **66**(14):7270-7275.

Davis, F., G., Preston-Martin, S. (1998). Epidemiology. Incidence and survival. In: Russel and Rubinsrein's Pathology of tumours on the nervous system, Binger DD, McLendon RE, Bruner JM (eds), 6<sup>th</sup> ed. Arnold: London. pp: 5-45.

Davis, P., J., Shih, A., Lin, H., Y., Martino, I., J., Davis, F., B. (2000). Thyroxine promotes association of mitogen-activated protein kinase and nuclear thyroid hormone receptor (TR) and causes serine phosphorylation of TR. *J Biol. Chem*; **275**(48):38032-38039.

DeAngelis, L. (2001). Medical progress: Brain tumours. *N. Eng. J. Med*; **344**(2): 114-123.

DeBosch, B., Treskov, I., Lupu, T. S., Weinheimer, C., Kovacs, A., Courtois, M. (2006). Akt1 is required for physiological cardiac growth. *Circulation*; **113**(17): 2097-2104.

Degens, H., Gilde, A. J., Lindhout, M., Willemsen, P. H., Van Der Vusse, G. J., Van Bilsen, M. (2003). Functional and metabolic adaptation of the heart to prolonged thyroid hormone treatment. *Am J Physiol Heart Circ Physiol*; **284**(1): 108-115.

Dorn, G. W. (2007). The fuzzy logic of physiological cardiac hypertrophy. *Hypertension*; **49**(5): 962-970.

Detillieux, K., A., Meij, J., T., Kardami, E., Cattini, P., A. (1999). Alpha1-Adrenergic stimulation of FGF-2 promoter in cardiac myocytes and in adult transgenic mouse hearts. *Am J Physiol*; **276**(3): 826-833.

Dhillon, A., S., Hagan, S., Rath, O., Kolch, W. (2007). MAP kinase signalling pathways in cancer. *Oncogene*; **26**(22):3279-3290.

Dillman, R., O., Duma, C., M., Schiltz, P., M., DePriest, C., Ellis, R., A., Okamoto, K., Beutel, L., D., De Leon, C., Chico, S. (2004). Intracavitary placement of autologous lymphokine-activated killer (LAK) cells after resection of recurrent glioblastoma. *J Immunother*; **27**(5):398-404.

Donahue, B., Scott, C., B., Nelson, J., S., Rotman, M., Murray, K., J., Nelson, D., F., Banker, F., L., Earle, J., D., Fischbach, J., A., Asbell, S., O., Gaspar, L., E., Markoe, A., M., Curran, W. (1997). Influence of an oligodendroglial component on the survival of patients with anaplastic astrocytomas: a report of Radiation Therapy Oncology Group 83-02. *Int J Radiat Oncol Biol Phys*; **38**(5):911-914.

Draman, M., B., Crutchfield, F., L., Schoenhoff, M., B. (1991). Transport of iodothyronines from bloodstream to brain: contributors by blood-brain and choroid plexus-cerebrospinal fluid barriers. *Brain Research*; **554**(1-2):229-236.

Gosteli-Peter, M., A., Harder, B., A., Eppenberger, H., M., Zapf, J., Schaub, M., C. (1996). Triiodothyronine induces over-expression of alpha-smooth muscle actin, restricts myofibrillar expansion and is permissive for the action of basic FGF and IGF-I in adult rat cardiomyocytes. *J Clin Invest*; **98**(8): 1737-1744.

Eber, B., Schumacher, M., Langsteger, W., Zweiker, R., Fruhwald, F. M., Pokan, R. (1995). Changes in thyroid hormone parameters after acute myocardial infarction. *Cardiology*; **86**(2): 152-156.

El-Habr, E., A., Tsiorva, P., Theodorou, M., Levidou, G., Korkolopoulou, P., Vretakos, G., Petraki, L., Michalopoulos, N., V., Patsouris, E., Saetta, A., A. (2010). Analysis of PIK3CA and B-RAF gene mutations in human astrocytomas: association with activation of ERK and AKT. *Clin Neuropathol*; **29**(4):239-245.

Esaki, T., Suzuki, H., Cook, M., Shimoji, K., Cheng, S. Y., Sokoloff, L. (2004). Cardiac glucose utilization in mice with mutated alpha- and beta-thyroid hormone receptors. *Am J Physiol Endocrinol Metab*; **287**(6): 1149-1153.

Fan, Q., W., Weiss, W., A. (2011). Autophagy and Akt promote survival in glioma. *Autophagy*; **7**(5):536-538.

Farwell, A., P., Lynch, R., M., Okulicz, W., C., Comi, A., M., Leonard, J., L. (1990). The actin cytoskeleton mediates the hormonally regulated translocation of type II iodothyronine 5 $\alpha$ -deiodinase in astrocytes. *J Biol Chem*; **265**(30):18546–18553.

Farwell, A., P., Tranter, M., P., Leonard, J., L. (1995). Thyroxine dependent regulation of integrin-laminin interactions in astrocytes. *Endocrinology*; **136**(9):3909–3915.

Ferreira, E., da Silva, A., E., Serakides, R., Gomes, M., G., Cassali, G., D. (2006). Ehrlich tumour as model to study artificial hyperthyroidism influence on breast cancer. *Pathology-Research and Practice*; **203**(1):39-44.

Fine, H., A., Dear, K., B., Loeffler, J., S., Black, P., M., Canellos, G., P. (1993). Meta-analysis of radiation therapy with and without adjuvant chemotherapy for malignant gliomas in adults. *Cancer*; **71**(8):2585-2597.

Fliers, E., Unmehopa, U., A., Alkemade, A. (2006). Functional neuroanatomy of thyroid hormone feedback in the human hypothalamus and pituitary gland. *Molecular and Cellular Endocrinology*; **251**(1-2):1-8.

Frelick, R., Huang, P., Topham, A. (1992). Brain and central nervous system tumours Delaware, 1980 to 1989. *Del Med J*; **64**(9):571-573.

Friedrichsen, S., Christ, S., Heuer, H. (2003). Regulation of iodothyronine deiodinases in the Pax8<sup>-/-</sup> mouse model of congenital hypothyroidism. *Endocrinology*; **144**(3):777-784.

Friesema E., C., et al. (1999). Identification of thyroid hormone transporters. *Biochem Biophys Res Commun*; **254**(2):497-501.

Friesema, E., C., et al. (2006). Mechanisms of disease: psychomotor retardation and high T3 levels caused by mutations in monocarboxylate transporter 8. *Nat Clin Pract Endocrinol Metab*; **2**(9):512-523.

Flamant, F., and Samarut, J. (2003). Thyroid hormone receptors: lessons from knockout and knock-in mutant mice. *Trends Endocrinol Metab*; **14**(2): 85-90.

Forini, F., Lionetti, V., Ardehali, H., Pucci, A., Cecchetti, F., Ghanefar, M. (2010). Early long-term L-T3 replacement rescues mitochondria and prevents ischemic cardiac remodeling in rats. *J Cell Mol Med*; **11**(11): 1582-4934.

Friberg, L., Werner, S., Eggertsen, G., Ahnve, S. (2002). Rapid down-regulation of thyroid hormones in acute myocardial infarction: is it cardioprotective in patients with angina? *Arch Intern Med*; **162**(12): 1388-1394.

Furlow J., D., Neff, E., S. (2006). "A developmental switch induced by thyroid hormone: *Xenopus laevis* metamorphosis," Trends in Endocrinology and Metabolism; **17**(2): 40–47.

Furlow, J. D., Yang, H. Y., Hsu, M., Lim, W., Ermio, D. J., Chiellini, G. (2004). Induction of larval tissue resorption in *Xenopus laevis* tadpoles by the thyroid hormone receptor agonist GC-1. J Biol Chem; **279**(25): 26555-26562.

Ganslandt, O., Buchfelder, M., Hastreiter, P., Grummich, P., Fahlbusch, R., Nimsky, C. (2004). Magnetic source imaging supports clinical decision making in glioma patients. Clin Neurol Neurosurg; **107**(1):20-26.

Garcia-Silva, S., and Aranda, A. (2004). "The thyroid hormone receptor is a suppressor of ras-mediated transcription, proliferation, and transformation," Mol Cell Bio; **24**(17):7514-7523.

Gerdes, A. M., and Iervasi, G. (2010). Thyroid replacement therapy and heart failure. Circulation; **122**(4): 385-393.

Gittoes, N., J., McCabe, C., J., Verhaeg, J., et al. (1998). An abnormality of thyroid hormone receptor expression may explain abnormal thyrotropin production in thyrotropin secreting pituitary tumours. Thyroid; **8**(1): 9-14.

Gloss, B., Trost, S., Bluhm, W., Swanson, E., Clark, R., Winkfein, R. (2001). Cardiac ion channel expression and contractile function in mice with deletion of thyroid hormone receptor alpha or beta. *Endocrinology*; **142**(2): 544-550.

Gonzalez-Sancho, J., M., Garcia, V., Bonilla, F., Munoz, A. (2003). Thyroid hormone receptors/THR genes in human cancer. *Cancer Lett*; **192**(2):121-132.

Grant, R., Collie, D., Counsell, C. (1996). The incidence of cerebral glioma in the working population: a forgotten cancer? *Br J Cancer*; **73**(2):252-254.

Greenlee, R., T., Murray, T., Bolden, S., Wingo, P., A. (2000). Cancer statistics 2000. *CA cancer J. Clin*; **50**(1): 7-33

Grossman, S., A., Batara, J., F. (2004). Current management of glioblastoma multiforme. *Semin Oncol*; **31**(5):635–644.

Grossman, W., Jones, D., and McLaurin, L. P. (1975). Wall stress and patterns of hypertrophy in the human left ventricle. *J Clin Invest*; **56**(1): 56-64.

Groves, M., D., Puduvalli, V., K., Hess, K., R., Jaeckle, K., A., Peterson, P., Yung, W., K., Levin, V., A. (2002). Phase II trial of temozolomide plus the matrix metalloproteinase inhibitor, marimastat, in recurrent and progressive glioblastoma multiforme. *J Clin Oncol*; **20**(5):1383-1388.

Guadano-Ferraz, A., Escamez, M., J., Rausell, E., et al., (1999). Expression of type 2 iodothyronine deiodinase in hypothyroid rat brain indicates an important role of thyroid hormone in the development of specific primary sensory systems. *Journal of Neuroscience*; **19**(9):3430-3439.

Guadano-Ferraz, A., Obregon, M., J., St Germain, D., L., et al., (1997). The type 2 iodothyronine deiodinase is expressed primarily in glial cells in the neonatal rat brain. *Proceedings of the National Academy of Sciences of the USA*; **94**(19):10391-10396.

Gudernatsch, J. F. (1912). "Feeding experiments on tadpoles—I: the influence of specific organs given as food on growth and differentiation. A contribution to the knowledge of organs with internal secretion," *Development Genes and Evolution*; **35**(3): 457–483.

Gurtner GC, Chang E.(2008). "Priming" endothelial progenitor cells: a new strategy to improve cell based therapeutics. *Arterioscler Thromb Vasc Biol*; **28**(6):1034-1035.

Gutin, P., H., Posner, J., B. (2000). Neuro-oncology: diagnosis and management of cerebral gliomas--past, present, and future. *Neurosurgery*; **47**(1):1-8.

Hagenbuch, B. (2007). Cellular entry of thyroid hormones by organic anion transporting polypeptides. *Best Pract. Res. Clin. Endocrinol. Metab*; **21**(2):209-221.

Harvey, C., B., Williams, G., R. (2002). Mechanism of thyroid hormone action. *Thyroid*; **12**(6): 441-446.

Hambleton, M., Hahn, H., Pleger, S. T., Kuhn, M. C., Klevitsky, R., Carr, A. N. (2006). Pharmacological- and gene therapy-based inhibition of protein kinase Calpha/beta enhances cardiac contractility and attenuates heart failure. *Circulation*; **114**(6): 574-582.

Henderson, K. K., Danzi, S., Paul, J. T., Leya, G., Klein, I., Samarel, A. M. (2009). Physiological replacement of T3 improves left ventricular function in an animal model of myocardial infarction-induced congestive heart failure. *Circ Heart Fail*; **2**(3): 243-252.

Henneman, G. (2001). Plasma membrane transport of thyroid hormones and its role in thyroid hormone metabolism and bioavailability. *Endocr. Rev*; **22**(4): 451-476.

Hennemann, G. (2005). Notes on the history of cellular uptake and deiodination of thyroid hormone. *Thyroid*; **15**(8): 753-756.

Herebergs, A., A., Goyal, L., K., Suh, J., H., et al. (2003). Propylthiouracil-induced chemical hypothyroidism with high dose tamoxifen prolongs survival in recurrent high grade glioma: a phase I, II study. *Anticancer Res*; **23**(1B):617-626.

Herdrich, B. J., Danzer, E., Davey, M. G., Allukian, M., Englefield, V., Gorman, J. H. (2011). Regenerative healing following foetal myocardial infarction. *Eur J Cardiothorac Surg*; **38**(6): 691-698.

Hers, I., Vincent, E., E., Tavaré, J., M. (2011). Akt signalling in health and disease. *Cell Signal*; **23**(10):1515-1527.

Heuer, H. (2007). The importance of thyroid hormone transporters for brain development and function. *Best practice and research clinical endocrinology and metabolism*; **21**(2):265-276.

Hickey, J., V. (2004). *Clinical practice of neurological and neurosurgical nursing*. 5<sup>th</sup> ed. Philadelphia Pa: Lippincott Williams & Wilkins; **10**(5): 236-244

Hirakawa, T., Ruley, H., E. (1988). Rescue of cells from ras oncogene-induced growth arrest by a second, complementing, oncogene. *Proc Natl Acad Sci*; **85**(5):1519-1523.

Hockey, B., Leslie, K., Williams, D. (2009). Dexamethasone for intracranial neurosurgery and anaesthesia. *J Clin Neurosci*; **16**(11):1389-1393.

Holland, F. W., 2nd, Brown, P. S., Jr., Weintraub, B. D., Clark, R. E. (1991). Cardiopulmonary bypass and thyroid function: a "euthyroid sick syndrome". *Ann Thorac Surg*; **52**(1): 46-50.

Huncharek, M., Muscat, J. (1998). Treatment of recurrent high grade astrocytoma; results of a systematic review of 1,415 patients. *Anticancer Res*; **18**(2B):1303-1311.

Hwang, S., L., Lin, C., L., Lieu, A., S., Hwang Y., F., Howng S., L., Hong, Y., R., Chang, D., S., Lee, K., S. (2008). The expression of thyroid hormone receptor isoforms in human astrocytomas. *Surgical Neurology*; **70**: 14-18.

Hynes, N., E., MacDonald, G. (2009). ErbB receptors and signaling pathways in cancer. *Curr Opin Cell Biol*; **21**(2):177-184.

Hyyti, O. M., Ning, X. H., Buroker, N. E., Ge, M., and Portman, M. A. (2006). Thyroid hormone controls myocardial substrate metabolism through nuclear receptor-mediated and rapid posttranscriptional mechanisms. *Am J Physiol Endocrinol Metab*; **290**(2): E372-379.

Ichiki, T. (2010). Thyroid hormone and atherosclerosis. *Vascul Pharmacol*; **52**(3-4): 151-156.

Iervasi, G., Pingitore, A., Landi, P., Raciti, M., Ripoli, A., Scarlattini, M. (2003). Low-T3 syndrome: a strong prognostic predictor of death in patients with heart disease. *Circulation*; **107**(5): 708-713.

Ischimura, K., Schmidt, E., E., Miyakawa, A., Goike, H., M., Collins, V., P. (1998). Distinct patterns of deletion on 10p and 10q suggest involvement of multiple tumour suppressor genes in the development of astrocytic gliomas of different malignancy grades. *Genes Chromosomes Cancer*; **22**(1):9-15.

Jansen, J., et al. (2005). Thyroid hormone transporters in health and disease. *Thyroid*; **15**(8):757-768.

Jeevanandam, V. (1997). Triiodothyronine: spectrum of use in heart transplantation. *Thyroid*; **7**(1): 139-145.

Jopling, C., Sleep, E., Raya, M., Marti, M., Raya, A., Belmonte, J. C. (2010). Zebrafish heart regeneration occurs by cardiomyocyte dedifferentiation and proliferation. *Nature*; **464**(7288): 606-609.

Jose, C., Hebert-Chatelain, E., Bellance, N., Larendra, A., Su, M., Nouette-Gaulain, K., Rossignol, R. (2011). AICAR inhibits cancer cell growth and triggers cell-type distinct effects on OXPHOS biogenesis, oxidative stress and Akt activation. *Biochim Biophys Acta*; **1807**(6):707-718.

Kalofoutis, C., Mourouzis, I., Galanopoulos, G., Dimopoulos, A., Perimenis, P., Spanou, D. (2010). Thyroid hormone can favorably remodel the diabetic myocardium after acute myocardial infarction. *Mol Cell Biochem*; **345**(1-2): 161-169.

Kamata, T., Feramisco, J., R. (1984). Epidermal growth factor stimulates guanine nucleotide binding activity and phosphorylation of ras oncogene proteins. *Nature*; **310**(5973):147-150.

Kamiya, Y., Puzianowska-Kuznicka, M., McPhie, P., Nauman, J., Cheng, S., Y., Nauman, A. (2002). Expression of mutant thyroid hormone nuclear receptors is associated with human renal clear cell carcinoma. *Carcinogenesis*; **23**(1):25-33.

Kaptein, E. M., Sanchez, A., Beale, E., Chan, L. S. (2010). Clinical review: Thyroid hormone therapy for postoperative nonthyroidal illnesses: a systematic review and synthesis. *J Clin Endocrinol Metab*; **95**(10): 4526-4534.

Keles, G., E., Berger, M., S. (2004). Advances in neurosurgical technique in the current management of brain tumours. *Semin Oncol*; **31**(5):659-665.

Kim, E., K., Choi, E., J. (2010). Pathological roles of MAPK signaling pathways in human diseases. *Biochim Biophys Acta*; **1802**(4):396-405.

Kim, S., P., Ha, J., M., Yun, S., J., Kim, E., K., Chung, S., W., Hong, K., W., Kim, C., D., Bae, S., S. (2011). Transcriptional activation of peroxisome proliferator-activated receptor-gamma requires activation of both protein kinase A and Akt during adipocyte differentiation. *Biochem Biophys Res Commun*; **399**(1):55-59.

Kimmel, D., W., Shapiro, J., R., Shapiro, W., R. (1987). In vitro drug sensitivity testing in human gliomas. *J Neurosurg*; **66**(2):161-171.

Kinugawa, K., Yonekura, K., Ribeiro, R., C., Eto, Y., Aoyagi, T., Baxter, J., D., Camacho, S., A., Bristow, M., R., Long, C., S., Simpson, P., C. (2001). Regulation of thyroid hormone receptor isoforms in physiological and pathological cardiac hypertrophy. *Circ Res*; **89**(7): 591-598.

Kimura, T., Kanda, T., Kotajima, N., Kuwabara, A., Fukumura, Y., Kobayashi, I. (2000). Involvement of circulating interleukin-6 and its receptor in the development of euthyroid sick syndrome in patients with acute myocardial infarction. *Eur J Endocrinol*; **143**(2): 179-184.

King, E. S. (1940). Regeneration in Cardiac Muscle. *Br Heart J*; **2**(3): 155-164.

Kinugawa, K., Yonekura, K., Ribeiro, R. C., Eto, Y., Aoyagi, T., Baxter, J. D. (2001). Regulation of thyroid hormone receptor isoforms in physiological and pathological cardiac hypertrophy. *Circ Res*; **89**(7): 591-598.

Kinugawa, K., Jeong, M. Y., Bristow, M. R., Long, C. S. (2005). Thyroid hormone induces cardiac myocyte hypertrophy in a thyroid hormone receptor alpha1-specific manner that requires TAK1 and p38 mitogen-activated protein kinase. *Mol Endocrinol*; **19**(6): 1618-1628.

Kinzler, K., W., Vogelstein, B. (1998). Landscaping the cancer terrain. *Science*; **280**(5366): 1036-1037.

Kleihues, P., Burger, P., C., Scheithauer, B., W. (1993). The new WHO classification of brain tumours. *Brain Pathol*; **3**(3):255-268.

Kleihues, P., Louis, D., N., Scheithauer, B., W., Rorke, L., B., Reifenberger, G., Burger, P., C., Cavenee, W., K. (2002). The WHO classification of tumours of the nervous system. *J Neuropathol Exp Neurol*; **61**(3):215-225.

Klemke, R., L., Cai, S., Giannini, A., L., Gallagher, P., J., de Lanerolle, P., Cheresch, D., A. (1997). Regulation of cell motility by mitogen-activated protein kinase. *J Cell Biol*; **137**(2):481-492.

Kohno, M., Pouyssegur, J. (2006). Targeting the ERK signaling pathway in cancer therapy. *Ann Med*; **38**(3):200-211.

Kress, E., Rezza, A., Nadjar, J., Samarut, J., Plateroti, M. (2008). The thyroid hormone receptor-alpha (TRalpha) gene encoding TRalpha1 controls deoxyribonucleic acid damage-induced tissue repair. *Mol Endocrinol*; **22**(1): 47-55.

Kress, E., Samarut, J., Plateroti, M. (2009). Thyroid hormones and the control of cell proliferation or cell differentiation: paradox or duality? *Mol Cell Endocrinol*; **313**(1-2):36-49.

Krishnan, R., Raabe, A., Hattingen, E., Szelényi, A., Yahya, H., Hermann, E., Zimmermann, M., Seifert, V. (2004). Functional magnetic resonance imaging-integrated neuronavigation: correlation between lesion-to-motor cortex distance and outcome. *Neurosurgery*; **55**(4):904-914.

Lai, J., Jin, H., Yang, R., Winer, J., Li, W., Yen, R., King, K., L., Zeigler, F., Ko, A., Cheng, J., Bunting, S., Paoni, N., F. (1996). Prostaglandin F<sub>2</sub> alpha induces cardiac myocyte hypertrophy in vitro and cardiac growth in vivo. *Am J Physiol*; **271**(6 Pt 2): 2197-2208.

Lauffenburger, D., A., Horwitz, A., F. (1996). Cell migration: a physically integrated molecular process. *Cell*; **84**(3):359-369.

Lebel, J., M., Dussault, J., H., Puymirat, J. (1994). Overexpression of beta 1 thyroid receptor induces differentiation in neuro-2<sup>a</sup> cells. *Proc Natl Acad Sci*; **91**(7):2644-2648.

Ledda-Columbano GM, Perra A, Piga R, Pibiri M, Loi R, Shinozuka H, Columbano A.(1999). Cell proliferation induced by 3,3',5-triiodo-L-thyronine is associated with a reduction in the number of preneoplastic hepatic lesions. *Carcinogenesis*; **20**(12):2299-2304.

Ledda-Columbano GM, Perra A, Concas D, Cossu C, Molotzu F, Sartori C, Shinozuka H, Columbano A. (2003). Different effects of the liver mitogens triiodo-thyronine and ciprofibrate on the development of rat hepatocellular carcinoma. *Toxicol Pathol*; **31**(1):113-120.

Lemke, D., M. (2004). Epidemiology, diagnosis, and treatment of patients with metastatic cancer and high-grade gliomas of the central nervous system. *Journal of infusion Nursing*; **27**(4):263-269.

Leonard, J., L., Farwell, A., P., Yen P., M., et al., (1994). Differential expression of thyroid hormone receptor isoforms in neurons and astroglial cells. *Endocrinology*; **135**(2):548-555.

Li, Z., Meng, Z., H., Chandrasekaran, R., Kuo, W., L., Collins, C., C., Gray, J., W., Dairkee, S., H. (2002). Biallelic inactivation of the thyroid hormone receptor  $\beta 1$  gene in early stage breast cancer. *Cancer research*; **62**(7):1939-1943.

Liappas, A., Mourouzis, I., Zisakis, A., Economou, K., Lea, R.-W., Pantos, C. (2011). Cell type dependent thyroid hormone effects on glioma tumour cell lines *Journal of Thyroid Research*: 856050.

Lin, H., M., Cheng, S., Y., (2002). Cyclin D1 is a ligand independent co-repressor for thyroid hormone receptors. *J Biol. Chem*; **277**(32):28733-28741.

Lin, H., Y., Sun, M., Tang, H., Y., Lin, C., Luidens, M., K., Mousa, S., A., Incerpi, S., Drusano, G., L., Davis, F., B., Davis, P., J. (2009). L-Thyroxine vs. 3,5,3'-triiodo-L-thyronine and cell proliferation: activation of mitogen-activated protein kinase and phosphatidylinositol 3-kinase. *Am J Physiol Cell Physiol*; **296**(5):C980-991.

Lin, H., Y., Tang, H., Y., Keating, T., et al. (2008). "Resveratrol is pro-apoptotic and thyroid hormone is anti-apoptotic in glioma cells: both actions are integrin and ERK mediated," *Carcinogenesis*; **29**(1): 62-69.

Lin, K., H., Zhu, X., G., Hsu, H., C., Chen, S., L., Shieh, H., Y., Chen, S., T., McPhie, P., Cheng, S., Y. (1997). Dominant negative activity of mutant thyroid hormone alpha1 receptors from patients with hepatocellular carcinoma. *Endocrinology*; **138**(12):5308-5315.

Lin, K., H., Zhu, X., G., Shieh, H., Y., Hsu, H., C., Chen, S., T., McPhie, P., Cheng, S., Y. (1996). Identification of naturally occurring dominant negative mutants of thyroid hormone alpha 1 and beta 1 receptors in a human hepatocellular carcinoma cell line. *Endocrinology*; **137**(10):4073-4081.

Lo, H., W. (2011). Targeting Ras-RAF-ERK and its interactive pathways as a novel therapy for malignant gliomas. *Curr Cancer Drug Targets*; **10**(8):840-848.

Loeser, A., A. (1954). "A new therapy for prevention of post-operative recurrences in genital and breast cancer; a six-years study of prophylactic thyroid treatment," *Br Med J*; **2**(4901): 1380-1383.

Lovely, M., P. (2002). Metastatic Brain Tumours: causes, survival, treatment and management. *Semin Oncol Nurs*; **14**(1): 73-80.

Lymvaios, I., Mourouzis, I., Cokkinos, D. V., Dimopoulos, M. A., Toumanidis, S. T., Pantos, C. (2011). Thyroid hormone and recovery of cardiac function in patients with acute myocardial infarction: A strong association? *Eur J Endocrinol*; **99**(10): 55-123.

Mahajan, A., McCutcheon, I., E., Suki, D. (2005). Case-control study of stereotactic radiosurgery for recurrent glioblastoma multiforme. *J Neurosurg*; **103**(2):210-217.

Mai, W., Janier, M., F., Allioli, N., Quignodon, L., Chuzel, T., Flamant, F., Samarut, J. (2004). Thyroid hormone receptor alpha is a molecular switch of cardiac function between fetal and postnatal life. *Proc Natl Acad Sci*; **101**(28):10332-10337.

Maldjian, J., A., Patel, R., S. (1999). Cerebral neoplasms in adults. *Semin Roentgenol*; **34**(2):102-122.

Mansen, A., Tiselius, C., Sand, P., Fauconnier, J., Westerblad, H., Rydqvist, B. (2011). Thyroid hormone receptor alpha can control action potential duration in mouse ventricular myocytes through the KCNE1 ion channel subunit. *Acta Physiol (Oxf)*; **198**(2): 133-142.

Martinez-Iglesias, O., Garcia-Silva, S., Regadera, J., et al. (2009). "Hypothyroidism enhances tumour invasiveness and metastasis development," *PLoS One*; **4**(7): 64-68.

Matsui, T., Li, L., Wu, J. C., Cook, S. A., Nagoshi, T., Picard, M. H. (2002). Phenotypic spectrum caused by transgenic overexpression of activated Akt in the heart. *J Biol Chem*; **277**(25): 22896-22901.

Maxwell, M., Naber, S., P., Wolfe., H., J., Hedley-Whyte, E., T., Galanopoulos, T., Neville-Golden, J., Antoniades, H., N. (1991). Expression of angiogenic growth factor genes in primary human astrocytomas may contribute to their growth and progression. *Cancer Res*; **51**(4):1345-1351.

McCormack, B., M., Miller, D., C., Budzilovich, G., N., Voorhees, G., J., Ransohoff, J. (1992). Treatment and survival of low-grade astrocytoma in adults--1977-1988. *Neurosurgery*; **31**(4):636-642.

McCubrey, J., A., Lahair, M., M., Franklin, R., A. (2006). Reactive oxygen species-induced activation of the MAP kinase signaling pathways. *Antioxid Redox Signal*; **8**(9-10):1775-1789.

McKenna, N., J., O'Malley, B., W. (2002). Combinational control of gene expression by nuclear receptors and coregulators. *Cell*; **108**(4):465-474.

Medema, R., H., de Vries-Smits, A., M., van der Zon., G., C., Maassen, J., A., Bos, J., L. (1993). Ras activation by insulin and epidermal growth factor through enhanced exchange of guanine nucleotides on p21ras. *Mol Cell Biol*; **13**(1):155-162.

Meischl, C., Buermans, H. P., Hazes, T., Zuidwijk, M. J., Musters, R. J., Boer, C. (2008). H9c2 cardiomyoblasts produce thyroid hormone. *Am J Physiol Cell Physiol*; **294**(5): C1227-1233.

Mitchell, A., M., et al. (2005). Thyroid export from cells contribution of P-glycoprotein. *J Endocrinol*; **185**(1):93-98.

Monden, T., Nakajima, Y., Hashida, T., Ishii, S., Tomaru, T., Shibusawa, N., Hashimoto, K., Satoh T., Yamada, M., Mori, M., Kasai K. (2006). Expression of thyroid hormone receptor isoforms down-regulated by thyroid hormone in human medulloblastoma cells. *Endocrine Journal*; **53**(2):181-187.

Morales, P., Bosch, A., Lopez, R., Nery, C., Borrás, F., Rosa, M. (1988). Radiotherapy and L-triiodothyronine in the treatment of high-grade astrocytoma. *J Surg Oncol*; **39**(2):119-121.

Morrison, D., K., Davis, R., J. (2003). Regulation of MAP kinase signaling modules by scaffold proteins in mammals. *Annu Rev Cell Dev Biol*; **19**:91-118.

Morrissey, R. P., Czer, L., and Shah, P. K. (2010). Chronic heart failure: current evidence, challenges to therapy, and future directions. *Am J Cardiovasc Drugs*; **11**(3): 153-171.

Mourouzis, I., Forini, F., Pantos, C., Iervasi, G. (2011). Thyroid hormone and cardiac disease: from basic concepts to clinical application. *Journal of thyroid research*; **11**(5): 1235-1345.

Mourouzis, I., Mantzouratou, P., Galanopoulos, G., Kostakou, E., Roukounakis, N., Kokkinos, A. D. (2011). Dose dependent effects of thyroid hormone on post-ischaemic cardiac performance: potential involvement of Akt and ERK signaling. *Mol Cell Biochem*; **10**(8): 135-177.

Nagahara, H., Mimori, K., Ohta, M., Utsunomiya, T., Inoue, H., Barnard, G., F., Ohira, M., Hirakawa, K., Mori, M. (2005). Somatic mutations of epidermal growth factor receptor in colorectal carcinoma. *Clin Cancer Res*; **11**(4):1368-1371.

Nauman, P., Bonicki, W., Michalik, R., Warzecha, A., Czernicki, Z. (2004). The concentration of thyroid hormones and activities of iodothyronine deiodinases are altered in human brain gliomas. *Folia Neuropathol*; **42**(2):67-73.

Nieder, C., Grosu, A. L., Mehta, M. P., Andratschke, N., Molls, M. (2004). Treatment of malignant gliomas: radiotherapy, chemotherapy and integration of new targeted agents. *Expert Rev Neurother*; **4**(4):691-703.

Nicoll, J. B., Gwinn, B. L., Iwig, J. S., Garcia, P. P., Bunn, C. F., Allison, L. A. (2003). Compartment-specific phosphorylation of rat thyroid hormone receptor alpha1 regulates nuclear localization and retention. *Mol Cell Endocrinol*; **205**(1-2): 65-77.

Nimsky, C., Fujita, A., Ganslandt, O., Von Keller, B., Fahlbusch, R. (2004). Volumetric assessment of glioma removal by intraoperative high-field magnetic resonance imaging. *Neurosurgery*; **55**(2):358-370.

Nishio, S., Morioka, T., Takeshita, I., Shono, T., Inamura, T., Fujiwara, S., Fukui, M. (1995). Chemotherapy for progressive pilocytic astrocytomas in the chiasmo-hypothalamic regions. *Clin Neurol Neurosurg*; **97**(4):300-306.

Normanno N, De Luca A, Maiello MR, Campiglio M, Napolitano M, Mancino M, Carotenuto A, Viglietto G, Menard S.(2006). The MEK/MAPK pathway is involved in the resistance of breast cancer cells to the EGFR tyrosine kinase inhibitor gefitinib. *J Cell Physiol*;**207**(2):420-427.

Odelberg, S. J. (2002). Inducing cellular dedifferentiation: a potential method for enhancing endogenous regeneration in mammals. *Semin Cell Dev Biol*, **13**(5): 335-343.

Ohgaki, H. (2005). Genetic pathways to glioblastomas. *Neuropathology*; **25**(1):1-7.

Ohgaki H, Kleihues P. (2007). Genetic pathways to primary and secondary glioblastoma. *Am J Pathol*;**170**(5):1445-1453.

Ohgaki, H. (2009). "Epidemiology of brain tumours," *Methods Mol Biol*; **472**: 323-342.

Ojamaa, K., Kenessey, A., Shenoy, R., and Klein, I. 2000. Thyroid hormone metabolism and cardiac gene expression after acute myocardial infarction in the rat. *Am J Physiol Endocrinol Metab*; **279**(6): 1319-1324.

Ojamaa, K. (2010). Signaling mechanisms in thyroid hormone-induced cardiac hypertrophy. *Vascul Pharmacol*; **52**(3-4): 113-119.

Oviedo N. J., Beane, W. S. (2009). “Regeneration: the origin of cancer or a possible cure?” *Seminars in Cell and Developmental Biology*; **20**(5): 557–564.

Pantos, C., Mourouzis, I., Malliopolou, V., Paizis, I., Tzeis, S., Moraitis, P., Sfakianoudis, K., Varonos, D., D., Cokkinos, D., V. (2005). Dronedarone administration prevents body weight gain and increases tolerance of the heart to ischemic stress: a possible involvement of thyroid hormone receptor alpha1. *Thyroid*; **15**(1): 16-23.

Pantos, C., Mourouzis, I., Tsagoulis, N., Markakis, K., Galanopoulos, G., Roukounakis, N. (2009). Thyroid hormone at supra-physiological dose optimizes cardiac geometry and improves cardiac function in rats with old myocardial infarction. *J Physiol Pharmacol*, **60**(3): 49-56.

Pantos, C., Mourouzis, I., Markakis, K., Tsagoulis, N., Panagiotou, M., and Cokkinos, D. V. (2008). Long-term thyroid hormone administration reshapes left ventricular chamber and improves cardiac function after myocardial infarction in rats. *Basic Res Cardiol*; **103**(4): 308-318.

Pantos, C., Mourouzis, I., Saranteas, T., Paizis, I., Xinaris, C., Malliopolou, V. (2005b). Thyroid hormone receptors alpha1 and beta1 are downregulated in the post-infarcted rat heart: consequences on the response to ischaemia-reperfusion. *Basic Res Cardiol*; **100**(5): 422-432.

Pantos, C., Malliopolou, V., Mourouzis, I., Thempeyioti, A., Paizis, I., Dimopoulos, A. (2006). Hyperthyroid hearts display a phenotype of cardioprotection against ischemic stress: a possible involvement of heat shock protein 70. *Horm Metab Res*; **38**(5): 308-313.

Pantos, C., Dritsas, A., Mourouzis, I., Dimopoulos, A., Karatasakis, G., Athanassopoulos, G. (2007a). Thyroid hormone is a critical determinant of myocardial performance in patients with heart failure: potential therapeutic implications. *Eur J Endocrinol*; **157**(4): 515-520.

Pantos, C., Mourouzis, I., Dimopoulos, A., Markakis, K., Panagiotou, M., Xinaris, C. (2007b). Enhanced tolerance of the rat myocardium to ischemia and reperfusion injury early after acute myocardial infarction. *Basic Res Cardiol*; **102**(4): 327-333.

Pantos, C., Mourouzis, I., Markakis, K., Dimopoulos, A., Xinaris, C., Kokkinos, A. D. (2007c). Thyroid hormone attenuates cardiac remodeling and improves hemodynamics early after acute myocardial infarction in rats. *Eur J Cardiothorac Surg*; **32**(2): 333-339.

Pantos, C., Mourouzis, I., Paizis, I., Malliopolou, V., Xinaris, C., Moraitis, P. (2007d). Pharmacological inhibition of TR $\alpha$ 1 receptor potentiates the thyroxine effect on body weight reduction in rats: potential therapeutic implications in controlling body weight. *Diabetes Obes Metab*; **9**(1): 136-138.

Pantos, C., Xinaris, C., Mourouzis, I., Malliopoulou, V., Kardami, E., Cokkinos, D. V. (2007e). Thyroid hormone changes cardiomyocyte shape and geometry via ERK signaling pathway: potential therapeutic implications in reversing cardiac remodeling? *Mol Cell Biochem*; **297**(1-2): 65-72.

Pantos, C., Mourouzis, I., Markakis, K., Tsagoulis, N., Panagiotou, M., Cokkinos, D. V. (2008a). Long-term thyroid hormone administration reshapes left ventricular chamber and improves cardiac function after myocardial infarction in rats. *Basic Res Cardiol*; **103**(4): 308-318.

Pantos, C., Mourouzis, I., Xinaris, C., Papadopoulou-Daifoti, Z., Cokkinos, D. (2008b). Thyroid hormone and "cardiac metamorphosis": potential therapeutic implications. *Pharmacol Ther*; **118**(2): 277-294.

Pantos, C., Xinaris, C., Mourouzis, I., Perimenis, P., Politi, E., Spanou, D. (2008c). Thyroid hormone receptor alpha 1: a switch to cardiac cell "metamorphosis"? *J Physiol Pharmacol*; **59**(2): 253-269.

Pantos, C., Mourouzis, I., Saranteas, T., Clave, G., Ligeret, H., Noack-Fraissignes, P. (2009a). Thyroid hormone improves postischaemic recovery of function while limiting apoptosis: a new therapeutic approach to support hemodynamics in the setting of ischaemia-reperfusion? *Basic Res Cardiol*; **104**(1): 69-77.

Pantos, C., Mourouzis, I., Tsagoulis, N., Markakis, K., Galanopoulos, G., Roukounakis, N. (2009b). Thyroid hormone at supra-physiological dose optimizes cardiac geometry and improves cardiac function in rats with old myocardial infarction. *J Physiol Pharmacol*; **60**(3): 49-56.

Pantos, C., Mourouzis, I., Galanopoulos, G., Gavra, M., Perimenis, P., Spanou, D. (2010). Thyroid hormone receptor alpha1 downregulation in postischemic heart failure progression: the potential role of tissue hypothyroidism. *Horm Metab Res*; **42**(10): 718-724.

Pantos, C., Mourouzis, I., Cokkinos, D. V. (2011a). New insights into the role of thyroid hormone in cardiac remodeling: time to reconsider? *Heart Fail Rev*; **16**(1): 79-96.

Pantos, C., Mourouzis, I., Saranteas, T., Brozou, V., Galanopoulos, G., Kostopanagioutou, G. (2011b). Acute T3 treatment protects the heart against ischemia-reperfusion injury via TRalpha1 receptor. *Mol Cell Biochem*; **353**(1-2): 235-241.

Pantos, C. I., Malliopolou, V. A., Mourouzis, I. S., Karamanoli, E. P., Tzeis, S. M., Carageorgiou, H. C. (2001). Long-term thyroxine administration increases heat stress protein-70 mRNA expression and attenuates p38 MAP kinase activity in response to ischaemia. *J Endocrinol*; **170**(1): 207-215.

Pantos, C. I., Malliopoulou, V. A., Mourouzis, I. S., Karamanoli, E. P., Paizis, I. A., Steimberg, N. (2002). Long-term thyroxine administration protects the heart in a pattern similar to ischemic preconditioning. *Thyroid*; **12**(4): 325-329.

Pantos, C., Malliopoulou, V., Mourouzis, I., Karamanoli, E., Moraitis, P., Tzeis, S. (2003a). Thyroxine pretreatment increases basal myocardial heat-shock protein 27 expression and accelerates translocation and phosphorylation of this protein upon ischaemia. *Eur J Pharmacol*; **478**(1): 53-60.

Pantos, C., Malliopoulou, V., Paizis, I., Moraitis, P., Mourouzis, I., Tzeis, S. (2003b). Thyroid hormone and cardioprotection: study of p38 MAPK and JNKs during ischaemia and at reperfusion in isolated rat heart. *Mol Cell Biochem*; **242**(1-2): 173-180.

Pantos, C., Mourouzis, I., Malliopoulou, V., Paizis, I., Tzeis, S., Moraitis, P. (2005a). Dronedaron administration prevents body weight gain and increases tolerance of the heart to ischemic stress: a possible involvement of thyroid hormone receptor alpha1. *Thyroid*; **15**(1): 16-23.

Paris, M., Brunet, F., Markov, G. V., Schubert, M., Laudet, V. (2008). "The amphioxus genome enlightens the evolution of the thyroid hormone signaling pathway," *Development Genes and Evolution*; **218**(11-12): 667–680.

Perra A, Simbula G, Simbula M, Pibiri M, Kowalik MA, Sulas P, Cocco MT, Ledda-Columbano GM, Columbano A.(2008). Thyroid hormone (T3) and TRbeta agonist GC-1 inhibit/reverse nonalcoholic fatty liver in rats. *FASEB*; **22**(8):2981-2989.

Pingitore, A., Iervasi, G., Barison, A., Prontera, C., Pratali, L., Emdin, M. (2006). Early activation of an altered thyroid hormone profile in asymptomatic or mildly symptomatic idiopathic left ventricular dysfunction. *J Card Fail*; **12**(7): 520-526.

Pingitore, A., Chen, Y., Gerdes, A. M., Iervasi, G. (2011). Acute myocardial infarction and thyroid function: New pathophysiological and therapeutic perspectives. *Ann Med*; **13**(1): 211-222

Porrello, E. R., Mahmoud, A. I., Simpson, E., Hill, J. A., Richardson, J. A., Olson, E. N. (2011). Transient regenerative potential of the neonatal mouse heart. *Science*; **331**(6020): 1078-1080.

Ranasinghe, A. M., Quinn, D. W., Pagano, D., Edwards, N., Faroqui, M., Graham, T. R. (2006). Glucose-insulin-potassium and tri-iodothyronine individually improve hemodynamic performance and are associated with reduced troponin I release after on-pump coronary artery bypass grafting. *Circulation*; **114**(1): 1245-250.

Ranasinghe, A. M., Bonser, R. S. (2011). Endocrine changes in brain death and transplantation. *Best Pract Res Clin Endocrinol Metab*; **25**(5): 799-812.

Rajabi, M., Kassiotis, C., Razeghi, P., Taegtmeyer, H. (2007). Return to the fetal gene program protects the stressed heart: a strong hypothesis. *Heart Fail Rev*; **12**(3-4): 331-343.

Pellettieri J, Sánchez Alvarado A.(2007). Cell turnover and adult tissue homeostasis: from humans to planarians. *Annu Rev Genet*;**41**:83-105.

Reiser, P., J., Kline, W., O. (1998). Electrophoretic separation and quantitation of cardiac myosin heavy chain isoforms in eight mammalian species. *Am J Physiol*; **274** (3 Pt 2): H1048–1053.

Robledo, M. (1956). Myocardial regeneration in young rats. *Am J Pathol*; **32**(6): 1215-1239.

Roger, V. L. (2010). The heart failure epidemic. *Int J Environ Res Public Health*; **7**(4): 1807-1830.

Rybin, V., Steinberg, S. F. (1996). Thyroid hormone represses protein kinase C isoform expression and activity in rat cardiac myocytes. *Circ Res*, **79**(3): 388-398.

Salcman M. (1980). Survival in glioblastoma: historical perspective. *Neurosurgery*; **7**(5):435-439.

Salcman M, Scholtz H, Kaplan RS, Kulik S. (1994). Long-term survival in patients with malignant astrocytoma. *Neurosurgery*; **34**(2):219-220.

Sanchez Alvarado, A. (2000). Regeneration in the metazoans: why does it happen? *Bioessays*; **22**(6): 578-590.

Sato, Y., Buchholz, D. R., Paul, B. D., Shi, Y. B. (2007). A role of unliganded thyroid hormone receptor in postembryonic development in *Xenopus laevis*. *Mech Dev*; **124**(6): 476-488.

Sehgal, S., Drazner, M. H. (2007). Left ventricular geometry: does shape matter? *Am Heart J*; **153**(2): 153-155.

Schnabel, K., Wu, C. C., Kurth, T., Weidinger, G. (2011). Regeneration of cryoinjury induced necrotic heart lesions in zebrafish is associated with epicardial activation and cardiomyocyte proliferation. *PLoS One*; **6**(4): 18503-18515.

Scruggs, S. B., Walker, L. A., Lyu, T., Geenen, D. L., Solaro, R. J., Buttrick, P. M. (2006). Partial replacement of cardiac troponin I with a non-phosphorylatable mutant at serines 43/45 attenuates the contractile dysfunction associated with PKCepsilon phosphorylation. *J Mol Cell Cardiol*; **40**(4): 465-473.

Sirlak, M., Yazicioglu, L., Inan, M. B., Eryilmaz, S., Taso, R., Aral, A. (2004). Oral thyroid hormone pretreatment in left ventricular dysfunction. *Eur J Cardiothorac Surg*; **26**(4): 720-725.

Shi, Y. B., Fu, L., Hsia, S. C., Tomita, A., Buchholz, D. (2001). Thyroid hormone regulation of apoptotic tissue remodeling during anuran metamorphosis. *Cell Res*; **11**(4): 245-252.

Slack, J., M., Lin, W., G., Chen, Y. (2008). "Molecular and cellular basis of regeneration and tissue repair: the *Xenopus* tadpole: a new model for regeneration research," *Cellular and Molecular Life Sciences*; **65**(1): 54–63.

Soonpaa, M. H., Field, L. J. (1998). Survey of studies examining mammalian cardiomyocyte DNA synthesis. *Circ Res*; **83**(1): 15-26.

Stock, A., Sies, H. (2000). Thyroid hormone receptors bind to an element in the connexin43 promoter. *Biol Chem*; **381**(9-10): 973-979.

Strandness, E., Bernstein, D. (1997). Developmental and afterload stress regulation of heat shock proteins in the ovine myocardium. *Pediatr Res*, **41**(1): 51-56.

Stupp R, Weber DC. (2005). The role of radio- and chemotherapy in glioblastoma. *Onkologie*; **28**(6-7):315-317.

Swynghedauw, B. (1999). Molecular mechanisms of myocardial remodeling. *Physiol Rev*; **79**(1): 215-262.

Tabatabai G, Hegi M, Stupp R, Weller M. (2012). Clinical implications of molecular neuropathology and biomarkers for malignant glioma. *Curr Neurol Neurosci Rep*; **12**(3):302-307.

Taegtmeyer, H., Sen, S., Vela, D. (2010). Return to the fetal gene program: a suggested metabolic link to gene expression in the heart. *Ann N Y Acad Sci*; **1188**: 191-198.

Tavi, P., Sjogren, M., Lunde, P. K., Zhang, S. J., Abbate, F., Vennstrom, B. (2005). Impaired Ca<sup>2+</sup> handling and contraction in cardiomyocytes from mice with a dominant negative thyroid hormone receptor alpha1. *J Mol Cell Cardiol*; **38**(4): 655-663.

Tongers, J., Losordo, D. W., Landmesser, U. (2011). Stem and progenitor cell-based therapy in ischaemic heart disease: promise, uncertainties, and challenges. *Eur Heart J*; **32**(10): 1197-1206.

Tseng, A., Stabila, J., McGonnigal, B., Yano, N., Yang, M. J., Tseng, Y. T. (2010). Effect of disruption of Akt-1 of lin(-)c-kit(+) stem cells on myocardial performance in infarcted heart. *Cardiovasc Res*; **87**(4): 704-712.

Tsonis PA. (2000). Regeneration of the lens in amphibians. *Results Probl Cell Differ*; **31**:179-196.

van der Heide, S. M., Joosten, B. J., Dragt, B. S., Everts, M. E., Klaren, P. H. (2007). A physiological role for glucuronidated thyroid hormones: preferential uptake by H9c2(2-1) myotubes. *Mol Cell Endocrinol*; **264**(1-2): 109-117.

van der Putten, H. H., Joosten, B. J., Klaren, P. H., Everts, M. E. (2002). Uptake of tri-iodothyronine and thyroxine in myoblasts and myotubes of the embryonic heart cell line H9c2(2-1). *J Endocrinol*; **175**(3): 587-596.

Venero, C., Guadano-Ferraz, A., Herrero, A. I., Nordstrom, K., Manzano, J., de Escobar, G. M. (2005). Anxiety, memory impairment, and locomotor dysfunction caused by a mutant thyroid hormone receptor  $\alpha 1$  can be ameliorated by T3 treatment. *Genes Dev*; **19**(18): 2152-2163.

Weller M. (2012). Microglia: a novel treatment target in gliomas. *Neuro Oncol*; **14**(8):957.

White, P., Burton, K. A., Fowden, A. L., Dauncey, M. J. (2001). Developmental expression analysis of thyroid hormone receptor isoforms reveals new insights into their essential functions in cardiac and skeletal muscles. *Faseb J*; **15**(8): 1367-1376.

Wikstrom, L., Johansson, C., Salto, C., Barlow, C., Campos Barros, A., Baas, F. (1998). Abnormal heart rate and body temperature in mice lacking thyroid hormone receptor  $\alpha 1$ . *Embo J*; **17**(2): 455-461.

Witman, N., Murtuza, B., Davis, B., Arner, A., Morrison, J. I. (2011). Recapitulation of developmental cardiogenesis governs the morphological and functional regeneration of adult newt hearts following injury. *Dev Biol*; **354**(1): 67-76.

Zielonko, J. (1874). Pathologisch-anatomische und experimentelle Studien über Hypertrophie des Herzens. *Virchows Arch. f. path. Anat*; **62**: 29-57.

